



Systematic Approaches to Comprehensive Analyses of Natural Organic Matter

Jerry A. Leenheer

U.S. Geological Survey

Received April 30, 2008; in final form December 11, 2008; accepted March 18, 2009.

Copyright © 2009 by Northeastern University
All Right Reserved
First Edition

Author:

Jerry A. Leenheer, U.S. Geological Survey, PO Box 25046, MS 408, Denver
Federal Center, Denver, CO 80225, USA

Editors:

Elham A. Ghabbour, Northeastern University, Boston, MA, USA
Geoffrey Davies, Northeastern University, Boston, MA, USA

Reviewers:

Russell F. Christman, University of North Carolina, Chapel Hill, NC, USA
Robert L. Wershaw, U.S. Geological Survey, Denver, CO, USA

DEDICATION

To my wife, Cora Jean, for her love,
support, and appreciation of humic
substances.

FOREWORD

The more that is learned of the chemistry of aquatic natural organic matter (NOM) the greater is the scientific appreciation of the vast complexity of this subject. This complexity is due not only to a multiplicity of precursor molecules in any environment but to their associations with each other and with other components of local environments such as clays, mineral acids and dissolved metals. In addition, this complex system is subject to constant change owing to environmental variables and microbial action. Thus, there is a good argument that no two NOM samples are exactly the same even from the same source at nearly the same time. When ubiquity of occurrence, reaction with water treatment chemicals, and subsequent human exposure are added to the list of NOM issues, one can understand the appeal that this subject holds for a wide variety of environmental scientists.

A significant amount of research was published on NOM prior to a full appreciation of this complexity, resulting in a certain degree of non-comparability of results owing to the use of different isolation and/or separation techniques. U.S. Geological Survey scientists were among the first to realize that the application of systematic fractionation methodology based upon NOM properties was the key to data comparability and were responsible for two pivotal developments in the 1980's. Robert Averett, then Chief of Water Quality for USGS, led a detailed agency study of the properties of Suwannee River Fulvic Acid and Ronald Malcolm of that agency urged the preparation and maintenance of Fulvic and Humic Acid standards that ultimately became one of the principal functions of the International Humic Substances Society. The publication in 1989 of the results of the USGS study of Suwannee River Fulvic Acid remains one of the under-heralded classics of NOM literature.

The enormous complexity and dynamic nature of NOM must not obscure the very simple fact that this system is composed of organic molecules. The only way to understand the interactions behind the complexity and to explain the properties of the system is to identify at least representative component molecular structures. Thus, a reductionist approach, employing the best that analytical chemistry has to offer, is likely to be the most rewarding strategy for achieving the goal of good science, i.e., the development of a predictive capacity with regard to the role NOM plays in the environment.

Jerry Leenheer was centrally involved with the entire USGS campaign to bring solid analytical chemistry to NOM research. It is no coincidence that his career has paralleled the growth of understanding of the chemistry of NOM, as his work has been a substantial contributor to most of it. He began his career with USGS in 1970 to begin work on organic solute migration in ground water, subsequently becoming Chief of the Subsurface Waste Injection Project and later, Project Chief of the Oil-Shale Wastewater and Water Quality Project. As his interests and influence expanded, he began the Comprehensive Organic Analysis of Water Project and since 1987 has been continuously devoted to the geochemical investigation of water and sediment ranging from the Arctic to the Amazon. Within this focus his interests have been wide, from isolation and fractionation methodology to advanced spectral analysis and model compound construction, and his record of peer reviewed publications is sufficient testimony to his success.

Although the insistence upon solid analytical chemistry is thematic in this account, Jerry Leenheer has drawn upon principles from biochemistry, plant science, soil science, hydrology, inorganic chemistry, and limnology where needed to guide the development of analytical and preparative scale methods and to inform his interpretation of analytical results. In this sense, the account presented here is both a guide and laboratory manual for anyone facing organic geochemical research questions. Of course, carefully isolated and separated NOM components are not needed for those experimental objectives aimed at the behavior of whole NOM mixtures, i.e., disinfection by-product formation and the behavior of engineered nanomaterials. Even for this latter eventuality, the explanation of whole system behavior often relies upon knowledge of the chemical and physical classifications of its parts.

Finally, it is very much in character for Jerry Leenheer to make this account available to the world of his professional colleagues in a format as accessible as *Annals of Environmental Science*. I extend my personal gratitude to Jerry Leenheer for preparing and sharing this detailed account and to our colleagues at Northeastern University for making it available.

R.F. Christman
Chapel Hill, North Carolina, USA

Contents

1 Preface 1

2 Introduction 1

- 2.1 Relationship of Comprehensive NOM Analyses to Research Objectives 1
 - 2.2 Knowledge Requirements 2
-

3 Controls on NOM Composition 3

4 Sampling NOM 5

- 4.1 Sampling Soil NOM 5
 - 4.2 Sampling Sediment NOM 6
 - 4.2.1 Large-Volume Sampling of Water and Suspended Sediment 6
 - 4.2.2 Small-Volume Sampling of Water and Suspended Sediment 8
 - 4.2.3 Bed-Sediment Sampling 9
 - 4.3 Sampling Dissolved Organic Matter (DOM) 9
-

5 NOM Fractionation and Isolation 11

- 5.1 DOM Fractionation and Isolation from Water 11
 - 5.1.1 DOC Fractionation 11
 - 5.1.2 DOM Fractionation of Fresh Water 13
 - 5.1.3 DOM Fractionation of Salt Water 19
 - 5.1.4 Dissolved Organic Nitrogen (DON) Fractionation 21
 - 5.2 Total Organic Matter (TOM) Fractionation of Soil and Sediments Suspended in Water 21
 - 5.3. NOM Sub-fractionations 22
 - 5.3.1 Solvent Solubility Separations 22
 - 5.3.2 Normal-Phase Chromatography on Silica Gel 24
 - 5.3.3 Reverse-Phase pH-Gradient Chromatography on XAD-8 Resin 24
 - 5.3.4 Reverse-Phase Solvent-Elution Chromatography on XAD-8 Resin 26
-



6	Characterization of NOM	28
6.1	Elemental Analyses	28
6.2	Molar Mass/Size Distributions	30
6.3	Density Analyses of Solvated NOM	34
6.4	Titrimetric Analyses	35
6.5	Infrared Spectrometry	37
6.6	Nuclear Magnetic Resonance Spectrometry	40
6.6.1	¹³ C-NMR Spectrometry	41
6.6.2	¹ H-NMR Spectrometry	43
6.6.3	¹⁵ N- and ³¹ P-NMR Spectrometry	46
6.6.4	²⁷ Al-, ¹¹ B-, ¹¹³ Cd-, ¹³³ Cs, and ²⁹ Si-NMR Spectrometry	46
6.6.5	Multidimensional-NMR Spectrometry	47
6.7	Mass Spectrometry	48
6.8	Ultraviolet/Visible Spectrometry	53
6.9	Fluorescence Spectrometry	55
6.10	X-ray Absorption Spectrometry	55
6.11	Degradative, Derivative, and Chromatographic Characterizations	56
6.11.1	Oxidative Degradations	56
6.11.2	Reductive Degradations	57
6.11.3	Degradations with Sodium Sulfide and Phenol	57
6.11.4	Hydrolytic Degradations	58
6.11.5	Thermal Degradations	58
6.11.6	Conclusions about NOM Characterizations	60



7	Comprehensive Structural Models of NOM	61
7.1	Analytical Requirements	61
7.2	NOM Source and Process Requirements	63
7.3	Geochemical Requirements	65
7.4	Successive Approximations of Structural Models of Suwannee River Fulvic Acid [100]	65
7.5	Ultrahigh-Resolution Mass-Spectrometric Molecular Model of Hydrophilic DOM in Seawater	68



8	Identification and Diagenesis of NOM Compound Classes and Precursors	69
8.1	Lignins	69
8.2	Tannins	70
8.3	Terpenoids	71
8.4	Polysaccharides and Proteins	73
8.5	Porphyryns	75
8.6	Lipids	77
8.7	Black Carbon	80



9	Examples of Comprehensive NOM Analyses	82
9.1	Dissolved Organic Matter in Recharge Waters, Santa Ana River Basin	82
9.2	Attenuation of Dissolved Organic Matter during Ground Water Recharge	86

- 9.3 Total Organic Matter in Stormflows, Santa Ana River Basin 86
- 9.4 Characterization of DOM in Domestic Waste-water Treatment-Plant Effluents 91
- 9.5 Characterization of DOM at the Stringfellow Hazardous-Waste Disposal Site, southern California 95
- 9.6 Characterization of Organic Matter in a Swine Waste-Retention Basin 97
- 9.7 Characterization of Organic Matter in Fog Water 97
- 9.8 Characterization of Organic Matter in Atmospheric Aerosols 99
- 9.9 Characterization of NOM in Hydrophobic Soils Altered by Fire 104
- 9.10 Characterization of DOM Incorporated in Calcium Carbonate Precipitated in Pyramid Lake, Nevada 105
- 9.11 Characterization of Humic acid Sub-fractions from Lignite and Soil Samples from Greece 111

10 The Paths to Molecular Characterization of NOM 114

- 10.1 Molecular Characterization of NOM Supramolecular Structures 114
- 10.2 Molecular Analyses of NOM 116

11 Acknowledgments 117

12 References 118



ABBREVIATIONS, ACRONYMS, AND SYMBOLS

A	acid
AMP	amphiphilic
APEC	carboxylated ethoxyalkylphenols
APEO	ethoxyalkylphenol surfactants
APT	attached proton test
B	base
Bz	benzenoid
cm ⁻¹	reciprocal centimeters (IR spectrometry wavenumber unit)
CAPEC	carboxylated alkylphenol ethoxycarboxylates
C:N	carbon to nitrogen ratio
CP/MAS	cross polarization magic angle spinning
CPOM	coarse-particulate organic matter
CRAMPS	combined rotation and multiple pulse
DATS	dialkyltetralin sulfonates
DDT	dichlorodiphenyltrichloroethane
DMF	N,N-dimethylformamide
DOSY	diffusion-ordered spectroscopy
DOC	dissolved organic carbon
DOM	dissolved organic matter
DON	dissolved organic nitrogen
E ₄ /E ₆	absorbance ratio at 465/665 nm
EEM	excitation, emission, intensity spectrometry
EOM	extractable organic matter
ESI	electrospray ionization
ET	electron transfer
EXAFS	extended X-ray-absorption fine-structure spectrometry
FA	fulvic acid
FT	Fourier transform
g	gram
GC	gas chromatography
HETCOR	heteronuclear-correlation spectroscopy
HMBC	heteronuclear multiple-bond connectivity
HPI	hydrophilic
HPLC	high performance liquid chromatography
HPO	hydrophobic
HSQC	heteronuclear single-quantum coherence
ICR	ion cyclotron resonance
IR	infrared spectrometry
k'	capacity factor
K	stability constant
L	liter
LAS	linear alkylsulfonate surfactants
LE	local excitation

M _n	number-average molar mass
M _w	weight average molar mass
meq	milliequivalent
MC	Mill Creek
MHz	megahertz
mL	milliliter
mg	milligram
mm	millimeter
ms	millisecond
mS	milliSiemen
MS	mass spectrometry
MSSV	microscale sealed-vessel
m/z	Mass/charge ratio
N	neutral
NA	not analyzed
nm	nanometers
NMR	nuclear magnetic resonance spectrometry
NOESY	nuclear Overhauser-effect spectroscopy
NOM	natural organic matter
(O+N)/C	polarity index
PEG	polyethylene glycol
PM	particulate matter
PPG	polypropylene glycol
ppm	parts per million (NMR spectrometry chemical shift unit)
RO	reverse osmosis
R/V	research vessel
SAR	Santa Ana River
SC	specific conductance
SEC	size-exclusion chromatography
SPC	sulfophenyl carboxylates
SRFA	Suwannee River fulvic acid
SUVA	specific UV absorbance
THMFP	trihalomethane formation potential
TOCSY	total correlation spectroscopy
TOF	time of flight
TOM	total organic matter
TPI	transphilic
USGS	U. S. Geological Survey
UV	ultraviolet
Vis	visible
XANES	X-ray-adsorption near-edge structure spectrometry
Φ	index of hydrogen deficiency
θ	number of rings
Ω	number of carbons per ring
φ	aromatic ring

1. PREFACE

Interest in the composition of natural organic matter (NOM) in various environments is increasing because of its significance in soil fertility, water quality, the global carbon cycle, and the maintenance of life itself. NOM composition cannot yet be described at the molecular level of characterization because of NOM complexity and its interactions with itself and environmental matrixes, but composition descriptions have progressed from the humus "black box" to compound-class descriptions that can be related to biochemical precursors modified by various diagenetic decay processes. The objective of this account is to present a number of comprehensive, systematic approaches to NOM analyses in a variety of soil, sediment, water, atmosphere, and rock environments. The focus of comprehensive NOM analyses is primarily based on analytical organic chemistry, but relevant information from biochemistry, plant science, soil science, hydrology, inorganic chemistry, and limnology is also included where needed. Comprehensive analysis is inclusive; its objective is to include all of NOM in its various fractions. Systematic analysis of NOM is based upon a hierarchical approach designed to quantitatively separate NOM into various fractions based on molecular size; polarity; acid, base, and neutral characteristics; specific gravity; extractability in various solvents; and volatility. The hierarchy level, fraction homogeneity, instrumental requirements, time, and cost of analyses are directly related to the number of NOM properties applied in the fractionation process.

Given the fact that each NOM analysis is a research endeavor, the intended audiences for this book are researchers. These researchers should have a fundamental understanding of analytical chemistry, organic chemistry, and inorganic chemistry to successfully apply and modify comprehensive NOM analyses for studies with specific objectives, particularly as applied to environmental samples with unique properties that require procedural modifications. Comprehensive NOM analyses are designed for the discovery of unknown components that comprise NOM. After their discovery, analytical methods for these previously unknown components can usually be developed that are more rapid, sensitive, and inexpensive. Thus, comprehensive NOM analysis is not intended for environmental monitoring studies. The analytical approach of comprehensive NOM analysis is reductionist, with the ultimate intent of separating pure NOM compounds that can be identified in a systematic manner similar to

that described in *The Systematic Identification of Organic Compounds* by Shriner, Fuson, and Curtin [1]. Obtaining pure NOM compounds that can be identified by conventional analyses is not yet possible, and the most homogeneous of NOM fractions still contains hundreds to thousands of compounds, as shown by high-resolution mass spectrometry. Consequently, NOM structures derived from analytical data are models of average data sets, and these models are only approximations.

Finally, there has been a revolution in the development of multidimensional spectra characterization methods and in ultrahigh resolution chromatography and mass spectrometry. Electrospray ionization/mass spectrometry has been especially useful in its application to NOM analyses. Fractions produced by comprehensive NOM analyses have been purified of inorganic components and have sufficient compound-class homogeneity to render these fractions especially suitable for advanced chromatographic and spectral analyses.

2. INTRODUCTION

2.1. Relationship of Comprehensive NOM Analyses to Research Objectives

Most NOM constituents in soil, sediment, and water environments do not exist as dissociated molecules, but instead are strongly associated with themselves through hydrogen-bonding and non-polar interactions [2,3], are strongly associated with trivalent metal cations such as iron(III) ion and aluminum [4,5], are moderately associated with divalent cations such as calcium, copper, lead, and zinc [6,7], and are weakly associated with boric acid [8] and silicic acid [9]. NOM constituents also strongly associate with clay minerals in soils and aquatic sediments to form coatings [5,10]. Recent research indicates that some NOM consists of supramolecular aggregates of relative low molar mass constituents [11,12]. Thus, NOM as it exists in the environment should be regarded as a dynamic combinatorial system [13] and as infinitely heterogeneous with regard to the molecular composition of NOM organic phases [14].

Comprehensive NOM analyses involving extensive fractionation may not be appropriate for research studies involving NOM phase characteristics such as non-polar organic-contaminant partitioning, metal binding with bulk NOM, and apparent molar mass measurements. Comprehensive NOM analysis is designed for studies of molecular characteristics such

as fundamental studies of structure and diagenesis from precursors. NOM reactivity studies such as reactions with various chemical disinfection agents, and its interaction with electromagnetic radiation, are also related to molecular characteristics of NOM.

The hierarchical approach for comprehensive analyses of dissolved organic matter (DOM) in water is diagrammed in Figure 1. The hierarchy level by which DOM is classified depends on the research objective, DOM mass and concentration requirements, analytical instrumentation availability, and the cost of analyses. Figure 1 illustrates how analytical cost increases exponentially as hierarchy levels increase. DOM characterization potential, defined as the percentage mass of DOM or dissolved organic carbon (DOC) indicated by the analytical requirements at each hierarchy level, decreases as hierarchy levels increase. DOM fractionation at hierarchy levels 1-3 is based upon dissolved organic carbon (DOC) analyses, has quantitative characterization potentials, and is usually defined as DOC fractionation. Analytical-scale DOC fractionation [15] has been used with various modifications for DOC-profiling studies [16,17]. DOM analyses at level 4 isolate organic matter fractions from water and inorganic solutes for various compound-class analyses; these level 4 analyses are

also known as preparative DOM fractionation [18]. DOM analyses at levels 5 and 6 involve advanced multidisciplinary research projects that are just beginning to yield molecular and specific complex information. Similar hierarchical analytical approaches for total organic matter (TOM) analyses in soils, sediments, and water have been devised and will be illustrated in this account.

2.2. Knowledge Requirements

NOM exists in a matrix of water, inorganic solutes, and minerals which must be either separated or accommodated for comprehensive NOM analyses. Therefore, a fundamental knowledge of water chemistry as given in the texts by Hem [19] and by Stumm and Morgan [20] is essential. The analyst should also be familiar with the chemical and physical separations of inorganic solutes taught in analytical chemistry courses. The soil and sediment matrix should be understood through courses and texts in soil chemistry and mineralogy and within the basic system of soil classification as given by the text *Soil Taxonomy* [21]. Various methods of soil analyses are given in the text by Jackson [22].

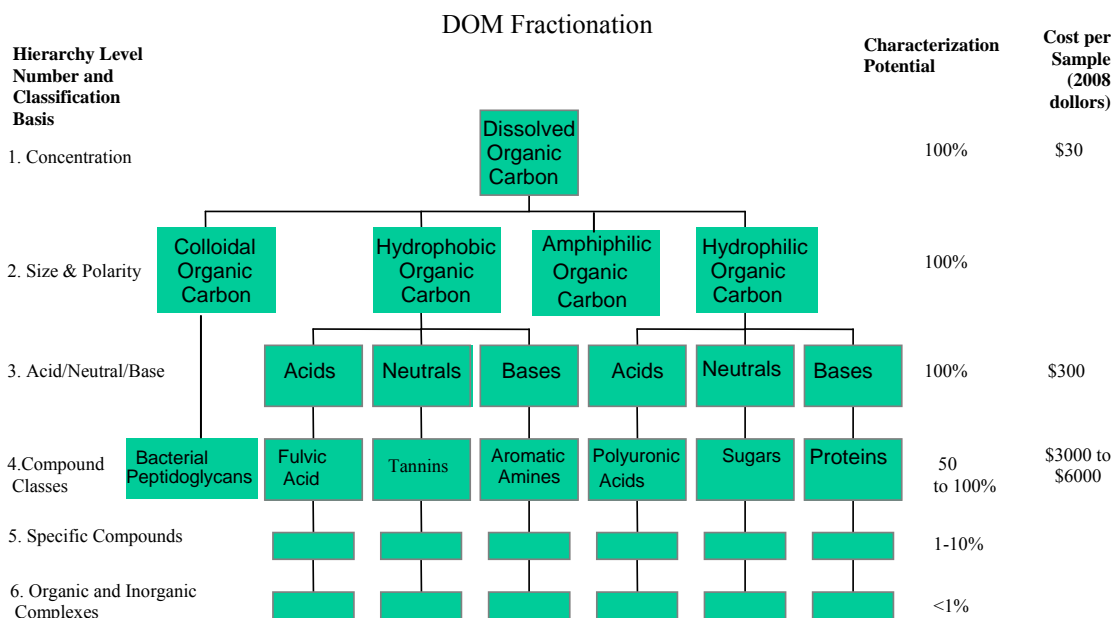


Figure 1 Diagram of hierarchical approach to dissolved organic matter fractionation

A firm background in organic chemistry is essential, and synthetic organic chemistry is helpful in the preparation of chemical derivatives of NOM for various analyses. With regard to analytical organic chemistry, the systematic analytical approach as given by Shriner et al [1] is very useful; however, the specific separation and characterization methods given in this account that were devised for monofunctional synthetic compounds are not applicable to NOM because of its complex polyfunctional nature. Analytical methods given in various biochemistry and plant chemistry texts [23] are more useful as applied to NOM analyses.

With regard to NOM analyses and properties in soils, the texts by Stevenson [5], Schnitzer and Khan [6], and Greenland and Hayes [24] are reasonably comprehensive. A discussion of the organic geochemistry of NOM in water with some analytical fractionation methods is presented in the text by Thurman [25]. Various processes that degrade or create NOM (through coupling and condensation reactions) are presented in the texts by Larson and Weber [26] and Stevenson [5]. Microbiological degradative processes are well covered in the text by Gibson [27]. Chemical descriptions of plant precursors to NOM are presented by Robinson [23], and autochthonous precursors are discussed in the limnology text by Wetzel [28]. A general knowledge of hydrology and geology is very useful for understanding the transport and fate of NOM in the global environment.

The major quantitative spectrometric methods used in comprehensive NOM analyses are infrared (IR) and nuclear magnetic resonance (NMR) spectrometry. A method which is useful but is still being developed for better application to comprehensive NOM analyses is mass spectrometry. For infrared spectrometry, the texts by Bellamy [29] and Stevenson [5] are useful for qualitative functional-group assignments, and the article by Wexler [30] is useful for quantitative interpretations. Applications of NMR spectrometry to NOM analyses are presented in texts by Wilson [31] and Nanny et al [32]. Spectral handbooks of known compounds by Pouchert [33] for IR spectra, by Simons [34] for ^1H -NMR spectra, and by Simons [35] for ^{13}C -NMR spectra are very useful for identification of structural features in NOM fractions.

The above citations for knowledge requirements are not meant to be comprehensive, and are not necessarily the most up-to-date and best references that might be used. Rather, they are the literature and

training that were used to develop the comprehensive NOM analyses presented in this account.

3. CONTROLS ON NOM COMPOSITION

Before attempting comprehensive NOM analysis, it is advantageous to understand which sources and biogeochemical processes are involved (Figure 2). NOM biomass is produced primarily by the photosynthetic activities of terrestrial and aquatic plants, algae, and photosynthetic bacteria. However, recent measurements indicate that bacterial biomass, much of which is produced by heterotrophic bacteria in secondary production processes, exceeds plant biomass on planet earth [36]. Fungi are another important secondary biomass source; thus, one should expect NOM to be derived from secondary production sources as much as primary production sources.

Proximity to the source is an important control on NOM composition. Autochthonous sources of NOM are usually more significant in samples where NOM inputs from allochthonous sources are minimal, such as lakes with algal blooms. Allochthonous NOM is also subjected to more degradative and removal processes during its transport, as illustrated in Figure 2. The trophic status of an environment is an important control on NOM concentration and composition. Eutrophic surface waters have both increased NOM production and degradation rates, provided oxygen is not limiting. Eutrophic ground waters (unlike ground waters with nutrient limitations), however, have only increased degradation rates because photosynthesis does not occur.

Aerobic degradation of NOM, both abiotic and biotic, adds oxygen in the form of hydroxyl, carbonyl, and carboxyl groups that generally increase NOM solubility, whereas anaerobic degradation removes oxygen and adds hydrogen that decreases NOM solubility. However, there are two important exceptions to oxidation increasing NOM solubility:

- 1) Oxidative coupling of phenols creates macromolecular insoluble humus [5] and insoluble theoburigin pigments in teas and wines [37]. Aldehyde oxidation products of NOM will also condense with reactive phenols as found in tannins, to produce insoluble macromolecular structures [23,38].
- 2) NOM oxidation, particularly of tannins and lignins, produces clustered carboxyl and phenolic groups that have high affinity for polyvalent metal cations [39,40]. This affinity will either

cause charge neutralization leading to flocculation, which is used to remove DOM by iron(III) chloride or alum in water treatment, or it will lead to DOM adsorption on sesquioxide iron and aluminum coatings on soil and sediment minerals, as shown in Figure 2.

At every step in the diagenesis from precursor to refractory NOM, molecular structures and the functional groups contained in them are major controls on ultimate composition. Compound classes that are readily biodegraded include aminoacids, proteins and peptides, carbohydrates, fatty acids, and straight-chain lipids [27] if they are not sequestered by

adsorption in mineral pores or by co-precipitation with sesquioxides and carbonate minerals. Functional groups that readily react and/or degrade include aldehydes (which condense with phenols or oxidize to carboxylic acids), primary amino groups that condense with carbonyl groups through the Maillard reaction [5], and ortho-phenol groups that rapidly oxidize to ortho-quinones which further oxidize with aromatic rings opening to aliphatic dicarboxylic acids [27]. Aromatic ring structures and conjugated aliphatic olefins that absorb ultraviolet light in the presence of reactive radicals are subject to oxidative degradation and oxidative coupling that forms new structures [41].

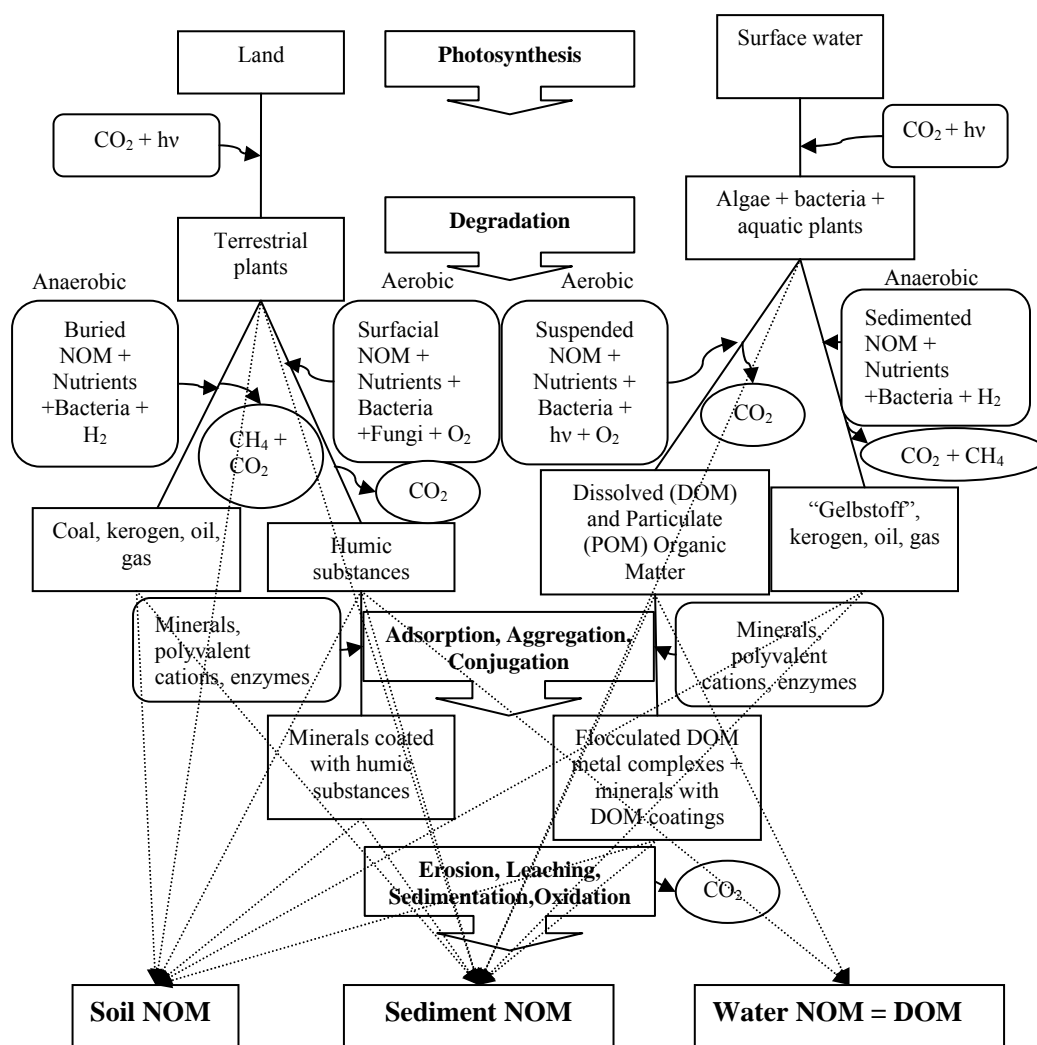


Figure 2 Derivation of NOM in soil, sediment, and water = NOM pools; = reactants; = gas products; = process; = NOM pool connectors; \rightarrow = reactant and product vectors; $\cdots\rightarrow$ = NOM pool input vectors, hv = electromagnetic radiation

A theory of marine fulvic acid formation involves oxidative coupling of unsaturated lipids [42]. Some of the most resistant structures to biodegradation are branched- and condensed-aliphatic and alicyclic-ring structures such as are found in terpenoid hydrocarbons, but even these structures can be biodegraded under certain conditions [43]. Terpenoid precursors have been found as major contributors to DOM in surface and ground water [44]. Refractory aliphatic structures found in certain soils and sediments are derived from plant waxes such as cutin [45]. Condensed aromatic ring structures resulting from pyrogenic processes (black carbon) have been found to be very refractory and a significant component of NOM in certain soils, although black carbon content has been previously overestimated by methodological artifacts [46].

The hydrologic processes of erosion, leaching, and sedimentation mix the various NOM pools shown in Figure 2 to such an extent that NOM in soils and sediments can be derived from almost any pool. Because of oxidative degradation and solubility limitations, NOM in water is derived primarily from two pools resulting from aerobic decay of plant and algal precursors with secondary inputs from bacteria and fungi. The flow-chart of Figure 2 is incomplete in that additional degradation of NOM from soil, sediment, and water pools after hydrologic mixing leads to NOM of increasing complexity with concurrent loss of identity of its precursor sources. Studies of “end-member” environments where NOM mixing and precursor sources are limited greatly simplify NOM characterization and aid in the understanding of NOM diagenesis [47,48].

4. SAMPLING NOM

Sampling of NOM in various environments is a complex procedure that involves considerations of sampling apparatus: sample containers, location, preservation, and shipment; sample separations involving centrifugation and/or filtration; and various field measurements and observations. NOM should be regarded as labile and reactive, as shown in Figure 2. NOM is also easily contaminated by synthetic chemicals and reagents used in the sampling process; however, because of its abundance relative to “trace contaminants,” NOM can generally be sampled without using ultra-clean procedures.

4.1. Sampling Soil NOM

Soil NOM usually is colored brown to black; thus, sampling of NOM in various soil horizons can be guided by color, although various iron and manganese minerals can also give brown to black coloration. The irregular nature of soil-horizon development (the soil pedon) is illustrated in Figure 3. Soil NOM deposited in the spodic horizon is black, whereas the sand subsoil is nearly white; however, the horizon boundaries are very irregular. Soil exposures in road cuts and trenches therefore offer better sampling options than samples taken from cores where these irregularities cannot be observed on a large-scale basis. Because soil NOM degrades and is contaminated with various particulates over time after exposure, soil should be sampled on freshly exposed surfaces cleaned with a knife or spade as shown in Figure 3.



Figure 3 A spodosol soil-horizon exposure in a road cut near Manaus, Brazil

Besides color, a number of rapid soil tests might be conducted during sampling, depending on the research objectives. These tests include soil pH, texture, porosity, moisture, salinity, oxygen content, organic matter content, and carbonate content. Tests could also be conducted for extractable phosphorus, nitrogen, potassium, sodium, calcium, magnesium, borate, chloride, and sulfate. A number of commercially field-test kits are available. The chemistry and physics involved with these tests are described by Jackson [22]. The types of soil-sampling equipment and sample containers are usually selected for convenience and durability for aerobic soils; anaerobic soils require specialized samplers, containers, and

preservatives designed to exclude oxygen. Wide-mouthed glass and plastic jars are typically used.

Soil samples are generally air-dried for storage, although they may be freeze-dried or frozen for long-term storage. Keep in mind that freezing ruptures plant and microbial cells, which releases water-soluble NOM that may not otherwise be present. Additional sample-preservation techniques include storage under nitrogen or argon (to prevent oxidation), refrigeration (to retard microbial degradation), and storage in dark containers to prevent photolytic degradation. Rapid processing of the sample is often the best option to minimize sample changes with time.

4.2. Sampling Sediment NOM

NOM in sediments suspended in water will receive the major emphasis with regard to sampling and analyses. NOM in bed sediments can be analyzed in a similar manner as soils, although specialized methods are required for sampling of bed sediments. Preliminary estimates of sediment concentration based upon turbidity or transparency measurements are necessary to determine the scale of the water/sediment sampling and separations that are required, depending on research objectives. Filtration of sediment is used to isolate small amounts of suspended sediment, whereas centrifugation and gravitational settling is required for separation of larger amounts of sediment. Sediments are also not uniformly distributed in water, as illustrated in Figure 4.



Figure 4 The confluence of the Rio Negro and the Rio Solimões near Manaus, Brazil

The Rio Negro in Brazil has little suspended sediment and is colored black by DOM, whereas the Rio Solimões has a muddy appearance because of its large concentration of suspended sediment. In addition

to lateral inhomogeneities in suspended sediment concentrations, there are vertical variations. There will be greater amounts of suspended-sediment concentration near the bottom in flowing rivers than at the top, although there may be floating NOM as shown by the grass rafts in the Rio Solimões in Figure 4. Therefore, to obtain representative samples of suspended sediment in rivers, depth-integrated and flow-weighted samples collected at equally spaced intervals across the river channel are composited as described by Meade et al [49].

4.2.1. Large-Volume Sampling of Water and Suspended Sediment

A large number of sampling approaches and systems have been developed for rivers, lakes, and oceans. It is not the intent of this account to describe them all. The sampling system used to measure contaminants in water and sediment in the Mississippi River from 1987 to 1992 will be described [49] because in this study considerable effort was made to obtain large-volume samples of water and sediment which were representative, quantitative, and uncontaminated by materials used in the sampling. The ship used to obtain the samples was the Research Vessel (R/V) *Acadiana* shown in Figure 5.



Figure 5 The research vessel (R/V) *Acadiana* at a sampling location on the Mississippi River

The braided steel line extending into the water enclosed a Teflon tube through which 500 to 1000 L of water were pumped into a laboratory on the stern of the vessel. Although this large sample was not depth-integrated, comparative studies with depth-integrated samples collected simultaneously were used to select the intake depth and determine sample volumes at each sampling location across the river, so that

sediment concentrations were comparable to the depth-integrated samples. A Teflon bellows pump driven by compressed air was used in this sampling system. Teflon plastic was used where possible, as its non-stick and non-contaminating characteristics were a great advantage for water and sediment sampling. Stainless-steel milk cans (shown on the top of the laboratory in Figure 5) were used for temporary storage of water during sampling, and glass carboys were also used for temporary storage and sample processing.



Figure 6 Centrifuge, sieve, and reservoirs used to process pumped-water sample in the laboratory on R/V *Acadiana*

The water sample was pumped through a 63 μ m nickel-wire sieve (to remove suspended sand) into a glass reservoir as shown in Figure 6. The sample was then passed from the reservoir by gravity-flow through a Sharples continuous-flow centrifuge to remove suspended silt and clay. The supernatant was collected in the stainless-steel milk cans for ultrafiltration to recover suspended colloids. The stainless-steel bowl of the centrifuge was lined with a Teflon sheet that could be removed, and the silt and clay were then recovered from it with a Teflon scraper as shown in Figure 7.

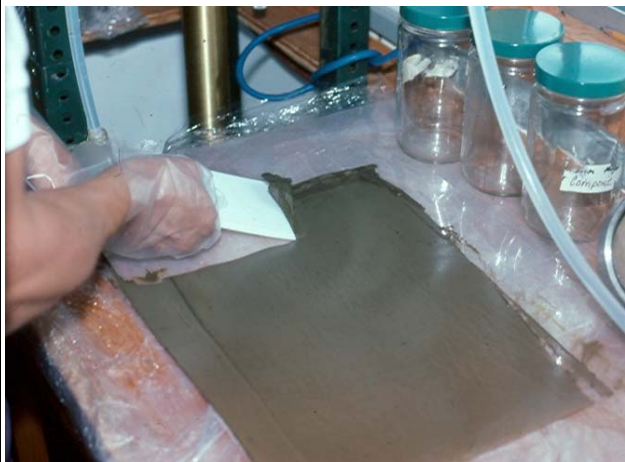


Figure 7 Removal of suspended silt and clay from Teflon centrifuge-bowl liner

Suspended-sediment colloids in the centrifuge supernatant were concentrated using a flat-plate tangential-flow ultrafilter that was also driven by a Teflon bellows pump (Figure 8). Regenerated cellulose membranes with a 30000 Dalton nominal pore-size cutoff were used. The number of ultrafilter plates in the filter assembly was dependent on the suspended-sediment concentration and the volume of water processed. The flat-plate ultrafilter was selected because trials with different types of tangential-flow ultrafilters showed that a significant percentage of the colloids stuck to the ultrafilter membranes. Spiral-wound ultrafilters could not be readily disassembled to remove adhered colloids, but flat-plate ultrafilters could. Removal of colloids that adhered to the flat plates is shown in Figure 9.

Retentate water that remained after processing 500 to 1000 Liters of sample was placed in a Teflon bag, and the adhered colloids were removed by rubbing the bag surface against the membrane surface to re-suspend the colloids in the retentate. The colloids

had little color, as shown in Figure 9, as compared to the silt and clay sediment shown in Figure 7.

Final isolation of the suspended colloids in dried form was accomplished by dialyzing the retentate concentrate contained in a cellulose dialysis bag (10000 Dalton nominal pore size) against deionized water, followed by freeze-drying. The color of these freeze-dried colloids was light brown to white, and its texture was like cotton.

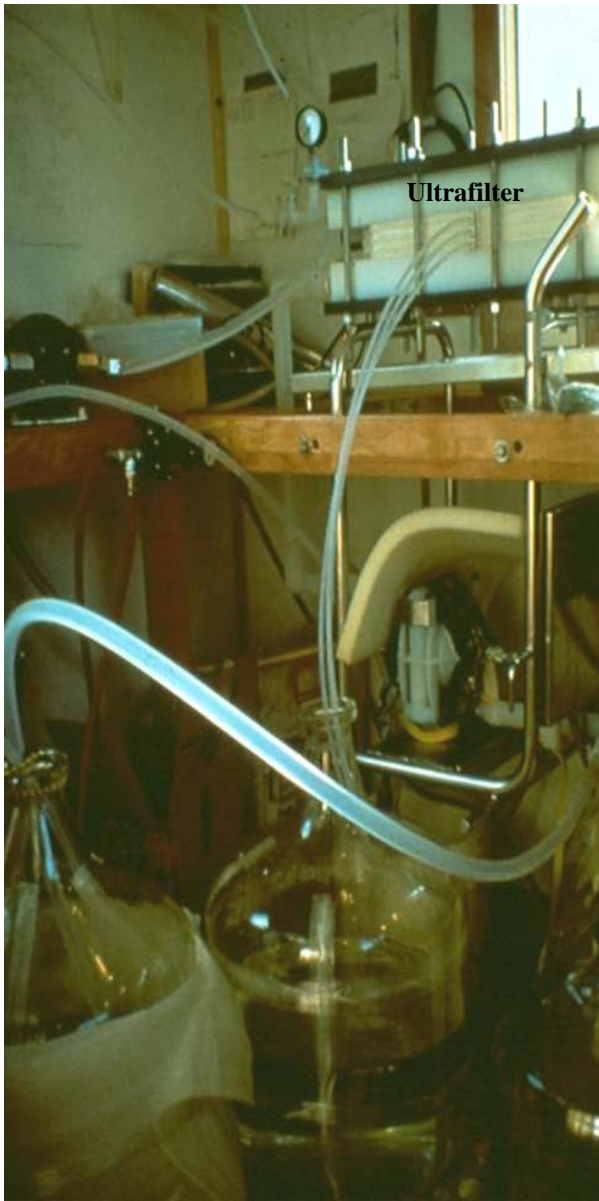


Figure 8 Tangential-flow ultrafilter used to concentrate suspended colloids onboard the RV *Acadiana*



Figure 9 Placing an ultrafilter plate inside the Teflon bag containing retentate water for removal of colloids that adhered to the ultrafilter membrane

4.2.2. Small-Volume Sampling of Water and Suspended Sediment

Small-volume (5 to 100 Liters of water), depth-integrated samples were collected from the bow of the R/V *Acadiana* at equally spaced intervals across the river. The sampling assembly is shown in Figure 10. The sampling bottle was positioned between the current meter and the sounding weight. The sampling bottle contained a collapsed Teflon bag that filled from an isokinetic Teflon nozzle; this nozzle is designed to admit water and suspended sediment in proportion to the velocity at which they are moving in the water current during lowering and raising of the sampling assembly. Depth-integrated samples from each sampling location were composited in the churn splitters as shown in Figure 11. The insides of the stainless-steel churn splitters were coated with Teflon, which minimized metal contamination and adherence of suspended sediments. Whole-water sub-samples

were taken from these churn splitters for various analyses, and a sub-sample was filtered on a previously weighed filter for gravimetric determination of suspended-sediment concentration.

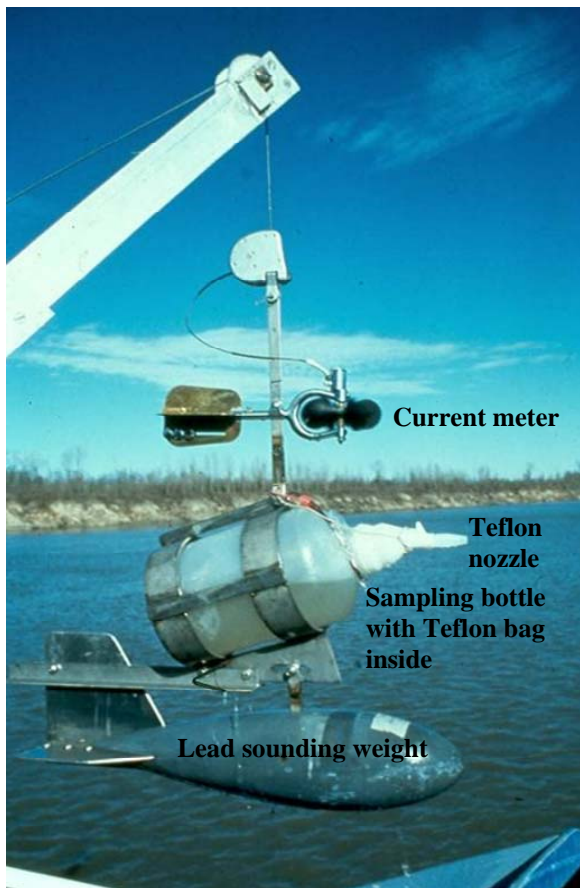


Figure 10 Sampling assembly used to obtain depth-integrated samples from the Mississippi River

4.2.3. Bed-Sediment Sampling

Bed-sediment samples were obtained in transects across the navigation pools of the Upper Mississippi River. A photograph of the clamshell sampler is shown in Figure 12. Also shown is the plastic gravity-core sampler. The upper 10 centimeters of bed sediment were collected by these grab samplers; the shallow depth of the navigation pools necessitated these samples being collected from a small boat.

4.3. Sampling Dissolved Organic Matter (DOM)

DOM is operationally differentiated from sediment NOM and colloidal NOM by the type of particulate-separation procedure used. These procedures may

include gravitation settling, centrifugation, filtration, ultrafiltration, and/or dialysis. They may be carried out during field sampling or in the laboratory after sampling. A combination of particulate-separation procedures in the field and laboratory is frequently used, depending on the research objectives.



Figure 11 Sub-sampling depth-integrated water and sediment samples from the Mississippi River with a churn splitter

A logical and practical particle-size cutoff by filtration is at 1 μm , which is the upper particle-size limit for colloids. Thus the filtrate will include both colloidal NOM and DOM; colloidal NOM can later be separated from DOM in the laboratory by dialysis [18]. Glass-fiber depth filters are preferred over membrane filters, which have problems with fouling, DOM adsorption, and/or contamination by leaching of organic wetting agents. Balston glass-cartridge depth filters with a 30 μm prefilter cartridge followed by a 1 μm cartridge have been used extensively for DOM sampling when recovery of sedimentary NOM is not

required [50]. This sampling and filtration apparatus has been packaged in a suitcase for field applications as shown in Figure 13.



Figure 12 Sampling bed sediment in a navigation pool in the Upper Mississippi River



Figure 13 Portable field-filtration assembly for sampling DOM



Figure 14 Polyethylene and glass carboys used as DOM sample containers

A Teflon bellows pump in the bottom of the suitcase is powered by a 12-volt direct current automobile battery; it pumps the water directly from the sampling site through the two glass-cartridge filters, with the filtrate being collected in a stainless-steel milk can. Teflon tubing with stainless-steel fittings is used throughout the field-filtration assembly of Figure 13. Peristaltic pumps and flexible plastic tubing were not used because of organic plasticizers that were released into water during sampling and filtration.

The use of stainless-steel milk cans for DOM samples was discontinued when a study of tannins in leaf leachates found problems with adsorption of these tannins on stainless steel during refrigerated storage of the samples [51]. The preferred containers for DOM samples are 20 L rectangular polyethylene carboys or glass carboys as shown in Figure 14.

Glass carboys have the advantage of being transparent, and they can be marked and calibrated to determine the volume of water. However, they are fragile and thus are not suitable for sample shipment. The rectangular polyethylene carboys are preferred because they can be closely packed for shipment on a pallet, they are durable during sample shipment, and they can readily be placed in ice coolers for refrigeration during shipment of the sample back to the laboratory. Leaching of plasticizers from ridged polyethylene containers has not been detected, and adsorption of polar DOM onto the polyethylene has not been a problem.

Measurements and observations of specific conductance, pH, color, odor, and turbidity should be made during sampling. A linear relationship exists between the specific conductance of water at pH values near neutrality and the salt content of water, as given by Equation 1 [52]:

$$\text{meq salt per Liter} = 12.5 \text{ SC} \quad (\text{Eq. 1})$$

where SC = specific conductance, mS/cm.

An estimate of the salt content of water is required for DOM separation procedures involving ion-exchange resins. Observations of color, both intensity and tint, are qualitative measurements that may relate to the concentration and nature of DOM. Observations of odor may relate to DOM source and nature, and the odor of hydrogen sulfide is an indication of anaerobic conditions. Lastly, turbidity is an estimate of suspended-sediment concentration, which is useful for the application of various sediment-separation methods.

5. NOM FRACTIONATION AND ISOLATION

The terms “fractionation” and “isolation” are often used interchangeably, but there are significant differences. Fractionation refers to chemical or physical processes that separate components of environmental samples into more homogeneous groupings based upon chemical or physical properties, e.g., acidity, anions, cations, polarity, molecular size. However, fractionation of NOM is usually accompanied by additional analytical procedures designed to isolate NOM from inorganic sample constituents and from reagents used in fractionation and isolation procedures. For example, hydrophilic anionic NOM constituents fractionated by anionic exchange resins must be further separated from inorganic anions such as sulfate to be “isolated” from the sample. Fractionation procedures are a part of isolation procedures, but isolation procedures extend beyond fractionation procedures, so “fractionation” is placed before “isolation” in descriptive terminology. Isolated NOM products are often solid or liquid mixtures and the isolation procedure can sometimes be designed to convert liquids, such as volatile fatty acids, to solids, such as sodium salts of fatty acids.

Various approaches to the isolation and fractionation of NOM have been developed and their relative advantages and disadvantages have been reviewed [53-55]. In sections 5.1 and 5.2, the efforts of U.S. Geological Survey (USGS) and other scientists to improve these procedures are described. Thematic in the development of these approaches has been the need to improve NOM recoveries and obtain more chemically meaningful subsets of NOM that are relatively free of mineral salts and other non-NOM organic components.

5.1. DOM Fractionation and Isolation from Water

Early approaches to fractionation of organic solutes in water and soil extracts frequently used ion-exchange celluloses and Sephadex gels to fractionate on the basis of apparent molecular size [56] and on acid, base, and neutral properties. An early fractionation scheme by Sirokina et al [57] used a sequence of diethylaminoethyl cellulose, carboxymethyl cellulose, and Sephadex to fractionate acidic DOM into high molar mass fulvic acid, humic acid, and polyphenol fractions, and into low molar mass carboxylic acid fractions. Basic DOM was fractionated into protein and amino acid fractions. Lastly, neutral DOM was fractionated into a polysaccharide and free-reducing sugar fraction. While gel-type adsorbents were

excellent in producing discrete fractions of differing NOM composition, they suffered from poor flow and capacity characteristics. Use of macroporous-resin adsorbents to concentrate and fractionate DOM became popular because they were developed with good flow and high-capacity characteristics.

The development of systematic NOM fractionation and isolation approaches for water using macroporous-resin adsorbents began with the hierarchical classification of organic solutes in water [58] and its accompanying analytical scheme called dissolved organic carbon fractionation analysis. This section will detail the developments and modifications of NOM fractionation approaches first in water, and then later its coupling to NOM fractionation and isolation in sediments and soils.

In the early 1970s, the state of organic-solute characterization in water is described in the report by Christman and Hrutford [59], who stated that the development of organic water-quality standards has “occurred on a piece-meal basis in response to current crises.” Analytical methods for these water-quality standards were limited in the following ways:

- 1) They were not capable of separating or recovering all organic solutes. They applied only to specific classes; many organic solutes were therefore not measured.
- 2) A materials balance based on organic carbon was seldom used. This means that the relationship between specific compounds and compound classes to total organic-solute concentrations was unknown.
- 3) Characteristics such as color, taste and odor, and oils and grease were nonspecific.
- 4) Most analytical schemes were based on methodology that incorporates liquid-liquid extraction or carbon adsorption to extract and concentrate organic solutes prior to analysis.

5.1.1. DOC Fractionation

DOC fractionation analysis was developed to provide the basis for comprehensive analyses of NOM in water. The original DOC fractionation analysis (Figure 15) separated DOC in a filtered water sample based upon its polarity (hydrophobic vs hydrophilic), and its acid, base, and neutral properties based upon adsorption chromatography. Macroporous-resin adsorbents were selected because of their high capacity, fast adsorption and desorption kinetics, physical stability, and high flow rates relative to small particle size and gel adsorbents. The polarity

fractionation for which the XAD resins were developed is described by Simpson [60]. Most DOM molecules are both amphiphilic and amphoteric; therefore, the DOC fractionation is operationally defined based upon its column-capacity factor (k') in which the predominant polarity property determines whether the molecule is classified as hydrophobic or hydrophilic. The use of pH adjustment for selective adsorption and desorption of hydrophobic acids and bases by XAD resins was previously reported by Burnham et al [61] and Junk et al [62].

These researchers used various organic solvents to desorb hydrophobic neutrals from the XAD resins. XAD-8 resin (a methacrylic-ester resin) was used as the adsorbent for DOC in water based upon the finding that aquatic fulvic acid could be quantitatively desorbed from this resin with dilute sodium hydroxide, whereas irreversible adsorption of fulvic acid on the styrene-divinyl-benzene resin adsorbents (XAD-2 and XAD-4) was observed [58]. Fractionation of hydrophilic acids, bases, and neutrals by ion-exchange resins was based upon the work of Rieman and Walton [63].

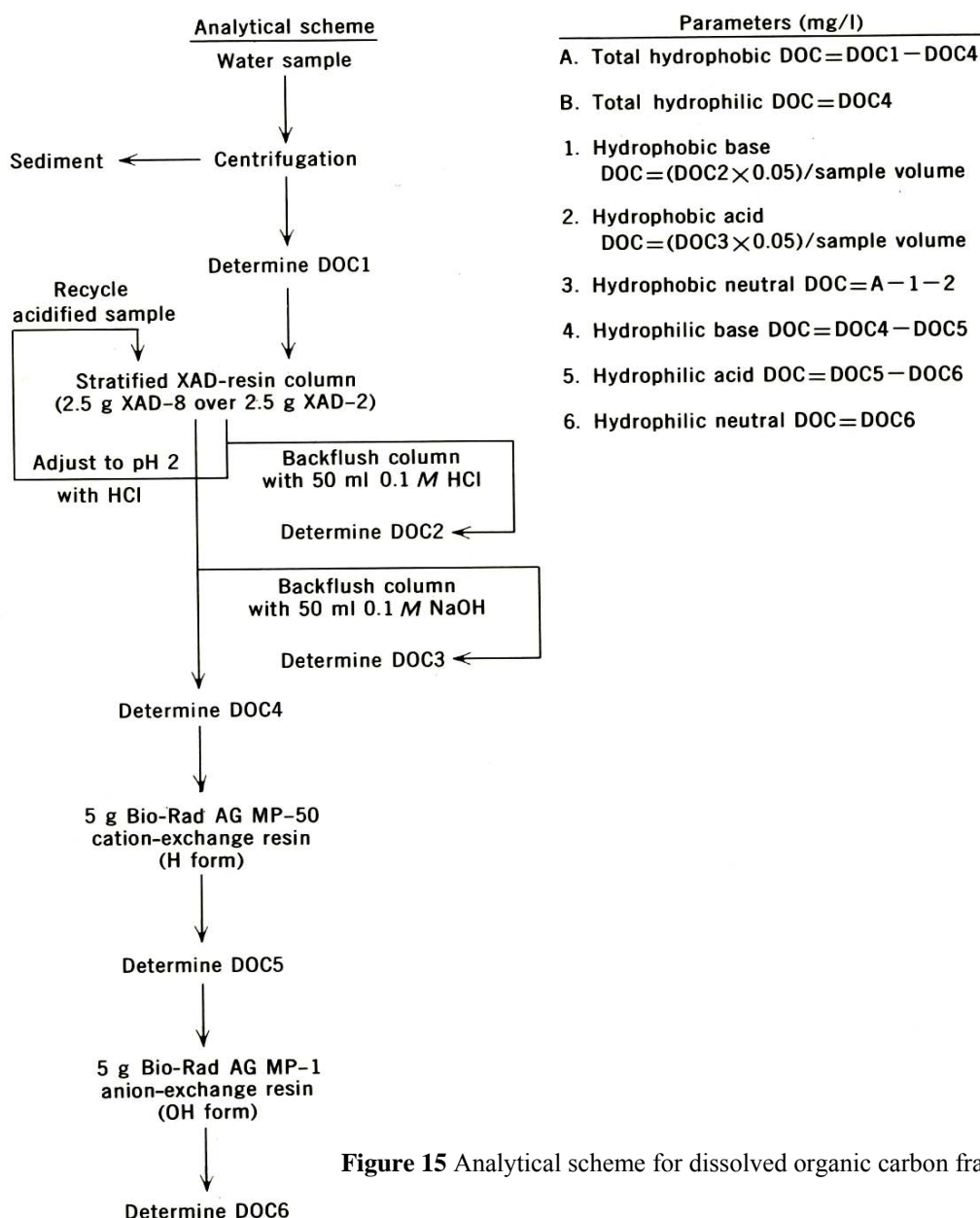


Figure 15 Analytical scheme for dissolved organic carbon fractionation [58]

After the development of DOC fractionation analysis, Thurman et al [64] determined that the logarithm of the column-capacity factor (k') of hydrophobic organic solutes on XAD-8 resin was inversely correlated with the logarithm of the aqueous molar solubility. Aiken et al [65] compared XAD-1, XAD-2, XAD-4, XAD-7, and XAD-8 resins for the concentration of fulvic acids from aqueous solution, and found that the methacrylic-ester resins (XAD-7 and XAD-8) had the best combination of properties for fulvic acid concentration. Aquatic humic substances, both humic and fulvic acid, were both concentrated and isolated from water with the following approach [66]:

- 1) adsorption on XAD-8 resin at pH 2,
- 2) desorption from the resin with 0.1 M sodium hydroxide,
- 3) removal of the sodium hydroxide by a hydrogen-form ion-exchange resin,
- 4) precipitation of humic acid at pH 1, and
- 5) removal of water by lyophilization.

DOC fractionation was achieved as a standard analytical method by Leenheer and Huffman [15] in which the limits of DOC concentration, sample volume, salt content, and analytical precision were defined.

5.1.2. DOM Fractionation of Fresh Water

The extension of the analytical DOC fractionation (in which DOC is measured as aqueous concentrations) to a preparative DOM fractionation (in which DOM fractions are isolated from water, weighed, and analyzed) was explored for the hydrophobic fractions in the original report [58], but the isolated fractions had ash contents ranging from 15 to 97% because of inadequate column-rinse and fraction-cleanup procedures. The first comprehensive approaches to various preparative DOM fractionation procedures were published by Leenheer [67], and the primary approach is shown in Figure 16. The major difference between the DOM fractionation scheme of Figure 16 and the DOC fractionation scheme of Figure 15 was the use of the weak-base anion-exchange resin Duolite A-7 for desorption of the hydrophilic acid fraction. Duolite A-7 has a phenol-formaldehyde matrix that becomes negatively charged at high pH, facilitating desorption of hydrophilic acid anions. An organic carbon recovery of 81% was obtained for a river-water sample. However, the isolated fractions still had significant salt contents, and eluents such as aqueous

ammonia and methanol were not satisfactory because their reactions with DOM.

The DOM fractionation procedure was scaled up to 10 L bed-volume columns and placed in a mobile field laboratory (Figure 17) to process large volumes of water on site [50]. The capacity of the column-adsorption system was monitored with a conductivity meter, where a rise in conductivity signaled that the ion-exchange columns were at capacity. The columns could be regenerated in the field to process multiple batches of water. Sodium-hydroxide solutions were substituted for aqueous ammonia to avoid undesirable DOM reactions with ammonia, and the MSC-1H resin was substituted for the Bio-Rad AG-MP-50 resin used previously owing to its similar properties and lower costs. Both the hydrophobic acid and hydrophilic acid fractions were concentrated simultaneously on the Duolite A-7 resin. The combined acid-fraction eluent from the Duolite A-7 resin was passed through an XAD-8 column in the laboratory to separate hydrophobic acids from hydrophilic acids. Improvements were also made in fraction-desalting procedures, such as using volatile trifluoroacetic acid in column rinses to remove salts from hydrophobic fractions, removal of chloride from the hydrophilic acid fraction with a silver-saturated cation-exchange resin, and removal of sulfate by crystallization of sodium sulfate decahydrate at low temperature in an ethanol-water mixture. However, borate, nitrate, phosphate, silica, and small amounts of sulfate still were undesirable inorganic constituents that remained in the hydrophilic acid fraction. Multigram quantities of DOM fractions were isolated from large-volume samples (300 L to 1340 L) in a number of surface- and ground water samples [50].

Another approach for desalting hydrophilic-DOM fractions was developed based upon zeotropic distillation. Zeotropic distillation is the separation of two miscible solvents that do not form azeotropes by distillation. Water can be distilled from higher-boiling-point organic solvents of DOM samples, in which inorganic salts precipitate as water is removed. The zeotropic-distillation procedure was originally developed using *N,N*-dimethylformamide to desalt hydrophilic NOM from saline waters in Big Soda Lake, Nevada [68]; however, *N,N*-dimethylformamide was difficult to evaporate in a vacuum-rotary evaporator because of its high boiling point, and it also partially hydrolyzed to dimethylamine and formic acid in the procedure. Acetic acid was found to be a better solvent for the zeotropic-distillation procedure as it is available in high purity, is a good solvent for DOM, and cannot form hydrolysis products [69].

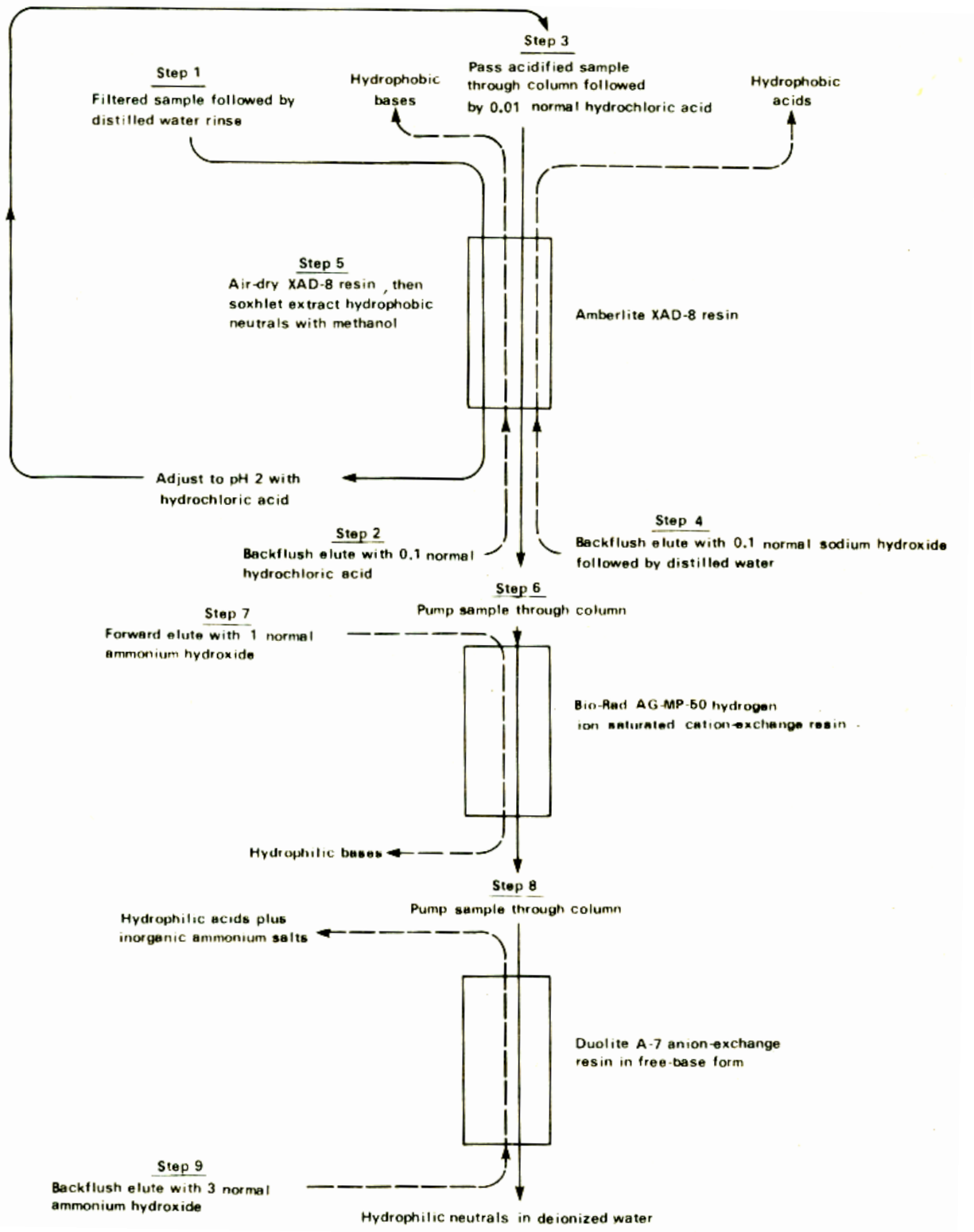


Figure 16 Analytical scheme for dissolved organic matter fractionation [67]

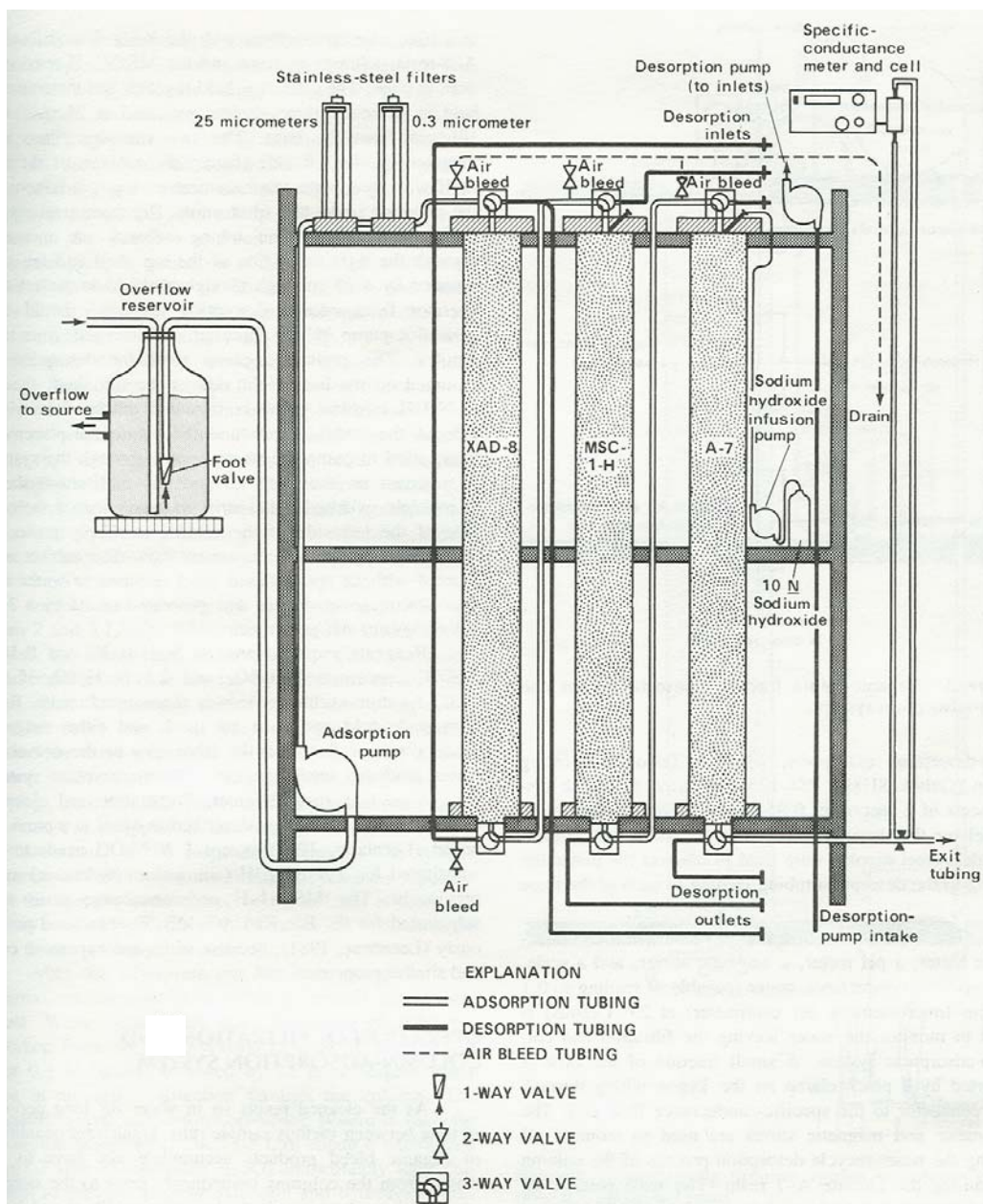


Figure 17 Large-volume DOM fractionation assembly [50]

The zeotropic-distillation procedure works well to remove sodium and potassium chlorides and sulfates that constitute the bulk of inorganic salts in natural waters, but weak inorganic acids (boric, silicic, and phosphoric acid), nitrates, and hydrated calcium and magnesium ions were not removed. Therefore, boric acid was removed from hydrophilic DOM by evaporation with methanol as volatile trimethyl borate; silicic acid was removed as silica gel which formed by

drying and re-dissolving the hydrophilic DOM concentrate; sulfate was removed by precipitation as barium sulfate at pH 1; and phosphate was removed by precipitation as magnesium ammonium phosphate [69]. At this point in the development of the comprehensive DOM fractionation procedure, there were no satisfactory methods to remove nitrate from the hydrophilic acid fraction.

The hydrophilic DOM fraction can be partially recovered and desalted from water by adsorption and desorption from XAD-4 resin after prior removal of the hydrophobic fractions with XAD-8 resin [16]. This DOM fraction recovered from XAD-4 resin has been called the hydrophilic, transphilic, or amphiphilic fraction, depending on the procedure and researcher. An attempt was also made to increase the percentage of the operationally defined hydrophobic DOM fraction on XAD-8 resin by lowering the column-capacity factor (k') from 10 to 1, but only 6% of the hydrophilic DOM was shifted into the hydrophobic DOM fraction for samples from the Mississippi River [69]. Another finding of the Mississippi River study was that a mixture of 75% acetonitrile/25% water is a very efficient eluent of the hydrophobic fractions from XAD-8 resin. Acetonitrile is a better eluent than the methanol used to elute the hydrophobic-neutral fraction in previous studies, as methanol transesterifies esters and slowly methylates carboxylic acid groups in DOM. Acetonitrile is also easily removed by vacuum-rotary evaporation and leaves no residues or reaction products in DOM isolates.

Tangential-flow ultrafiltration was developed as a method to concentrate and isolate colloidal DOM from the Mississippi River [70], and the apparatus is shown in Figures 8 and 9. As most of NOM colloids are submicron particles that pass through filters, it is operationally defined as DOM. A major portion of these DOM colloids have hydrophilic-neutral properties, and an attempt was made to develop a column to concentrate and isolate hydrophilic-neutral components that elute at the end of the DOM fractionation procedure. As borate forms complexes with cis-diol groups in carbohydrates and ortho-phenols, a borate-saturated anion-exchange resin will concentrate certain carbohydrates and phenols.

A borate-saturated anion-exchange resin (Bio-Rad AG-MP-1) column was added after the Duolite A-7 resin column of Figure 17 and was tested on a low DOC ground water, a high DOC landfill leachate, and a tertiary sewage effluent [71]. Hydrophilic DOM was eluted from the borate column with 20% acetic acid, and the concentrate was evaporated. Borate and silica were also eluted, and borate was removed by methanol evaporation, while silica was removed as silica gel. A portion of the hydrophilic DOM was recovered, but hydrophilic colloids were mostly lost or irreversibly adsorbed in this four-column DOM fractionation system.

Two case studies with the goal of maximum DOC recovery and fractionation were conducted on water samples from the Suwannee River, Georgia, and the

South Platte River near Denver, Colorado [72]. Additional procedural modifications tested to better recover DOM were:

- 1) use of vacuum-rotary evaporation prior to DOM adsorption on XAD-8 and XAD-4 resins to decrease the column-capacity factors from $k'=100$ to $k'=5$;
- 2) derivatization (methylation and acetylation) of hydrophilic DOM followed by adsorption on XAD-8 and XAD-4 resins; and
- 3) adsorption of hydrophilic DOM on alumina followed by elution with 0.1 M NaOH.

Despite these modifications to optimize DOM recovery, about 20% of the DOC in the Suwannee River and 36% of the DOC in the South Platte River was not recovered. This study [72] also assessed DOM preconcentration by reverse osmosis and ultrafiltration combined with resin-adsorption and metal-oxide (alumina, iron oxide, and magnesium oxide) adsorbents on various waters. Quantitative DOM recoveries with desalting of isolate fractions were not obtained with any combination of methods, and it was concluded that most DOM losses occurred with the hydrophilic organic-colloid fraction.

Another method was devised to recover the hydrophilic organic-colloid fraction [18,73]. This comprehensive isolation approach combined reverse osmosis (RO) concentration (for large samples), rotary-vacuum evaporation of the sample to a salt slurry, transfer of the salt slurry to dialysis bags, and dialysis to separate colloidal NOM from inorganic salts and low molar mass DOM before resin adsorbents were used. For membrane dialysis, Spectra/Por regenerated cellulose membranes of 2000 and 3500 Dalton cutoffs were tested on salt-saturated concentrates. Osmotic pressure caused the 2000 Dalton membrane to burst; therefore, the 3500 Dalton dialysis membrane was chosen for the colloid-size cutoff. Membrane dialysis is a three-step procedure whereby:

- 1) salts and low molecular-weight DOM are removed by dialysis against deionized water;
- 2) precipitated silica gel is removed by dialysis against 0.2 M hydrofluoric acid; and
- 3) the hexafluorosilicic acid reaction product and unreacted hydrofluoric acid are removed by dialysis against deionized water.

Application of this colloid-isolation procedure coupled with the DOC fractionation procedure [50]

gave DOC recoveries of 77% for a tertiary sewage-treated wastewater with a sodium-softening step, and 97% recovery when the sodium-softening step was omitted [73].

The preparative DOM fractionation procedure for fresh-water samples that gave the greatest DOC recoveries is presented in Figure 18. This procedure was designed to assess total organic matter mobilized during stormflows in the Santa Ana River in southern California [74,75]. Therefore, very heavy suspended-sediment loads had to be accommodated and separated by a combination of gravitational settling, centrifugation, and filtration.

The hydrophobic-neutral fraction was isolated before the sample was evaporated because the limited solubility of this fraction caused it to precipitate as a film on the flask during rotary evaporation, and this film was not readily transferred into the dialysis bag. There were negligible losses of the colloid fraction on the XAD-8 resin column at the ambient pH values of the water sample during adsorption of the hydrophobic-neutral fraction.

After adsorption of the hydrophobic-neutral fraction, the sample was acidified to pH 4 with HCl to convert carbonate and bicarbonate salts to chloride salts with removal of carbon dioxide during evaporation. Carbonate salts form a scale on the evaporation flask that is very difficult to transfer into the dialysis bags. The pH will decrease to pH 1 as the sample is concentrated during evaporation, but the sulfate/bisulfate equilibrium will buffer the pH to prevent further decreases in pH for samples that contain sulfate. It is important that the vacuum is sufficient to maintain the boiling point of the sample between 25° to 30° C to minimize hydrolysis of acid-labile functional groups in DOM under these acidic conditions.

The salt slurry is transferred from the rotovap flask into the dialysis bags with the aid of a funnel, a Teflon film scraper, a nylon bristle brush, and a squirt bottle containing deionized water. The initial dialysis step to remove inorganic salts is carried out in a 1 L graduate cylinder, and the dialysis steps with hydrofluoric acid to remove silica and with water to remove HF and its reaction products are carried out in a 4 L polyethylene beaker. The combined-permeate sample is pumped through the MSC-1H column, the XAD-8 column, and the XAD-4 column in series. The MSC-1H column was placed before the XAD columns (as opposed to after the XAD columns, as in Figure 17) for two reasons:

- 1) Ion exchange of sample cations with hydrogen ions will depress the pH to 2 or less, which is necessary for adsorption of hydrophobic acids on XAD-8 resin and amphiphilic acids on XAD-4 resin.
- 2) Neutralization of the column effluent with NaOH to pH 4 will convert inorganic acids to sodium salts that are most efficiently removed by the zeotropic-distillation procedure.

The hydrophobic-neutral, hydrophobic acid, and amphiphilic-acid-plus-neutral fractions will initially freeze-dry as sticky isolates that are difficult to weigh and transfer. These isolates are sticky because the small amount of HCl in the column rinse forms a negative azeotrope with water that is not completely removed by freeze-drying, and it causes the sample to retain some water. To remove this HCl and water to obtain powder isolates, the isolates were redissolved in a minimum volume (about 1 mL) of 25% acetonitrile/25% water and diluted with 50 mL of deionized water; this mixture was then freeze-dried a second time. A glass Erlenmeyer vacuum-filtration flask with a 47 mm, 1µm-porosity glass-fiber filter was used to filter the sodium salts from the sample during the zeotropic-distillation procedure. Water was evaporated in a small vacuum-rotary evaporator until salts began to form, and then the sample was diluted with an equal volume of glacial acetic acid and evaporated until the salt slurry was about 80% salt by volume. The salt was removed by filtration and the salts were rinsed with about an equal volume of glacial acetic acid passed through the salt cake on the filter. A second cycle of this procedure is necessary to remove additional salt, but the procedure should not be repeated to the point where the salt becomes colored, which indicates loss of hydrophilic-acid-plus-neutral constituents. The filtrate was diluted with an equal volume of deionized water to convert neutral ion-pairs to anions and cations, which were required for the selective precipitation and ion-exchange procedures used in the final step in Figure 18.

Barium formate is used to precipitate barium sulfate, as volatile formic acid is readily removed later by evaporation after ion-exchange conversion to an acid. Formic acid is an antioxidant that prevents oxidation by nitric acid of the hydrophilic acids plus neutrals. Coprecipitation of hydrophilic acids with barium sulfate is minimized by the acetic acid in the sample, and constituents such as oxalic acid that do co-precipitate are recovered by the 1.0 M HCl rinse [73].

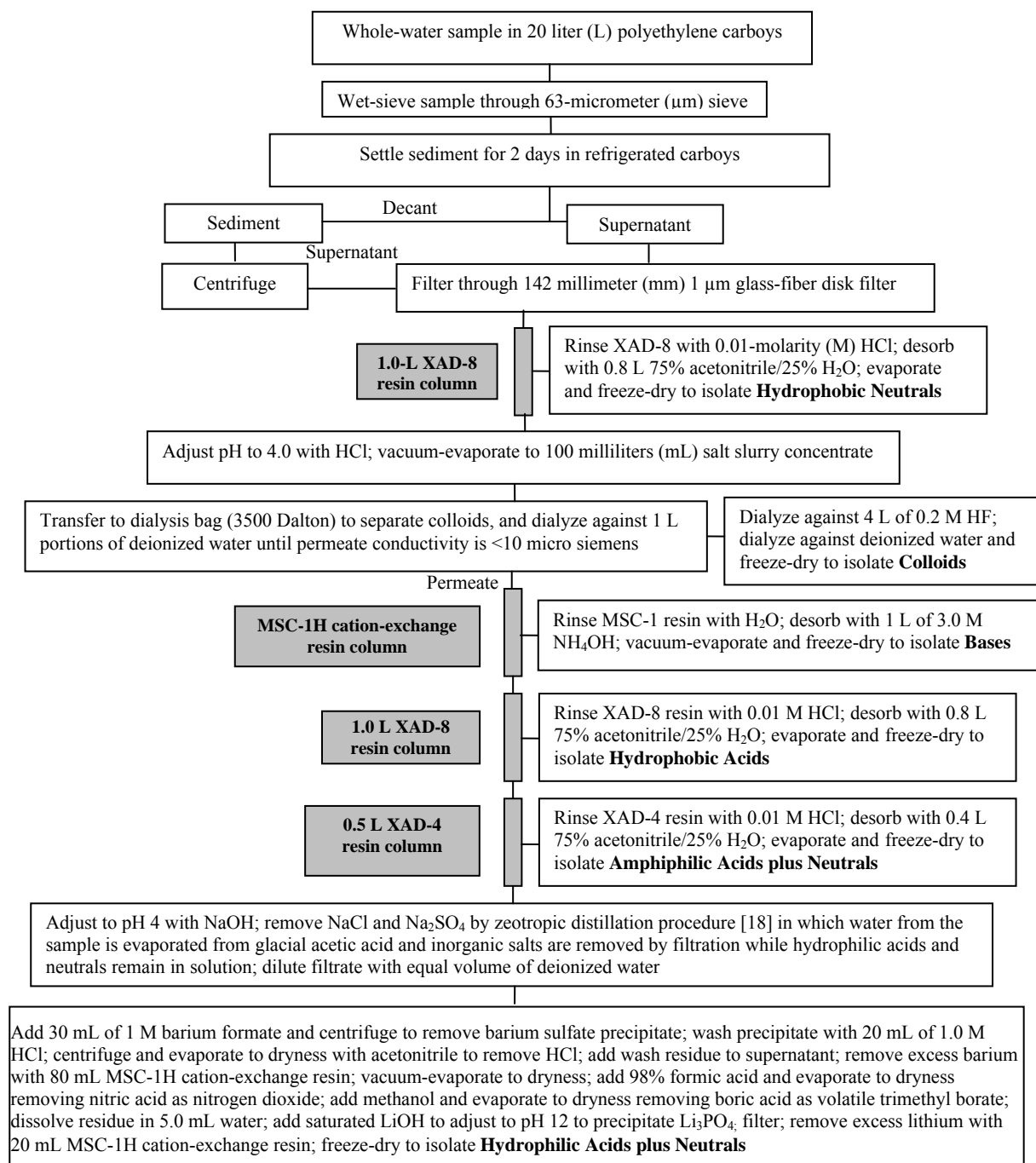


Figure 18 Flow-chart of final dissolved organic matter fractionation for fresh-water samples

The removal of nitric acid by its reduction to nitrogen dioxide should not be attempted with large amounts of nitric acid in the rotovap flask, as an explosion will occur in the flask [18]. If the previous zeotropic-distillation procedure and drying procedure

with repeated additions of acetonitrile are performed, only small amounts of nitric acid will remain in the sample. Most of the nitrate has been removed previously as sodium nitrate, and volatile nitric acid has been removed with acetonitrile.

Most natural water samples do not contain enough phosphate to merit its removal by precipitation as Li_3PO_4 , and this final precipitation can be omitted from the procedure. The hydrophilic-acid-plus-neutral fraction frequently freeze-dries as a sticky hygroscopic solid in the hydrogen form. To accurately weigh this fraction, freeze-drying should be performed in a previously tared test tube and the weight determined by difference. If a dry powder is required for spectral measurements such as NMR, the hydrophilic-acid-plus-neutral fraction can be dissolved in water, titrated to pH 8 with NaOH, and freeze-dried as the sodium salts.

5.1.3. DOM Fractionation of Salt Water

Comprehensive isolation and fractionation of DOM from salt-water samples present special problems for the removal of salt from the hydrophilic fractions. The high ratio of salt to DOM results in hydrophilic-DOM losses during removal of salt in the zeotropic-distillation step, and there is a greater percentage of calcium and magnesium chlorides (difficult to remove by zeotropic distillation) in salt-water samples than in fresh-water samples. The large amount of salt also is difficult to manage for the isolation of colloids by dialysis.

Comprehensive DOM fractionation of salt water was first attempted on a sample from the Great Salt Lake [76]. The Great Salt Lake was selected because its surface DOC concentration is about 60 times greater than DOC in seawater, which reduced the required sample volume accordingly. The DOM fractionation procedure of Figure 18 was used on a 38 L sample with the following modifications:

- 1) The dialysis permeate was acidified with HCl to pH 2 and passed through the XAD-8 and XAD-4 columns to isolate the hydrophobic acid and amphiphilic DOM fractions before isolation of the hydrophilic base fraction on the MSC-1H column.
- 2) The sample effluent from the XAD-4 column was vacuum-evaporated with acetic acid to remove salts readily removed by zeotropic distillation (NaCl , KCl , Na_2SO_4 , CaSO_4). The sample was evaporated to remove acetic acid, redissolved in water, and passed through a sodium-form MSC-1 resin to replace calcium and magnesium cations with sodium. Then the zeotropic-distillation step was repeated to remove the sodium salts. Two cycles of the sodium-softening steps and zeotropic-distillation

step sufficed to remove most of the salt.

- 3) The hydrophilic base fraction was next isolated on the MSC-1H resin and the hydrophilic-acid-plus-neutral fraction was isolated as presented in Figure 18. DOC recoveries from the Great Salt Lake ranged from 44 to 62%.

The second attempt to comprehensively isolate and fractionate DOM from salt water was performed on a sample from the deep South Atlantic Ocean [77]. Because of the low DOC concentration (0.55 mg/L), a large sample was required to isolate sufficient DOM in each fraction for analyses. The large mass of salt in a large sample rendered dialysis impractical for separation of colloids as had been performed in the Great Salt Lake sample, so the colloids were removed by ultrafiltration on board ship during sampling. Organic colloids were directly isolated by dialysis on a separate 33 L sample of unfiltered seawater. The ultrafilter permeate was acidified to pH 1 on board ship for preservation, and 700 L of the acidified permeate was sent airfreight to the U.S. Geological Survey laboratory in Denver, Colorado, for development of the comprehensive DOM fractionation method in sea-water samples.

The 700 L sample was split into 100 L portions for development and optimization of the method. The DOM fractionation procedure used for the Great Salt Lake sample (without the colloid-isolation step) was used on the first portion. This procedure was not successful for isolating the hydrophilic-acid-plus-neutral fraction because the large amounts of calcium and magnesium chloride relative to hydrophilic DOM resulted in the buildup of unacceptable levels of resin bleed from the large MSC-1 columns during ion-exchange of calcium and magnesium with sodium. Another problem was that calcium and magnesium chlorides formed neutral ion-pairs that were not efficiently converted to sodium salts by ion exchange.

The focus of method development shifted to direct removal of calcium and magnesium chlorides by zeotropic distillation of water from acetic acid. This procedure was ultimately successful after its optimization during processing of 100 L permeate portions 2-7 (Figure 19). Calcium and magnesium chlorides are more soluble in acetic acid than are sodium and potassium chlorides and sulfates. They also form fine crystal needles that are difficult to filter and rinse. A large Buchner funnel with a fritted-glass filter was used to filter and rinse the calcium and magnesium chloride crystals that formed after slow room-temperature overnight cooling to facilitate the growth of large crystals. Six cycles of the zeotropic-

distillation procedure were required for sufficient removal of the calcium and magnesium chlorides. The seventh portion was spiked with 1,2-trans-cyclohexane dicarboxylic acid (a hydrophobic acid), tartaric acid (a hydrophilic acid), and arginine hydrochloride to evaluate fraction recoveries. Recovery of the surrogate standards added to

permeate portion 7 ranged from 94% for 1,2-trans-cyclohexane dicarboxylic acid to 21.5% for tartaric acid; arginine hydrochloride was not recovered. A total of 52.5% of the DOC was directly recovered, but after adjustment for internal-standard recovery, 67.4% of the DOC was accounted for.

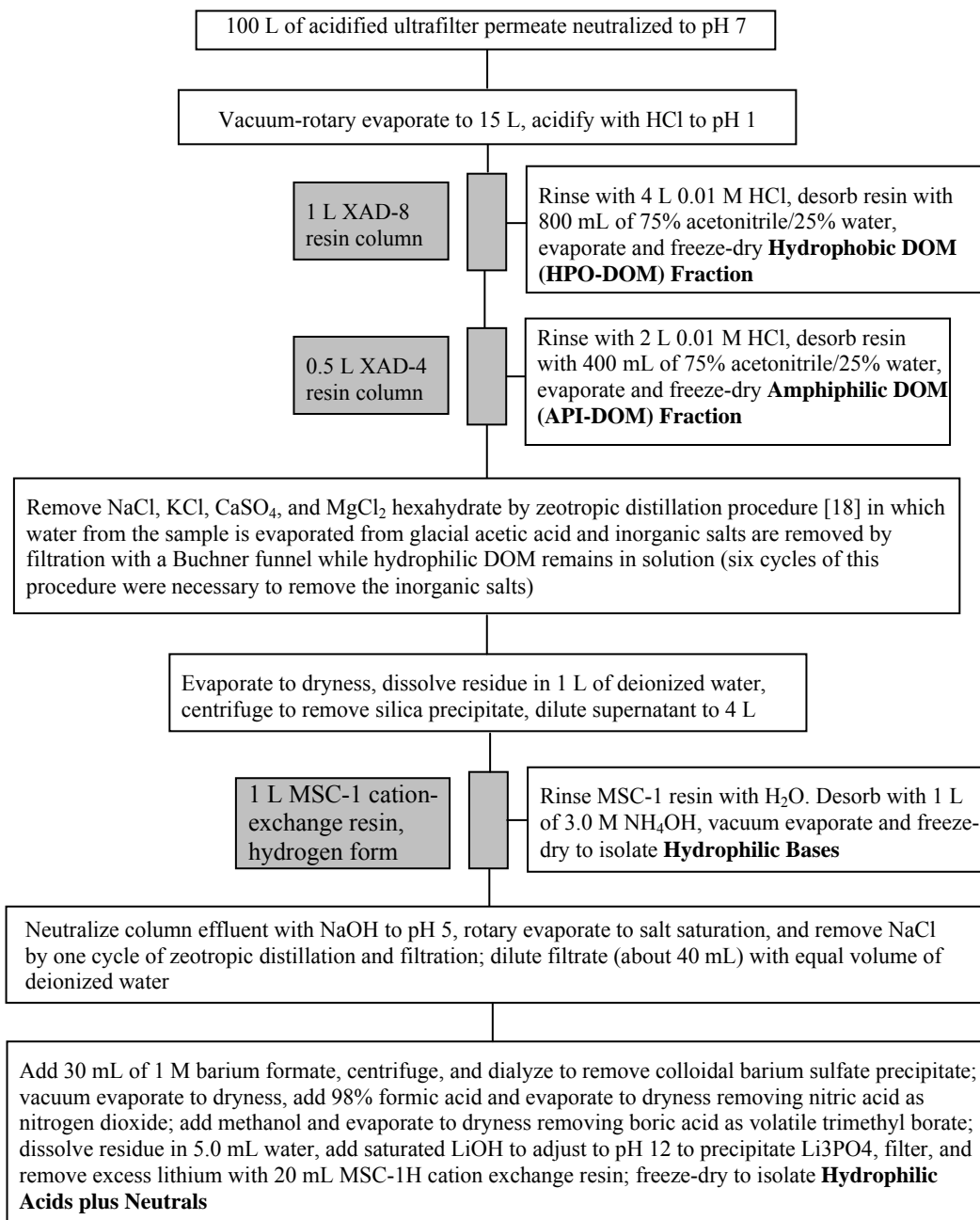


Figure 19 Flow-chart of DOM fractionation and isolation procedure for seawater

5.1.4. Dissolved Organic Nitrogen (DON) Fractionation

A preparative dissolved organic fractionation method was developed to enrich isolated fractions in organic nitrogen for nitrogenous disinfection by-product research [78]. A flow-chart of the method is presented in Figure 20. The method was developed and tested on DOM derived from an algal culture, a bacterial culture, a mesotrophic lake during the beginning of an algal bloom, and an effluent from a sewage-treatment plant. The method was based on the assumption that most organic nitrogen in natural organic matter is contained in proteins and aminoacids, as shown by ¹⁵N-nuclear-magnetic-resonance data [79]. Proteins, peptides, and certain aminoacids are retained on the macroporous styrene/divinylbenzene resins (XAD-2 and 4) at pH values greater than 10, whereas the macroporous methylmethacrylate resin XAD-7 did not adsorb these compounds at pH>10 [80].

The DON fractionation method originally used the macroporous styrene/divinylbenzene resin XAD-1 in place of the XAD-8 column in Figure 20, but problems with irreversible adsorption of the blue dye Erioglaurine, found in the hydrophobic-neutral fraction in the effluent from a sewage-treatment plant, led to modification of the DON fractionation method presented in Figure 20. This improvement in the method was based upon the finding that strongly adsorbed hydrophobic-neutral compounds could be desorbed from the XAD-8 resin with 75% acetonitrile/25% water, and that proteins and peptides in the hydrophobic-base fraction desorbed at pH 13 with 0.1 M NaOH could be re-adsorbed at this pH on XAD-4 resin and separated from the hydrophobic acid fraction.

Membrane dialysis and the resin-adsorption sequences were performed at pH 1 to disrupt NOM/metal aggregates better than previous fractionations that were conducted at pH 2 or greater. The membrane-dialysis procedure was also placed before the resin-adsorption sequences for DON fractionation (Figure 20) rather than after the adsorption of the hydrophobic-neutral fraction (Figure 18) in DOM fractionation. This was done because disruption of NOM/metal aggregates was judged to be more important for a clean separation of organic-nitrogen fractions and removal of iron(III) and aluminum in DON fractionation than it was for recovery of the hydrophobic-neutral fraction in DOM fractionation.

DON fractionation, with its nine fractions, was found to be more complex and labor-intensive than DOM fractionation, with its six fractions. Application

of the preparative scheme in Figure 20 showed that organic nitrogen is concentrated in the aminoacid, amphiphilic-neutral-plus-base, colloid, hydrophilic base, and hydrophobic-base fractions; organic nitrogen is depleted in the amphiphilic acid, hydrophilic-acid-plus-neutral, hydrophobic acid, and hydrophobic-neutral fractions [78].

5.2. Total Organic Matter (TOM) Fractionation of Soil and Sediments Suspended in Water

A comprehensive fractionation method presented in the flow-chart of Figure 21 was developed for TOM contained in soil, sediment, and water [81]. This method fractionates TOM based upon apparent molecular size, TOM extractability in aqueous and non-aqueous solvents, TOM affinity for various resin adsorbents, and TOM acid/base/neutral characteristics. TOM fractions obtained are isolated from water, inorganic salts, and various inorganic minerals. These fractions are suitable for elemental, spectroscopic, and titrimetric characterizations.

The TOM fractionation method has been applied to soils [82], sediments suspended in water [74,83], and hog manure [84]. For waters with low suspended-sediment concentrations such as in the Neversink Reservoir study [83], the steps that separate sediment by sedimentation and centrifugation can be deleted, and sediment is separated from dissolved constituents by filtration. Separation of coarse-particulate organic matter by sieving and differential sedimentation in water does not cleanly separate this fraction from attached mineral matter; additional dispersion steps, such as ultrasonic cleaning, and chemical treatments with HF may be required if this fraction is to be purified of inorganic constituents.

Treatment of soils and sediments with 0.1 M HCl is performed to remove carbonates, oxy-hydroxide coatings, and exchangeable cations that bind NOM to soil and sediment surfaces [10]. After freeze-drying acid-treated soils and sediments, lipids can be extracted with 2:1 methylene chloride/methanol solution. This solution should be evaporated in a beaker or watch-glass in a hood, as evaporation in a vacuum-rotary evaporator may introduce silicone-grease contaminants extracted from the seals in the rotary evaporator.

Humic acid is extracted from soils and sediments with 0.1 M sodium hydroxide under a nitrogen atmosphere to minimize oxidation of phenols to quinones. The alkaline extract is transferred to a dialysis bag and dialyzed against 0.2 M HF to precipitate the humic acid and to convert extracted silica to fluorosilicic

acid, which is removed by dialysis. Iron(III) complexed with extracted humic acid is also removed as soluble iron(III) chloride by this procedure.

The insoluble humin fraction in soils and sediments is separated from the glass-fiber and silicate constituents that dissolve when treated with 0.2 M HF. Carrying out this dissolution procedure in dialysis bags retains organic colloidal humin constituents which may be lost if centrifugation is used to separate insoluble humin from the HF solution and its reaction products. Hydrofluoric acid reacts with aluminum constituents of clay minerals to form insoluble aluminum fluorides. It was found that dialysis of humin residues containing aluminum fluorides against 0.1 M sodium hydroxide removes the aluminum fluorides as determined by infrared-spectrometry assay. It is not known which soluble aluminum species form when aluminum fluoride is treated with sodium hydroxide, as insoluble cryolite is supposed to be the product of this reaction [19]. Perhaps there are soluble intermediate aluminum fluoride-hydroxide species formed before cryolite precipitates. It is important that aluminum fluorides be removed before humin is separated from other mineral constituents resistant to HF treatment by density separations, because humin is strongly attached to aluminum fluoride by electrostatic interactions. Quartz is the major mineral constituent that remains after HF and

sodium hydroxide treatments; it is readily separated from humin by centrifugation in sodium polytungstate solution of density 2.2.

5.3. NOM Sub-fractionations

NOM fractions obtained from the fractionation procedures presented in Figures 18-21 may be insufficiently homogeneous with regard to compound-class composition or some other property under investigation. Therefore, additional sub-fractionation procedures may be applied to better characterize NOM components.

5.3.1. Solvent Solubility Separations

Various organic solvents, aqueous solvents, and solvent combinations have been extensively investigated for extraction of humic substances from soil [55,85]. Weakly basic solvents that donate electrons (acetone, acetonitrile, dioxane, tetrahydrofuran, and tertiary amines) selectively extract carboxylic acid constituents from NOM fractions, and weakly acidic solvents that donate protons (alcohols, carboxylic acids, N,N-dimethylformamide, and water) selectively solubilize basic constituents from NOM fractions.

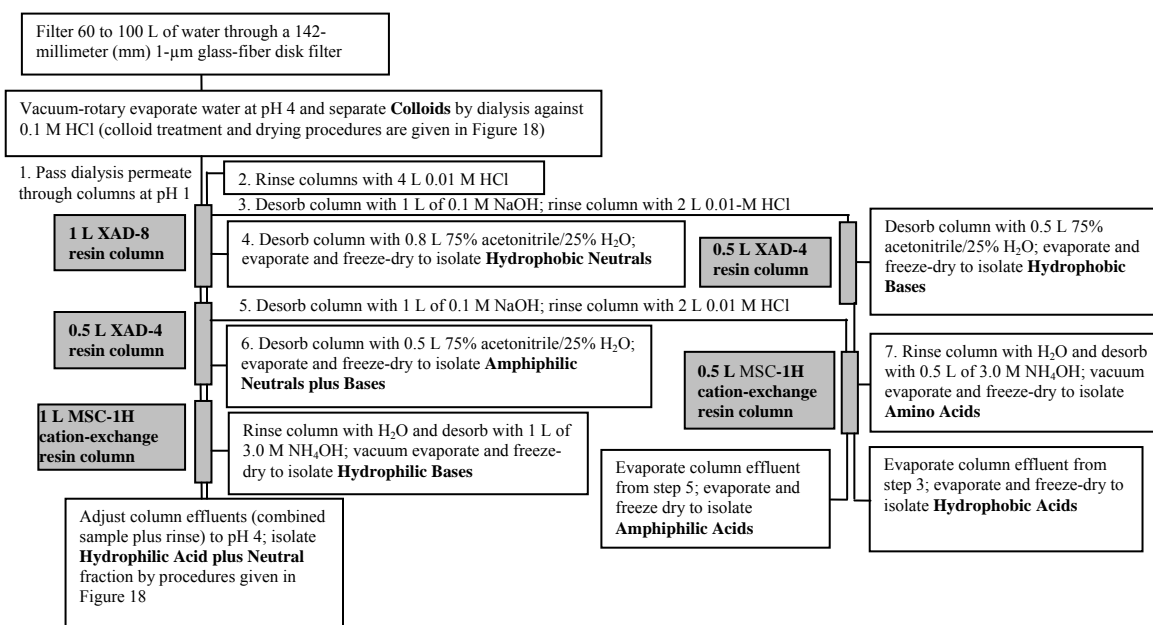


Figure 20 Flow-chart of dissolved organic nitrogen fractionation (numbered steps must be performed in sequence)

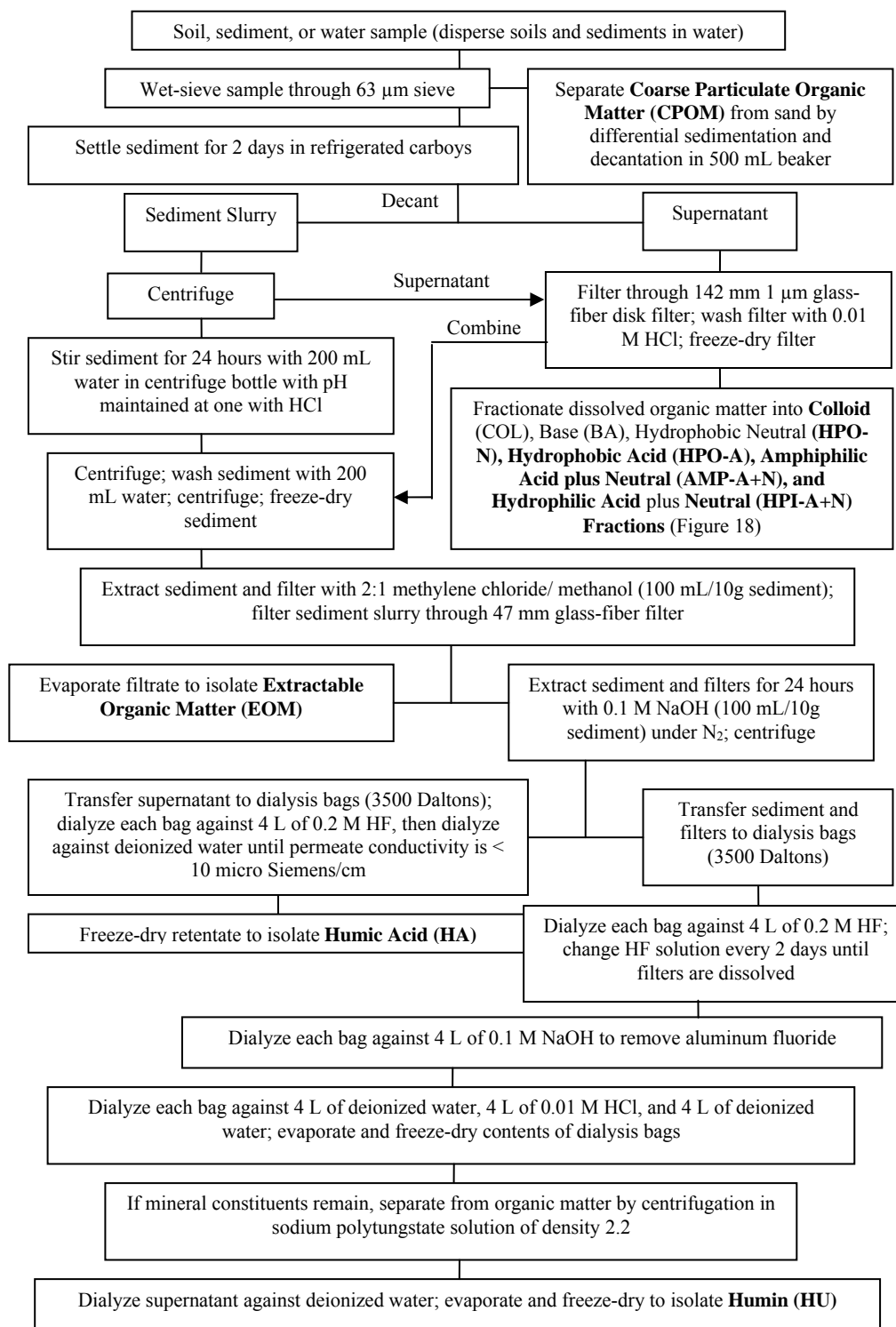


Figure 21 Flow-chart of total organic matter fractionation

Because much of NOM is both amphoteric and amphiphilic, the most effective solvent combinations are those that both donate electrons and protons to disrupt hydrogen-bonding aggregation interactions in NOM and also have hydrocarbon moieties that disrupt hydrophobic interactions. Such solvent combinations include acetonitrile/water, acetone/water, dimethylsulfoxide/water/HCl, and water/5 M urea (which has recently been found to solubilize much of the humin fraction in soil [85]).

A mixture of 2:1 methylene chloride/methanol, as was utilized in the TOM fractionation procedure of Figure 21, is an efficient extractant for lipids in soils and sediments. When alcohols are used as solvents, they should be immediately removed by evaporation to minimize esterification and transesterification reactions in NOM.

Sub-fractionation of the hydrophobic-base/neutral fraction from lake water isolated on XAD-1 resin in the initial DON fractionation procedure [78] by extraction with ethyl acetate was very effective in separating DOM derived from lipids (with a C:N ratio of 68.6) from DOM derived from protein and porphyrins (which have a C:N ratio of 9.4). The lipid-derived organic matter was extracted by slurring the hydrophobic-base/neutral fraction with 50 mL of ethyl acetate and stirring for 24 hours. The suspension was filtered through a 1 μ M glass-fiber filter, and the ethyl-acetate filtrate was evaporated and freeze-dried to isolate the lipid-derived sub-fraction of the hydrophobic-neutral fraction. Material retained on the filter was dissolved by slowly passing 50 mL of 75% acetonitrile/25% water through the filter. This filtrate was evaporated and freeze-dried to isolate the hydrophobic-base sub-fraction.

5.3.2. Normal-Phase Chromatography on Silica Gel

A two-stage fractionation of Suwannee River fulvic acid was performed by normal-phase chromatography on silica gel [86]. The fraction yields are diagrammed in Figure 22 and are listed in Table 1. Table 1 also presents the solvent-elution sequence. Six grams of the tetrabutylammonium salt of Suwannee River fulvic acid dissolved in 22 mL of chloroform were applied to a 2 L bed-volume column of 100-200 mesh silica gel previously conditioned with tetrabutylammonium acetate dissolved in chloroform. After the first-stage fractionation, solvents were evaporated from each fraction and the fractions were converted to the acid form by passage through a MSC-1H hydrogen-form cation-exchange resin. The acid-form fractions were then dissolved in a minimum volume of

tetrahydrofuran and fractionated using the solvent-elution sequence of Table 1 on silica-gel columns, with fraction loadings of 2.5 mg sample per 1 mL of bed volume. Fraction boundaries were determined by the cessation of color eluted from the column by each solvent mixture.

The solvent-elution sequence progressed from solvents of increasing polarity as electron donors to solvent mixtures with proton donors of increasing acidity. Quantitative recovery of the fulvic acid was obtained after each stage of the fractionation, with no irreversible adsorption on the silica gel that would be indicated by residual color remaining on the column. The first-stage fractionation, which fractionated the conjugate-base form of the fulvic acid, gave fractions of increasing acid-group content (after fraction conversion to the acid form) with increasing fraction number, whereas the reverse trend was observed in the second-stage fractionation of the acid-form fractions. The silica-gel sub-fractionation procedure produced number-average molar masses (determined by equilibrium centrifugation) ranging from 200 to 1540 Daltons, weight average molar masses ranging from 820 to 2920 Daltons, molecular-polydispersity ratios ranging from 1.09 to 5.27, and acid-group contents ranging from 2.96 to 7.16 meq/g [86]. The molecular-polydispersity ratio tended to decrease as the acid-group content increased. These fractionation results indicated that silica-gel normal-phase chromatography fractionated fulvic acid by hydrogen-bonding interactions, as contrasted with hydrophobic interactions of fulvic acid by reverse-phase chromatography on the XAD resins. Silica-gel sub-fractionations of Suwannee River fulvic acid fractions previously separated by pH-gradient chromatography on XAD-8 resin were used for studies of acid-group structures [40,87,88] and for studies of metal-binding structures [39,89,90]. Silica-gel chromatography of Suwannee River fulvic acid followed by solvent-elution fractionation of sub-fractions on XAD-8 resin was used to separate terpenoid-derived fulvic acid from tannin-derived fulvic acid [91].

5.3.3. Reverse-Phase pH-Gradient Chromatography on XAD-8 Resin

A large-scale (40 grams) sub-fractionation of Suwannee River fulvic acid using an increasing pH gradient on a 9.4 L column of XAD-8 resin was conducted to study metal-binding structures [39] and strong-acid carboxyl group structures [40]. The fulvic acid was dissolved in 500 mL of water and adjusted to pH 1 with HCl. In the pH 1-3 range, the pH was

controlled by adjusting the HCl concentrations to the desired pH and rinsing the column with 25 L of eluent at the desired pH. Above pH 3, 25 L solutions of citrate and phosphate buffers were used to control the pH. The pH was raised in increments of 0.5 units up to pH 8, and then it was increased by 1.0 pH-unit increments up to pH 12. The citrate and phosphate buffers were removed by acidifying the eluents to pH 2 with HCl, reconcentrating the fractions on a 2 L column of XAD-8 resin, and eluting the fractions with

75% acetonitrile/25% water followed by evaporation and freeze-drying of each fraction. A plot of the mass versus elution pH is shown in Figure 23. Values for a four pK_a model for Suwannee River fulvic acid [88] are also plotted in Figure 23, and the mass eluted generally parallels the successive ionization of carboxylic acid groups from pH 1 to 5.5. Elutions of fractions above pH 5.5 were attributed to ionization of weak carboxylic- and phenolic-hydroxyl groups in fulvic acid structures.

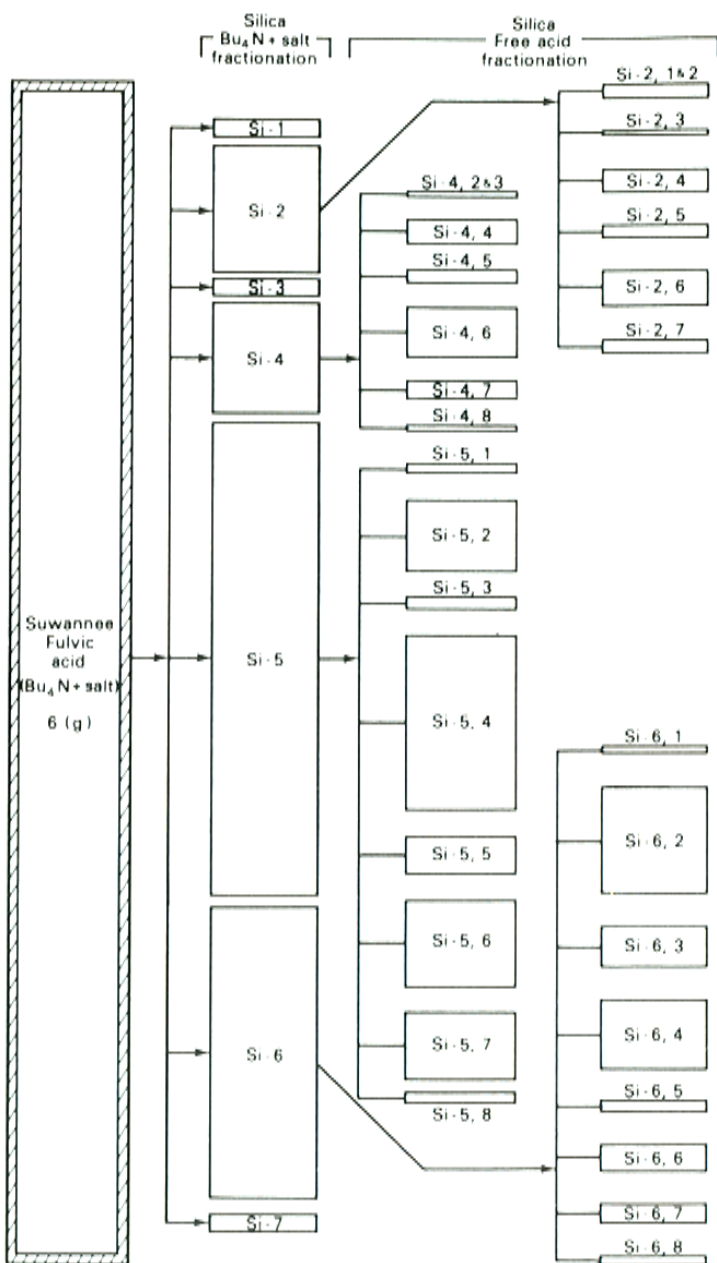


Figure 22 Two-stage fractionation of Suwannee River fulvic acid on silica gel (bar sizes are proportional to yield)

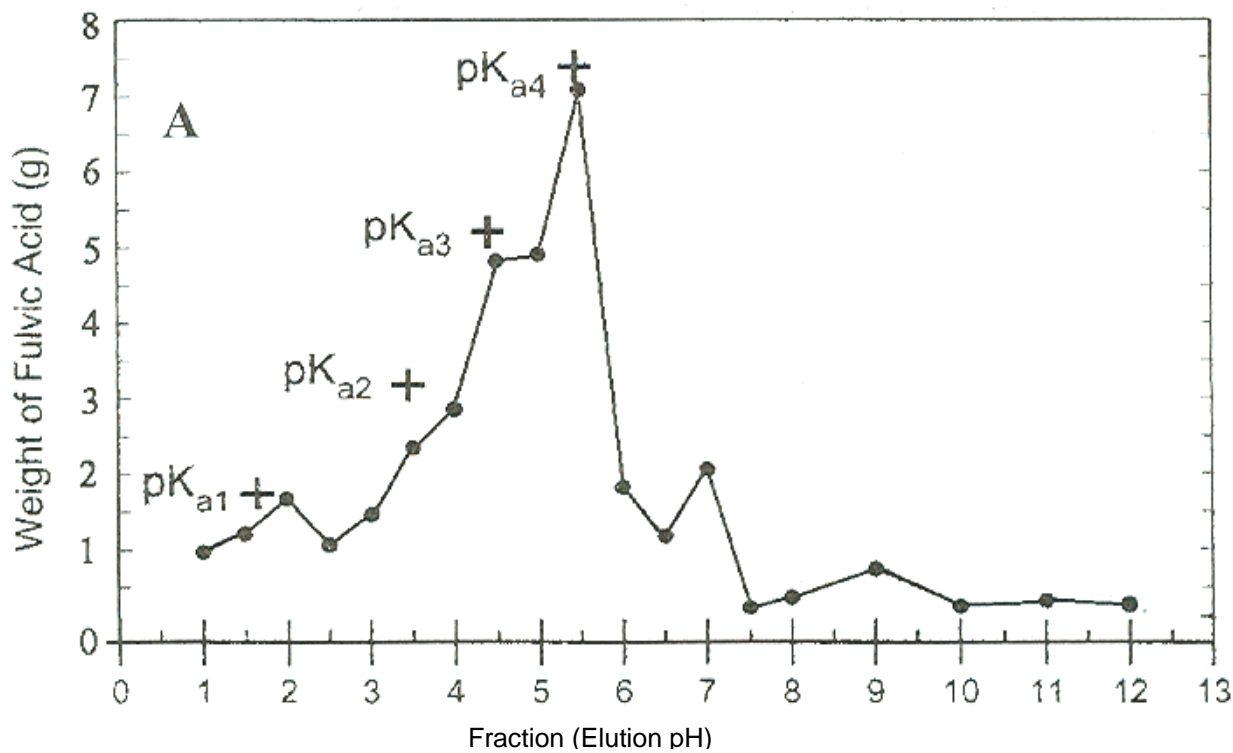


Figure 23 Reverse-phase pH-gradient fractionation of Suwannee River fulvic acid on XAD-8 resin, showing results from four pK_a model (see section 6.4 of this account)

Humic acid can also be sub-fractionated by a decreasing pH-gradient fractionation. Humic acid extracts from a soil and a lignite in Greece were sequentially dialyzed (12000-15000 Dalton membrane) against 0.1 M HCl to remove exchangeable metals and against 0.2 M HF to remove silica. Lastly, they were dialyzed against 0.1 M citric acid adjusted to pH 10 to disaggregate the humic acid and to remove iron and aluminum by complexation with citric acid. Humic acid retained in the dialysis bag was sequentially dialyzed against deionized water, 0.1 M HCl, and deionized water again, and it was then freeze-dried. Humic acid in the dialysis permeate from the sodium-citrate treatment was passed through a 1 L column of XAD-8 resin and rinsed with citric acid buffer at pH 10; this was followed by a 0.01 M HCl rinse to convert the adsorbed humic acid to the acid form. Humic acid was then eluted with 75% acetonitrile/25% water followed by evaporation and freeze-drying. Humic acid in the eluent that did not adsorb at pH 10 was acidified to pH 5, and the procedure was repeated. The humic acid eluent was successively acidified to pH 3 and pH 2, and the procedure was repeated until all of the humic acid in

the permeate was sub-fractionated.

5.3.4. Reverse-Phase Solvent-Elution Chromatography on XAD-8 Resin

Silica-gel chromatography of 3.47 grams of Suwannee River fulvic acid followed by solvent-elution chromatography on XAD-8 resin was used to separate terpenoid-derived fulvic acid from tannin-derived fulvic acid [91]. The mass fractionation of this two-stage sub-fractionation procedure is shown in Figure 24. The free-acid form of the fractions obtained from the silica gel was dissolved in water acidified to pH 2 with formic acid and then adsorbed on XAD-8 resin columns. The column was eluted with a discrete series of solvent mixtures ranging from 5 to 75% acetonitrile. Solvents (including formic acid) were removed by evaporation and freeze-drying. The advantage of solvent-elution chromatography compared to pH-gradient chromatography is that solvents are easily removed, as opposed to additional adsorption and elution procedures used to remove pH buffers.

Table 1 Yields of silica-gel fractionation of Suwannee River fulvic acid

<i>Fraction Number (from Figure 22)</i>	<i>Elution Solvent</i>	<i>Weight (mg)</i>	<i>Percent Yield</i>
Si-1	chloroform	72	1.35
Si-2	methyl ethyl ketone	658	12.32
Si-3	50% methyl ethyl ketone, 50% acetonitrile	66	1.23
Si-4	acetonitrile	559	10.45
Si-5	75% acetonitrile, 25% 2-propanol	2420	45.21
Si-6	75% acetonitrile, 25% water	1500	28.15
Si-7	75% acetonitrile, 25% water, 0.25 M oxalic acid	70	1.30
Si-2,1 and 2	chloroform and diethyl ether	57	1.21
Si-2,3	75% diethyl ether, 25% methyl ethyl ketone	23	0.49
Si-2,4	methyl ethyl ketone	105	2.23
Si-2,5	acetonitrile	49	1.04
Si-2,6	75% acetonitrile, 25% 2-propanol	187	4.00
Si-2,7	75% acetonitrile, 25% water	58	1.23
Si-4,2 and 3	diethyl ether and 75% diethylether, 25% methyl ethyl ketone	6.8	0.14
Si-4,4	methyl ethyl ketone	127	2.72
Si-4,5	acetonitrile	54	1.15
Si-4,6	75% acetonitrile, 25% 2-propanol	244	5.21
Si-4,7	75% acetonitrile, 25% water	62	1.31
Si-4,8	75% acetonitrile, 25% water, 0.25 M oxalic acid	3.6	0.08
Si-5,1	chloroform	25	0.54
Si-5,2	diethyl ether	360	7.68
Si-5,3	75% diethyl ether, 25% methyl ethyl ketone	42	0.89
Si-5,4	methyl ethyl ketone	913	19.47
Si-5,5	acetonitrile	162	3.45
Si-5,6	75% acetonitrile, 25% 2-propanol	391	8.33
Si-5,7	75% acetonitrile, 25% water	362	7.71
Si-5,8	75% acetonitrile, 25% water, 0.25 M oxalic acid	67	1.26
Si-6,1	chloroform	15	0.33
Si-6,2	diethyl ether	548	11.69
Si-6,3	75% diethyl ether, 25% methyl ethyl ketone	200	4.27
Si-6,4	methyl ethyl ketone	336	7.18
Si-6,5	acetonitrile	37	0.80
Si-6,6	75% acetonitrile, 25% 2-propanol	136	2.89
Si-6,7	75% acetonitrile, 25% water	88	1.88
Si-6,8	75% acetonitrile, 25% water, 0.25 M oxalic acid	31	0.65

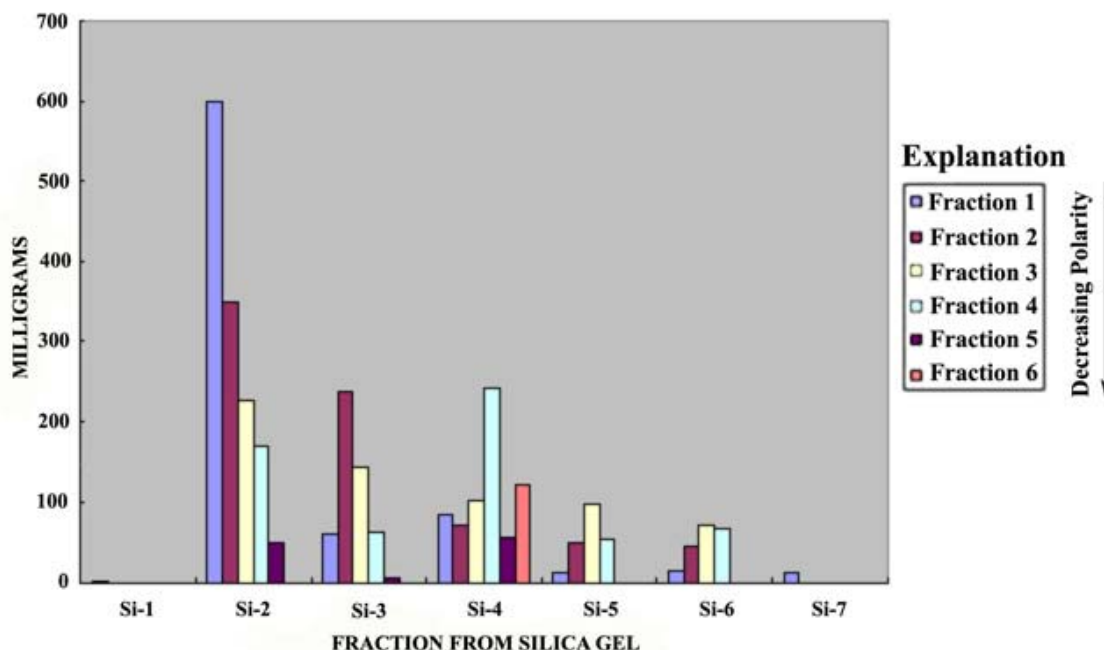


Figure 24 Normal-phase silica-gel sub-fractionation and reverse-phase solvent-gradient sub-fractionation of Suwannee River fulvic acid; fractions 1-6 were eluted with a gradient ranging from 5% acetonitrile to 75% acetonitrile in water

6. CHARACTERIZATION OF NOM

NOM is partially characterized by its fractionation patterns based on concentration, polarity, size, solubility, and acid, base, and neutral characteristics at the first three levels of the hierarchical classification (Figure 1). To proceed to the compound-class level 4 of Figure 1, additional analyses of NOM fractions are required. These analyses are selected as if the NOM fractions were pure compounds to obtain comprehensive organic-structural information which can then be used in successive approximations to model compound-class structures.

6.1. Elemental Analyses

Major elements typically determined for NOM include carbon, hydrogen, oxygen, nitrogen; minor elements include halogens, sulfur, and phosphorus. Specific methods for elemental analyses of NOM are reported by Huffman and Stuber [92]. In addition to elemental analyses, determination of moisture content and ash content is critical for accurate determination of elemental content. Much of NOM is polar and hygroscopic, which means it rapidly absorbs water after freeze-drying. Salt hydrates which may be co-

isolated with hydrophilic-DOM fractions also contain much water, which will make major contributions to hydrogen and oxygen content. Thus, it is critical that NOM be separated from these inorganic salt hydrates before elemental analyses are conducted. Huffman and Stuber [92] found that separate determination of water content followed by correction of hydrogen and oxygen content was preferable to vacuum drying of NOM with direct determination of hydrogen and oxygen content, because certain NOM samples rapidly regained moisture after vacuum drying.

It is also important that NOM fractions have low ash contents, especially for oxygen analyses. Oxygen in NOM is commonly reported by difference between 100% minus the sum of the other major elements determined with a C, H, and N analyzer. Problems with this difference-oxygen determination are:

- 1) Errors with carbon, hydrogen, and nitrogen determinations are additive and are summed in the oxygen calculation.
- 2) The minor elements are included in this difference calculation.
- 3) The ash may include elements already determined, such as carbonates, sulfates, and oxides.

Direct determination of oxygen on samples with low ash content therefore minimizes errors.

An independent evaluation of the accuracy of elemental analyses upon which the empirical formula is based is to determine the heat of combustion by calorimetry [93]. The sum of the heats of combustion for various bonds (C-H, C-C, C=C, C-O, and C=O) in a molecule equals the total heat of combustion for the molecule. The various bond types can be determined from a quantitative ¹³C-NMR spectrum. Using this approach, the calculated heat of combustion, 926.3 kcal/mol, was similar to the calorimetric value, 930.4 kcal/mol, for the Suwannee River fulvic acid [93]. Lack of agreement between the calculated and the experimental heats-of-combustion determinations indicates errors either in the elemental analyses or in the quantitation of the ¹³C-NMR spectrum.

Various elemental ratios of NOM are used in analytical chemistry and biogeochemistry applications. The index of hydrogen deficiency (Φ) is a measurement of the number of rings and double bonds in a NOM fraction whose empirical formula is determined from elemental analyses and whose molar mass is arbitrarily set at 1000 Daltons. It is calculated using numbers of carbon, hydrogen, oxygen, and nitrogen atoms in the empirical formula with Equation 2:

$$\Phi = [(2C + 2) - (H - N)]/2 \quad (\text{Eq 2})$$

The average oxidation state of carbon in NOM

can be determined by assuming that carbon is bonded to hydrogen (+1), oxygen (-2), nitrogen (-3), or sulfur (-2) [94]. By combining the index of hydrogen deficiency with a measurement (or estimate) of carboxyl group content, it is possible to estimate the relative proportions of aliphatic carbon, aromatic carbon, and other forms of carbon in NOM [94].

The atomic C:N ratio is used to distinguish terrestrial-plant material (C:N>20) from autochthonous phytoplankton and bacteria (C:N<10) in aquatic sediments, and it has been used to characterize source inputs in particulate organic matter in major world rivers [95]. This C:N-ratio indicator is based upon the Redfield ratio (C:N:P = 106:16:1), which is the molecular ratio of carbon, nitrogen, and phosphorus in phytoplankton [96]. An example of C:N ratios indicative of NOM sources is shown in Figure 25 for a total organic matter fractionation of water samples from Mill Creek in a stormflow study conducted in cooperation with the Orange County Water District [74]. The NOM fractions from the base-flow samples where autochthonous inputs are expected to dominate generally have the lowest C:N ratios, and the NOM fractions where allochthonous inputs are expected to dominate generally have the largest C:N ratios. Exceptions to this trend are the coarse-particulate organic matter fraction (CPOM) and the humic acid and humin fractions extracted from fine-particulate sediment, which have the largest C:N ratio for the first recessional-flow sample.

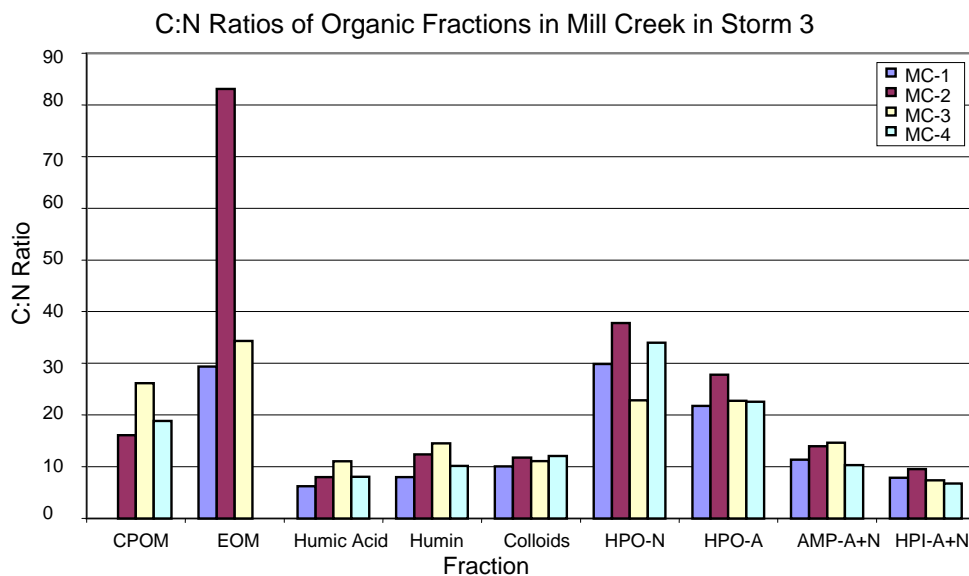


Figure 25 C:N ratios of organic fractions in Mill Creek, Chino, California, in storm 3, February 20-23, 2004 (fractions are defined in Figure 21); MC-1 is a base-flow sample, MC 2 is a peak-flow sample, MC-3 and 4 are recessional-flow samples

This difference in C:N-ratio trends is indicative of differential transport, characteristic of particulate NOM compared to dissolved NOM. The dramatic differences in C:N ratios of the extractable organic matter fraction reflect nitrogen-rich chlorophyll extracted from algae in the base-flow sample. Polar NOM fractions generally have lower C:N ratios than non-polar fractions [74]. The ratio of (O+N)/C is called the polarity index; it has been used to predict the sorption of non-polar chemicals to NOM in soils and sediments [97].

Two-dimensional plots (H/C and O/C) and three-dimensional plots (H/C, O/C and N/C) are used to type different NOMs and are derived originally from typing of coals [98]. An example of two-dimensional Van Krevelen diagrams is shown in Figure 26; it types hydrophobic (fulvic)-acid fractions and "hydrophilic" (actually amphiphilic)-acid fractions isolated from Antarctic lakes and compares them to other fulvic acids isolated from various temperate environments in North America [99].

6.2. Molar Mass/Size Distributions

Determination of molar mass/size distributions of NOM constituents is very difficult because of the interactive nature of NOM molecules with themselves, with media that fractionate NOM based on molecular size, and with various inorganic constituents in the water, soil, and sediment environment, and because of various molecular configurations that NOM and its aggregates can form as a function of pH, temperature,

and ionic strength.

In natural waters, the NOM molecules (represented as HO-R-O⁻M⁺ in Figure 27) exist in equilibrium with aggregates and precipitates that form by hydrogen bonding, covalent bonding with silica and boron, and metal complexation [100]. The degree (number of molecules in the aggregate) of NOM aggregation depends on the chemistry of the specific NOM in question and the inorganic chemistry of water. In soils and sediments, NOM often exists as surface coatings that interact with iron and aluminum sesquioxide coatings as shown in Figure 28 [10]. NOM aggregates in water and NOM coatings in soils and sediments act as an amorphous phase in certain of its properties, such as organic-contaminant sorption. Extraction, fractionation, and isolation of NOM from soil, sediment, and water disrupt aggregates and NOM coatings to varying degrees, depending on the procedure. The existence of NOM-metal aggregates in certain molar mass measurements such as size-exclusion chromatography (SEC) partially explains differences in NOM molecular and size measurements by various methods [7]. In a study of soil humic acids that compared size-exclusion chromatography molecular measurements with multi-dimensional NMR molecular measurements, the SEC measurements gave humic acids colloidal-size properties of 6000 Daltons or greater, whereas the NMR measurements showed that humic acid components had molar masses of 2000 Daltons or less and were held together as colloidal aggregates by complexation with metal cations [11].

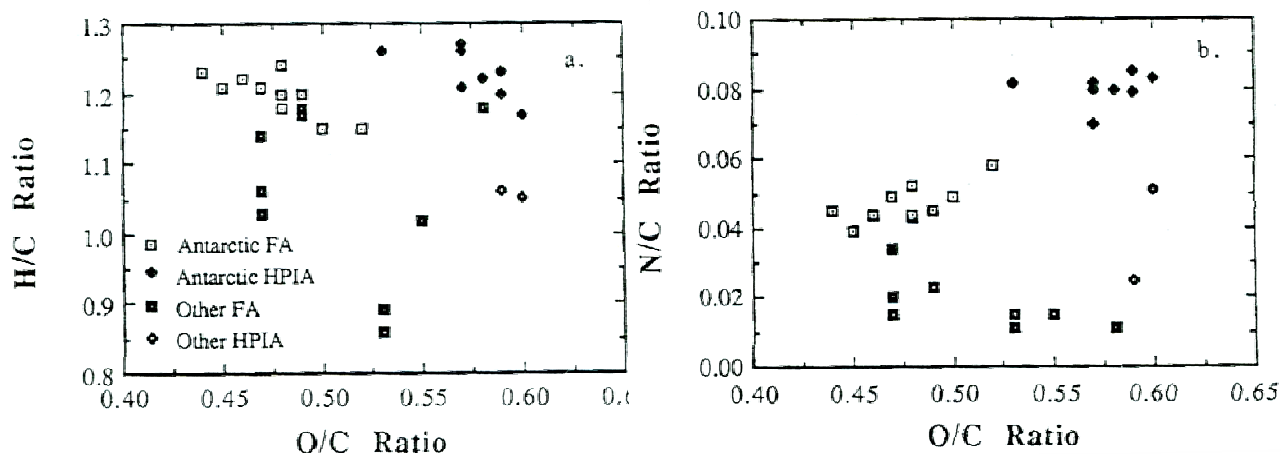


Figure 26 Van Krevelen diagrams comparing H/C and O/C ratios (a) and N/C and O/C ratios (b) for Antarctic fulvic acid (FA) and hydrophilic acid (HPIA) samples with those from other aquatic environments [99]

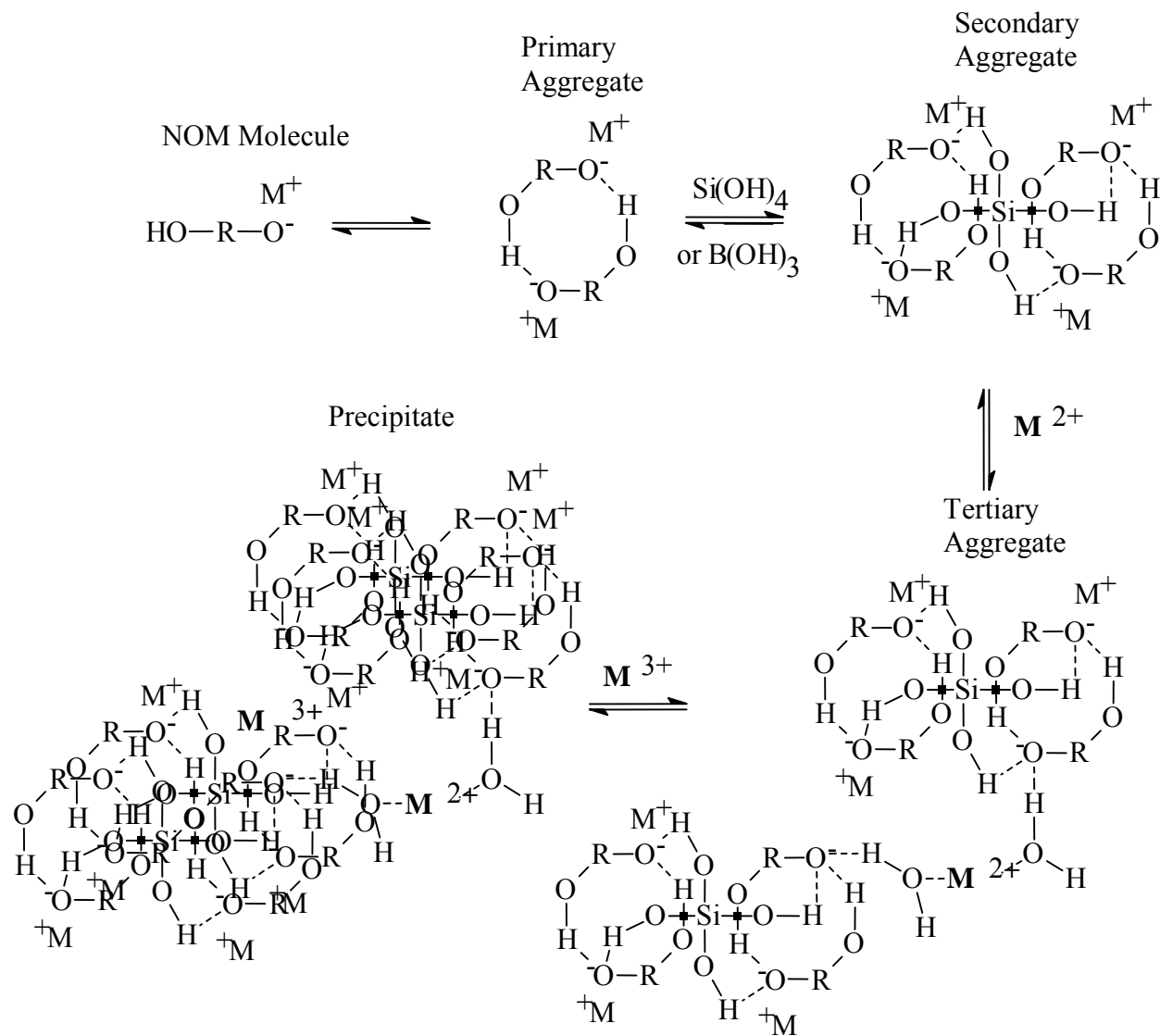


Figure 27 Equilibria and inorganic species involved with NOM aggregate formation (M = metal, R = hydrocarbon structure) [100]

Table 2 Number average (M_n) and weight average (M_w) molar mass measurements of Suwannee River fulvic acid by various methods. Molar mass units are grams per mole. M_w/M_n = Index of polydispersity

Method [Reference]	Sample State	Sample Medium	M_n	M_w	M_w/M_n
Equilibrium ultracentrifugation [86]	Potassium salt	0.2 M KCl, pH 8 in water	1060	1340	1.27
Equilibrium ultracentrifugation [86]	Free acid	Tetrahydrofuran	470	1110	2.36
Equilibrium ultracentrifugation [86]	Methylated	N,N-dimethyl-formamide	530	1250	2.36
Equilibrium ultracentrifugation [86]	Methylated	Acetonitrile	530	1190	2.25
Size-exclusion chromatography with UV detection [101]	Sodium salt	0.1 M phosphate buffer (water), pH 6.8	1385 (estimate from size)	2114 (estimate from size)	1.53
Size-exclusion chromatography with DOC detection [101]	Sodium salt	0.1 M phosphate buffer (water), pH 6.8	1166 (estimate from size)	2114 (estimate from size)	1.81
Field-flow fractionation with UV detection [102]	Sodium salt	005 M Na ₂ SO ₄ + .003 M NaN ₃ in water	1658 (estimate from size)	2364 (estimate from size)	1.43
Field-flow fractionation with DOC detection [102]	Sodium salt	005 M Na ₂ SO ₄ + .003 M NaN ₃ in water	1518 (estimate from size)	1900 (estimate from size)	1.25
Mass spectrometry [103]	Free acid	Vacuum	591	914	1.55
Mass spectrometry [104]	Methylated	Vacuum	581	695	1.20
Vapor pressure osmometry [105]	Free acid	Tetrahydrofuran	756		
Small-angle X-ray scattering [105]	Sodium salt	1% fulvic acid solution at pH 9 in water	711 (estimate from size)		

The variability of number average (M_n) and weight average (M_w) molar mass and size measurements determined by different methods is shown for the Suwannee River fulvic acid in Table 2. The salt-form molar mass measurements are generally two to three times greater than the free-acid-form measurement, with the exception of the small-angle X-ray-scattering measurement [105]. Major contributions to the apparent molar mass increase (as determined by equilibrium ultracentrifugation) of Suwannee River fulvic acid when converted from the free-acid to the salt form were attributed to electrostatically bound salt cations and the addition of four to six water molecules in the hydration sphere of cation-carboxylate ion-pairs [86].

Molar mass estimates based upon molecular-size separations (size-exclusion chromatography and field-flow fractionation) are calibrated with standards

(usually polyethylene glycol or polystyrene sulfonate) and have errors caused by variable molecular configurations, hydration spheres, charge effects, and interactions with the fractionating matrix (in the case of size-exclusion chromatography). Note that direct measurement of fulvic acid molecular size by small-angle X-ray scattering (Table 2) gives an estimated molar mass that is more consistent with the free-acid and methylated forms of Suwannee River fulvic acid. On-line DOC detectors give lower number-average molar masses than ultraviolet (UV) detectors for gel-permeation chromatography and field flow fractionation data in Table 2. For unfractionated DOC, the high molar mass colloid fraction is almost undetectable by UV measurement, and DOC detectors give much lower molar masses for gel permeation chromatography than UV detectors [101].

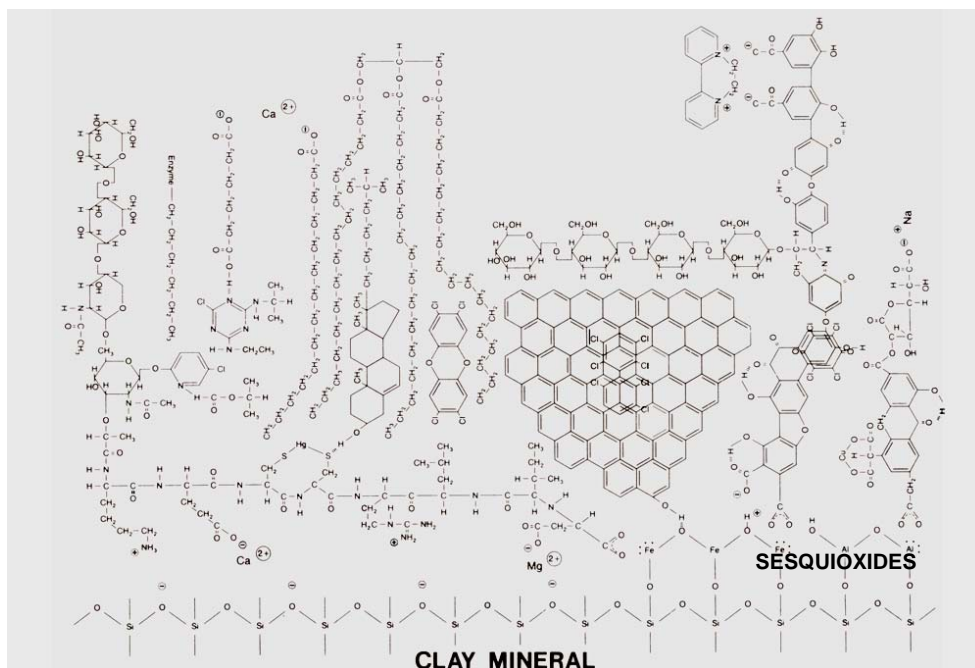


Figure 28 Hypothetical molecular representation of NOM coating on soil and sediment [10]

A recent study [106] of differences in molecular composition of Suwannee River fulvic acid size fractions separated by gel permeation chromatography coupled with an ion-cyclotron mass spectrometer found that the high-molar mass fraction gave a distribution including low molar mass ions, suggesting either aggregation or fragmentation of the high molar mass fraction.

Mass spectrometry gives accurate measurements of mass-to-charge ratios, but conversion of this ratio to NOM molar masses may yield low estimates of mass by multiple charging of large NOM molecules, as shown in a study of polyacrylic acid oligomers [104]. It may also yield low estimates by loss of water in the formation of cyclic anhydrides and lactones when introducing acid NOM molecules into a vacuum, and because of molecular fragmentation by cleavage of labile ester and carboxyl groups [103]. Electrospray-ionization/mass spectrometry minimizes molecular fragmentation. High molar mass biased measurements by mass spectrometry may be caused by molecular aggregates [104,107] and by cationic adducts (NH^+ , Na^+ , K^+). Amphiphilic NOM molecules with surface-active properties are selectively ionized and better detected by electrospray ionization than are polar NOM molecules without surface-active properties [108].

Colligative-property measurements (boiling point, freezing point, osmotic pressure, and vapor pressure) can be used to determine the molar concentration of NOM dissolved in water or organic solvents. Number-average molecular masses can thus be calculated from NOM weights and molar concentration determinations. These measurements are valid only if a suitable solvent is found for a NOM isolate. Corrections need to be made for ionization and inorganic-solute impurities if water is used as a solvent, and for water adsorbed to NOM if anhydrous organic solvents are used [56]. Solvation of NOM aggregates can also introduce a high molar mass bias. The number-average molar mass value for Suwannee River fulvic acid as determined by vapor-pressure osmometry in Table 2 compares well with number average molar mass values determined by small-angle X-ray scattering, mass spectrometry, and equilibrium ultracentrifugation of the free-acid and methylated forms of fulvic acid.

With the exceptions of the non-humic colloid fraction and coarse-particulate organic fractions in soil, sediment, and water, molecular-size and -mass estimates for humic substances have been decreasing. This is due to improvements in molar mass and size determinations, and to improvements in isolation and fractionation methods that remove inorganic components and produce more compound-class homo-

geneous fractions. This size and mass decrease is good news, in that the goal of ultimate molecular-level characterization of NOM components is more readily achieved with small molecules.

6.3. Density Analyses of Solvated NOM

Density analyses of NOM and its fractions solvated in various solvents give valuable information regarding NOM-aggregation and NOM-conformation characteristics. This information is required to interpret NOM molecular-size and -mass determinations discussed in the previous section [86]. Density is significant in the determination of chemical structures because of the additivity of atomic volumes and densities incorporated into molecular densities [109]. This additivity rule known as Traube's Rule is valid only if there are:

- 1) no intermolecular interactions (aggregation),
- 2) no intramolecular interactions such as molecular-conformation changes to form H-bonded or metal-chelate ring structures, or
- 3) no changes in solvent densities such as occur in the hydration sphere of ions where water density increases through the process of electrostriction.

Electrostriction effects on density can be detected and quantified (number of water molecules in the hydration sphere) by varying the ionic strength of the water solvent. Aggregation effects on density can be detected by varying the concentration of the solute, and intramolecular interactions can be detected if solute densities are concentration independent and their values are greater than are determined by Traube's Rule.

An extensive study of the significance of density determination in solvated structures of Suwannee River fulvic acid was conducted; those densities were compared to the density of standards in various solvents [110]. Densities for various standards and Suwannee River fulvic acid were determined by pycnometry at 20° C [111]. Using both experimental and handbook data, the following densities (data in g/mL in parentheses) were determined for structural groups known to be present in Suwannee River fulvic acid: methyl (0.32), methylene (0.83), methine (1.33), primary alcohol (1.27), secondary alcohol (1.76), tertiary alcohol (2.31), phenol (2.16), anomeric carbon in sugars (1.57), methyl ether (0.62), methylene ether (1.10), methine ether (1.56), aromatic ether (1.93), aliphatic ketone (1.74), aromatic ketone (1.81),

aliphatic carboxyl (1.90), aromatic carboxyl (2.04), aliphatic ester (1.89), phenolic ester (2.46), unsubstituted aromatic carbon (0.88), and carbon-substituted aromatic carbon (1.41). The computed density value using Traube's Rule for quantitatively determined structural groups in Suwannee River fulvic acid [112] was 1.45 g/mL. Only one solvent mixture (94% dimethylsulfoxide, 5% water, 1% hydrochloric acid) for Suwannee River fulvic acid gave an experimentally determined density value of 1.47 g/mL that was comparable to the computed value.

Density versus concentration plots for other solvents for the acid and methylated forms of Suwannee River fulvic acid are shown in Figure 29 [86]. The density-concentration dependence of Suwannee River fulvic acid solvated in water, N,N-dimethylformamide (DMF), and tetrahydrofuran indicates intermolecular aggregation. However, when dioxane was used as the solvent for the free acid it had density values independent of concentration (Figure 29) indicating intramolecular cyclic associations which give density values considerably above the Traube's-Rule value of 1.45 g/mL. The density values for the methylated forms were concentration independent and generally fell below the Traube's-Rule value for the free acid, but the value of 1.38 g/mL was the calculated Traube's-Rule value for the methylated form, agreeing closely with the densities for methylated fulvic acid in DMF.

Solution-state density determinations aid in the interpretation of other data collected in solution. Solution NMR and IR measurements generally are performed at large concentrations in solvents where density measurements indicate NOM exists as aggregates, whereas solution UV measurements are performed at low concentrations where aggregation is minimal. Methylation appears to greatly decrease NOM aggregation. Certain solvent mixtures such as 94% dimethylsulfoxide, 5% water, and 1% hydrochloric acid appear to disrupt both inter- and intramolecular interactions in humic substances, as predicted by Hayes [55]. Lastly, the solution density study for the Suwannee River fulvic acid tends to support the low range of number average molar mass values near 500 Daltons in Table 2, as determined by equilibrium ultracentrifugation and mass spectrometry. The vapor-pressure osmometry determination in tetrahydrofuran and small-angle X-ray-scattering determinations occur at concentrations where density determinations indicate there may be a degree of aggregation.

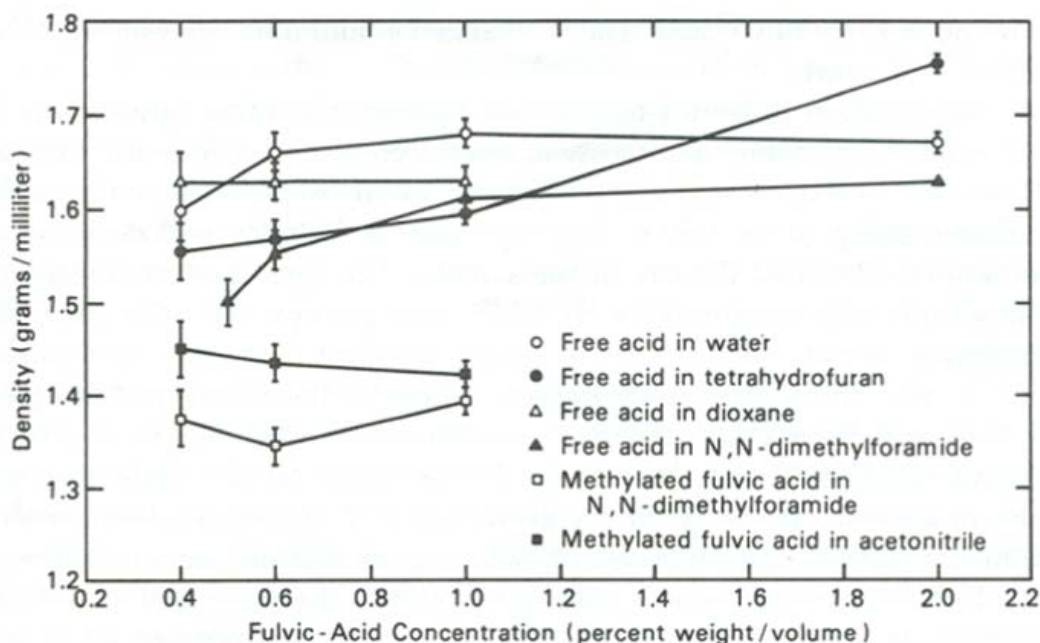


Figure 29 Density-concentration curves for Suwannee River fulvic acid in various solvents [86]

6.4. Titrimetric Analyses

The literature on titrimetric analyses of NOM is very extensive. An overview of titrimetric methods used for DOM is provided by Perdue [113] and Perdue and Richie [94]. An overview of titrimetric methods used for soil organic matter is provided by Stevenson [5]. The titrimetric methods presented in this section will focus on methods that are especially useful in providing structural information regarding the distribution of carboxyl, phenolic-hydroxyl, and metal-binding functional groups.

Aquatic DOM and soil fulvic acids have the greatest amount of acidic and metal binding functional groups when compared to other DOM fractions. Fulvic acids that are not sub-fractionated into more homogeneous fractions appear to have a continuous distribution of proton binding pK_a values between 1 and 10 that can be modeled with simple statistical-distribution models [114]. If one uses only pH titration data by themselves with unfractionated fulvic acid, it is not possible to distinguish polyprotic acids from mixtures of monoprotic acids; but it is generally accepted that carboxyl groups can be quantified by titration to pH 8, and one-half of the phenolic-hydroxyl groups are titrated between pH 8 and 10 [115].

Extensive studies [40,87,88] of the strong acid

carboxyl groups in Suwannee River fulvic acid have combined the sub-fractionations (described in Section 5) with titrimetric, spectrometric (^{13}C -NMR, UV, and IR), hydrolysis, and chemical standard characterizations. The titrations were performed using 200-400 mg of fulvic acid suspended in 4 mL of 0.5 M NaCl and titrating with 0.5 M NaOH. The large concentrations were necessary to accurately determine the pK_a values of the strong-acid groups. The effect of the phase change (solid to dissolved) of fulvic acid with increasing pH was minimized by titrating in 0.5 M NaCl to minimize electrostatic field effects. These studies found that keto-acids and aromatic-carboxyl groups were minor groups that contributed to the strong acid ($pK_a < 3$) characteristics [87], but that aliphatic carboxyl groups in unusual and/or complex configurations accounted for the majority of the strong-acid characteristics [88]. An additional study [40] found that carboxyl groups clustered in aliphatic, alicyclic ring structures could explain strong acid characteristics by electrostatic field theory [116]. The chemical standard, tetrahydrofuran tetracarboxylic acid, was shown to have similar acidity characteristics to carboxyl groups in Suwannee River fulvic acid; possible diagenetic pathways were presented whereby these aliphatic, alicyclic-carboxyl groups could be derived in fulvic acid [40]. Tetraprotic aliphatic alicyclic structures thus appear to be the best models

for describing the acidity characteristics of the strong acid fraction of the Suwannee River fulvic acid. The four pK_a values of this tetraprotic carboxylic acid model are shown in Figure 23.

Alkaline hydrolysis of humic substances typically releases simple aliphatic acids and phenolic acids in aquatic [117] and soil [118] humic substances. These hydrolysis products have been attributed to the presence of phenolic esters in humic substances. Hydrolyzable tannins produced by plants consist of phenolic acids (especially gallic acid) esterified to sugar [23]. Hydroxy acids with the hydroxyl group on the γ -carbon or δ -carbon relative to the carboxyl group will spontaneously form five- and six-membered-ring lactones in aqueous acid solution and will hydrolyze in aqueous alkaline solutions. Phenolic esters in particular are readily hydrolyzed under alkaline conditions and will affect the titrimetry of certain NOM isolates. A titrimetric study [115] of Suwannee River fulvic acid found both reversible and irreversible ester-hydrolysis reactions that affect time-dependent titrimetric characteristics as shown in Figure 30. These hydrolysis reactions began near pH 7, and the hydrolysis rate increased as the pH increased. Another study [119] of hydrolysis of Suwannee River fulvic acid found the hydrolysis reactions to be mainly irreversible, and it confirmed the disappearance of the ester group by infrared spectrometry. To minimize ester hydrolysis, direct forward titrations of acid groups by base up to pH 10 should take 2 minutes or less. Ester group content is about 40% of the carboxylic acid group content in Suwannee River fulvic acid [112].

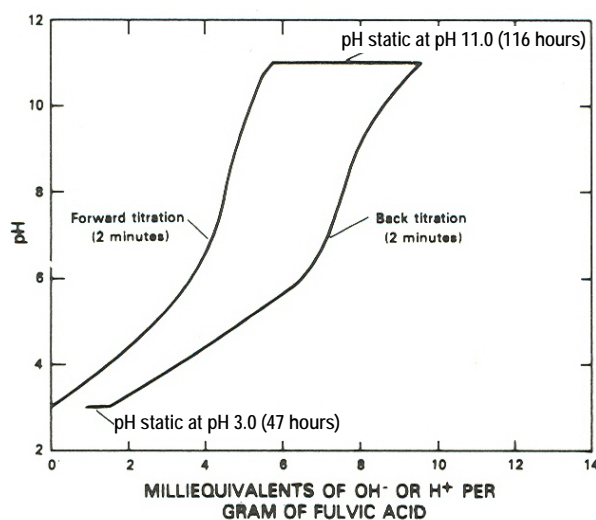


Figure 30 Acid-base titration hysteresis experiment with Suwannee River fulvic acid [115]

Acid groups in NOM fractions that are insoluble in water may be indirectly titrated by equilibration with various basic reagents at defined pH values. The barium-hydroxide method for total acidity equilibrates NOM with 0.1 M BaOH near pH 13, and the calcium acetate method for carboxyl group acidity equilibrates NOM with 1.0 M calcium acetate near pH 8 [5]. After equilibration, NOM is removed by filtration, and excess barium hydroxide or liberated acetic acid is titrimetrically determined. Ester hydrolysis can be a significant error in the total acidity method, and incomplete separation of NOM by filtration can lead to errors with both methods.

The Boehm titration has been used to determine strong acids (titrated at pH 8), moderate acids (titrated from pH 8 to 10), and weak acids (titrated from pH 10-13) in chars [120,121]. This indirect-titration method equilibrates the char with sodium bicarbonate, that titrates carboxylic acids; with sodium carbonate, that titrates low pK_a phenols and hydrolyzes lactones; and with sodium hydroxide, that titrates high pK_a phenols. This method also suffers from solubilization of NOM from chars at high pH, and this NOM cannot be removed by filtration while titrating excess reagent to quantify acid group content. However, it at least recognizes the presence of lactones that affect the total- and moderate-acidity results. The report by Rutherford et al [121] showed the development of carboxyl, lactone, and phenol groups by Boehm titration and infrared spectrometry during progressive thermal degradation of wood and wood components in the process of char formation.

Potentiometric titration can also be used with specific-ion electrodes to study metal binding by NOM or NOM fractions [5, pp. 405-428]. An example of a titration with a cupric ion-specific electrode using fractions of Suwannee River fulvic acid derived from the pH-gradient fractionation shown in Figure 23 is illustrated in Figure 31 [90]. Inflections in the titration curves of certain fractions shown in Figure 31 indicate specific binding sites of fulvic acid component structures for Cu^{2+} , whereas the Cu^{2+} titration curves for unfractionated fulvic acid (data not shown) do not show any inflections because of the mixture of different binding sites. Not all of the fractions showed inflections in their Cu^{2+} ion titration curves. Cupric ion titrimetry was also used to show how different DOM fractions isolated from the South Platte River upstream from Denver, Colorado, had substantially different stability constants (K_{Cu}) [122]. For the hydrophobic and amphiphilic acid fractions, Cu^{2+} was bound by low-affinity carboxylic acid (\log_{Cu} near 1) and high-affinity phenol (\log_{Cu} near 8), but the

amphiphilic neutral fraction, that was mainly proteinaceous, bound Cu^{2+} with amino groups that had the largest stability constants (\log_{Cu} near 10).

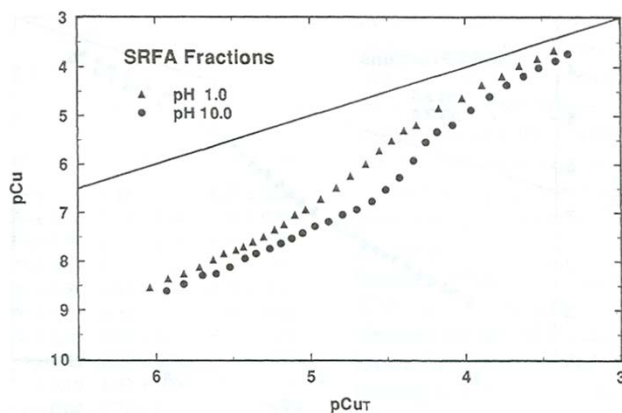


Figure 31 pCu versus pCu_T for 55 mg/L of Suwannee River fulvic acid (SRFA) fractions in 1.0 mM KClO₄ at pH 6 (fractions refer to pH of elution in Figure 23) [90]

6.5. Infrared Spectrometry

A concise presentation of the theory and methods of infrared spectrometry as applied to humic substances is given by Stevenson [5]. Comprehensive interpretation of FT-IR spectra of pure compounds is difficult because so many absorption bands are generated; however, the complex mixture properties of NOM and its fractions simplify interpretation of the spectra because only the strongest bands can be identified and associated with the predominant structures. For interpretation of the spectra of pure compounds, the reader is referred to Pouchert [33], and for the analyses of complex biomolecular structures and humic substances to Bellamy [29] and Stevenson [5], respectively. It is important to examine and compare the complete spectrum of reference compounds as well as peak frequencies for spectra interpretation, as there is considerable variation in peak intensities and peak profiles for various structures and for functional groups within a compound.

Infrared spectra collected by the author used 2 to 5 mg of sample in KBr pellets, which provide spectra free from interferences from solvents or carriers such as Nujol. The Perkin Elmer System 2000 FT-IR spectrometer employed a pulsed-laser source and a deuterated triglycine sulfate detector. The instrument was set up to scan from 4000 to 400 cm^{-1} , averaging ten scans at 1.0 cm^{-1} intervals with a resolution of 4.0 cm^{-1} . All spectra were normalized after acquisition to

a maximum absorbance of 1.0 for comparative purposes. Infrared peaks presented in the absorbance mode were preferred to the transmittance mode, because absorbance is linearly related to peak intensity.

Infrared spectrometry is essential for NOM studies both as a monitoring tool for NOM extraction, fractionation, and isolation procedures, and as a characterization tool for determination of NOM structures and functional-group content. Infrared absorption peak frequencies for various inorganic solutes that frequently co-isolate with DOM and its fractions are listed in Table 3. These inorganic solute peaks are monitored for their presence or absence in DOM fractionation and isolation procedures. For TOM isolation and fractionation procedures as presented in Figure 21, certain minerals and their reaction products with hydrofluoric acid are frequently detected by infrared spectrometry. Table 4 presents characteristic IR peak frequencies for these compounds.

Table 3 Characteristic infrared spectral peaks of inorganic solutes (in KBr pellets)

Inorganic Solute	Characteristic IR Peak Frequencies (cm^{-1})
Ammonium chloride	3137, 3024, 1402
Boric acid	3212, 2260, 1450, 1194, 548
Calcium and magnesium hydrates	3400, 1640
Sodium bicarbonate	2541, 1920, 1695, 1618, 1307, 1000, 837, 696
Sodium carbonate	1440, 880
Sodium nitrate	1385, 838
Phosphoric acid	1007, 490
Disodium hydrogen phosphate	1159, 1074, 950, 860, 544, 521
Silicic acid	1093, 964, 798, 468
Sulfuric acid	1288, 1176, 1071, 1012, 889, 852, 617, 577, 455
Sodium hydrogen sulfate	1251, 1182, 1046, 865, 607, 577, 481
Sodium sulfate	1122, 640, 608

Certain compound classes in NOM and its fractions can readily be determined by FT-IR spectrometry. A listing of characteristic peak frequencies for these compound classes are listed in Table 5. Infrared spectra for various NOM fractions containing the compound classes in Table 5 are shown in Figures 32-34.

Table 4 Characteristic infrared spectral peaks of certain inorganic compounds and minerals

Inorganic compound	Characteristic IR Peak Frequencies (cm ⁻¹)
Barium sulfate	1190, 1077, 638, 610
Calcium carbonate	1460 (broad), 875, 712
Calcium sulfate dihydrate (gypsum)	3400, 1640, 1150, 590
Kaolin	3695, 3619, 1115, 1034, 914, 752, 692, 645, 542, 471
Silicon oxide (quartz)	1340, 1106, 470
Sodium hexafluoroaluminate (cryolite)	600 (broad)
Sodium hexafluorosilicate	720 (broad)

Carbohydrates contain two broad peaks near 3400 cm⁻¹ (the OH stretch of alcohols) and 1100 cm⁻¹ (the C-O stretch of alcohols). The carbohydrate spectrum of Figure 32 was from the hydrophilic-acid-plus-neutral fraction in a DOM fractionation of beer [123]. Carbohydrate-rich NOM isolates usually contain carbohydrate acids as shown by the carboxylic acid peak near 1720 cm⁻¹ in Figure 32.

Aminosugars usually are the dominant constituent of the colloid fraction in DOM [18]. The amino group in the carbohydrate is acetylated, and this N-acetyl group gives rise to characteristic peaks in the infrared spectrum of the colloid fraction from the Great Salt Lake [76] as shown in Figure 32. In addition to the broad carbohydrate peaks discussed previously, the keto-form of the amide carbonyl stretch gives a peak at 1660 cm⁻¹ (amide 1 peak), the enol-form of the amide C=N stretch gives a peak at 1550 cm⁻¹ (amide 2 peak), and the methyl bending of the acetyl group gives a peak at 1380 cm⁻¹. Carboxylic acids in this colloid fraction are clearly differentiated from amides by the peak at 1720 cm⁻¹.

Proteins and peptides in NOM give characteristic infrared spectra, as illustrated by Figure 32 for the base/neutral fraction from the DON fractionation of soluble microbial products from a bacterial culture [78]. The amide 1 and amide 2 peaks are similar to those of N-acetyl aminosugars, but the amide 2 peak occurs near 1540 cm⁻¹ and differs by about 10 cm⁻¹. The 1370 cm⁻¹ methyl-bending peak of aminosugars is not present in the protein spectrum. A weak N-H stretching band near 3100 cm⁻¹ is also characteristic of proteins.

Infrared spectra of humic substances are generally dominated by OH group stretches, C=O group stretches, and C-O stretches. An excellent review of "typing" by infrared spectrometry of humic substances from different fractions, sources, and composition is given in the text by Stevenson [5]. The infrared spectrum of the Suwannee River fulvic acid sub-fraction derived from terpenoids [44] is shown in Figure 33. The broad OH-stretch peak from 3600 to 2200 cm⁻¹ results mainly from the OH of the carboxyl group with sharp C-H stretch peaks (3000 to 2800 cm⁻¹) superimposed upon the broad OH peak. The shoulder from 2700 to 2200 cm⁻¹ arises from OH in carboxyl groups that are hydrogen-bonded to carbonyl groups in carboxyl, ester, or ketone groups. The dominant carbonyl peak near 1720 cm⁻¹ is a combination of carboxyl, ester, and ketone groups, and the broad peak near 1200 cm⁻¹ is the C-O stretch of carboxyl and ester groups. Distinct peaks for methyl and methylene hydrocarbons (2960, 2920, 1460, and 1380 cm⁻¹) are not apparent in terpenoid structures, as alicyclic-ring hydrocarbons give broad C-H stretching and bending frequencies [33].

The infrared spectrum (Figure 33) of the Suwannee River fulvic acid sub-fraction derived from condensed tannins [91] differs from the terpenoid-derived fulvic acid by the peak at 1620 cm⁻¹.

Table 5 Infrared frequency peaks for various compound classes in NOM isolates

Compound Class	Peak Frequencies (cm ⁻¹) and Structure (φ = aromatic ring)
Carbohydrates	3400-3300 (O-H), 1100-1000 (C-O)
Humic substances	3600-3300 (O-H), 2700-2200 (COOH), 1760 (COOR), 1720 (COOH), 1660-1600 (C=C-C=O), 1280-1150 (φ-O, COOH)
Hydrocarbons	2960 (CH ₃), 2940(CH ₂), 1460 (CH ₂), 1380 (CH ₃)
Lignin	1600 (φ-C=O), 1510 (φ), 1460 (CH ₂), 1420 (φ), 1267 (φ-O), 1127 (O-CH ₃), 1035 (φ)
Lipids	2960 (CH ₃), 2940 (CH ₂), 1740 (COOR), 1720 (COOH), 1460 (CH ₂), 1380 (CH ₃)
Proteins	3100 (N-H), 1660 (Amide 1 peak, N-C=O), 1540 (amide 2 peak, N=C-O)
N-Acetyl aminosugars	1660 (amide 1 peak, N-C=O), 1550 (amide 2 peak, N=C-O), 1380(CH ₃)
Aromatic sulfonic acids	1180, 1125, 1040, (φ-SO ₃ H), 1010 (φ-H)

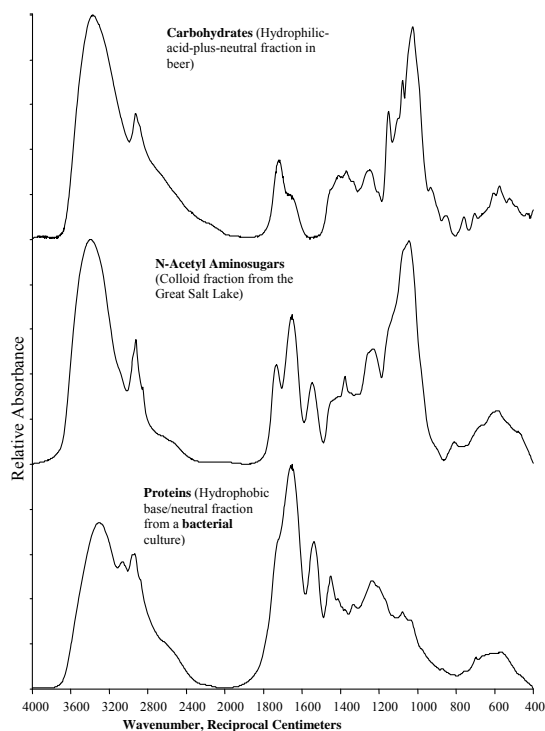


Figure 32 Infrared spectra of carbohydrates, N-acetyl aminosugars, and proteins in various NOM fractions

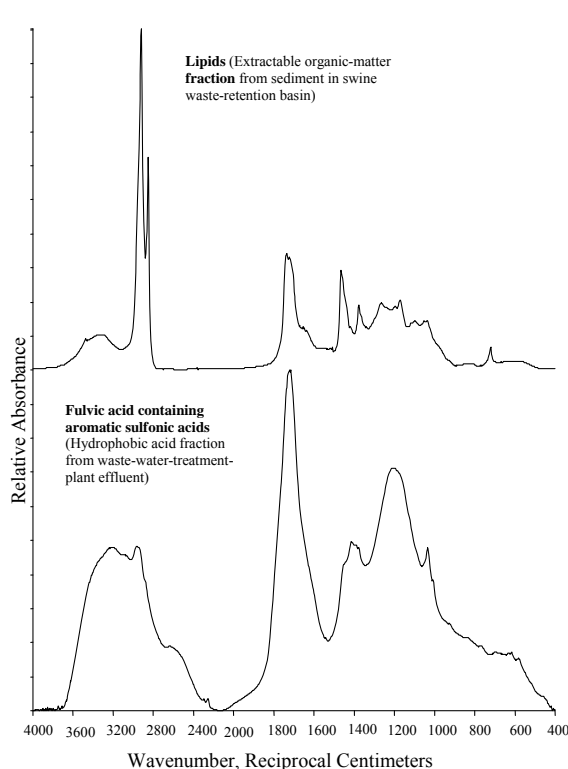


Figure 34 Infrared spectra of lipids and aromatic sulfonic acids in NOM fractions

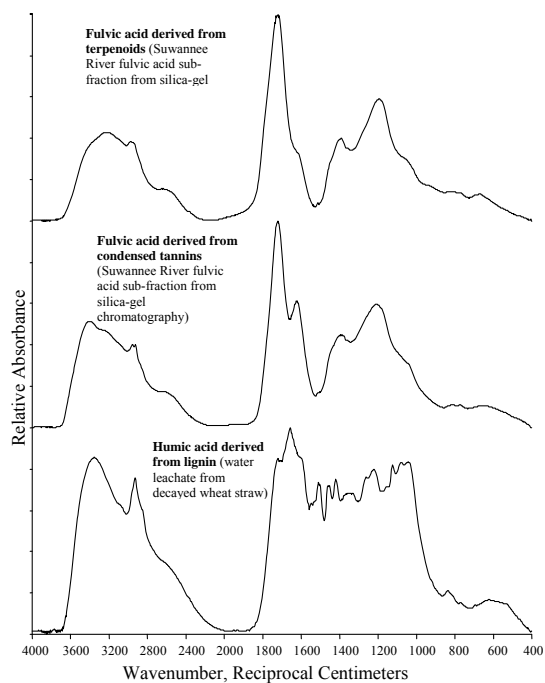


Figure 33 Infrared spectra of humic substances derived from terpenoids, condensed tannins, and lignins

The 1620 cm^{-1} peak is typically attributed [5] to aromatic ring C=C vibrations plus hydrogen-bonded conjugated ketones (flavones, quinones, keto-form of phenols, and aromatic ketones); however, aromatic C=C vibrations give sharp peaks, and their integrated intensities are 20 to 50 times lower than the C=O stretch of conjugated ketones [30]. Therefore, it is attractive to assume that the 1620 cm^{-1} peak in this fulvic acid sub-fraction, and in humic substances in general, should be mostly attributed to various conjugated ketone groups.

The infrared spectrum (Figure 33) of humic acid derived from decayed wheat straw [124] shows distinct aromatic ring C=C vibrations at 1510 and 1420 cm^{-1} . The 1510 cm^{-1} peak is especially diagnostic of humic substances derived from lignin, as this small but well-resolved peak occurs in a spectral region where few other peaks occur. The 1127 cm^{-1} peak is diagnostic of aromatic methoxy groups in lignin.

Aliphatic straight-chain lipids and straight-chain hydrocarbons are relatively simple to discern by infrared spectrometry, as shown by the infrared spectrum (Figure 34) of the extractable organic matter fraction in sediment from a swine waste-retention

basin [84]. The straight-chain methylene groups give sharp peaks at 2960 and 1460 cm^{-1} . The aliphatic ester groups in lipids give a broader peak at 1740 cm^{-1} . Aromatic sulfonic acids in fulvic acid fractions are also readily detected by the sharp 1040 cm^{-1} peak, with a satellite 1010 cm^{-1} peak in the infrared spectrum (Figure 34) of the hydrophobic acid fraction isolated by DON fractionation of a sewage-treatment-plant effluent [125].

Ester and ketone carbonyl group stretches occur near the same frequencies as the carboxylic acid stretch, but these ester and ketone peaks may be revealed by converting the carboxylic acids to carboxylate salts by titration with base to pH 8. The infrared spectrum of the tetrabutylammonium salt of Suwannee River fulvic acid is presented in Figure 35 [115]. The ester peak occurs near 1760 cm^{-1} , a frequency that indicates phenolic esters and five-member-ring lactones. The peak at 1680 cm^{-1} most likely indicates aromatic ketones, but could also have some contribution from aromatic esters. Tetrabutylammonium salts gave sharper ester and ketone peaks than sodium salts, possibly because of better disruption of hydrogen bonding of the carbonyl groups with the tetrabutylammonium salts.

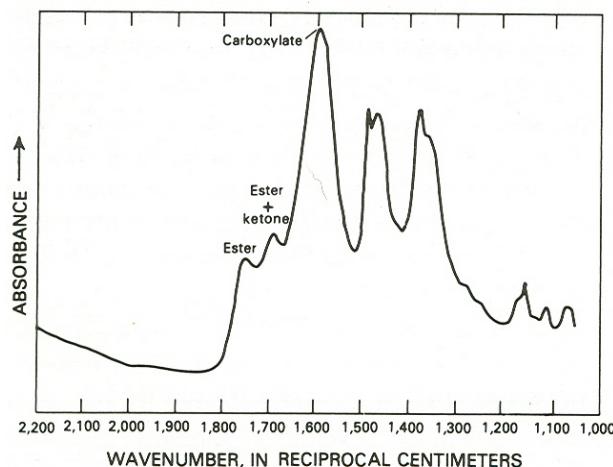


Figure 35 Infrared spectrum of tetrabutylammonium salt of Suwannee River fulvic acid [115]

Infrared spectrometry is basically used for qualitative characterization of certain functional groups and hydrocarbon structures in NOM, although “rough quantitative estimates of the concentrations of certain groups in material of unknown structure can be made” [126]. For solid-state infrared spectra, both peak intensities and frequencies are affected by

hydrogen bonding, electrostatic field effects, pi-electron conjugation, and steric effects [30]. Solution-state infrared spectra can be collected with DOM samples solvated by water using attenuated total-reflectance cells; quantitative determination of carboxylic acid content in fulvic acid [127] and the pK_a values of carboxylic acids were measured by the integrated intensity (acid content) and frequency (pK_a) [128] of the antisymmetric-carboxylate peak near 1600 cm^{-1} . Peak frequency shifts with trace-metal complexation with NOM also have been used to qualitatively determine functional groups (amino, carboxyl, conjugated ketone) binding with various trace metals [5].

6.6. Nuclear Magnetic Resonance Spectrometry

The structural information provided by nuclear magnetic resonance (NMR) of various elements in NOM is essential for comprehensive analytical studies. The optimum NMR-active nuclei of elements in NOM include ^{13}C , ^1H , ^{15}N , and ^{31}P . In addition, ^{17}O , ^{33}S , ^{35}Cl , ^{81}Br , and ^{127}I are also NMR-active nuclei, but quadrupolar effects for these nuclei lead to line broadening that greatly limits resolution. Although F is not an element that occurs in significant percentages in NOM, ^{19}F -NMR is useful for characterization of NOM functional groups by derivatization with ^{19}F reagents [129] and for studies of fluorinated contaminant interactions with NOM [130]. Inorganic NMR-active nuclei that interact with NOM include ^{27}Al , ^{11}B , ^{113}Cd , ^{133}Cs , ^{23}Na , and ^{29}Si . ^1H -NMR has been found useful for studies of NOM solvation and non-ionic organic-contaminant interactions with NOM [130]. Comprehensive reviews of the theory and applications of NMR are provided by Nanny et al [32] for environmental chemistry and by Wilson [31] for geochemistry and soil chemistry.

Solution-state NMR methods generally have better line resolution than solid-state methods; however, given the molecular complexity of NOM and its fractions, high resolution NMR is not necessarily advantageous. Solution-state ^{13}C -NMR and ^1H -NMR were used to characterize the International Humic Substances Society collection of reference fulvic and humic acids [131]. A problem for solution-state NMR is that certain NOM preparations may not be completely soluble. Solid-state NMR methods mostly avoid the solubility problem, although partial hydration of soluble samples by adsorbed water may result in changes and even loss of signal [132]. It is therefore necessary to completely dry the sample before spectrometric analysis.

6.6.1. ¹³C-NMR Spectrometry

¹³C-NMR spectrometric characterization of NOM is essential for quantitative structural analyses. For solid-state, cross-polarization, magic angle spinning (CP/MAS) ¹³C-NMR, sensitivity is greatly improved (compared to direct polarization of carbon in both liquid- and solid-state) by cross-polarization of carbon by protons in NOM structures [31]. Line resolution is improved and spinning side bands are eliminated by a combination of magic angle spinning and proton decoupling. Quantitative CP/MAS ¹³C-NMR of NOM is compromised by the unequal distribution of protons attached to carbon in NOM structures such that protonated carbons give greater responses than nonprotonated carbons. The solution to this differential response problem was elucidated by Alemany et al [133], who found that a contact time near 5 milliseconds was a reasonable compromise between loss of sensitivity (because of relaxation of carbon polarization) and a quantitative-equivalent response between protonated and nonprotonated carbons. A separate study by Wershaw et al [38] that compared quantitative solution-state ¹³C-NMR spectra of various DOM samples with CP/MAS ¹³C-NMR spectra of these samples confirmed that a 5 millisecond contact time gave the best quantitative results.

Table 6 Structural assignments for ¹³C-NMR spectra (ϕ = aromatic carbon)

Chemical Linkage	Compound Type	Chemical Shift Range (ppm)
C-H	Aliphatic hydrocarbon	0-55
C-N	Amines, Amides, Proteins	40-55
O-CH ₃	Methoxy groups in tannins and lignins	55-60
C-O	Aliphatic alcohols, ethers, and esters	60-90
O-C-O	Anomeric carbon in carbohydrates, Lactols	90-110
ϕ	Aromatic carbon	95-165
ϕ-O	Aromatic esters, ethers, and phenols	135-165
ϕ-SO ₃ H	Aromatic sulfonic acids	140-145
O=C-O,	Carboxylic acids, Esters,	160-190
O=C-N	Amides	
O=C-	Flavones, Quinones	170-200
C=C		
O=C-C	Aliphatic and aromatic ketones	190-220

For studies performed by the author, CP/MAS ¹³C-NMR spectra were preferred because of superior sensitivity compared to liquid-state spectra and because of their applicability to insoluble NOM samples. An example of the utility of the method is contained in the NOM structural assignments shown in Table 6. CP/MAS ¹³C-NMR spectra were obtained on 5 to 200 mg of NOM isolated from water or inorganic soil and sediment matrixes; freeze-dried samples were packed in ceramic rotors. CP/MAS ¹³C-NMR spectra were obtained on a 200 megahertz (MHz) Chemagnetics CMX spectrometer with a 7.5 mm-diameter probe. The spinning rate was 5000 Hertz. The acquisition parameters included a contact time of 5 milliseconds, pulse delay of 1 second, and a pulse width of 4.5 microseconds for the 90° pulse.

There is considerable overlap in the chemical shifts for various types of structures; therefore, determination of various structures in NOM NMR spectra is somewhat of a subjective exercise that depends on the judgment of the analyst. However, comparison with infrared spectra greatly strengthens spectral interpretation. For example, amide, carboxylic acid, ester, and quinone groups overlap in ¹³C-NMR spectra, but these groups are much better resolved in the infrared spectra.

CP/MAS ¹³C-NMR spectra for NOM fractions containing various compound classes are shown in Figures 36 and 37. The carbohydrate spectrum of Figure 36 was from the hydrophilic-acid-plus-neutral fraction in a DOM fractionation of beer [123]. The major peak near 75 parts per million (ppm) is from secondary alcohol carbon atoms in carbohydrates, and the peak near 175 ppm is from anomeric carbons. Carbohydrate acids are indicated by the carboxylic acid peak near 175 ppm in Figure 36.

N-acetyl aminosugars, isolated as colloids in the DOM from Anaheim Lake [18], give the CP/MAS ¹³C-NMR spectrum shown in Figure 36. In addition to the carbohydrate peaks, the methyl carbon of the N-acetyl group gives a peak near 20 ppm and the carbonyl carbon of the N-acetyl secondary amide gives a peak at 175 ppm. The carbonyl carbon peak has greater intensity than the methyl carbon peak because it includes both the amide and carboxyl carbonyl carbons which are not differentiated as they are in the infrared spectrum of colloids in Figure 32.

A CP/MAS ¹³C-NMR spectrum of proteins isolated in the amphiphilic neutral fraction from the South Platte River [122] is shown in Figure 36. Multiple peaks in the 40-55 ppm range indicate various C-N linkages in amide and amino groups in proteins. As with N-acetyl aminosugars, the carbonyl

carbon peak at 172 ppm overlaps the carboxylic acid carbon peak in this protein fraction. The remaining peaks indicate various aliphatic carbon (20-35 ppm), alcohol (75 ppm), and aromatic carbon (130 ppm) structures that occur in proteins.

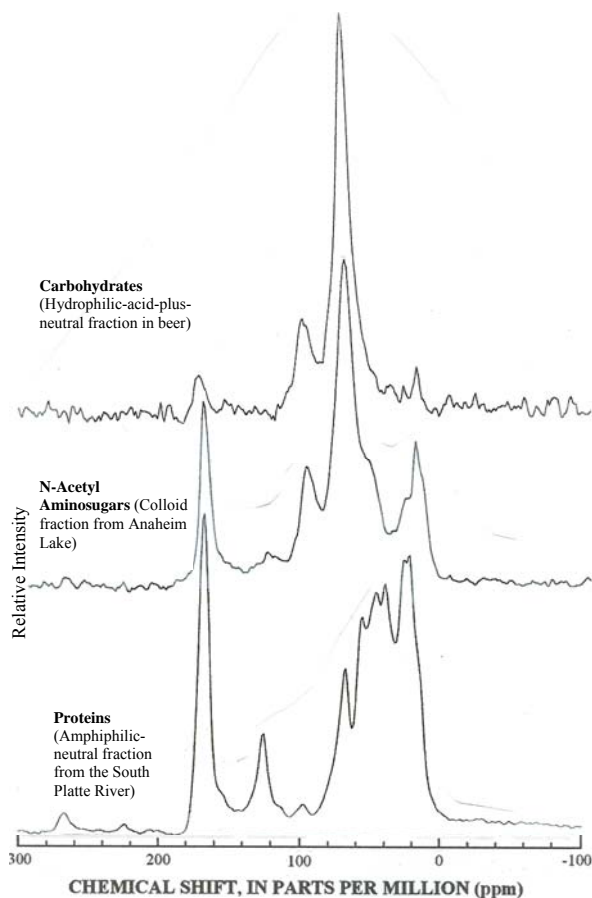


Figure 36 CP/MAS ^{13}C -NMR spectra of carbohydrates, N-acetyl aminosugars, and proteins in various NOM fractions

The Suwannee River fulvic acid sub-fraction derived from terpenoids [44] has the CP/MAS ^{13}C -NMR spectrum shown in Figure 37. Abundant methyl groups in terpenoid structures are indicated by the peak at 20 ppm, and carbon atoms in aliphatic, alicyclic ring structures are indicated by the peak at 40 ppm. These terpenoid structures also contain aromatic and alkene carbon atoms indicated by the broad peak near 130 ppm, but a distinct peak for phenolic carbon near 150 ppm is not observed. This fulvic acid sub-fraction, which resulted from partial oxidation of terpenoid precursors, is also rich in carboxylic acids, as indicated by the peak near 175 ppm.

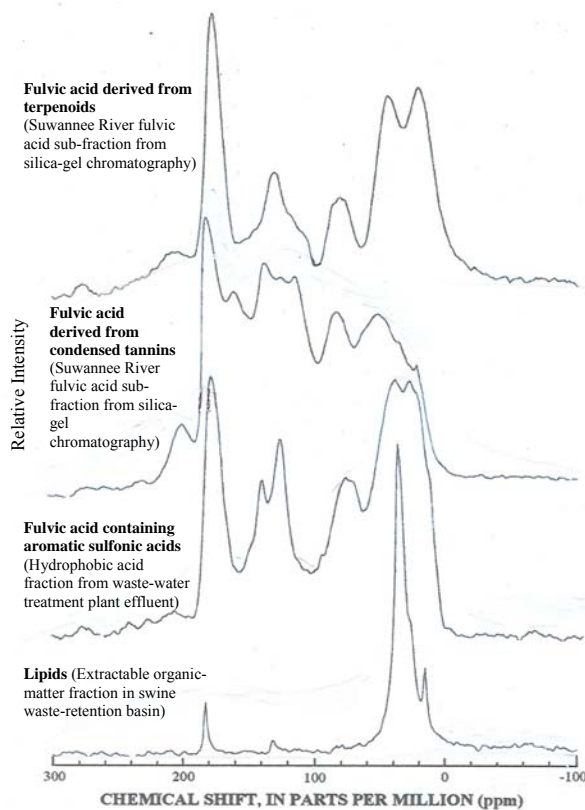


Figure 37 CP/MAS ^{13}C -NMR spectra of fulvic acid derived from terpenoids and condensed tannins; fulvic acid containing aromatic sulfonic acids; and lipids

The CP/MAS ^{13}C -NMR spectrum (Figure 37) of the Suwannee River fulvic acid sub-fraction derived from condensed tannins [91] differs from the terpenoid-derived fulvic acid by the diminished methyl peak near 20 ppm, the aromatic carbon peak at 107 ppm, and the phenolic carbon peak near 155 ppm. The aromatic carbon peak at 107 ppm is indicative of carbon-substituted aromatic carbons between meta-hydroxy groups in the A-ring of condensed tannins [38,134]. CP/MAS ^{13}C -NMR dipolar-dephased spectra (which detect only quarternary-substituted carbon and methyl carbon atoms) are useful in distinguishing lignin- [135] from tannin- [135] from terpenoid- [44] derived NOM. Figure 38 illustrates how CP/MAS ^{13}C -NMR dipolar-dephased spectra can distinguish between terpenoid-derived fulvic acid and tannin-derived fulvic acid. Terpenoid-derived fulvic acid (sub-fractions F 2/1 and F 2/4) has significant peaks at 42 ppm (quarternary aliphatic C-C) and 85 ppm (quarternary aliphatic C-O), whereas tannin-derived fulvic acid (sub-fractions F 3/2, F 4/4, F 5/3, and F 6/3) has significant peaks at 107 ppm

(quaternary aromatic C-C between meta C-O) and 155 ppm (quaternary aromatic meta C-O). There is some cross-over of diagnostic terpenoid peaks with tannin peaks which may indicate incomplete mixture separation or coupling of terpenoid with tannin components in the fulvic acid. A number of spectral-editing pulse sequences in liquid-state ^{13}C -NMR spectrometry, such as the attached proton test (APT), can also be used to differentiate methyl, methylene, methane, and quaternary carbon, as illustrated by Thorn et al.'s characterization of the structural differences in the various humic and fulvic acid standards of the International Humic Substances Society [131].

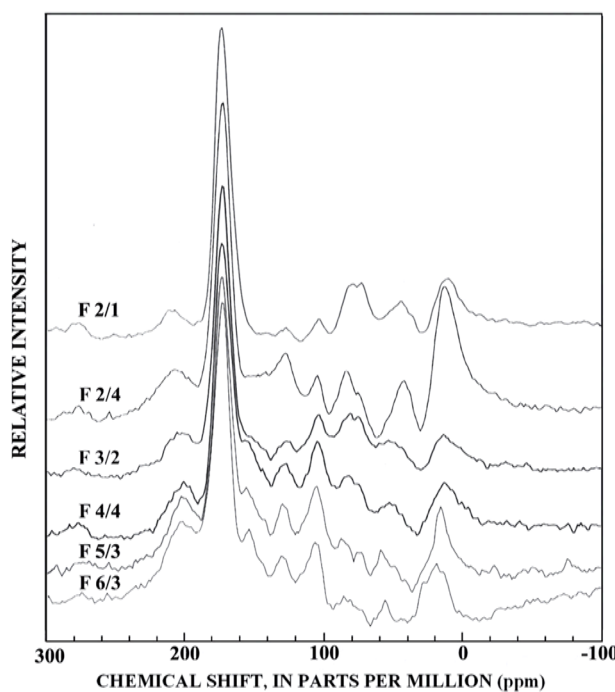


Figure 38 CP/MAS ^{13}C -NMR dipolar-dephased spectra of selected major numbered sub-fractions of Suwannee River fulvic acid [44]

Aromatic sulfonic acids derived from anionic surfactants are indicated by the 140 ppm peak of the C-SO₃H linkage in the CP/MAS ^{13}C -NMR spectrum (Figure 37) of the hydrophobic acid fraction from a waste water effluent discharged into the Santa Ana River basin in southern California [125]. Straight-chain methylene structures in NOM give a sharp peak near 30 ppm, as shown by the CP/MAS ^{13}C -NMR spectrum of lipids (Figure 37) in the extractable

organic matter fraction in sediment from a swine waste-retention basin [84].

A series of CP/MAS ^{13}C -NMR spectra of the conversion of lignin to black carbon char during heating at 350°C for various times is shown in Figure 39 [136]. Unheated lignin gives characteristic peaks at 55 ppm (OCH₃) and 147 ppm (aromatic C-O). During the first 8 hours of heating, methoxy groups are lost from lignin and the residue is mainly aromatic black carbon. Further heating to 72 hours produces aromatic carboxylic acid and phenolic lactone structures (broad peak near 165 ppm). Heating of bark, cellulose, and wood produces similar results [136]. Black carbon char residues are common constituents of many soils and sediments and can be detected by ^{13}C -NMR spectrometry [137,138].

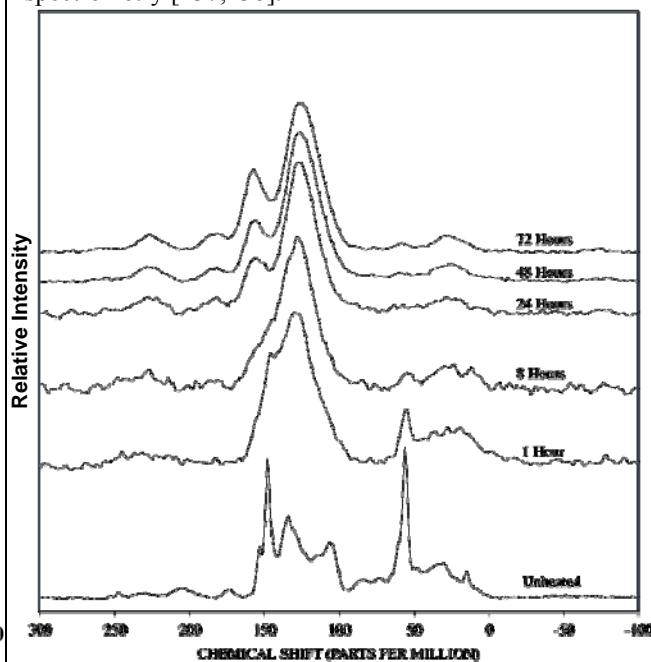


Figure 39 CP/MAS ^{13}C -NMR spectra of lignin heated at 350° C for various times [136]

6.6.2. ^1H -NMR Spectrometry

Quantitative and qualitative structural information on the hydrogen distributions in NOM can be obtained by ^1H -NMR spectrometry. This information is useful for apportioning hydrogen in an empirical formula into a quantitative, average structural model as was done for the Suwannee River fulvic acid [139]. For NOM samples that are soluble in deuterated water or deuterated organic solvents, liquid-state ^1H -NMR spectra provide information about exchangeable (OH, NH, and COOH) and non-exchangeable (CH, CH₂,

CH₃, and aromatic H) hydrogen distribution [140]. Sample preparation, sample drying involving deuterium exchange, sample concentration, spectral acquisition parameters, phasing, and solvent selection are all important considerations in obtaining high-quality spectra. In solid-state ¹H Combined Rotation and Multiple Pulse (CRAMPS) NMR, line widths are broad, and inclusion of exchangeable protons over a wide range of chemical shifts tends to smear out the spectra so that little useful information is obtained for NOM samples if the ratio of exchangeable to non-exchangeable protons is large. ¹H-CRAMPS-NMR

has been used to estimate aromatic and aliphatic protons in coal [31].

Solution-state ¹H-NMR spectra of Suwannee River fulvic acid in various solvents are shown in Figure 40 [140]. The exchangeable-proton OH peak may be combined with OH of protic solvents such as methanol or water, or it may be a broad peak in aprotic solvents such as dioxane-*d*₈ or DMF-*d*₇. Total exchangeable protons in Suwannee River fulvic acid were quantitated by the integral of the OH peak of the sample dissolved in dioxane-*d*₈ (Figure 40) after subtraction of aromatic hydrogen in the spectrum of the sample dissolved in deuterium oxide [140].

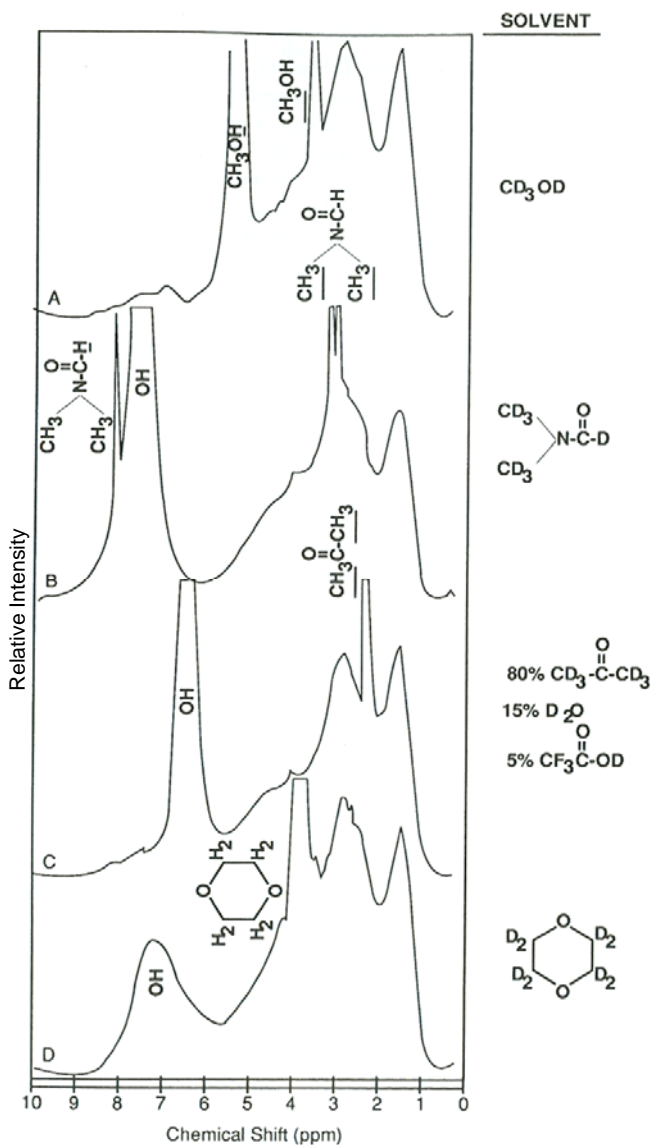


Figure 40 ¹H-NMR spectra of 100 mg/mL of Suwannee River fulvic acid dissolved in (A) methanol-*d*₄; (B) N,N-dimethylformamide-*d*₇; (C) 80% acetone-*d*₆, 15% D₂O, 5% trifluoroacetic acid-*d*₁, (D) dioxane *d*₈; spectra were acquired on a Varian FY-80A NMR spectrometer [140]

exchangeable ^1H -NMR spectra are dominated by methyl and methylene groups, as the ratio of hydrogen to carbon is 3:2:1 for methyl, methylene, and methine groups, respectively. Aliphatic hydrogen atoms are divided into three peaks noted on Figure 41: aliphatic 1 hydrogens are attached to methyl and methylene groups removed two or more carbon atoms from a carbonyl group or aromatic ring; aliphatic 2 hydrogens are attached to methyl, methylene, and methane groups adjacent to a carbonyl group or aromatic ring; and aliphatic 3 hydrogen atoms are attached to hydroxyl, ester, or ether carbons. The structural information provided by the aliphatic 1 and 2 peaks in ^1H -NMR spectrometry is not provided by ^{13}C -NMR spectrometry in which there is greater peak overlap of various aliphatic carbon structures. Aliphatic ketones are a significant component of the aliphatic 2 peak, because when ketones were reduced with sodium borohydride to alcohols, about one-third of the hydrogen atoms in the aliphatic 2 peak were shifted to the aliphatic 3 peak [143]. Olefinic hydrogen atoms are not seen as a separate peak; they overlap with hydrogen atoms in anomeric carbon and ester structures. Aromatic hydrogen gives a broad peak with a sub-peak near 6.8 ppm that is assigned to hydrogen atoms alpha to an aromatic C-O linkage.

6.6.3. ^{15}N - and ^{31}P -NMR Spectrometry

Nitrogen and phosphorus are significant elements in NOM as shown by the C:N:P Redfield ratio in phytoplankton of 106:16:1. The low natural abundance of ^{15}N of 0.37% results in a receptivity that is about fifty-fold lower than that of a ^{13}C -NMR study of NOM. The first ^{15}N -NMR studies of NOM were therefore obtained with ^{15}N -enriched composts and melanoidins. However, improvements in NMR instrumentation have enabled characterization of nitrogen in plant composts and native humic materials by natural abundance ^{15}N CP/MAS and solution-NMR spectrometry [79]. For all NOM samples of this study, 80 to 90% of the nitrogen occurred in a single peak near -250 ppm, which corresponds to amide nitrogen. This was surprising to NOM researchers, considering that various types of heterocyclic nitrogen (pyrroles, indoles, purines, and pyrimidines) had been postulated to account for nitrogen in NOM structures. However, proteins, peptides, N-acetyl aminosugars, and lactams (from porphyrin degradation) are all amides that contribute to this single peak in the ^{15}N -NMR spectra. The remaining 10 to 20% of the nitrogen corresponded to various types of aminoacids found in side chains in proteins and peptides.

Thorn [144] has used ^{15}N -NMR with ^{15}N -labeled reagents to investigate reactions and fixation of ammonia, aniline, hydroxylamine, nitrite, and nitroaromatic explosives to NOM. In the hydroxylamine study [145], ketone and quinone groups in humic and fulvic acids reacted to form the expected oximes, but ^{15}N -NMR also revealed unexpected hydroxamic acid, nitrile, oxazole, oxazolone, isocyanide, amide, and lactam derivatives.

Organic phosphorus is found in NOM metabolites, phospholipids, and in nucleotides in NOM. ^{31}P is found at 100 % natural abundance, and it can be detected by NMR at high sensitivity. However, because of the low percentage of organic phosphorus in NOM, extensive concentration, purification, and isolation procedures must be employed that do not hydrolyze organic phosphate esters. For NOM in lake water concentrated by ultrafiltration and reverse osmosis, Nanny and Minear [146] found broad, poorly resolved peaks between -10 to 10 ppm, whose chemical shifts indicated mono- and di-ester phosphates. Resolution was improved by adding the lanthanide-shift reagent PrEDTA. A small peak between 20 and 30 ppm indicated phosphonates (C-P linkage) in certain lake water samples. Phosphonates originate from cellular membranes and algal cells. ^{31}P -NMR studies of alkaline extracts of soils and sewage sludges detected mono- and di-ester phosphates as the predominant form of organic P, but phosphonates, pyrophosphate, polyphosphates, and orthophosphates were also detected [147].

6.6.4. ^{27}Al -, ^{11}B -, ^{113}Cd -, ^{133}Cs -, and ^{29}Si -NMR Spectrometry

NMR spectrometry of selected inorganic species with isotopes suitable for NMR spectrometry has yielded significant information about complexing groups in NOM structures. An ^{27}Al -NMR study [148] of reaction of aquatic humic substances with aluminum at pH 2.5 to pH 4.5 found that aluminum formed five-membered-ring inner-sphere chelate complexes that give peaks at 6.5 ppm (1:1 aluminum:NOM complex), 12.4 ppm (1:2 complex), and 16.5 ppm (1:3 complex). Various model organic acids were also studied, and from similarities in the ^{27}Al -NMR spectra the NOM-complexing groups were ascribed to α -hydroxy aliphatic carboxylic acids. The relative concentration of the higher ratio NOM complexes increased as the NOM concentration increased. At higher pH values various hydroxy-aluminum complexes formed.

Boric acid concentrations in water are significantly correlated with DOM concentrations, which provides circumstantial evidence for boric acid complex formation with DOM [8]. Specific evidence of the nature of these complexes was provided by a solid-state magic angle spinning ^{11}B -NMR spectroscopy study of boric acid adsorption on calcium-flocculated Aldrich humic acid [149]. Significant boric acid complexation with humic acid was observed between pH 6 and 12, with the maximum adsorption between pH 9.5 and 10. Five- and six-membered-ring chelates were formed with 1,2- and 1,3- diols at pH 8 to 11. Borate complexes were also formed with dicarboxylate structures at pH values from 6 to 9.

^{113}Cd is an excellent isotope for NMR studies because of its relatively high natural abundance and broad range of chemical shifts (900 ppm). A ^{113}Cd -NMR study of cadmium binding to Suwannee River DOM found that cadmium was principally complexed to oxygen (carboxyl and hydroxyl functional groups) at pH values from 3.5 to 11 [150]. Cadmium binding to nitrogen functional groups increased with pH until up to one-third of the cadmium was bound with nitrogen. A small amount of cadmium binding with sulfur functional groups at alkaline pH values was also detected. The binding exchange rate was faster in acid solutions, where free Cd^{2+} ions predominate.

Cesium ion (Cs^+) is an alkali metal cation expected to have only weak interactions with NOM because of its low charge density. A ^{133}Cs NMR study [151] of cesium interaction with Suwannee River DOM found the cesium was bound at pH values from 3.4 to 9.0 through outer-sphere complexes that rapidly exchange with free Cs^+ in the bulk solution. Cesium binding with NOM at constant cesium concentrations also decreased as the pH increased.

Aqueous silicic acid and mineral silicates are found in high concentrations in soil, sediment, and water. ^{29}Si -NMR has been extensively used to investigate silicate minerals, but there are no known studies at this time (2008) where it has been used to investigate silicate NOM interactions. However, a ^{29}Si -NMR study [9] found that aqueous solutions of various polyols rapidly form stable five- and six-coordinated silicate ions in alkaline solutions. The authors suggested that this finding plays a significant role in the biological uptake and transport of silicon, and in mineral diagenesis. As various polyhydroxy species are common in certain NOM fractions, such as the colloidal fraction, ^{29}Si -NMR spectrometry would be a promising area of investigation for future research.

6.6.5. Multidimensional NMR Spectrometry

Multidimensional NMR spectrometry generates multiple variable plots in which the variables are NMR nuclei (^{13}C versus ^1H), nuclear Overhauser effects (spatial interactions between nuclei), and a variety of pulse sequences that affect nuclei coupling and relaxation. Multidimensional NMR experiments can be performed in both the solid and liquid state. They have acronym names such as total correlation spectroscopy (TOCSY), correlation spectroscopy (COSY), nuclear Overhauser effect spectroscopy (NOESY), heteronuclear single quantum coherence (HSQC), heteronuclear multiple bond connectivity (HMBC), diffusion ordered spectroscopy (DOSY), and heteronuclear correlation spectroscopy (HETCOR) [152]. In a study of humic substances isolated from a variety of soils, Simpson et al [153] applied a wide range of multidimensional solution-state NMR spectral methods to show that soil humic substances are aggregates of relatively low molar mass aliphatic acids, ethers, esters, alcohols, lignins, polysaccharides, and polypeptides.

An example of a solid-state HETCOR experiment performed by Mao et al [154] on the hydrophilic colloid fraction isolated from biosolids is shown in Figure 42. These colloids give a ^{13}C -NMR spectrum nearly identical to the spectrum shown in Figure 36 and a similar infrared spectrum to that shown in Figure 32. By varying cross-polarization times and pulse sequences, different contour plots (plots a and b in Figure 42) were obtained that correlated carbons and protons separated by different distances. An advantage of the solid-state HETCOR experiment is that NOM solubility is not a limitation, and that both exchangeable and non-exchangeable protons can be correlated with carbon structural units. Exchangeable N-H hydrogen on N-acetyl groups in aminosugars near 7 ppm in the ^1H -NMR spectrum in Figure 42 correlates with the amide carbonyl peak near 175 ppm in the ^{13}C -NMR spectrum. If carboxylic acid groups were present in these colloids, the exchangeable carboxylic acid protons would be expected to give ^1H -NMR signals from 10 to 20 ppm, as was seen in a solid-state HETCOR spectrum of a peat humic acid [155]. Structural information that is not available with other spectral methods can be obtained in these multidimensional NMR experiments.

The HETCOR experiment on peat humic acid [155] revealed that carboxylic acids in this sample are predominantly near $-\text{O}-\text{CH}_n-$ protons. Specific structural information for CH_3 , $(\text{CH})_n$, OCH_3 , N-C-H, O-alkyl, anomeric carbon, aromatic, aromatic C-O,

COOH, and ketone/quinone groups was given by a HETCOR experiment on peat humic acid.

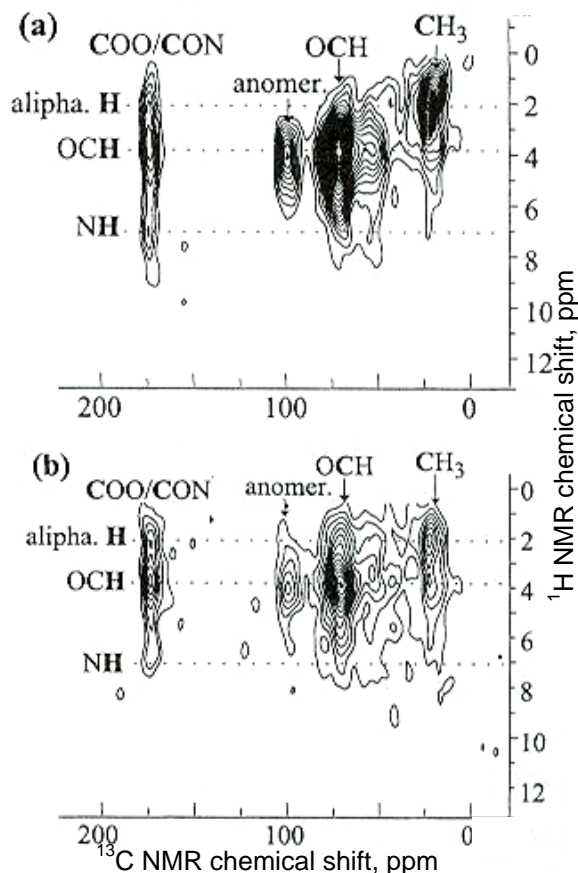


Figure 42 Two-dimensional HETCOR NMR spectra of > 12000 Dalton components of the hydrophilic colloid fraction isolated from biosolids: (a) showing correlations of protons and carbons separated by three or less bonds, and (b) showing correlations of protons and carbons separated by less than 6 Angstroms. Reprinted with permission from reference [154], Figure 4. Copyright 2003, American Chemical Society.

6.7. Mass Spectrometry

Mass spectrometry is a powerful technique for NOM characterization, but its application to NOM and interpretation of the mass spectra is a challenging exercise of current research interest. A comprehensive general reference for the principles and applications of various types of mass spectrometry is the text by Herbert and Johnstone [156]. Electrospray-ionization/mass spectrometry (ESI/MS) since its introduction by Yamashita and Fenn [157] is particularly suitable for

NOM analyses, given the nonvolatility and charge characteristics of most NOM molecular components. The reader is referred to the text edited by Cole [158] for descriptions of the fundamentals, instrumentation, and applications of ESI/MS.

Numerous studies have coupled gas chromatography with electron-ionization mass spectrometry to identify products of degradative studies of NOM [24,117], but the sum of the products typically accounted for only a few percent of the carbon in the NOM mass. Direct mass spectrometric analyses of NOM were partially successful using fast-atom-bombardment mass spectrometry [105], in that the molecular distribution of ions approximately corresponded to molar mass distributions determined by other methods, but the carbon accounting question remained. Ions were obtained at almost every mass unit up to 1000 Daltons, and the distribution lacked features from which additional structural information could be obtained.

The first application of ESI/MS to NOM analyses was a study of ground water organic acids by McIntyre et al. [159], who found this technique provided detailed molar mass data while minimizing fragmentation. An example of the molecular ion distribution for the Suwannee River fulvic acid given by low-resolution ESI/quadrupole MS is shown in Figure 43 [103]. Ions produced in both negative- and positive ion spectra were generally odd, which indicates an absence of nitrogen; the number- and weight average ion distributions (reported in Table 2) agreed well with equilibrium ultracentrifugation determination of molar mass distribution. This study [103] also determined the ESI/quadrupole MS of 15 selected carboxylic acids with both positive- and negative ion detection. The dominant ions generally detected were $[\text{M} + \text{Na}]$ for positive ions, and $[\text{M} - \text{H}]$ for negative ions; however, decarboxylation $[\text{M} - \text{H} - \text{COOH}]$ gave dominant ions for phenylmalonic acid, chelidonic acid, and coumarin-3-carboxylic acid. Dehydration $[\text{M} + \text{Na} - \text{H}_2\text{O}]$ gave a dominant ion for galacturonic acid; the triply-charged negative ion $[\text{M} - 3\text{H}]^{3-}$ was the dominant ion for glycyrrhizic acid, and lasalocid acid fragmented to produce a dominant positive ion at m/z 377. Molecular aggregate ions of lower intensity were detected as dimers (tricarballic acid, coumarin-3-carboxylic acid, cyclopentane tetracarboxylic acid, coumalic acid, chelidonic acid, chlorogenic acid, galacturonic acid, and lasalocid acid), trimers (coumalic acid and coumarin-3-carboxylic acid), and tetramers (coumalic acid). Glycyrrhizic acid gave almost no positive ions. Therefore, this ESI/quadrupole MS study indicated aggregation,

decarboxylation, dehydration, fragmentation, and lack of detection as likely problems in the interpretation of ESI/MS spectra of NOM as a molar mass distribution.

An additional factor for ESI/MS molecular ion distributions are variabilities in molar responses (ionization efficiencies) [108]. For an equimolar mixture of 10 carboxylic acids of different polarities, the molar response for negative ions systematically increased as the polarity decreased. Lasalocid acid, whose structure is mainly aliphatic and alicyclic hydrocarbon, has a molar response that is 126 times

that of highly polar citric acid. Methylation of these two acids decreased the molar response difference to a factor of 26. Methylation of Suwannee River fulvic acid decreased the molecular ion distribution (Table 2), indicating that molecular aggregation through hydrogen-bonding of free acid groups skewed the molecular ion distribution to greater masses. Other types of mass spectrometry (ESI/time-of-flight (TOF)) [107] and ESI/ion-cyclotron resonance (ICR/MS) [106] have also detected significant amounts of molecular aggregates in fulvic acid.

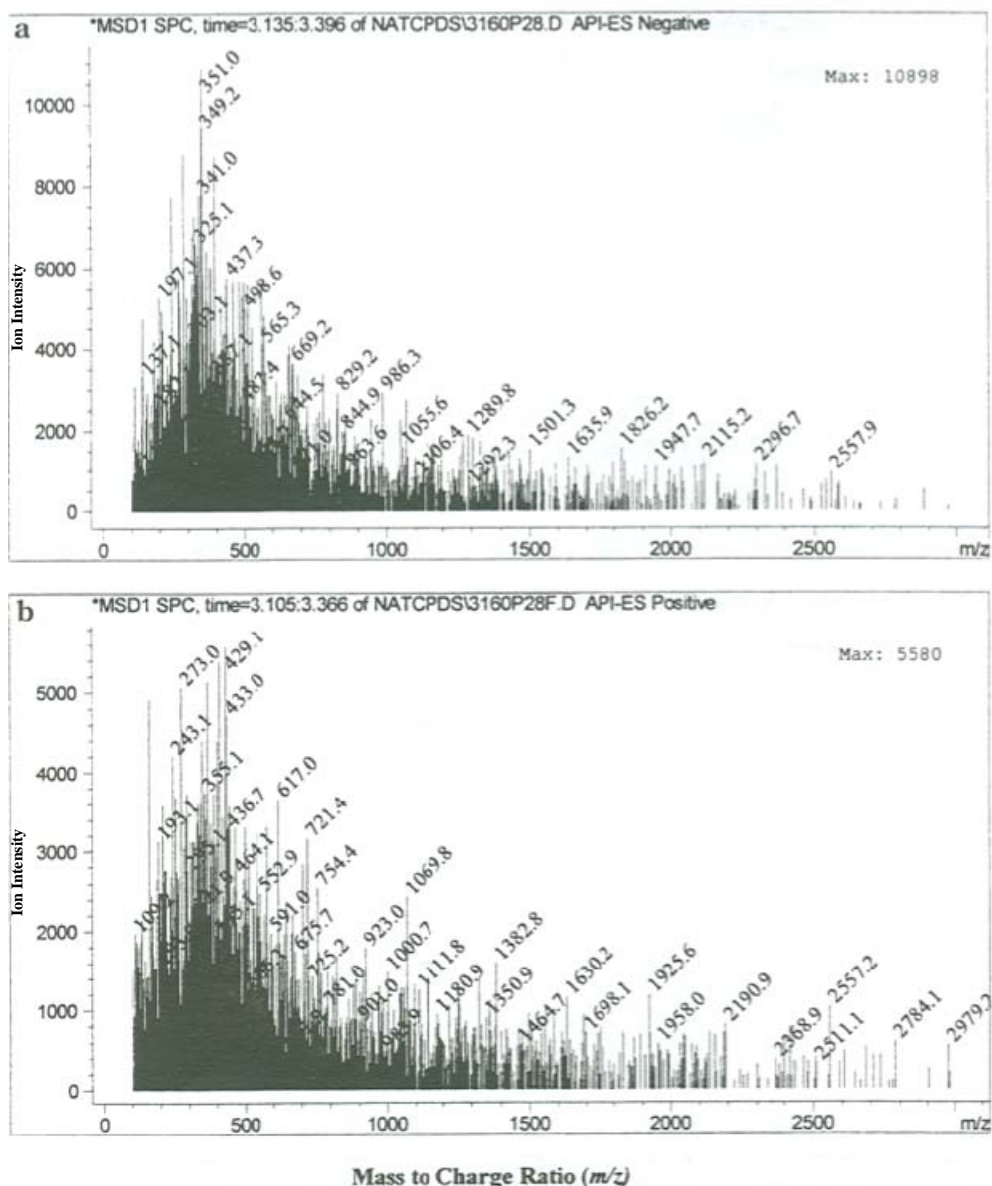


Figure 43 Electrospray spectra of Suwannee River fulvic acid in (a) negative ion mode and (b) positive ion mode [103]

The formation of multiply-charged ions is a function of molecular distance between charged groups in molecular structures. Polycarboxylic acid standards (up to four carboxyl groups/molecule) did not form multiple-charged ions for molar masses up to about 200 Daltons because electrostatic field effects favored single-charged ions [103]. However, the linear polymer of poly(acrylic acid) of average molar mass 2000 Daltons produced numerous multiple-charged ions that greatly decreased the apparent molar mass distribution to number-average values near 400 [104]. The same multiple-charging effect with size was noted for glycyrrhizic acid. Polyacrylic acid also formed cyclic six-membered ring anhydrides accompanied by the loss of water between adjacent carboxyl groups.

Mass spectrometers with ion storage systems such as ion traps [103] and ion cyclotrons [106] give lower ion mass distributions for Suwannee River fulvic acid than for ESI/quadrupole MS [103]. These lower distributions likely result from decarboxylation,

dehydration, disaggregation, and fragmentation reactions in ion storage systems. ESI/ion-trap MS can give multiple daughter ion mass spectra that can provide detailed information about NOM structure.

An example of a multiple-daughter ion ESI/ion-trap MS spectra of Suwannee River fulvic acid is shown in Figure 44. The m/z 329 negative ions selected from the spectrum presented in Figure 43 were successively fragmented in four stages following water loss from each stage. The negative ions at m/z 329 are a mixture of compounds and isomers, with the number of peaks and the complexity of the spectrum (Figure 44, spectrum A) reflecting the mixture characteristics. The dominant peaks occur at intervals of m/z 18, indicating dehydration, and m/z 44, indicating decarboxylation. As the number of MS stages of the product ions increases, the spectra become increasingly simple until only one product ion at m/z 109 which cannot be further fragmented is detected (Figure 44, spectrum D).

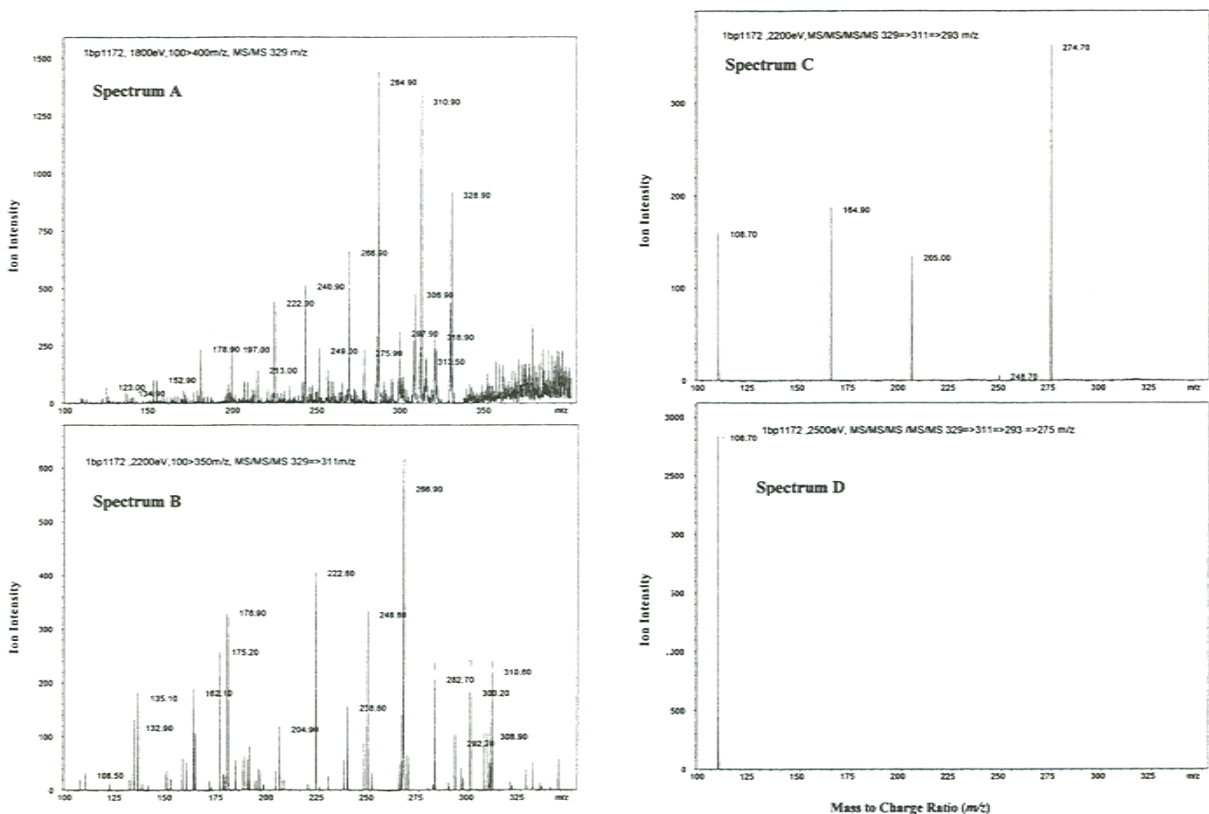
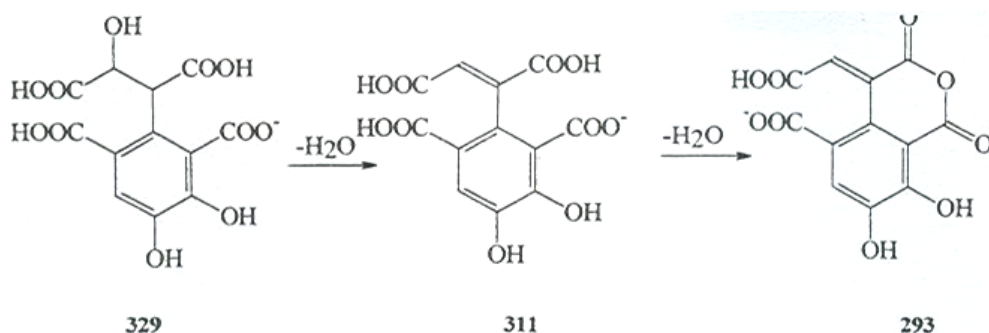


Figure 44 A series of MSⁿ ($n = 2-4$) which follow the loss of water (m/z 18) from the m/z 329 ion of Suwannee River fulvic acid, m/z 329→311→293→275 [103]

Dehydration steps leading to the m/z 293 product ion



Hypothetical fragmentation of the m/z 293 product ion

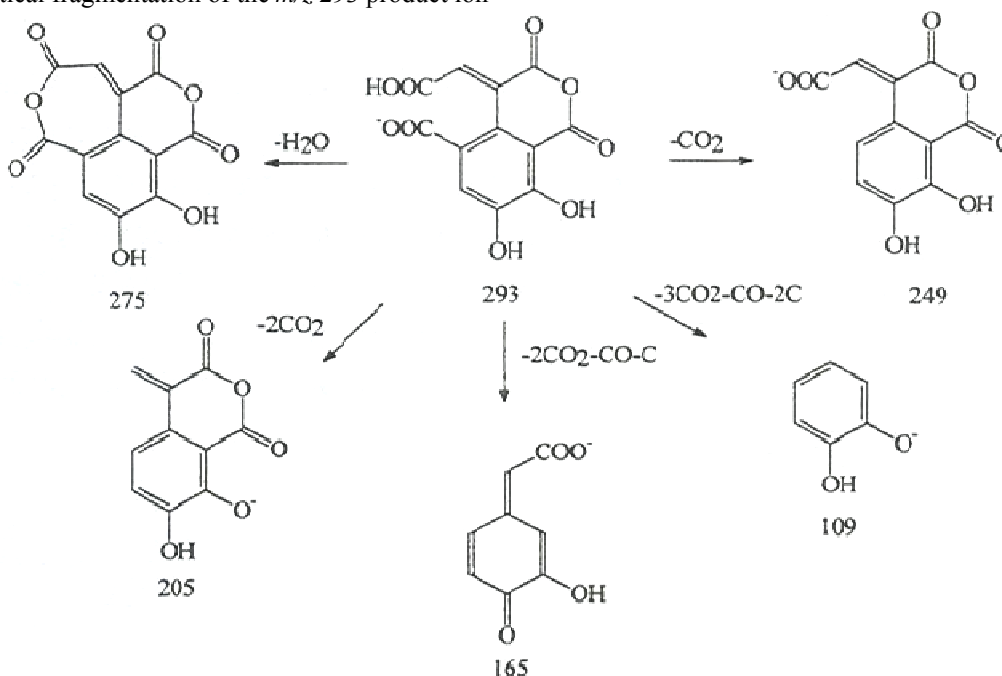
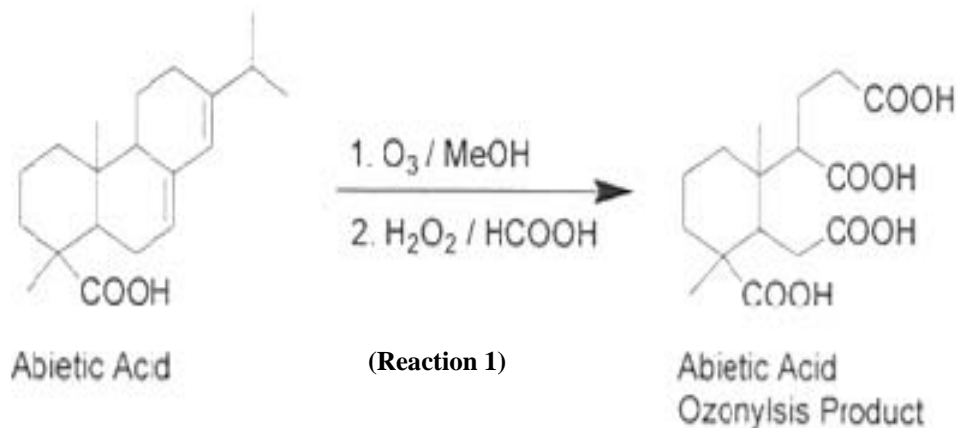


Figure 45 Hypothetical fragmentation pathway for multiple ESI/ion-trap MS spectra presented in Figure 44

The simplicity of the fragmentation pattern for the m/z 293 ion (Figure 44, spectrum C), and the similarity of this fragmentation pattern to multiple MS spectra for certain polycarboxylic acid standards, suggest that the m/z 293 ion is derived from a single compound in Suwannee River fulvic acid. A hypothetical fragmentation pathway involving alcohol dehydration, cyclic-anhydride formation, decarboxylation, and neutral water, carbon dioxide, carbon monoxide, and carbon losses that leads to the final m/z 109 ion is presented in Figure 45.

A high-resolution ESI/MS study [160] of ionization and fragmentation of Suwannee River

fulvic acid noted a homologous series of ions separated by two Daltons (attributed to differences in double bonds and ring structures) and by ion clusters separated by 14 Daltons (attributed to differences in methylene groups). These ion series were investigated in greater detail in a study of terpenoid precursors of fulvic acid [44]. An example of these homologous-ion series is shown in Figure 46 in the ESI/MS spectrum (spectrum A) of fulvic acid isolated from ground water in Australia. These ion clusters were postulated to be derived from oxidation of terpenoid precursors such as abietic acid. An abietic acid standard was oxidized with ozone as shown in Reaction 1.



The similarity of the homologous series of ion clusters produced by abietic acid oxidation and the similarity of the product ion MS/MS spectra shown in Figure 46 is strong evidence of the terpenoid source of this fulvic acid and of the oxidation process that gives a homologous series of carboxylic fulvic acid molecules.

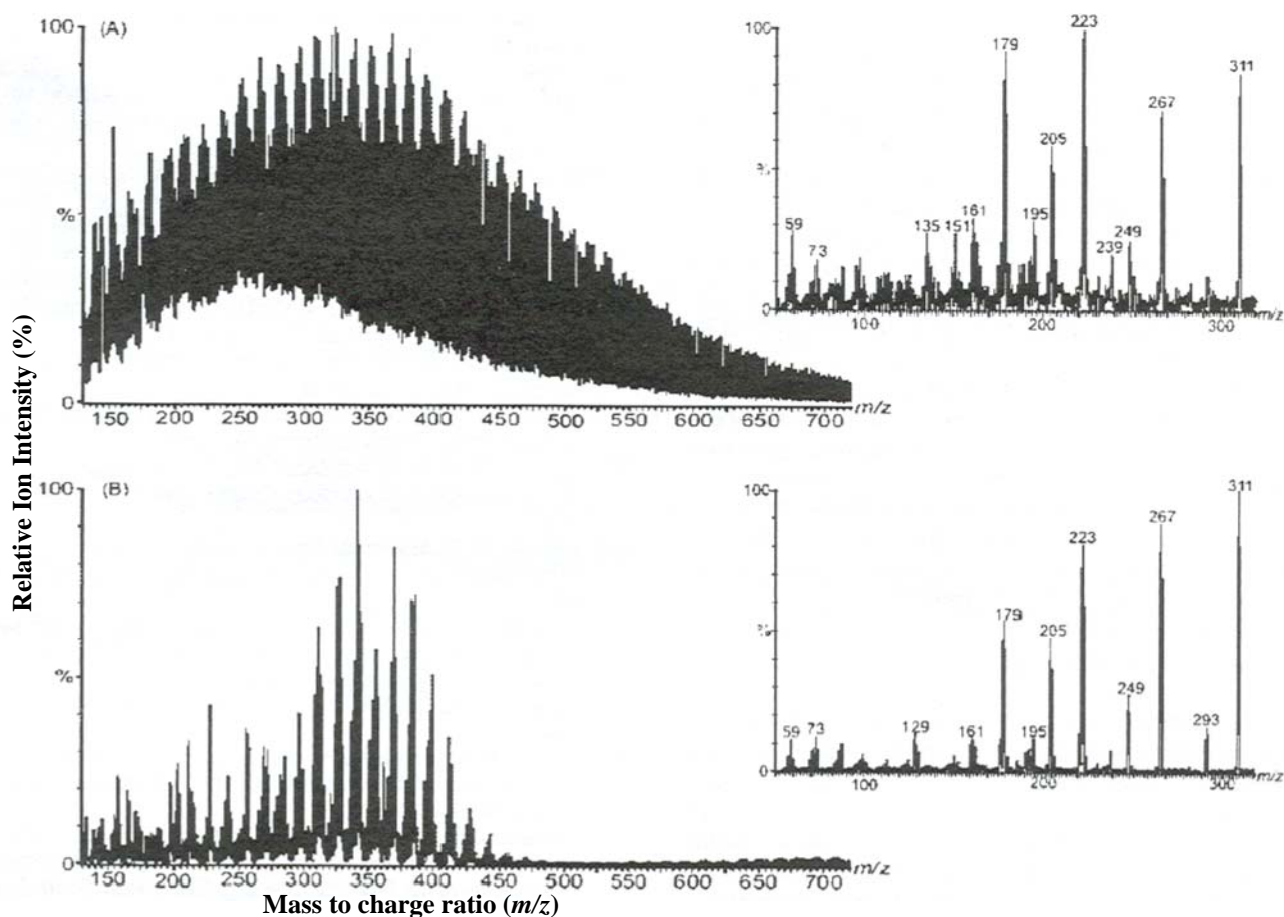


Figure 46 Electrospray-ionization mass spectra (ESI/MS) of fulvic acid isolated from the Tomago Sand Beds (A) and the ozonation product of abietic acid (B); product-ion spectra (ESI/MS/MS) of m/z 311 ion for each sample are shown as spectra C and D.

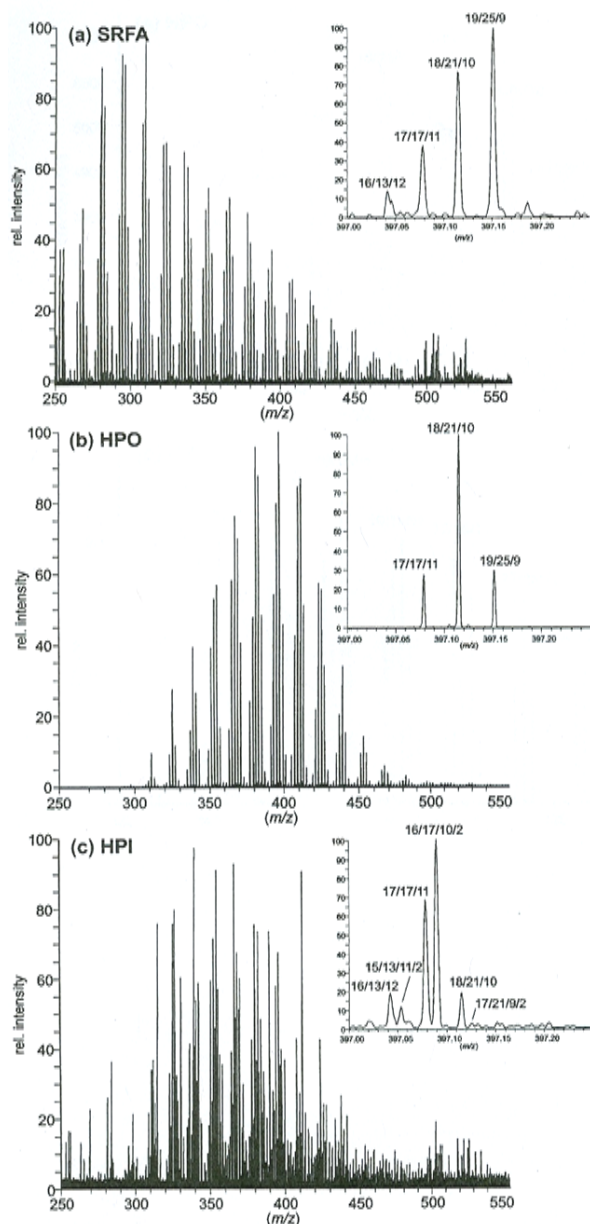


Figure 47 FT-ICR-MS scan spectra (ESI-negative) of (a) Suwannee River fulvic acid (SRFA) isolated from fresh water and of dissolved organic matter from the deep South Atlantic Ocean, separated into (b) a hydrophobic fraction (HPO), and (c) a hydrophilic fraction (HPI); insets show the extended mass spectra for m/z 397.000-397.25 (in panels a and b, the numbers denote the number of C/H/O atoms of the anions; in panel c, they denote the number of C/H/O/N atoms of the anions). Reprinted with permission from reference [77], Figure 1. Copyright 2008, American Chemical Society.

The most exciting development in mass spectrometry is the ultrahigh mass resolution provided by electrospray ionization Fourier-transform ion-cyclotron-resonance mass spectrometry (FT-ICR-MS) [160,161]. For the first time, individual NOM molecules can be separated with baseline resolution, as shown in Figure 47, for the mass spectra of DOM fractions isolated from the deep ocean [77]. Each peak in low resolution mass spectra contains several peaks of differing elemental composition in the ultrahigh resolution of FT-ICR-MS, as shown in Figure 47.

Elemental composition can be computed from accurate mass measurements, and elemental analyses of various NOM anions are shown in Figure 47. The hydrophilic NOM fraction isolated for the first time from seawater contained up to three nitrogen atoms per molecule. This nitrogen was neutral in character, and was part of the aliphatic, alicyclic-ring structure [77].

The molecular composition of NOM analyzed by FT-ICR-MS can be plotted as a van Krevelen diagram [161,162]. Precursor compound classes can be mapped on the Van Krevelen plots and the various diagenetic reactions (methylation, demethylation, hydrogenation, dehydrogenation, hydration/condensation, oxidation/reduction) that alter the elemental composition of NOM precursors are shown as line patterns on the plots. As FT-ICR-MS is the only technique that achieves molecular separations of complex NOM mixtures, it would be useful to couple this technique with tandem mass spectrometry and possibly other spectral characterization methods to achieve ultimate molecular characterization of NOM. However, the various advanced mass spectrometric characterizations presented in this section still give qualitative rather than quantitative data about NOM because of the many limitations concerning the introduction and detection of NOM molecules in mass spectrometers.

6.8. Ultraviolet/Visible Spectrometry

Ultraviolet (UV)/Visible (Vis) spectrometry spans about 180 nanometers (nm) to 760 nm in the electromagnetic spectrum, with 380 nm being the division between ultraviolet and visible spectrometry. Ultraviolet light is absorbed by pi-electron transitions in simple chromophores, with one or a few double bonds such as exist in an aromatic ring; visible light is absorbed by extended conjugated double-bond systems that exist in dyes and pigments. The UV spectra of NOM dissolved in water [72] are mostly featureless spectra which increase exponentially as the wavelength decreases, as shown in Figure 48.

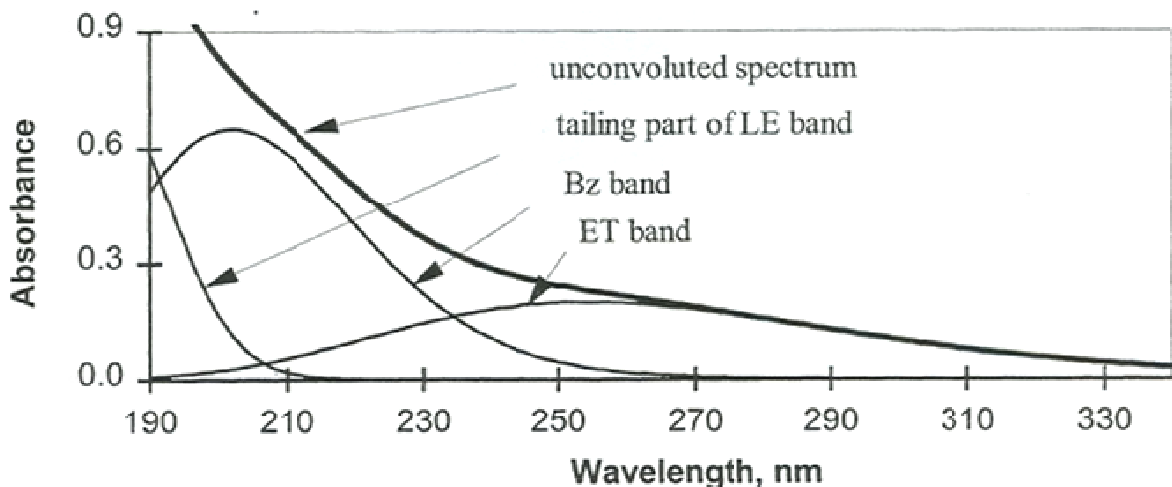


Figure 48 Summation of three composite absorption bands (LE, local excitation; Bz, benzenoid; and ET, electron transfer) and formation of unconvoluted UV-absorbance spectrum of NOM. Reprinted with permission from reference [72], Figure 2.2, Copyright 2000, American Water Works Association

Korshin et al. [163] proposed modeling the UV-absorbance spectra of NOM as a composite of three Gaussian bands in aromatic chromophores of NOM, as shown in Figure 48. These bands are the local excitation (LE), benzenoid (Bz), and electron-transfer (ET) bands in simple aromatic compounds. The broad peak shape of each of these bands and the lack of peaks in the composite spectrum result from overlap of these bands at differing wavelengths in the complex mixture known as NOM.

The ratio of the UV adsorbance at 254 nm (UV_{254}) near the peak of the ET band to the DOC concentration is often used to estimate the aromatic carbon content of NOM in solution [164]. This ratio has become known as the specific UV absorbance (SUVA) of NOM. Chin et al [165] correlated SUVA of aquatic humic substances measured at 280 nm with aromatic carbon content and weight average molar mass determined by high-performance size-exclusion chromatography. Visible absorbance (or "color") of NOM solutions at 400 nm was found to correlate with trihalomethane formation potential (THMFP) when reacted with chlorine [166], and SUVA was also found to generally correlate with THMFP [167]. However, SUVA has its limitations as a predictor for THMFP. This is because activated aromatic rings such as meta-hydroxybenzene structures in tannins give high yields of chlorinated disinfection by-products such as trihalomethanes, whereas deactivated aromatic rings without phenols (aromatic carboxylic acids and sulfonic acids) give low yields. Non-humic materials, operationally defined as NOM fractions with low

SUVA values such as the hydrophilic fractions in Colorado River water, also produce greater than predicted amounts of various chlorinated disinfection by-products [168].

The tail of the exponentially decreasing UV spectrum of NOM with wavelength continues into the visible region, but the spectral characteristics of the visible spectrum of NOM cannot be explained by superposition of numerous independent chromophores, as was done in Figure 48. The visible absorption tail appears to result from intramolecular charge-transfer interactions between hydroxy-aromatic donors and quinoid acceptors formed by the partial oxidation of phenols [169]. These authors monitored UV/Vis spectral changes during laser irradiation that was used to selectively destroy certain chromophores in Suwannee River humic and fulvic acid. The authors believed that these charge-transfer complexes are intra- rather than inter-molecular aggregates because of the independence of molar absorptivity with variable fulvic acid concentrations over the UV/Vis spectrum. Examples of NOM precursors that can form charge-transfer complexes with partial oxidation include lignin, polyphenols, tannins, and melanins.

The slope of the absorbance tail of humic substances in the visible region can be measured as the ratio of absorbance at 465 nm and 665 nm (the E_4/E_6 ratio). This ratio has been used by soil scientists to characterize humic substances, but varying interpretations of the meaning of this ratio existed for several years. The definitive study of the E_4/E_6 ratio

was conducted by Chen et al [170], who found that the ratio was inversely and linearly correlated with the molar mass determined by reduced viscosity. The E_4/E_6 ratio was also affected by pH, correlated with free radical concentration, was independent of humic- or fulvic acid concentration, and was not related to the relative concentration of condensed aromatic rings. The findings of this E_4/E_6 ratio study are in general agreement with the later study by Del Vecchio and Blough [169], who explain the visible absorption tail to be related to intra-molecular charge-transfer complexes.

6.9. Fluorescence Spectrometry

Fluorescence spectrometry is an attractive analytical tool because it is at least an order of magnitude more sensitive to NOM than is UV spectrometry. However, it has limited use for NOM structural characterization, as less than 1% of the aromatic structures in NOM emit light as fluorophores [171]. NOM fluoresces when irradiated at different wavelengths, and a spectral three-dimensional plot of excitation, emission, and intensity is known as an EEM spectrum. An example of an EEM spectrum of Suwannee River fulvic acid is shown in Figure 49 [172]. EEM spectral plots have been broadly related to different types of NOM as shown in Table 7 [173].

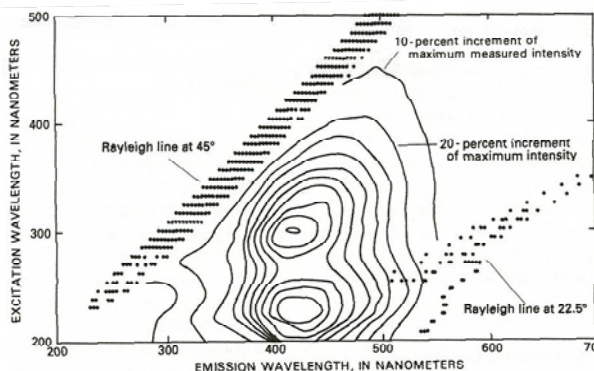


Figure 49 EEM spectrum of Suwannee River fulvic acid at pH 4.5 [172]

The Suwannee River fulvic acid EEM spectrum in Figure 49 is obviously “humic-like” according to Table 7, and these “humic-like” fluorophores in DOM have been identified as quinone structures [174] as changes in the EEM spectra of humic DOM from oxidizing and reducing environments were similar to spectra changes of quinone standards in the oxidized

and reduced state. EEM spectra of DOM fractions obtained from various New Jersey surface waters and treatment plant effluents gave distinctive plots that were characteristic of DOM sources and fraction composition [175]. Terrestrial sources of fulvic acid can be readily distinguished from microbial sources of fulvic acid in filtered whole-water samples by EEM spectrometry [176]. Various sources of DOM in the Santa Ana River, which drains a complex urbanized basin in southern California, were identified by EEM spectroscopy under both stormflow and base-flow conditions [177].

Table 7 Major component types in EEM spectra [173]

Range of Excitation (nm)	Range of Emission (nm)	Component Type
330-350	420-480	Humic-like
250-260	380-480	Humic-like
310-320	380-420	Marine humic-like
270-280	300-320	Tyrosine-like, protein-like
270-280	320-350	Tryptophan-like, protein-like, or phenol-like

NOM fluorescence is affected by the molecular size, the molecular conformation, and the extent of complexation with metal ions and with other organic molecules, leading to either fluorescence quenching or enhancement depending on the nature of the interaction [72,172]. NOM fractions with low molecular size have high excitation and emission intensity, and the position of the maximum in the emission spectrum shifts to lower wavelengths as the molecular size decreases.

6.10. X-ray Absorption Spectrometry

The development of better data analysis methods and the availability of synchrotron-based radiation sources [178] have led to the recent application of X-ray absorption spectrometry in structural studies of NOM. X-ray absorption spectrometry can be applied to most organic and inorganic elements, but the information obtained for organic elements in NOM is not sufficiently detailed and unique (with the exception of sulfur) when compared to other spectral methods previously discussed. Extended X-ray absorption fine-structure spectrometry (EXAFS) is sensitive to short-range order in crystalline and non-crystalline samples, and it is useful for studying NOM interactions with cations in inner-sphere complexes. X-ray adsorption

near-edge structure spectrometry (XANES) requires synchrotron radiation sources, and it gives information about binding energy and oxidation state of the selected element [179].

The nature of copper complexation with aquatic fulvic acids was investigated by both EXAFS [178] and XANES [180]. The EXAFS study revealed that copper was bound to a heterogeneous assemblage of functional groups that could not be approximated by specific binding sites found in salicylate or tetrahydrofuran carboxylate standards. The XANES study confirmed the non-uniform nature of copper binding sites, and found that at low copper concentrations ($Cu/C < 0.005$), nitrogen-containing functional groups were likely engaged in the complexation.

Sulfur XANES was used to identify multiple organic sulfur oxidation states in aquatic and soil humic substances [181]. Organic sulfur structures exist in oxidation states of -1 (thiols), 0 (thiol ethers), +2 (sulfoxides), +4 (sulfites and sulfones), +5 (sulfonates), and +6 (sulfate esters). Reduced sulfur species (thiols and thiol ethers) were the most abundant in Suwannee River humic and fulvic acid, whereas oxidized sulfur species (sulfate esters) were the most abundant in humic acids from a bog and a mineral soil. Significant amounts of sulfur species in the intermediate +2, +4, and +5 oxidation states were found for all samples. The finding of reduced thiols in these humic substances is significant in that they form strong complexes with the toxic trace metals Cd, Co, Ni, Pb, Zn, and Hg. A XANES study of Hg^{2+} binding to soil organic matter found very large binding constants ($K = 10^{32}$), with Hg^{2+} bound in two-fold coordination involving one reduced S and one O or N atom [182].

6.11. Degradative, Derivatative, and Chromatographic Characterizations

Separations of molecular species of NOM by high-resolution gas or liquid chromatography have generally not been successful because of the non-volatility of NOM (for gas chromatography), and because molecular complexity and aggregate properties (shown in Figure 27) cause liquid chromatograms of NOM and its fractions to resemble broad rather than sharply defined peaks. Therefore, chromatography of NOM is limited to the low-resolution fractionations and sub-fractionations discussed previously. However, if NOM is degraded by oxidation, reduction, hydrolysis, sodium sulfide or phenol cleavage, or thermal methods, and the degradation products are derivatized to increase their volatility for

gas chromatography or detectability for liquid chromatography, valuable structural information can be obtained by identifying low molar mass NOM-degradation products.

6.11.1. Oxidative Degradations

Various oxidative degradation methods have been used to investigate NOM structure because their application to studies of the structure of coal and lignin [4,117,118,183-185]. Alkaline permanganate oxidation has been the most commonly applied procedure, but NOM oxidations with alkaline cupric oxide, alkaline nitrobenzene, chlorine, nitric acid, and peracetic acid have been tested. These oxidative procedures yield a mixture of aliphatic mono- and polycarboxylic acids, benzene polycarboxylic acids, and phenolic carboxylic acids, which may have chlorine or nitrate substituents depending on the oxidant. Milder oxidants such as alkaline cupric oxide may also yield aromatic aldehydes. With alkaline permanganate oxidation, permethylation of carboxylic acids and phenols in NOM increases the yields of oxidation products because of stabilization of phenols in alkaline media, and postmethylation is required to extract and analyze the oxidation products by gas chromatography and mass spectrometry. Yields of identifiable oxidation products of NOM are variable, but yields of 25% are near the upper limit for aquatic humic substances [183].

For soil humic substances, the phenolic carboxylic acid oxidation products are indicative of lignins because of the substitution patterns at the 3, 4, and 5 positions, whereas phenolic carboxylic acid oxidation products of aquatic humic substances with meta-substituted phenols indicated condensed tannin components [4]. The alkaline cupric oxide oxidation method was refined to characterize lignin sources of NOM by the suite of 11 phenolic aldehydes, phenolic carboxylic acids, and phenolic acetophenone oxidation products [186]. This lignin oxidation product method has been extensively applied to determine lignin sources of NOM in natural waters, but while the method has been useful in identifying lignin characteristic of woody angiosperm and woody gymnosperm plants as primary sources of DOM, the method only collectively accounts for about 0.6% of the DOC [94].

The aromatic carboxylic acid oxidation products range from mono- to hexacarboxylic acids, which indicates significant substitution in aromatic ring structures of NOM. Short-chain aliphatic mono- and polycarboxylic acids are produced as oxidation products of DOM, whereas long-chain fatty acids are

found in the oxidation products of humic acid and humin fractions of soils and sediments. Little useful information about polar functional groups in NOM (with the exception of phenols) is provided by oxidative degradation as many of these groups are oxidized to carbon dioxide and water. Schnitzer [118] proposed on the basis of degradative and non-degradative methods that humic substances are not single molecules but are rather aggregates of molecules held together by hydrogen bonding, van der Waals forces, aromatic charge-transfer complexes, and radical-coupling reactions. Later spectrometric studies of humic substances have substantiated much of Schnitzer's hypothesis about humic aggregate characteristics.

Oxidation of DOM with chlorine has been extensively studied, as halomethanes, haloacetic acids, haloacetonitriles, and halo ketones are disinfection by-products that are of health concerns in drinking water [26,183]. The keto-forms of resorcinol and phloroglucinol structures in condensed tannins are ketones that are very reactive with chlorine to produce halomethanes. β -hydroxy acids in hydrophilic DOM produce haloacetic acids, and proteins produce haloacetonitriles [26].

6.11.2 Reductive Degradations

Reductive degradation of humic substances for structural studies has been attempted with catalytic hydrogenation, hydriodic acid, n-butylsilane, sodium amalgam, sodium in liquid ammonia, and zinc dust [6,185,187,188]. Reduction with n-butylsilane [188] is the only method that does not cleave backbone structures of humic substances. This method reduces polycarboxylic acids, alcohols, aldehydes, ketones, and methyl esters to alkanes, with phenols being converted to silyl ethers. Ester linkages are reduced to ethers. When applied to three fulvic acids, the yields of GC-amenable materials were about 30%, excluding siloxanes. This new (2007) method has significant potential for deriving new information regarding humic backbone structures.

The sodium amalgam method of reduction has also provided useful information in giving good yields of identifiable compounds and in preservation of aliphatic structures that were destroyed with oxidative methods. Sodium amalgam and sodium in liquid ammonia cleave ether linkages in NOM structures. Up to 35 different phenolic compounds have been identified in sodium amalgam degradations of soil humic substances that were derived from lignin, tannin, and fungal sources [187]. Reduction of an

aquatic humic acid with sodium in liquid ammonia produces aliphatic alcohols, aliphatic acetates, and phenolic anisolic acids that were not found as degradation products of this humic acid with cupric oxide, permanganate, and chlorine oxidations, or from hydrolysis with sodium hydroxide [117]. A major problem with sodium amalgam reduction and other methods of reduction is that certain reduced products readily re-oxidize and couple upon exposure to atmospheric oxygen so that both yields and products are highly variable, depending on the experimental conditions.

Hydriodic acid in the presence of red phosphorus to combine with any iodine liberated is the basis of the Zeisel method to cleave ethers [1]. Fused aromatic ring compounds were identified as the "core structure" of certain humic acids after hydriodic acid reduction and dehydrogenation with a palladium carbon catalyst [189]. The products of reacting humic substances with zinc dust also produces fused aromatic ring compounds [189]. Hydriodic acid reduction of Suwannee River fulvic acid under much milder conditions in glacial acetic acid was used to show that most of the strong-acid acidity was caused by carboxyl groups on carbons adjacent to ether linkages [88]. Catalytic hydrogenation of humic substances produces low yields of identifiable products, and the high temperatures and pressures involved with the procedure cause structural rearrangements such that little useful structural information is obtained [187].

6.11.3. Degradations with Sodium Sulfide and Phenol

Applications of sodium sulfide and phenol degradations to NOM and the mechanisms of these degradations are summarized in a review by Hayes and O'Callaghan [190]. Both sodium sulfide and phenol degradations give greater yields of organic solvent-soluble degradation products than oxidative or reductive degradation methods. A mixture of hot aqueous sodium hydroxide and sodium sulfide is the basis of the Kraft process for the delignification of wood. Various functional groups in lignin and NOM are cleaved, oxidized, reduced, and polymerized by alkaline sodium sulfide solutions. A gas-chromatographic/mass spectrometric analysis of methylated sodium sulfide degradation products of humic acids revealed aliphatic alcohols, aliphatic mono- and polycarboxylic acids, phenols, and aryl-aliphatic carboxylic acids. The major finding was that phthalic acid was the only aromatic carboxylic acid detected in small amounts, which indicates that the aromatic

polycarboxylic acids found in oxidative-degradation procedures are likely produced by oxidation of substituted aromatic structures.

When phenol is refluxed (185°C) with a catalyst (p-toluene sulfonic acid) and NOM, extensive cleavage and substitution with phenyl groups occur, such that refractory and insoluble materials such as coal can be brought into solution in various organic solvents. Jackson et al. [191] applied phenol degradation to soil humic acids and used a combination of column chromatography, gas-liquid chromatography, and thin-layer chromatography to identify the products. A complex mixture of benzophenone, di-, tri-, and tetraphenyl methane, diaryl ether, and xanthone products was found. The complexity of the degradation products causes difficulty in reconstructing the NOM structures from which NOM is derived.

6.11.4. Hydrolytic Degradations

A comprehensive review of various hydrolytic degradations applied to NOM characterization is given by Parsons [192]. When hydrolyzed with bases such as alkali hydroxides or ammonia, soil and aquatic humic materials give many of the same products as discussed previously for oxidative and reductive degradations [117,118], although the yields of identifiable products are lower. This finding suggests that humic molecules have chemically labile linkages such as phenolic esters that are readily hydrolyzed.

Non-humic aminosugars, carbohydrates, and proteins in NOM are also characterized by hydrolysis [192]. Carbohydrates are typically hydrolyzed to monosaccharides with concentrated sulfuric acid; the monosaccharides may be derivatized to alditol acetates for GC analyses or analyzed by various liquid chromatographic methods. Hydrolysis of carbohydrates with concentrated hydrochloric acid creates furfural by-products, which reduce yields and polymerize; however, hydrolysis with HCl has been used to remove carbohydrates and proteins from humic substances prior to additional characterization studies [118].

Hydrolysis of proteins with 6 M HCl to aminoacids followed by derivatization (ninhydrin or o-phthalaldehyde) and liquid chromatography is the common method of protein analyses in NOM [193]. The aminoacids tryptophan, methionine, and cysteine are frequently lost during hydrolysis, and threonine and serine are also slowly degraded. Formation of melanoidins, with aminoacids reacting with monosaccharides in hydrolysis solutions by the Maillard

reaction, causes additional losses of both carbohydrates and aminoacids in their analyses. Acid hydrolysis of proteins and aminosugars (which are also frequently analyzed with proteins) typically accounts for 40 to 70% of the total organic nitrogen in NOM [193], and the remaining unaccounted-for nitrogen has been assumed to be various types of heterocyclic N structures such as purines, pyrimidines and pyrroles. However, this assumption was not substantiated when Martens and Loeffelmann [194] found that hydrolysis of NOM in soil with 4 M methanesulfonic acid increased the recovery of nitrogen in aminosugars and proteins from 46% (when hydrolyzed with 6 M HCl) to 86% (when hydrolyzed with 4 M methanesulfonic acid). This significant finding is substantiated by the ¹⁵N-NMR studies of NOM that found most of the nitrogen in NOM is in the form of amides [79].

6.11.5. Thermal Degradations

Thermal degradations of NOM have several advantages over the chemical degradations discussed previously:

- 1) Volatile degradation products can be directly analyzed by gas chromatography and mass spectrometry without derivatization.
- 2) They can be directly performed on the whole soil, sediment, or water sample.
- 3) Extraction and purification of degradation products from chemical reagents is not necessary or is minimal.
- 4) Pyrolyzers can be directly interfaced to gas chromatographs and mass spectrometers.
- 5) Pyrolytic procedures can be automated to increase the precision of the analyses.

A review of various analytical pyrolytic methods applied mostly to soil NOM is given by Bracewell et al [195], and a more recent comprehensive review of analytical pyrolysis applied to air, water, soil, and waste materials is given by Page [196]. Pyrolysis products may be analyzed by GC, MS, or GC/MS (which provides the best separation and identification). Conversion of about 50% of the NOM mass to identified pyrolysis fragments is typical, and the fragments can be related to NOM compound classes by various multivariate factor analysis methods. Compound classes identified in soil NOM include polysaccharides, N-acetyl aminosugars, proteins, lignins, lipids, polycarboxylic acids, aromatic hydrocarbons, and phenols.

A pyrolysis method used to estimate the relative proportions of major compound classes in aquatic NOM was developed by Bruchet et al [197]. This method directly pyrolyzed residues of evaporated water samples, as inorganic salts in the residue do not significantly interfere. Pyrolysis fragments used to identify and quantify NOM compound classes in water are listed in Table 8. A study of polar NOM in drinking water sources [198] by analytical pyrolysis found that N-acetyl aminosugar colloids were not being recovered in the DOM fractionation methods of Figures 16 and 17; this led to the DOM fractionation method of Figure 18 [18].

Table 8 Specific pyrolysis fragments of compound classes in fresh-water samples

Compound Class	Common Pyrolysis Fragments
Polysaccharides	Methylfuran, furfural, acetylfuran, methylfurfural, levoglucosenone, hydroxypropanone, cyclopentenone, methylcyclopentenone, acetic acid
N-acetyl amino sugars	Acetamide, N-methylacetamide, propionamide, acetic acid
Proteins	Acetonitrile, benzonitrile, phenylacetone, pyridine, methylpyridine, pyrrole, methylpyrrole, indole, methylindole, toluene, styrene, phenol, <i>p</i> -cresol
Polyphenolic	Phenol, <i>o</i> -, <i>m</i> -, <i>p</i> -cresol, methylphenols, dimethylphenols
Lignins	Methoxyphenols
Tannins	Catechol
DNA	Furfuryl alcohol
Polyhydroxy-butyrate	Butenoic acid

Conventional pyrolysis methods give little information about carboxylic acid structures in NOM, as decarboxylation occurs during pyrolysis. Pyrolysis of NOM in the presence of tetramethylammonium hydroxide forms methylesters (from carboxylic acids) and methylethers (from phenols) that preserve these acid structures during pyrolysis [199]. This alkylation/pyrolysis method that has become known as thermochemolysis was applied to a number of soil humic acids, and significant yields of aliphatic mono- and di-carboxylic acids, triterpenoid compounds, and aromatic phenolic acids from lignins were found that were not detected by conventional pyrolysis [200].

Pyrolysis and thermochemolysis was applied to hydrophobic neutral and hydrophobic acid fractions of landfill leachate that were shown by NMR, IR, and mass-spectral characterizations to be derived from terpenoid precursors such as resin acids in paper-sizing agents [44]. The terpenoid constituents of the aquatic fulvic acid fractions did not give well-resolved pyrolysis and thermochemolysis fragments. The GC/MS total ion current profiles showed that most of the mass in the chromatogram was in broad, unresolved sections upon which were well-resolved peaks related to lignin, polyethylene and polypropylene glycols, mono- and dicarboxylic acids, and petroleum-related hydrocarbons. Therefore, the molecular complexity of certain classes of compounds such as terpenoids in their degraded state limits their characterization by pyrolysis or thermochemolysis.

An opposite strategy to characterizing NOM by thermal degradation is the removal of the oxygen functional groups that give rise to molecular complexity, leaving the core hydrocarbon structures that may have less mixture complexity. Hydrous pyrolysis of NOM involves extended heating (several days) at 300-360°C in sealed vessels in the presence of water. The analytical method for hydrous pyrolysis is called microscale sealed-vessel (MSSV) pyrolysis. Hydrous pyrolysis has been extensively investigated in petroleum formation [201], and it involves complex radical cracking and recombination mechanisms where by various carbonyl groups in NOM are oxidized/decarboxylated to CO₂, and aliphatic hydroxyl and ether oxygens are dehydrated and may be substituted with hydrogen derived from water. The results are hydrocarbon oils that are well suited for GC/MS analysis. MSSV analyses were applied to hydrophobic neutral and hydrophobic acid fractions of DOM isolated from various surface and ground waters [202], and partial-ion chromatograms of GC/MS analyses of the MSSV pyrolysates are shown in Figure 50.

The alkyl naphthalene and cadalene structures in Figure 50 indicate core fulvic acid structures derived from sesquiterpenoid structures shown in Robinson [23], whereas retene indicates cyclic diterpenoid precursors. The alkylphenols are derived from tannin and lignin precursors. Cyclic tetraterpenoid hopane indicators of bacteria were found in the MSSV pyrolysate of the Great Salt Lake hydrophobic-neutral fraction [202], whereas flash pyrolysis of this fraction did not find hopanes. MSSV pyrolysis of Suwannee River fulvic acid produced mostly alkyl benzenes, naphthalenes, anthracenes, and phenanthrenes indicative of terpenoids, and alkyl phenols indicative of tannins and lignins. Hopanes were not found in the

Suwannee River fulvic acid, which was expected, given the oligotrophic characteristics of the water.

The alkyl naphthalene and cadalene structures in Figure 50 indicate core fulvic acid structures derived from sesquiterpenoid structures shown in Robinson [23], whereas retene indicates cyclic diterpenoid precursors. The alkylphenols are derived from tannin and lignin precursors. Cyclic tetraterpenoid hopane indicators of bacteria were found in the MSSV

pyrolysate of the Great Salt Lake hydrophobic-neutral fraction [202], whereas flash pyrolysis of this fraction did not find hopanes. MSSV pyrolysis of Suwannee River fulvic acid produced mostly alkyl benzenes, naphthalenes, anthracenes, and phenanthrenes indicative of terpenoids, and alkyl phenols indicative of tannins and lignins. Hopanes were not found in the Suwannee River fulvic acid, which was expected, given the oligotrophic characteristics of the water.

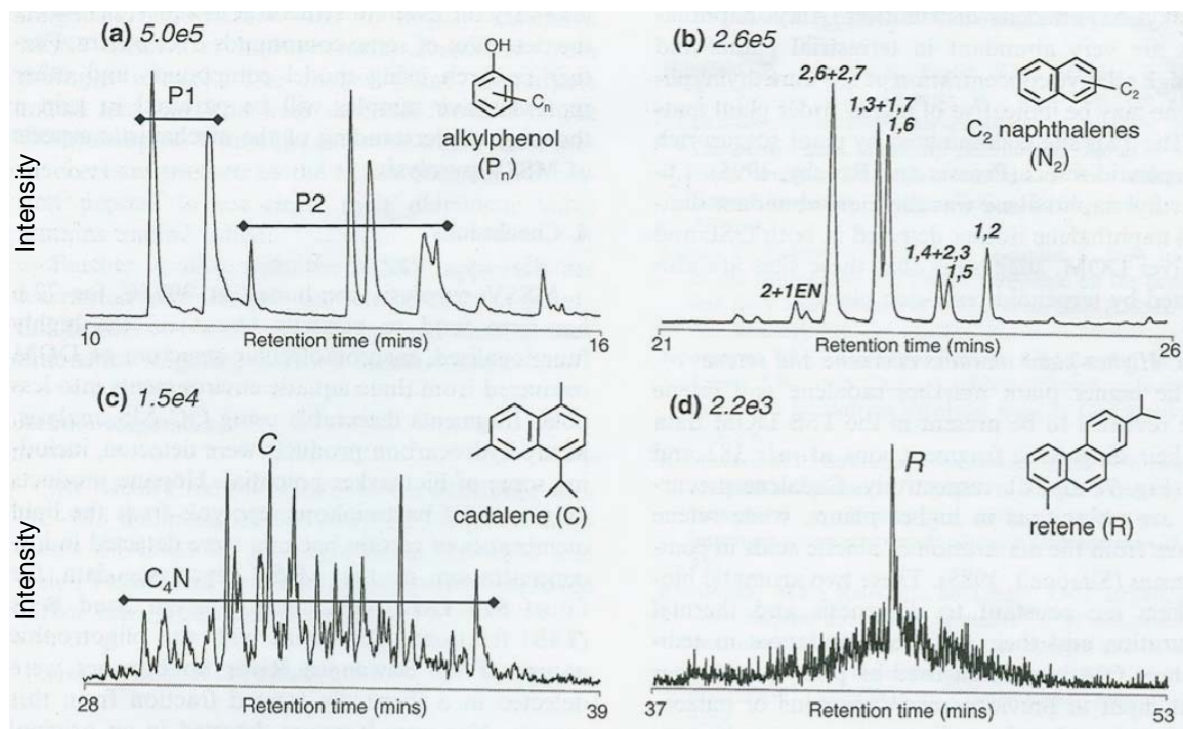


Figure 50 Partial-ion chromatograms reconstructed from the full scan analyses of the 300°C/72h (MSSV) pyrolysates of Tomago Sand Beds ground water hydrophobic acids: (a) m/z 107 showing alkylphenols; (b) m/z 156 showing ethyl- and dimethylnaphthalenes; (c) m/z 183 showing cadalene amongst the tetramethyl naphthalene distributions; (d) m/z 219 showing retene; relative abundances of a-d are indicated in italics. Reprinted with permission from reference [202], Figure 7. Copyright 2006, Elsevier.

6.11.6. Conclusions about NOM Characterizations

There are many independent methods used to obtain physical and chemical information about NOM in soil, sediment, and water. Furthermore, the existence of humic substance standard and reference samples made available by the International Humic Substances Society means that many NOM characterizations have been performed on identical samples. Integration of this information into physical and structural models has been attempted by numerous researchers, but often this information is fragmentary as discussed by

Christman et al. [183]. Their hypothetical model for fresh water humic acids was presented to show how little absolute structural information has been obtained from hydrolysis degradation, and the model was to be used as an abstraction to help derive new structural hypotheses. Since the model of Christman et al [183] was presented, much of the unknown macromolecular structure of various NOM fractions has become known as presented in this section, and better model approximations can be presented. There is a growing recognition among researchers that data from multiple characterization methods must be correlated with each

other to derive more detailed structural information about NOM and to validate results obtained from different methods [203]. This multimethod approach is well recognized as the scientific method that is used to discover and unify information based upon consilience, defined by Wikipedia [204] as “the unity of knowledge (literally a ‘jumping together’ of knowledge), which has its roots in the ancient Greek concept of an intrinsic orderliness that governs our cosmos, inherently comprehensible by logical process.”

7. COMPREHENSIVE STRUCTURAL MODELS OF NOM

The NOM models presented in this section are presented as comprehensive because they incorporate (a) quantitative data from multiple independent methods used to verify and constrain the data; (b) natural product source structures from plant and microbial precursors; (c) products from aerobic and anaerobic diagenetic processes; and (d) various biogeochemical controls on NOM composition (Figure 2). These models are still approximations or abstractions of actual structures, but they are designed to incorporate all relevant data. The goal of the reductionist approach is to improve model accuracy via the application of multiple fractionation methods in order to reduce NOM heterogeneity.

7.1. Analytical Requirements

Quantitative elemental analyses and quantitative ^{13}C -NMR spectra are the most important requirements for model construction, followed by infrared spectra and acid-base titrimetry. Choice of the molar mass of the model is based on measured molar mass distributions and averages determined by consilience between various methods. Therefore, the primary determinants of the model are the empirical formula (based upon elemental analyses and the chosen molar mass) and the distribution of carbon structures (aliphatic and aromatic plus olefinic) based upon quantitative ^{13}C -NMR spectrometry. Quantitative determinants of oxygen structural distributions separated into ketone, carboxylic acid + ester + amide + quinone, phenol + phenolic ether + phenolic ester, anomeric oxygen of carbohydrates, and aliphatic alcohols, esters, and ethers are also from ^{13}C -NMR spectrometry. Oxygen in carboxylic acids is quantitatively determined by titrimetry, and the percentages of oxygen in ester, amide, and quinone groups (relative to quantitatively

determined carboxylic acids) may be estimated by infrared spectrometry. Amide oxygen may also be estimated by the nearly 1:1 relationship of amides to nitrogen content in most NOM samples. Ether plus alcohol/phenol can be estimated as a residual of unaccounted-for oxygen, or alcohols and phenols can be directly determined by selective acetylation followed by acetyl group measurement by ^1H -NMR.

Proton distributions can be separated into exchangeable and non-exchangeable protons by ^1H -NMR, and non-exchangeable proton structures can be partitioned into structures presented in Figure 41. However, reasonable estimates of the distribution of protons between methyl, methylene, methane, and aromatic/olefinic structures can be derived from ^{13}C -NMR spectra. Use of spectral-editing pulse sequences in ^{13}C -NMR spectrometry is very useful for distinguishing methyl, methylene, methane, and quaternary carbon structures. Infrared spectrometry also qualitatively differentiates between methyl and methylene structures. Therefore, ^1H -NMR spectrometry of NOM, while desirable, is not a necessary analytical requirement for structural models.

The final requirements of structural NOM models are the determination of the index of hydrogen deficiency (Φ), the number of rings (θ), and the number of carbons per ring (Ω). An example of the data used to determine structural models of DOM fractions isolated from the Great Salt Lake is shown in Table 9 [76]. Structural models derived from the data of Table 9 are presented in Figure 51.

Molar masses of the hydrophobic acid, amphiphilic DOM, and hydrophilic-acid-plus-neutral models of Figure 51 were based on median values of negative ion ESI/MS distributions, and the empirical formulas of Table 9 were normalized to C_{40} for comparative purposes. Consequently, when model molar masses are considerably less than the empirical formula masses, elements such as nitrogen, sulfur, and halides may not be incorporated into models if their values in model-adjusted empirical formulas are less than 0.5. Only the primary structural data derived from elemental analyses and ^{13}C -NMR spectra are shown in Table 9; additional structural information derived from CPDAS/ dipolar-dephased ^{13}C NMR spectra, infrared spectra, and ESI/MS was also incorporated into the model structures of Figure 51. After the initial experience of constructing the structural model of Suwannee River fulvic acid in which an exhaustive (and expensive) data set was collected [112], subsequent studies found that more limited data sets yielded satisfactory compound-class structural models of the type shown in Figure 51.

Table 9 Data used to determine structural characteristics of DOM fractions from the Great Salt Lake [76]

Determination	Method	Hydrophobic Acids	Amphiphilic DOM	Hydrophilic Acids + Neutrals	Colloids
Empirical Formula (1000 Dalton)	Elemental Analyses	C _{46.7} H _{60.5} O ₂₂ N _{1.5}	C _{42.9} H ₅₇ O _{23.5} N _{2.3}	C _{33.3} H _{53.3} O _{23.8} N _{3.4} S _{0.8} Cl _{2.8}	C _{37.9} H _{63.2} O _{29.2} N _{2.9}
(Normalized to C ₄₀)		C ₄₀ H _{51.8} O _{18.9} N _{1.3}	C ₄₀ H _{53.1} O _{21.9} N _{2.1}	C ₄₀ H ₆₄ O _{28.6} N ₄ .1S ₁ Cl _{3.4}	C ₄₀ H _{66.7} O _{30.8} N _{3.1}
Aliphatic C-H plus C-N Carbons	%C from ¹³ C-NMR times #C's in 1000 Dalton formula	23.2	19.2	13.4	9.4
Aliphatic C-O Carbons	%C from ¹³ C-NMR times #C's in 1000 Dalton formula	8.2	10.2	9.4	19.1
Anomeric O-C-O Carbons	%C from ¹³ C-NMR times #C's in 1000 Dalton formula	1.1	1.1	1.7	4.5
Aromatic plus Olefinic Carbons	%C from ¹³ C-NMR times #C's in 1000 Dalton formula	4.5	3.2	1.4	0.4
Carbonyl C=O Carbons	%C from ¹³ C-NMR times #C's in 1000 Dalton formula	9.8	9.3	7.4	4.5
Index of Hydrogen Deficiency(Φ)	$\Phi = [(2C + 2) - (H + Cl - N)]/2$	18.2	16.6	8.0	8.8
# Rings (θ)	$\theta = \Phi - C=O - C - 0.5$ (aromatic plus olefinic C)	6.2	5.7	-0.1	4.1
# C per Ring (Ω)	$\Omega = \text{Total C} / \theta$	7.5	7.5	No rings	9.2

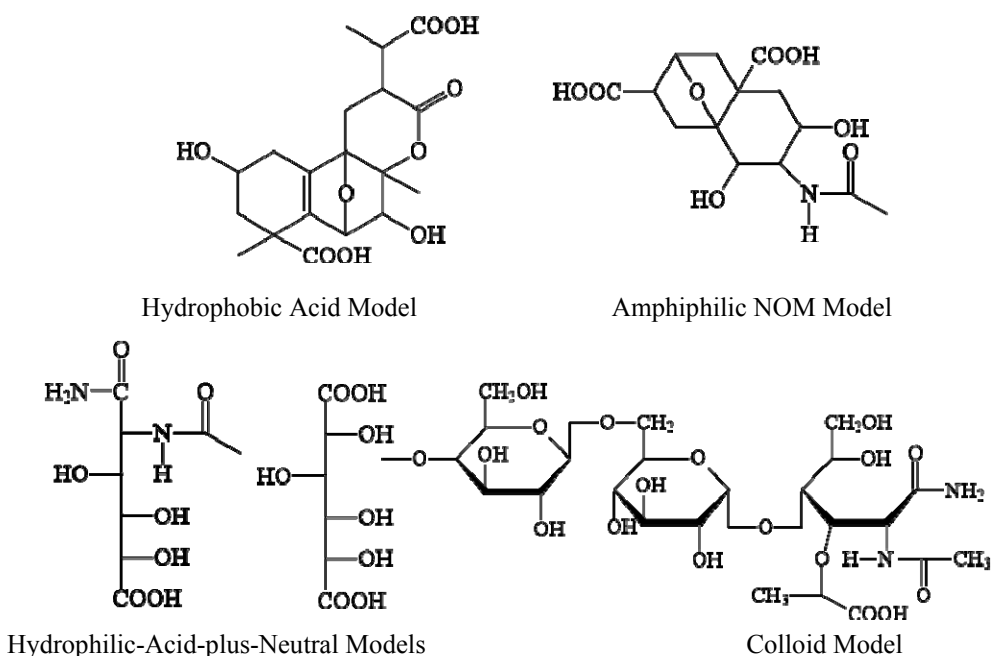


Figure 51 Structural models of DOM fractions isolated from the Great Salt Lake [76]

The models in Figure 51 indicate that the hydrophobic acids are derived from terpenoid precursors, and that the hydrophilic-acid-plus-neutral and colloid fractions are derived from N-acetyl aminosugar precursors. The amphiphilic DOM model is likely a mixture of compounds from terpenoid and aminosugar precursors, and additional sub-fractions of amphiphilic DOM are needed to obtain compound-class homogeneity.

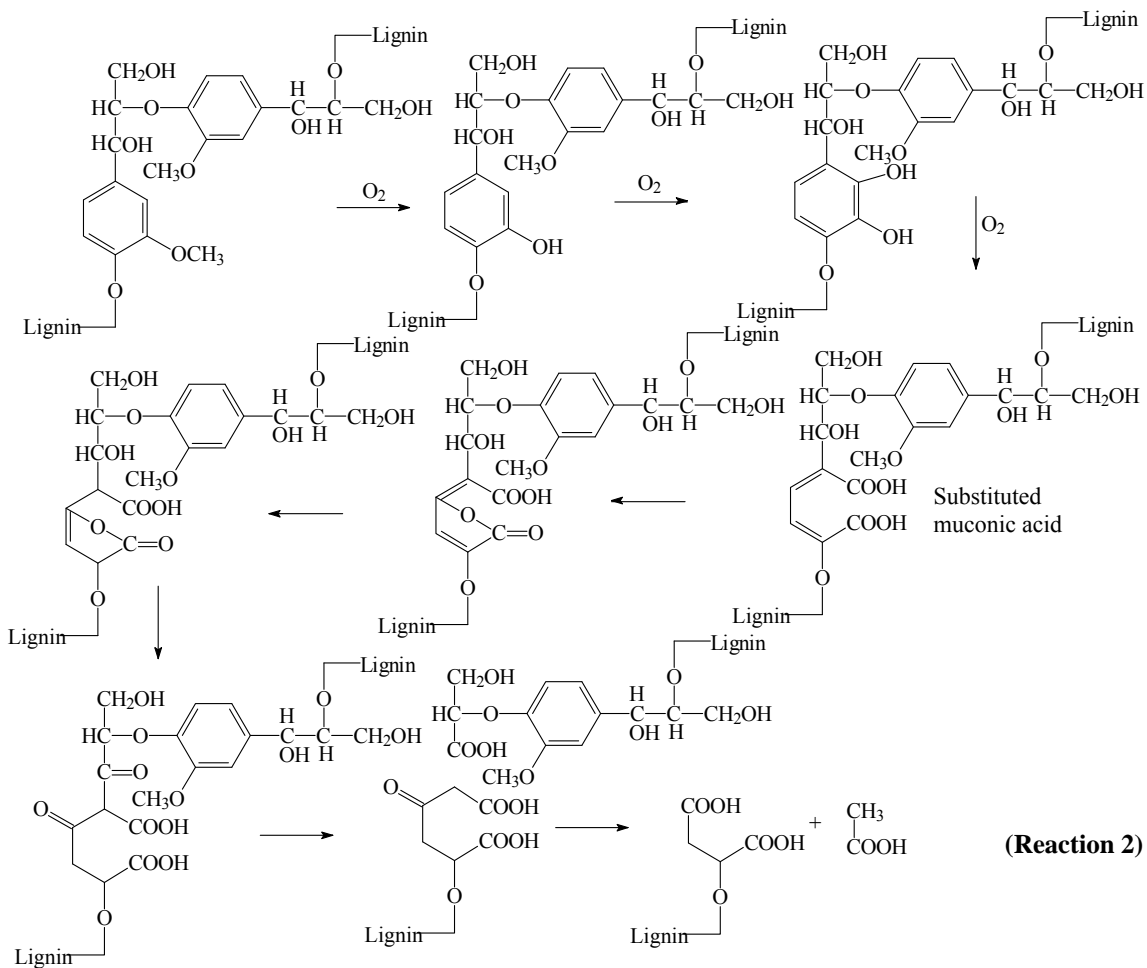
7.2. NOM Source and Process Requirements

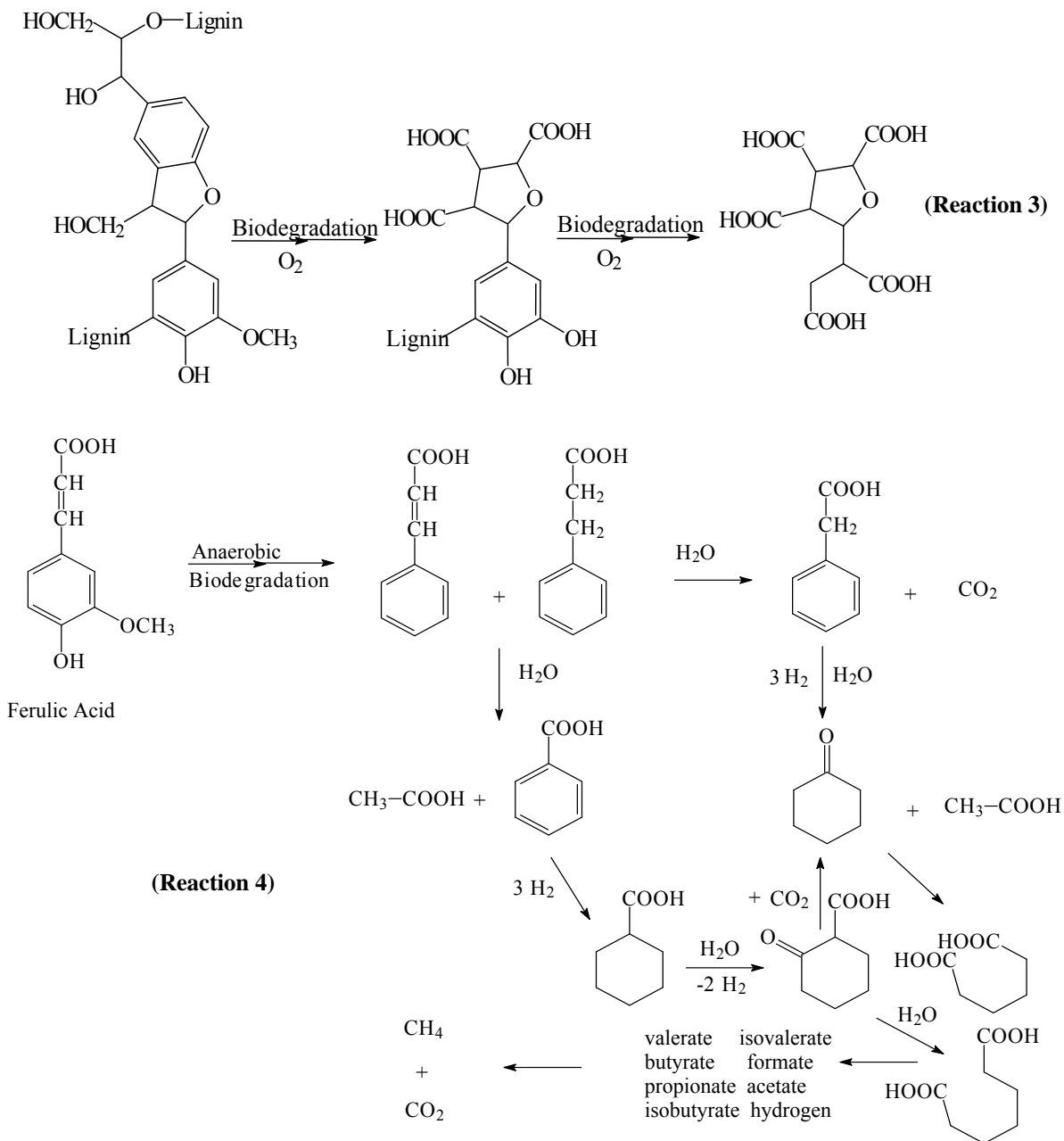
Sources and processes that result in certain DOM fractions such as the colloids (derived from bacterial cell-wall aminosugars) and the hydrophilic acids (derived from oxidation of aminosugars) are readily discerned from the analytical evidence presented in Table 9, but the source terms and diagenetic pathways of other NOM sources such as lignin are much more

complex. Lignin is known to degrade through both aerobic and anaerobic degradation pathways [27].

Under aerobic conditions, lignin is degraded by various wood fungi rather than by bacteria. A hypothetical catabolic sequence [205] for the aerobic degradation of lignin based on the β -keto adipate pathway is presented in Reaction 2. This catabolic sequence produces substituted succinic acid structures that have been postulated to explain clustering of carboxyl groups on tetrahydrofuran ring structures when these ring structures are present in the original lignin precursors [40]. This reaction sequence is shown in Reaction 3.

Carboxyl group clusters on tetrahydrofuran rings have been used to explain the strong acid characteristics of certain fractions of Suwannee River fulvic acid for which pK_1 values as low as 0.5 have been measured [40]; they have also been incorporated into structural models used to explain strong acid characteristics [88].



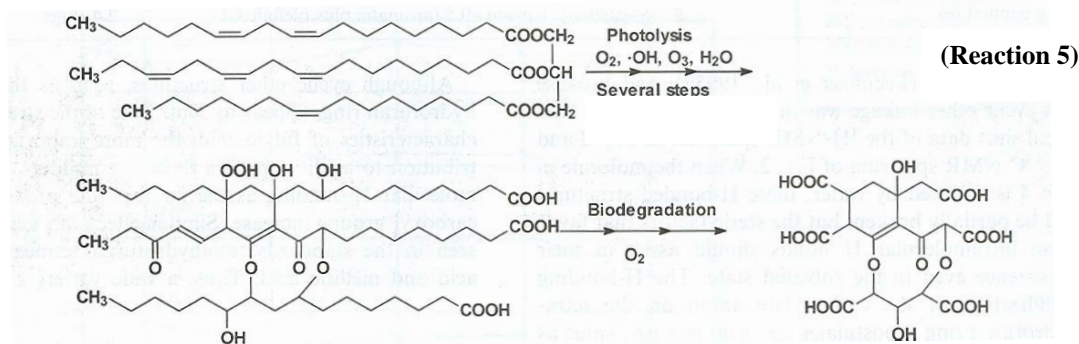


Lignin is also known to bacterially degrade under anaerobic conditions to produce methane and other by-products [206]. A proposed pathway [207] for the degradation of ferulic acid, a lignin monomer, is presented in Reaction 4.

Other lignin monomers, such as caffeic acid and homoprotocatechuic acids, also lost ring substituents during anaerobic biodegradation [206]. These losses of ring substituents and propane side chains result in the loss of lignin identity with regard to spectral characterizations.

A study of the organic composition of hog-lagoon wastewater [84] found that the major constituent of the hydrophobic acid fraction of this wastewater was hydrocinnamic acid. This is likely an anaerobic metabolite of lignin constituents in hog feed as shown in Reaction 4.

Both abiotic processes, such as photolysis that produces marine fulvic acid from unsaturated lipids [208], and biotic processes should be considered in structural models of NOM, as shown in Reaction 5 [40].



Radical-coupling processes involving double bonds in unsaturated lipids with reactive oxygen species and light create the cross-linked structures, and microbial degradation of aliphatic-hydrocarbon chains through aerobic α - and ω -oxidation processes [209] result in the accumulation of carboxyl groups on alicyclic ring structures that are resistant to both photolytic and microbial degradation.

7.3. Geochemical Requirements

A fundamental factor that determines whether NOM resides in soil, sediment, or water is solubility. The dependence of organic compound structure and functional group arrangements as a function of pH in water is presented by Shriner et al [1]. Certain organic compounds will also form insoluble complexes and precipitates with inorganic elements as presented in Figure 27, and they will adsorb on mineral surfaces as presented in Figure 28. Certain NOM precursors such as tannins are much more soluble than lignins and lipids, which become part of DOM only after extensive degradation. Thus the inorganic composition of soil, sediment, and water is an important factor in determining plausible structural models of NOM.

Functional groups in NOM structures are an important determinant of whether NOM will adsorb on sediment. Free phenolic hydroxyl groups and phenols in combination with carboxylic acid groups such as are found in salicylate structures form very strong complexes with iron and aluminum in sesquioxide mineral coatings. Phenols in NOM structures therefore act as solubility controls on DOM composition in surface and ground water [210]. When surface water infiltrates into ground water, DOM composition changes based upon adsorption and biodegradation reactions. The sorption process of

structural DOM models illustrative of certain compound classes is shown in Figure 52 for a soil/aquifer treatment study performed for the Orange County Water District in southern California [125]. Tannins and terpenoids are adsorbed on sesquioxide coatings on sediments by interactions with phenolic and carboxylic acid groups, and colloids adsorb by interactions with amino and carboxylic acid groups. However, terpenoid-derived fulvic acid does not adsorb because of the absence of phenolic hydroxyl groups and because carboxyl groups are spaced on alicyclic ring structures such that they do not form strong complexes with sesquioxides.

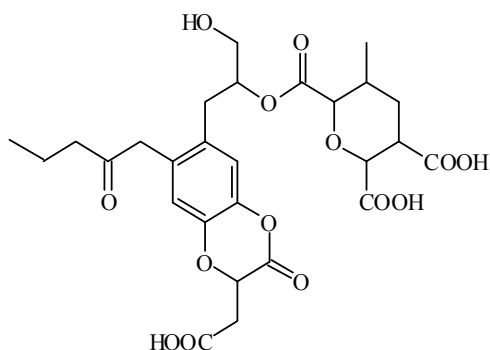
Studies of fulvic acids isolated from wheat straw [124] and from the Neversink Reservoir water supply of New York City [83] found methoxy-lignin structures that did not bind to iron and aluminum sesquioxides, indicating that methylation of phenols prevents adsorption. Therefore, both fulvic acid ligand structures and mineral coatings containing iron and aluminum sesquioxides act as solubility controls on DOM concentrations and composition in natural water.

7.4. Successive Approximations of Structural Models of Suwannee River Fulvic Acid [100]

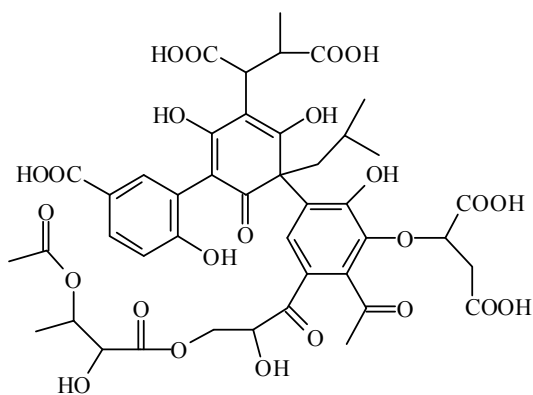
Suwannee River fulvic acid (SRFA), isolated for the International Humic Substances Society standard and reference samples, was extensively characterized by the U.S. Geological Survey [211]. Part of this characterization was assembling the characterization data into an average structural model presented below [139].

This and other structural models were derived without considering possible organic precursors and diagenetic processes that produce fulvic acid.

The second model was derived from quantitative characterization of fractions resulting from two-stage normal-phase chromatography of SRFA on silica gel [88]. This model, presented below, revealed that the strong acid acidity, with pK_a values as low as 2, resulted from carboxyl groups being clustered together next to aliphatic C-O linkages in ethers and esters.



The third model was derived from quantitative characterization of a SRFA fraction that was assayed to have the greatest binding constants for Ca^{2+} , Cd^{2+} , Cu^{2+} , Ni^{2+} , and Zn^{2+} [39]. This fraction was derived from a pH-gradient fractionation of SRFA on XAD-8 resin following by a normal-phase fractionation of a high-affinity metal binding fraction on silica gel. The model is presented below.



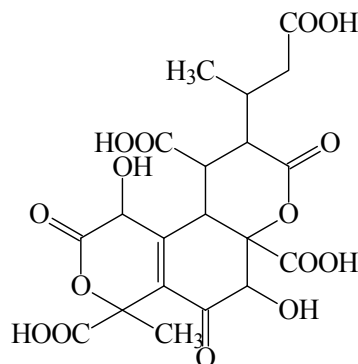
This third model had greater molar mass, phenol content, and carboxyl group content than the average model structure for unfractionated SRFA. The carboxyl, ether, and phenol groups were clustered to favor metal-chelate structures with large binding constants. This was the first model designed with a possible precursor structure, because the m-hydroxybenzene aromatic ring is present as condensed tannins.

The fourth model was derived from electrospray-ionization/multistate tandem mass-spectrometric separation of SRFA negative ions as shown in Figure 45 presented in section 6.7 about mass-spectrometric

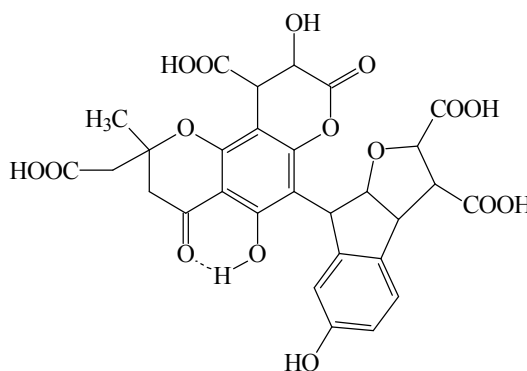
characterization.

The fifth model represented another fraction from the pH-gradient fractionation followed by the silica-gel fractionation of SRFA [40]. The selected fraction was exceptionally acidic ($pK_{a1} = 0.5$) and was composed of aliphatic structures with an average of five carboxyl groups per molecule. The strong acidity was attributed to electrostatic field effects of clustered carboxyl groups on a tetrahydrofuran ring structure. For the first time, a diagenetic reaction sequence presented in Reaction 3 (discussed previously) was considered along with lignin precursors in the derivation of this model.

The sixth set of models was based on a study of precursors from which SRFA was derived [91]. The fractionation sequence was normal-phase fractionation on silica gel followed by reverse-phase fractionation on XAD-8 resin. Characterization of the fractions by infrared, ^{13}C -NMR, and ESI/MS indicated that SRFA was primarily derived from terpenoid and tannin precursors, with lignin precursors present in lesser amounts. Models of the tannin-and terpenoid-derived fulvic acids are presented below.



Terpenoid Fulvic acid Model



Tannin Fulvic acid Model

These models have recognizable structures that can be related back to parent terpenoids and tannins based on plausible diagenetic reaction sequences.

The six models of SRFA presented in this section show progressive refinements in structural model approximations. The first model was based entirely upon quantitative chemistry data. Carboxyl group acidity and metal binding properties were added as analytical constraints in models 2 and 3. ESI/MS data was added in model 4, and organic precursor and diagenetic reaction sequences were added as constraints on the models in models 5 and 6. Several different fractionation sequences were developed based on the objective of the study, and the decreased mixture heterogeneity of the fractions greatly improved the validity of the models.

7.5. Ultrahigh-Resolution Mass-Spectrometric Molecular Model of Hydrophilic DOM in Seawater

Ultrahigh-resolution mass-spectrometry can resolve complex DOM mixtures into molecules, or more likely, into molecular isomeric mixtures of the same elemental composition as shown in Figure 47. Therefore, the elemental analyses and molar masses are true molecular properties that are not estimated by average assumptions of NOM fraction models presented previously. However, other essential spectrometric characterizations such as IR and NMR spectrometry cannot yet be made on NOM molecules separated by ultrahigh-resolution mass spectrometry because of mass limitations. Therefore, IR and NMR spectrometric analyses of NOM fractions analyzed by ultrahigh-resolution mass-spectrometry must be applied to estimate structural characteristics of molecular models. This exercise in molecular modeling will be applied to the hydrophilic-acid-plus-neutral DOM fraction isolated from the deep South Atlantic Ocean and analyzed by FT-ICR-MS [77].

The negative ion [M-1] of greatest intensity in the hydrophilic-acid-plus-neutral fraction has a molar mass of 340 Daltons and a molecular formula of $C_{14}H_{16}O_8N_2$. The C:N ratio of this molecular formula is 7, whereas the C:N ratio of the whole hydrophilic-acid-plus-neutral fraction is 11.5. This is reasonable, as several molecules in this fraction have lesser percentages of nitrogen [77].

The IR spectra of the free acid and sodium-salt forms of the hydrophilic-acid-plus-neutral fraction are presented in Figure 53. These IR spectra have some unusual features not typically seen in DOM fractions. The broad C-O peak near 1100 cm^{-1} has greater intensity than the broad OH stretch peak near 3400

cm^{-1} , which indicates ester and ether C-O linkages. As esters are not indicated near $1740\text{-}1770\text{ cm}^{-1}$, ether linkages are the more likely. The sodium salt form spectrum, in which carboxylate groups are shifted to peaks near 1600 cm^{-1} and 1400 cm^{-1} , indicates a broad peak near 1680 cm^{-1} that did not shift with conversion to the salt form. This peak is likely an amide peak, but a secondary amide II peak near 1550 cm^{-1} that is typical for proteins and aminosugars in DOM fractions is not seen. Primary amides are also not likely because of the low intensity in the 3400 cm^{-1} region where the NH_2 stretch occurs. The most likely amides are lactams of five- to seven-membered rings where the amide II band does not occur [33].

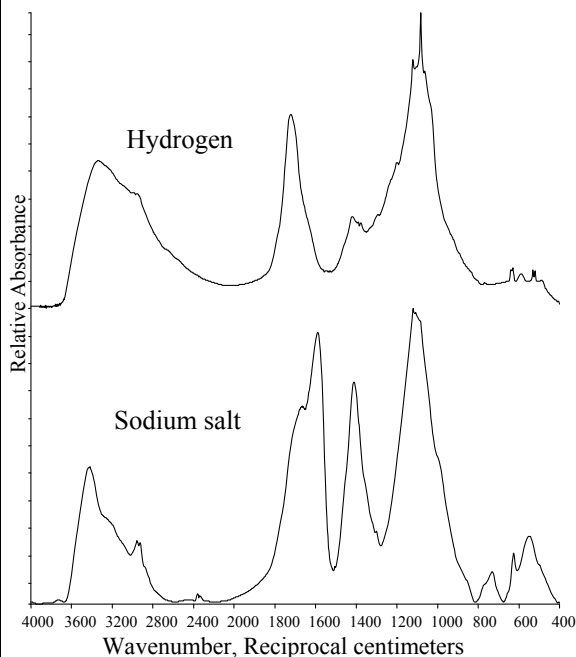


Figure 53 Infrared spectra of hydrophilic-acid-plus-neutral fraction isolated from the deep South Atlantic Ocean

The normal CP/MAS ^{13}C -NMR and CP/MAS ^{13}C -NMR dipolar-dephased spectra of the hydrophilic-acid-plus-neutral fraction are shown in Figure 54. The normal spectrum indicates that the carbon in this fraction is almost entirely aliphatic, with aliphatic carboxyl and amide carbonyl groups (peak at 175 ppm), aliphatic alcohol and ether groups (peak at 70 ppm), and aliphatic amide C-N linkage (shoulder at 55 ppm) being the major polar functional groups. The dipolar-dephased spectrum indicates the peak near 20 ppm is the methyl group, and the peak near 75 ppm indicates quarternary C-O linkages. The shoulder near

55 ppm indicates quarternary C-N linkages. Quarternary aliphatic C-C linkages near 55 ppm were not detected in the hydrophilic-acid-plus-neutral DOM fraction.

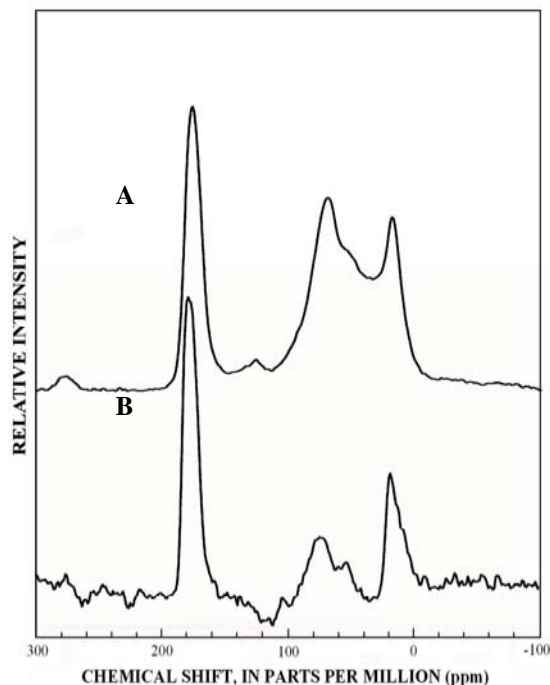
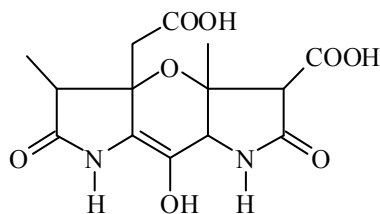


Figure 54 Normal CPMAS-¹³C-NMR spectrum (A) and dipolar-dephased spectrum (B) of hydrophilic-acid-plus-neutral fraction from deep South Atlantic Ocean

After considering the consilience of data for the molecular model, the hydrocarbon structure should be mostly aliphatic; the oxygen should be distributed between carboxyl, ether, and amide structures and most of the C-O linkages should be quarternary; and the nitrogen should be in neutral lactam structures. Basic amine structures are ruled out by the fraction isolation procedure. Source considerations implicate porphyrin precursors from chlorophyll in algae. Porphyrins are biologically degraded to pigments such as urobilins [212], which are dipyrrolylmethane compounds joined at the two α -pyrrolyl positions by methylene bridges to ether pyrrolenone or pyrrolidone rings. Pyrrolidone rings are aliphatic five-member lactams that fit the infrared data. Low-resolution positive ion MS/MS product ion spectra found losses of formic, acetic, and propanoic acid [77]. This is indicative of the methyl, ethyl, and propyl side chain known to exist on pyrrole rings in porphyrins; therefore, the carboxyl groups in the model were

derived from oxidation of the terminal carbon in methyl and ethyl groups. The molecular model is presented below.



One possible mechanism for the intramolecular ether bridge is oxidative radical cross-linking with olefinic double bonds in pyrrole rings, as shown for unsaturated lipids in the formation of fulvic acid in seawater in Reaction 5. The analytical constraints of the index of hydrogen deficiency determined by the molecular formula and the aliphatic structure dictate the five- and six-membered aliphatic, alicyclic rings of the model.

8. IDENTIFICATION AND DIAGENESIS OF NOM COMPOUND CLASSES AND PRECURSORS

The objective of this section is to apply the comprehensive information discussed in the previous section to the identification and diagenesis of NOM compound classes and precursors. Special emphasis will be given to subtle, but significant, differences in distinguishing between compound classes with similar characteristics, such as lignins and tannins that both have polyphenolic characteristics.

8.1. Lignins

Because of its abundance in the biosphere, lignin is undoubtedly the precursor of a substantial proportion of NOM in soils, sediment, and water. Lignin has an aromatic ring structure substituted with an aliphatic-substituted phenylpropane side chain at the 1 position, and ortho-substituted phenol, methoxy, or substituted aryl ether substituents at the 3-, 4-, and 5-positions. This is the molecular basis for spectrometric and degradative methods for identification of lignin and its degradation products. Lignin loses its aromatic ring structure and hence its identity when aerobically degraded, as shown in Reactions 2 and 3. Anaerobic degradation removes phenolic constituents from aromatic rings as shown in Reaction 4, and this process also causes a loss of lignin identity. The ¹³C-

NMR spectra of humic and fulvic acids extracted from peat have large aromatic carbon contents, but they have low phenolic carbon content [131]. Peats are known to be derived from plants high in lignin, and they form in swamps under anaerobic conditions. The loss of phenolic ring constituents under anaerobic conditions could explain the aromatic carbon profile of the ^{13}C -NMR spectra of peat humic and fulvic acid [131], in which carbon- and hydrogen-substituted aromatic structures predominate.

Other plant precursors, such as condensed tannins, have ortho-phenol structures in the B-ring, and hydrolyzable tannins have ortho-phenolic carboxylic acids such as gallic acid esterified to carbohydrates [23]. These ortho-phenol structures may be misinterpreted to be derived from lignin. To make matters even more confusing, lignin and tannins may oxidatively couple during plant senescence to form complex macromolecular structures such as theorubigin structures found in tea pigments [37]. The polyphenolic model of humus formation stresses phenolic coupling reactions that form macromolecular humus structures [5]. Therefore, the identity of both lignin and tannin precursors in NOM must be qualified by considerations of alternative precursors and diagenetic transformations.

Lignin precursor structures in NOM can be identified by degradative methods [186] or by nondegradative spectral profiles. The presence of the aromatic methoxy group is generally characteristic of lignin, although some tannin structures also have methoxy substituents [23]. Methoxy groups ($\text{O}-\text{CH}_3$) give peaks near 1127 cm^{-1} in the infrared spectra (Table 5, Figure 33) and near 55 ppm in the ^{13}C -NMR spectra (Table 6, Figure 39). Aromatic skeletal vibrations in lignin give a sharp peak near 1510 cm^{-1} in the infrared spectra, and unsubstituted carbons ortho to aromatic C-O structures in lignin give peaks from 105 to 120 ppm in the ^{13}C -NMR spectra, depending on ring substitution.

8.2. Tannins

Tannins are major constituents in plant leaves and vegetative litter [135]. During leaf senescence and litter decomposition, a complex assemblage of soluble and insoluble humic structures is formed from tannins, lignins, carbohydrates, and proteins [51,213]. The A-ring of condensed tannins and flavonoids is based upon substituted phloroglucinol and resorcinol structures that exist in tautomeric equilibrium with mono-, di- and triketone structures, depending on the substituents in the ring [23]. An example of a

substituted phloroglucinol-ring structure in the monoketone tautomer is shown in the model of the Suwannee River metal binding structure [39], which was presented earlier as the third approximation of a Suwannee River fulvic acid molecule. These ketone tautomers give rise to conjugated ketone structures that give strong infrared peaks from $1660 - 1620\text{ cm}^{-1}$, depending on the amount of hydrogen bonding. The unsubstituted sites of both the phenol form and the keto form of the A-ring of condensed tannins are very reactive with oxygen and a variety of plant constituents to form completely substituted A-ring degradation products in the hydrophobic acid model of Figure 55.

Condensed tannins and flavonoids are antioxidants that rapidly degrade to phloroglucinol and phenolic acids when exposed to molecular oxygen [214]. Phloroglucinol is a very reactive phenol that condenses with aldehydes and oxidatively couples with phenols and alkenes to form carbon- and oxygen-substituted structures to completely substitute the aromatic ring [23]. Lastly, biotic oxidation [27] of labile organic structures results in carboxyl groups accumulating on refractory ring and branched-chain structures. This process leads to the water-soluble hydrophobic acid component of DOM in which substituted A-ring structures can be identified. The B-ring structures may be completely degraded in this process, or they may be coupled to substituted A-ring structures.

The ^{13}C -NMR spectrum of a tannin-derived fulvic acid fraction is shown in Figure 37. This diagnostic spectral profile has a phenol peak near 155 for meta C-O structures, and a peak near 107 ppm for substituted aromatic structures between meta C-O structures. The 107 ppm peak is often confused with an anomeric carbon peak of carbohydrates, but fractionation and sub-fractionation procedures can remove carbohydrates as shown in the spectrum of Figure 36. The dipolar-dephased spectrum of tannin-derived fulvic acid give the diagnostic quarternary carbon peak at 107 ppm for condensed tannin structures, as was reported by Wilson and Hatcher [134]. The complex hydrophobic acid structure of Figure 55 is difficult to identify by oxidative, reductive or pyrolytic methods, although simple phloroglucinol and resorcinol compounds have been reported as degradation products. The use of combined fractionation and non-degradative characterization methods found much greater amounts of tannin-derived fulvic acid in the Suwannee River than suggested by previous studies [91].

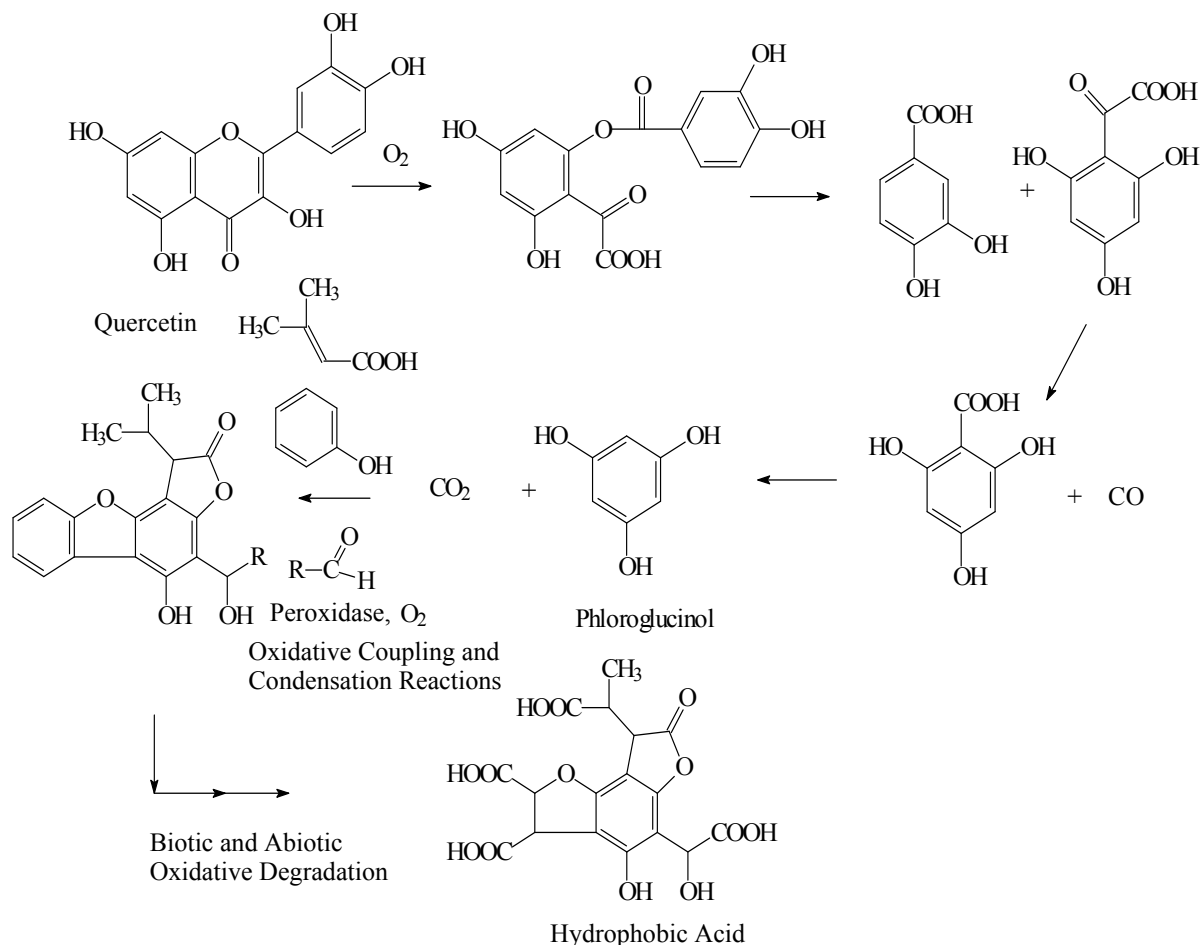


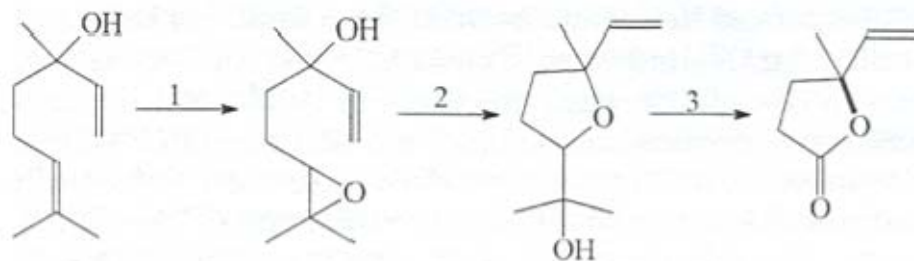
Figure 55 Hypothetical degradation of the flavonoid quercetin to a hydrophobic acid molecule [100]

8.3 Terpenoids

Terpenoids are a diverse group of compounds (resins, steroids, alkaloids, pigments, glycosides, etc) whose basic skeletons are all derived from mevalonic acid [23]. Terpenoid structures are built up of isoprene or isopentane units, which result in alicyclic rings, as found in steroids, branched methyl groups, and quarternary C-C and C-O linkages. Detection of these unique combinations of linkages in various fulvic acid isolates derived from landfill leachates, surface waters, and ground waters was the basis for concluding that terpenoids are major precursors for aquatic fulvic acids [44]. Terpenoid-derived fulvic acids are readily separated from fulvic acid isolates by extraction with ethyl acetate or by silica gel chromatography as discussed in Section 5. The methyl groups and quarternary C-C and C-O linkages are readily

detected by CP/MAS dipolar-dephased ^{13}C -NMR spectrometry as shown in Figure 38.

Terpenoids such as steroids and hopanoids are difficult to degrade biologically and have been used by organic geochemists as biomarkers in sediments [215]. The metabolic pathways of the biodegradation of terpenoid structures are presented by Trudgill [43]. Two of these pathways, which form hydrophobic acid constituents of fulvic acid using abiatic acid in this case, are presented in Figure 56. The aromatization pathway may explain a portion of the aromatic carbon structures observed by ^{13}C -NMR spectra that cannot be readily explained by phenolic acids derived from lignins and tannins. The Baeyer-Villiger pathway may partially explain ester structures that are usually found in terpenoid-derived fulvic acid. Lactone ester structures with quarternary C-O linkages are also formed in terpenoids during biodegradation as shown in Reaction 6 [216].



(Reaction 6)

Both metabolic pathways in Figure 56 produce hydrophobic fulvic acid structures in which carboxyl groups are scattered around the perimeter of the rings. This scattered carboxyl group arrangement does not facilitate metal binding or adsorption by sesquioxide coatings on mineral surfaces. Therefore, terpenoid-derived DOM acids are not removed by adsorption on mineral surfaces during infiltration of surface water into ground water [125], nor are these acids removed by coagulation/flocculation by ferric chloride or alum

during water treatment [72,198]. Many of the methyl groups, quaternary linkages, and ring structures in the parent terpenoids are preserved in the hydrophobic acid metabolites such that they can be used for identification purposes. Additional degradation of terpenoid-derived hydrophobic acids will increase carboxyl groups and degrade hydrocarbon structures so that these polar metabolites will be shifted into amphiphilic and hydrophilic DOC fractions.

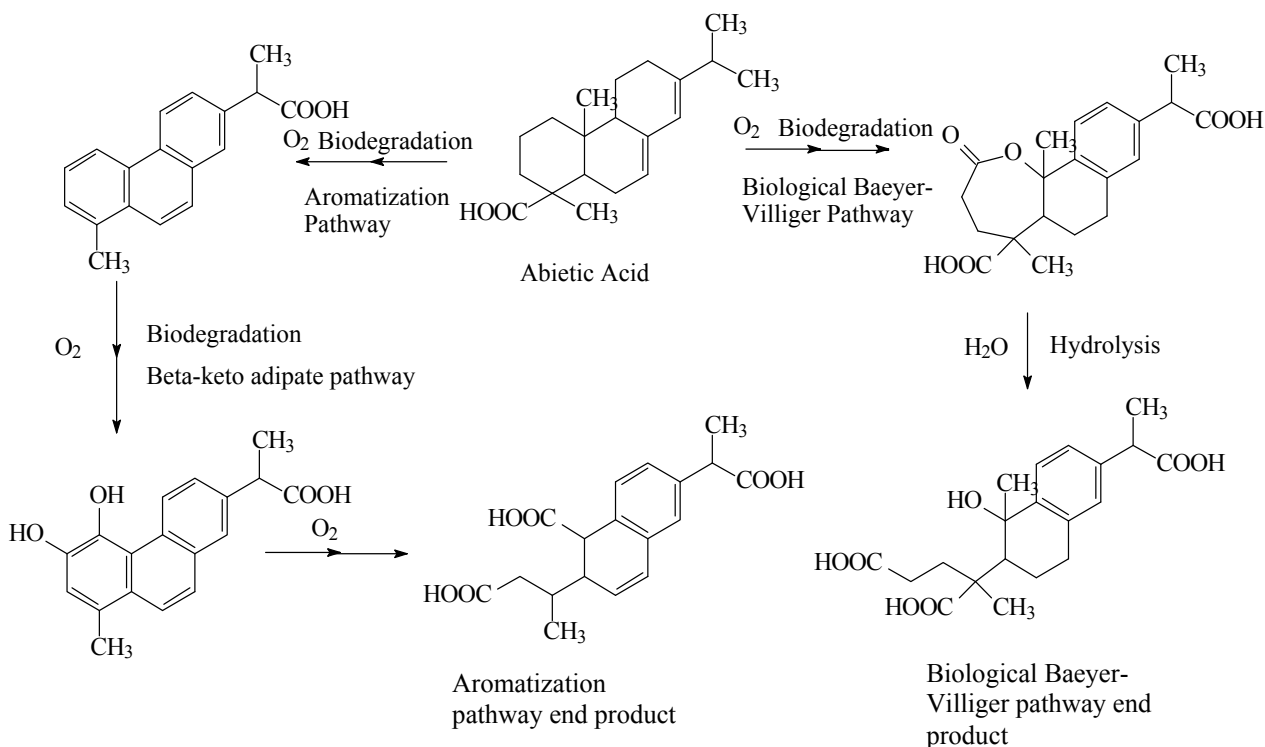


Figure 56 Possible metabolic pathways for the biodegradation of abietic acid [100]

8.4. Polysaccharides and Proteins

In NOM, polysaccharides and proteins (a) are linked together in peptidoglycans in cell walls, (b) react together to form melanoidins, and (c) are relatively labile to biodegradation processes. Aminosugars, polysaccharides, and proteins have distinctive infrared spectra as presented in Figure 32 and have distinctive ¹³C-NMR spectra as presented in Figure 36. The identifying spectral peaks were discussed in Section 6.

Aminosugars have been measured to constitute 10-20% of the organic nitrogen in mineral soils [217], but aminosugars constituted only 8-10% of nitrogenous compounds extracted from Lake Ontario sediments [218]. Aminosugars constitute highly variable percentages of DOM, depending on the source of organic matter and the trophic state of the water [198]. In general, aminosugars constitute a much higher percentage of DOM than is found for soil and sedimentary organic matter. Additionally, aminosugar nitrogen exceeds protein nitrogen in DOM, whereas protein nitrogen greatly exceeds aminosugar nitrogen in soils and sediments, suggesting that aminosugars dissolve in water and wash out of soils and sediments.

The origin and diagenesis of aminosugar residues

found in NOM in soil, sediment, and water is presented in Figure 57. The sources of aminosugars in NOM are cell wall membranes found in bacteria and fungi [219]. Free aminosugars are not found in soil, but the amino group exists in the acetylated form. Aminosugars in bacterial cell walls are combined with a short-chain peptide containing both L- and D-aminoacids in structures called peptidoglycans [219]. A study [154] of aminosugars in municipal biosolids found that the peptide chain was biodegraded to form the N-acetyl aminosugar in Figure 57. Additional degradation of aminosugars to N-acetyl aldaric acids was found for the hydrophilic acid fraction in the Great Salt Lake [76].

Aminosugars have only recently been isolated from other DOM components and inorganic salts by using semi-permeable membranes in dialysis or ultrafiltration assemblies [18, 220]. The aminosugars are colorless substances with minimal UV and fluorescence properties. Their molar masses have been estimated to range from 5000-20000 Daltons by size-exclusion chromatography [101]. This large size classifies them as colloids, although they are operationally classified as part of DOM because of their passage through a 0.45µm membrane filter.

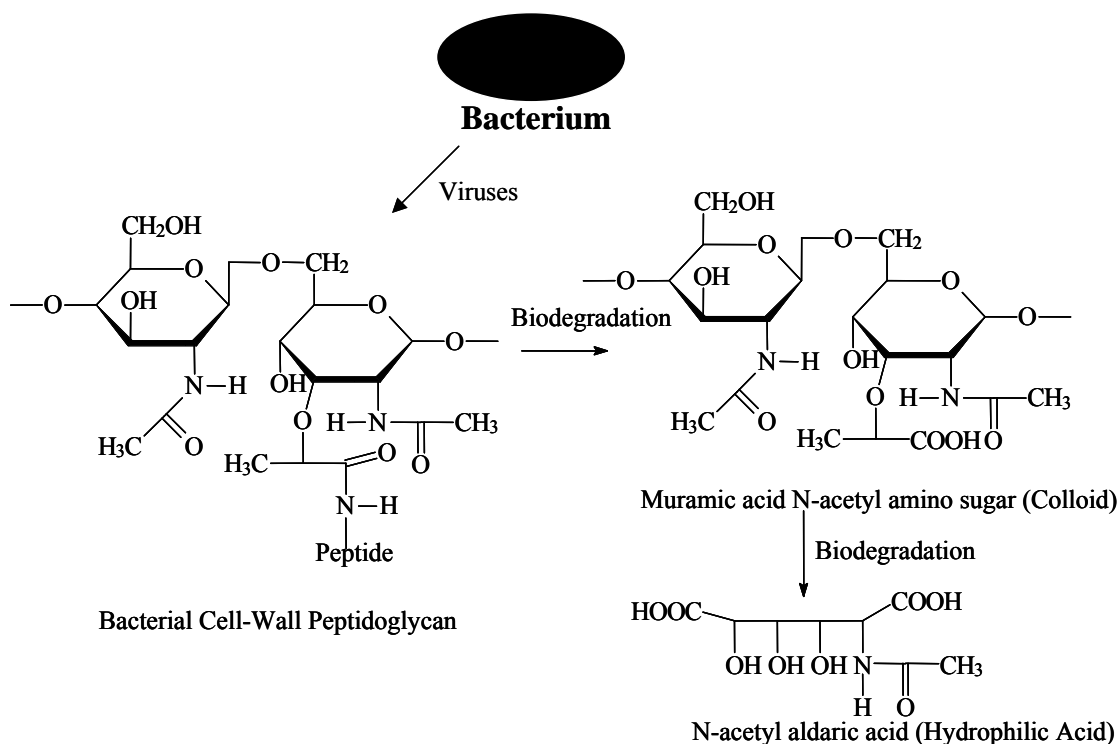
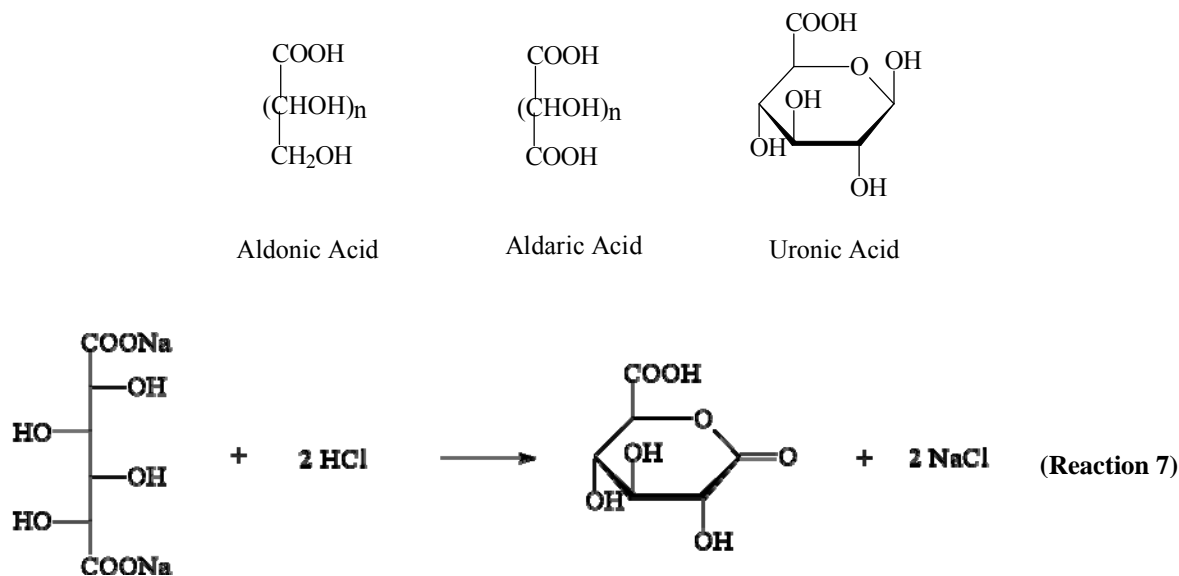


Figure 57 NOM diagenesis from bacterial cell walls



Aminosugars can clearly be identified from their infrared (Figure 32) and ^{13}C -NMR spectra (Figure 36), with characteristic peaks discussed in Section 6. When DOM fractions derived from peptidoglycans are pyrolyzed, both the colloid fraction and the hydrophilic-acid-plus-neutral fractions produce aceta-mide from the N-acetyl functional group [197].

Carbohydrates of the homopolysaccharide class can also be readily identified from the infrared (Figure 32) and the ^{13}C -NMR (Figure 36) spectra, with characteristic peaks discussed in Section 6. Carbohydrates are oxidized to sugar acids. The sugar acids consist of aldonic, aldaric, and uronic acids. Their structures are shown above. Aldonic and aldaric acids exist in open-chain forms as salts, but when acidified they form five- and six-membered lactone rings as shown below in Reaction 7.

Aldonic and aldaric acids are low molar mass hydroxy acids that result from oxidation of the anomeric carbon in polysaccharide structures, whereas uronic acids are frequent constituents of heteropolysaccharides such as aldobiuronic acid, chondroitin, hyaluronic acid, and heparin [219]. Uronic acids have been reported to constitute 30-40% of the weight as compared to the weight of neutral sugar content of soil polysaccharides [185]. Glucuronic acid is used biochemically to render soluble various hydrocarbons, steroids such as estrogen, and certain pesticide contaminants by the formation of glucuronide conjugates [221].

For water samples, sugar acids can be expected to occur in the transphilic and hydrophilic acid fractions of DOM, although hydroxypolycarboxylic acids also occur as metabolites from a wide variety of organic precursors [219]. The ^{13}C -NMR spectra of all DOM fractions isolated from Anaheim Lake are shown in Figure 58. The transphilic (TPI-A) and hydrophilic acid (HPI-A+N) fractions have a major peak between 60-90 ppm in the ^{13}C -NMR spectra; this peak represents C-O linkages typical of aliphatic hydroxyl groups in sugars. However, the anomeric carbon peak near 100 ppm is absent for the hydrophilic acid fraction and is greatly reduced in intensity (as compared to the colloid fraction) for the transphilic-acid fraction. This indicates that the sugars have been oxidized to either aldonic acid, aldaric acid, or N-acetyl aldaric acid if carbohydrates and aminosugars are precursors of these fractions [125].

Monosaccharides (reducing sugars) derived from polysaccharides and aminoacids (derived from proteins) are known to react to form melanoidins by the Maillard reaction, more commonly known as the Browning reaction. This reaction is shown in Figure 59. The Browning reaction is the basis for the melanoidin theory of humus formation presented in the book by Stevenson [5]. The melanoidin theory was frequently invoked to account for unidentified nitrogen in NOM, but recent ^{15}N -NMR studies and better methods to analyze for hydrolyzed aminoacids and aminosugars have mostly closed the nitrogen balance in soils and sediments [194].

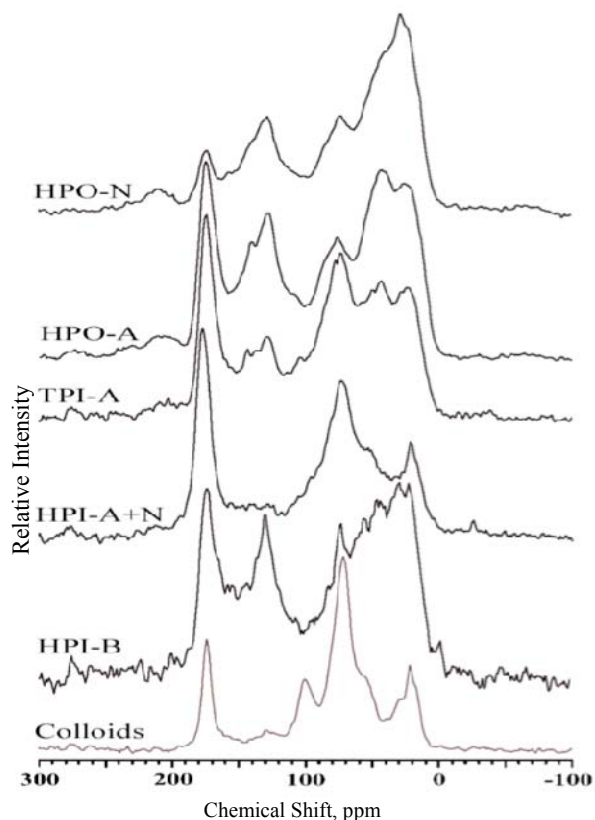


Figure 58 CP/MAS ^{13}C -NMR spectra of DOM fractions from Anaheim Lake sampled August 30, 2001 [125]

There are no specific characterization methods for melanoidins in NOM as there are for other precursors or their degradation products, although pyrolysis/MS procedures indicate that certain furan structures are derived from secondary polysaccharides produced by the Browning reaction [195]. Oxime structures initially formed in the Browning reaction have not been detected in significant amounts in humic substances by ^{15}N -NMR spectrometry, and furan structures have not been found as distinct peaks by either ^{13}C -NMR or infrared spectrometry. The aldehydes, aminoacids, and furans produced by the fragmentation step in the Browning reaction of Figure 59 likely condense and couple with each other and with other reactive precursors such as lignins and tannins to produce amorphous NOM structures that have lost their structural identity. These low molar mass fragments are also subject to rapid mineralization by biotic and abiotic degradation processes.

Proteins and peptides can be identified from their infrared (Figure 32) and ^{13}C -NMR spectra (Figure 36), with characteristic peaks discussed in Section 6. The

DON fractionation method [78] has shown that proteins are generally not conjugated with carbohydrates through the Browning reaction, because relatively homogeneous protein fractions are found in the hydrophobic base/neutral fraction, as shown in the infrared spectra of Figure 60.

The broad C-O peak of carbohydrates near 1100 cm^{-1} is not a major peak in either the hydrophobic base/neutral fraction or in the aminoacid fraction, whereas the carbohydrate peak is a major peak for the colloid fraction in which aminosugars predominate. Although biodegradable, proteins are stabilized by adsorption on clay mineral surfaces as shown in Figure 28.

8.5. Porphyrins

Porphyryns derived from pigments are sufficiently refractory to degradation to be used as biomarkers in sediments [222]. The model of the hydrophilic-acid-plus-neutral fraction isolated from Atlantic Ocean seawater also is suggestive of porphyrin precursors as discussed in Section 7. The infrared and ^{13}C -NMR spectra (Figure 58) of the hydrophilic base fraction from Anaheim Lake and in ground water from recently infiltrated Anaheim Lake water [125] had spectral characteristics that did not match protein and aminoacid constituents known to isolate in this fraction.

The aromatic carbon content of the hydrophilic base fraction in the CP/MAS ^{13}C -NMR spectrum of Figure 58 was significantly greater than the aromatic carbon content of the CP/MAS ^{13}C -NMR spectrum of protein in Figure 36. To identify this unknown NOM material, multiple-tandem positive ion ESI/MS spectra of this hydrophilic base fraction were determined. The results are shown in Figure 61, in which the three major ions all indicated the same compounds $[\text{M}+\text{H}]$ at m/z 587.6, $[\text{M}+\text{Na}]$ at m/z 610.6, and $[\text{M}+\text{K}]$ at m/z 625.6. Multiple mass spectra of the m/z 587.6 positive ion produced ions consistent with the chlorophyll degradation product shown in Figure 61. The porphyrin ring of chlorophyll was opened and the esterified phytol side chain was lost during biodegradation. The nitrogen atoms in conjugated pyrrole structures in this degraded porphyrin are very weak bases, but they are apparently sufficiently basic to isolate on the hydrogen-form cation exchange resin used to separate hydrophilic bases. More research needs to be performed on the fate and structures of porphyrins in NOM, as these initial findings suggest that porphyrin degradation products may be significant in certain environments.

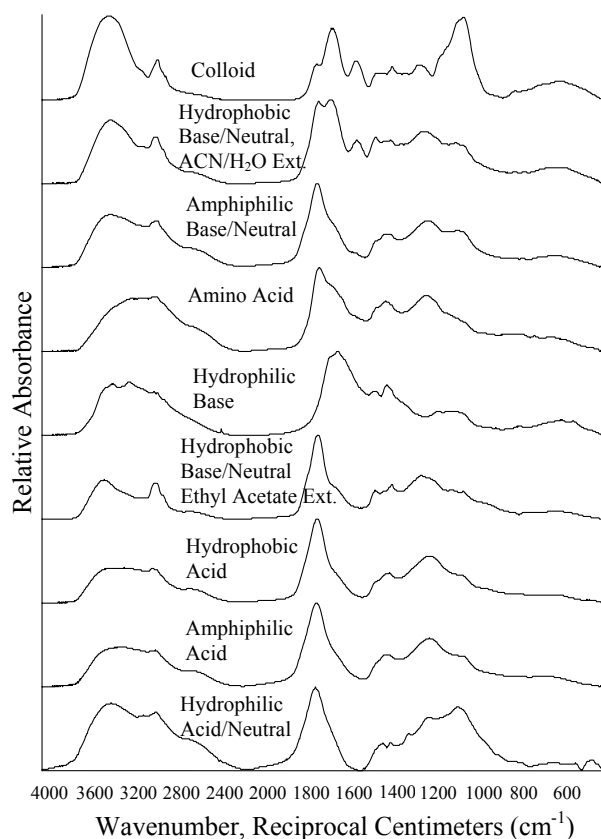


Figure 60 Infrared spectra of dissolved organic fractions from Saguaro Lake [78]

8.6. Lipids

The lipids discussed in this section are limited to straight-chain aliphatic hydrocarbon structures such as fatty acid esters (saponifiable lipids) and various plant biopolymers such as cutins and suberins. Technically speaking, plant biopolymers are not saponifiable lipids, but they have straight-chain aliphatic hydrocarbon structures very similar to saponifiable lipids. Branched-chain hydrocarbon structures found in various terpenoid hydrocarbons will not be discussed here as they have been previously covered in section 8.3.

The analyses and nature of lipid compound-class constituents in NOM is of considerable interest because they have been related to non-polar, contaminant-partitioning interactions [223]. In plants and microbial cells, saponifiable lipids generally constitute 5-25% of cellular mass, and they exist as free fatty acids, triglycerides, phospholipids, and glycolipids [23]. The fatty acids in lipid structures may exist in crystalline, gel, and fluid states as shown in Figure 62; non-polar contaminants readily partition

into the gel and fluid forms as evidenced by the linear adsorption isotherms of contaminant uptake into NOM [223]. Both crystalline and non-crystalline domains of the poly(methylene) chains of lipid structures in humic acids, humins, and peats have been detected by solid-state ^{13}C -NMR and wide-angle X-ray scattering [224]. The poly(methylene) chains of lipids in NOM are readily detected by the sharp, intense peak near 2920 cm^{-1} in infrared spectra (Figure 34) and by the peak near 30 ppm in ^{13}C -NMR spectra (Figure 37). Lipid poly(methylene)-chain structures dominate the extractable organic matter fraction from suspended sediment in a stormflow sample from Mill Creek, and they are also a significant structural component of the humin fraction as shown in the infrared spectra of a TOM fractionation in Figure 63 [74]. Extractable lipids are readily biodegraded [27], but their abundance in plant and microbial biomass and their preservation in organic coatings on mineral surfaces (Figure 28) results in extractable lipids being a major NOM fraction in certain environments, e.g., water in a swine waste-retention basin [84].

The aliphatic poly(methylene)-chain moieties in NOM that are not solvent extractable during various fractionation steps, as shown for the humin fraction in Figure 63, have also been shown to be resistant to saponification. Tegelaar et al [225] ascribed these moieties (based upon pyrolysis and ^{13}C -NMR evidence) that are resistant to both biological and chemical degradation to cutin and suberin, which are long-chain polyester structures. Cutin is a component of the cuticular extracellular membrane of plant leaves, fruits, and non-woody stems. An average structure of cutin is presented below [226].

The monomers in cutins consist of C_{20} – C_{30} fatty acids and primary alcohols along with ω -hydroxy C_{16} – C_{24} fatty acids. The fatty acids of cutin may also be chemically conjugated with polysaccharides in plant cuticles [225]. Long-chain aliphatic structures in a fulvic acid extracted from a forest soil were identified by three-dimensional NMR spectrometry as being derived from leaf cuticles by detection of specific hydroxy fatty acid monomers [153].

Suberin is found as an intracellular compound associated with lignin in cork cell walls (barks) of woody plants. A structural model of suberin is presented below [227].

Less is known about the exact chemical structure of suberin, and the direct conjugation of phenolic structures in lignin with the aliphatic fatty acids is speculative in the model presented above. Suberin is more resistant to degradation than cutin; it is found as a maceral called suberinite in certain coals [228].

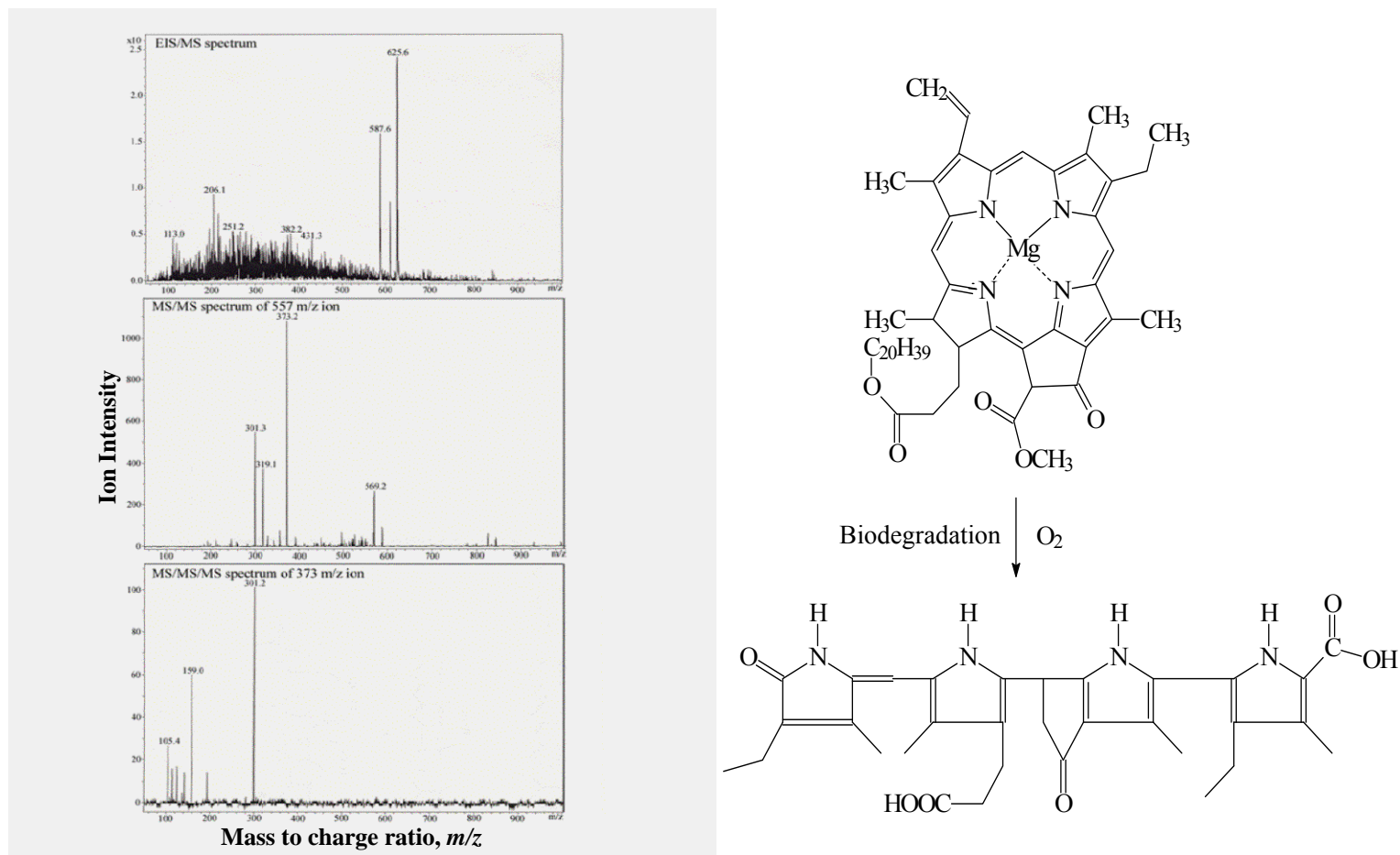


Figure 61 Multiple-tandem positive ion ESI/MS spectra of the hydrophilic base fraction from ground water infiltrated from Anaheim Lake, California [125]; daughter ion spectra were obtained on the 557 positive ion that indicated the proposed degradation product of chlorophyll

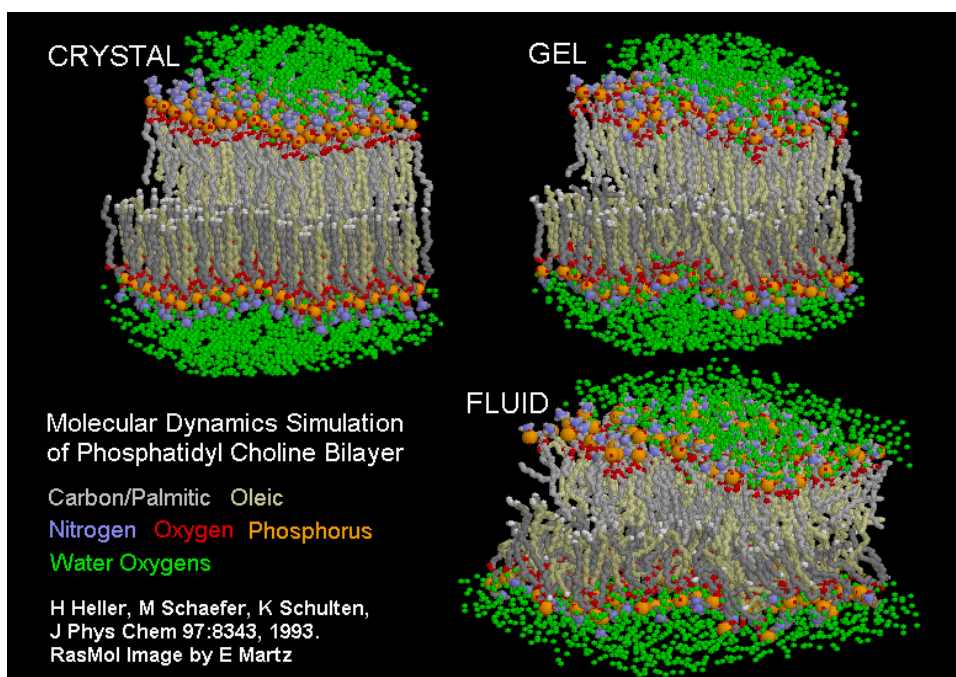
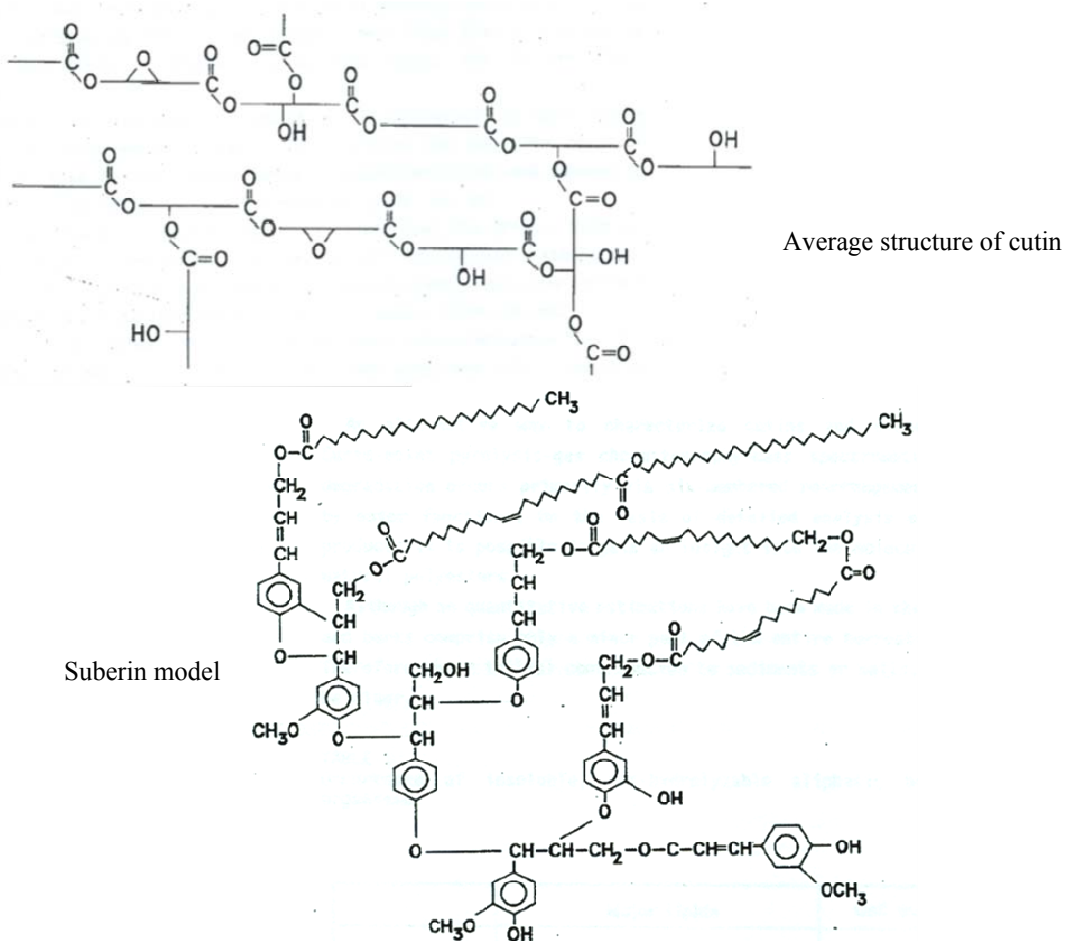


Figure 62 Cellular lipid bilayer structure in crystalline, gel, and fluid forms. Reprinted with permission from the author, Eric Martz, Image credit <http://molvis.org>.

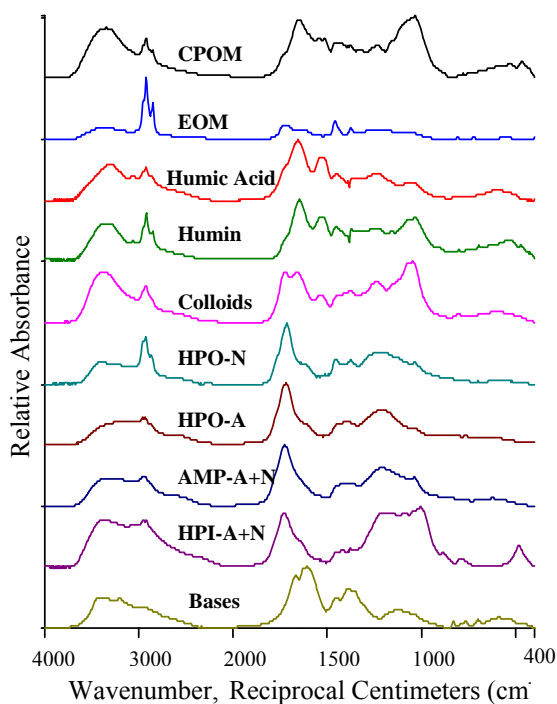


Figure 63 Infrared spectra of fractions obtained from TOM fractionation of Mill Creek sampled during stormflow [74]; fraction acronyms are defined in Figure 21

8.7. Black Carbon

Black carbon is a form of NOM altered by heat and described by its appearance. While easy to describe, black carbon is very difficult to analyze in soil, sediment, and water because it exists in a variety of forms depending on the precursors and temperatures under which it was produced, as shown in the ^{13}C -NMR spectra of Figure 39 [136]. There is general agreement that the core structures in black carbon are condensed polyaromatic rings, but condensed aromatic ring structures such as retene are also found in NOM as a natural constituent not produced by heat. Quantitative analyses of black carbon in soils and sediment are desired owing to its significance in sequestering carbon in the global carbon cycle [229], because of its role in improving soil fertility [230], and because of its properties as an adsorbent for non-polar organic contaminants [231].

Most methods for black carbon analyses have focused on removal of all carbon compounds from soil and sediment except black carbon. This has been done by thermal oxidation, photo-oxidation, and chemical oxidation with various reagents, with quantification of the remaining black carbon in the residue by carbon

analysis. The authors of a comparative study of analytical methods noted that black carbon values in individual soil samples varied by over two orders of magnitude [232]. Certain NOM structures such as the poly(methylene) chains found in cutins and suberins are resistant to chemical and photochemical oxidation and require strong oxidants such as dichromate to remove; however, part of the black carbon is oxidized, and the remaining black carbon is more polar and less effective as a sorbent for non-polar organic contaminants [231]. Thermal oxidation methods tend to create black carbon from NOM that leads to overestimates in soils and sediments [46]. UV photo-oxidation methods also tend to give overestimates of black carbon in soils and sediments because the minerals present protect NOM from oxidation.

The best method for determining black carbon in soils and sediments is based upon mild oxidation with sodium hypochlorite, which oxidizes aromatic polyphenolic constituents of NOM; partial demineralization with hydrofluoric acid to enrich black carbon and remaining NOM; and removal of iron oxides that interfere with NMR analyses with hydrofluoric acid. One can then conduct quantitative elemental carbon and ^{13}C -NMR analyses of the residue, because the aromatic carbon of the residue is a measure of black carbon [138]. Quantitative determination of the aromatic carbon in black carbon by solid-state ^{13}C -NMR is difficult because most of the carbon is not protonated; however, various pulse sequences have been developed to achieve reasonably quantitative estimates of black carbon [137,138]. The mild-oxidation method of Simpson and Hatcher [138] probably results in a small amount of black carbon being lost in a fulvic acid fraction in supernatant waters discarded during the oxidation and demineralization steps. These losses are probably minimal because humic acids containing black carbon are not extracted during this procedure.

The molecular structures of humic acids derived from black carbon in a volcanic ash soil were determined by ultrahigh resolution FT-ICR-MS [232]. The ^{13}C -NMR spectrum of this humic acid revealed almost no aliphatic carbon; the aromatic carbon was mostly not protonated and was extensively carboxylated. The FT-ICR-MS analyses revealed three different types of highly carboxylated aromatic compounds: linearly fused aromatic structures, aromatic structures linked by carbon-carbon single bonds, and highly condensed aromatic structures. This finding provides evidence that black carbon exists as a continuum in the environment, from elemental carbon in graphite and fullerene structures to oxidized

carboxylated humic and fulvic acids. Low temperature charring also results in phenol groups and lactones [121], and nitrogen and sulfur heteroatoms such as those found in aza-arenes and thiophenes are also incorporated into black carbon.

An example of the continuum of black carbon incorporation into various NOM fractions is provided by the stormflow study of the Santa Ana River [74] that sampled runoff from the first storm after the major wildfires in southern California in October-November, 2003. Stormflow runoff was sampled in an urban drain from an area that had received extensive ashfall. The appearance of the water after the sediment had settled was olive brown with colloidal matter remaining in suspension, as shown in Figure 64.



Figure 64 Stormflow sample from an urban drain into the Santa Ana River; sample is contained in a separatory funnel used to separate sediment NOM from dissolved and colloidal NOM

A total organic matter fractionation was conducted on this sample using the procedure shown in Figure 21. The ^{13}C -NMR spectra of this comprehensive NOM fractionation are shown in Figure 65.

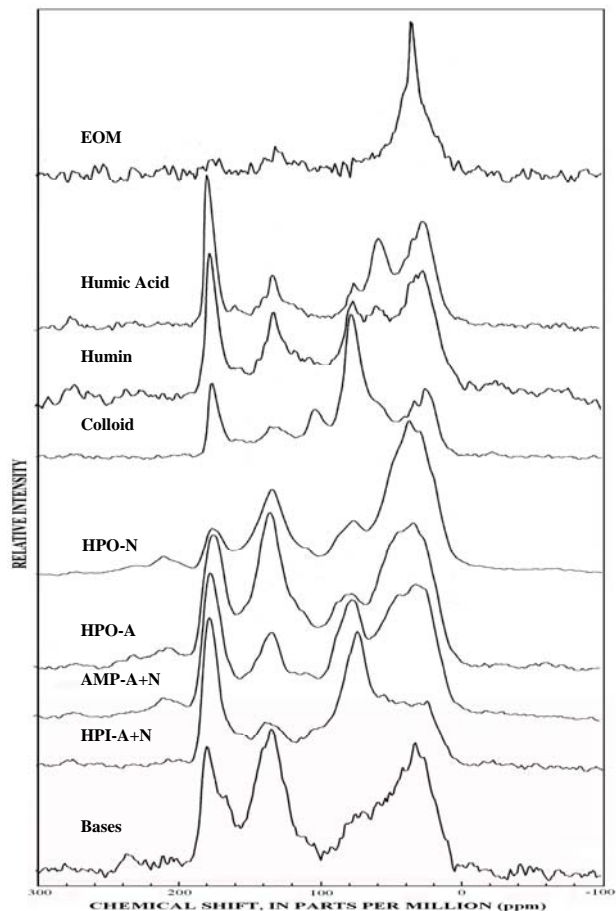


Figure 65 ^{13}C -NMR spectra of NOM fractions obtained from stormflow sample from urban drain into the Santa Ana River

The presence of black carbon was qualitatively detected by increases in the symmetrical aromatic carbon peak at 95-165 ppm, indicative of black carbon in every fraction with the exception of the extractable organic matter fraction. These increases were noted by comparison with fraction ^{13}C -NMR spectra in a baseflow sample collected prior to the storm, and by comparison with similar stormflow samples collected in the Santa Ana River basin in a previous study [125] that predated the forest fire. Even the colloid fraction, which typically has almost no aromatic carbon (Figure 36) and is white in color after isolation, had more aromatic carbon and was grey in color after isolation. What is remarkable about the colloid color is that the relatively small increase in colloid aromatic carbon when comparing the ^{13}C -NMR spectra of Figures 36 and 68 was sufficient to darken the color of the isolate to grey.

The increases in aromatic carbon contents of the hydrophobic acid, hydrophobic neutral and base fractions were especially pronounced when compared with water samples collected before the fire, indicating that significant black carbon components of NOM are soluble in water. With regard to the effect of fires on soil carbon, a study of pine forest soils near Seville, Spain, sampled before and after a fire, determined significant increases in aromatic carbon with fire as determined by solid-state ^{13}C -NMR spectrometry [233,234].

9. EXAMPLES OF COMPREHENSIVE NOM ANALYSES

Several examples of comprehensive NOM analyses in soil, sediment, surface water, ground water, seawater, wastewater, fog water, atmospheric aerosols, and limestone will be presented in this section. These examples demonstrate how the experimental approach and the NOM characterizations can be designed to meet the objectives of a particular study.

9.1. Dissolved Organic Matter in Recharge Waters, Santa Ana River Basin

The objectives of this study [125,235] were to assess DOM concentrations, composition, and properties of waters used to recharge the lower Santa Ana River alluvial aquifers that are used as a barrier to prevent saltwater infiltration and as a water supply for Orange County, California. The cooperative study was funded by the Orange County Water District and the USGS was part of the Santa Ana River Water Quality and Health study [236].

A map of the Santa Ana River Basin with sampling sites for the study is presented in Figure 66. Waters used to recharge the alluvial aquifers of the Santa Ana River basin in Orange County, California, include the Santa Ana River, wastewater effluents, and imported Colorado River water. The Santa Ana River has its headwaters in the San Bernardino Mountains, but its water quality is greatly affected by urban inputs of the San Bernardino and Riverside metropolitan regions, and by agricultural inputs of dairy farming in the Chino valley (Figure 66).

These inputs are via smaller creeks (Chino Creek and Mill Creek), which drain into the Prado Wetlands along with the Santa Ana River above Prado dam. The ground water recharge basins, such as Anaheim Lake and Kraemer Basin, located near the Forebay Recharge Facilities, were originally constructed as

gravel pits. These recharge basins accept the majority of the flow of the Santa Ana River below Prado Dam, and the water infiltrates into aquifers underlying parts of Orange County.

Water samples (40-120 L) filtered onsite (Figure 13) included two reclaimed water effluents (each sampled twice), and four surface-water samples from the Santa Ana River basin and Anaheim Lake selected to assess variations in season and water flow as well as the effect of the Prado Wetlands on DOM composition. Stormflows (high-flow) periodically occur during the rainy season (October to March), and base-flow (low-flow) conditions predominate during the dry season (April to September). DOM in these samples was fractionated according to the flow-chart procedure described in Figure 18.

Bar-chart diagrams of the DOM fractionations are presented in Figure 67. The Santa Ana River Prado Wetland Inlet base-flow sample has very similar DOC concentrations and DOM fractionation pattern to the Colorado River reported previously [198]. At stormflow, the DOC concentration in the Prado Wetland Inlet sample doubles compared to the base-flow sample, with the largest DOM fraction increase being observed in the colloid fraction. A very large increase in the colloid fraction is observed at stormflow in the Mill Creek sample. The large increase in the colloid fraction concentrations during stormflow is a significant finding that may be related to fouling of the infiltration basins. The exceptionally high colloid concentrations from Mill Creek during stormflow may be related to excess rinse water runoff and/or input of animal manure from the dairy farms of the Chino Valley.

At base-flow, the DOC concentration is only about 0.5 mg C/L greater at the Cattail site (located toward the end of water passage through the wetland) than the Santa Ana River, Prado Wetland Inlet site, and the DOM fractionation patterns are very similar. The Cattail site was sampled 7 days after stormflow in the Santa Ana River to allow maximum leaching of DOM from the wetland vegetation, but in this case DOC decreased slightly during the passage of water through the wetland. The largest DOM fraction decrease during stormflow was observed in the HPI-B fraction; the other fractions had similar patterns between the Prado Wetlands Inlet and the Cattail site samples. As with the other base-flow and stormflow samples, stormflow caused a large increase in the colloid DOM concentrations at the Cattail site, indicating that sedimentation in the wetland does not significantly remove colloids. The wetlands also may be a source of colloidal DOM.

The Anaheim Lake sample collected on February 6, 2001, had a greater DOC concentration and different DOM fractionation than the Prado Wetlands Cattail site sample. The algal bloom that was occurring in Anaheim Lake during the sampling may have caused these differences. The greatest DOM increase was observed in the HPO-A fraction. The Anaheim Lake sample collected on August 30, 2001, had a lower DOC concentration and had a DOM fractionation pattern typical for baseflow samples such as the Prado Wetlands Inlet sample.

These differences in DOM fractionation patterns demonstrate the dynamic nature of DOC concentration and composition changes as a function of environment, flow, season, and water source. More specific information about DOM composition can be obtained by infrared and ^{13}C -NMR analyses of each water sample. Infrared and ^{13}C -NMR analyses of an Anaheim Lake sample collected on August 30, 2001

are presented in Figure 68. The side-by-side presentation of the spectra in Figure 68 along with the fractionation bar diagrams of Figure 68 allows a comprehensive compound-class assessment of DOM.

The composition of the HPO-N, HPO-A, and the AMP-A+N fractions are derived primarily from terpenoid hydrocarbon precursors recently reported to be major precursors of DOM in water [44]. The split aliphatic hydrocarbon peaks (15 ppm and 45 ppm) of the HPO-A and AMP-A+N fractions as well as the symmetrical aromatic hydrocarbon peak (100-160 ppm) of the HPO-N fraction in the ^{13}C -NMR spectra of Figure 68 are diagnostic of terpenoid hydrocarbon precursors such as abietic acid. Lesser amounts of aromatic sulfonates in the HPO-N, HPO-A and AMP-A+N fractions derived from degradation of anionic sulfonate surfactants are shown by small peaks near 1040 cm^{-1} in the infrared spectra and 140 ppm in the ^{13}C -NMR spectra.

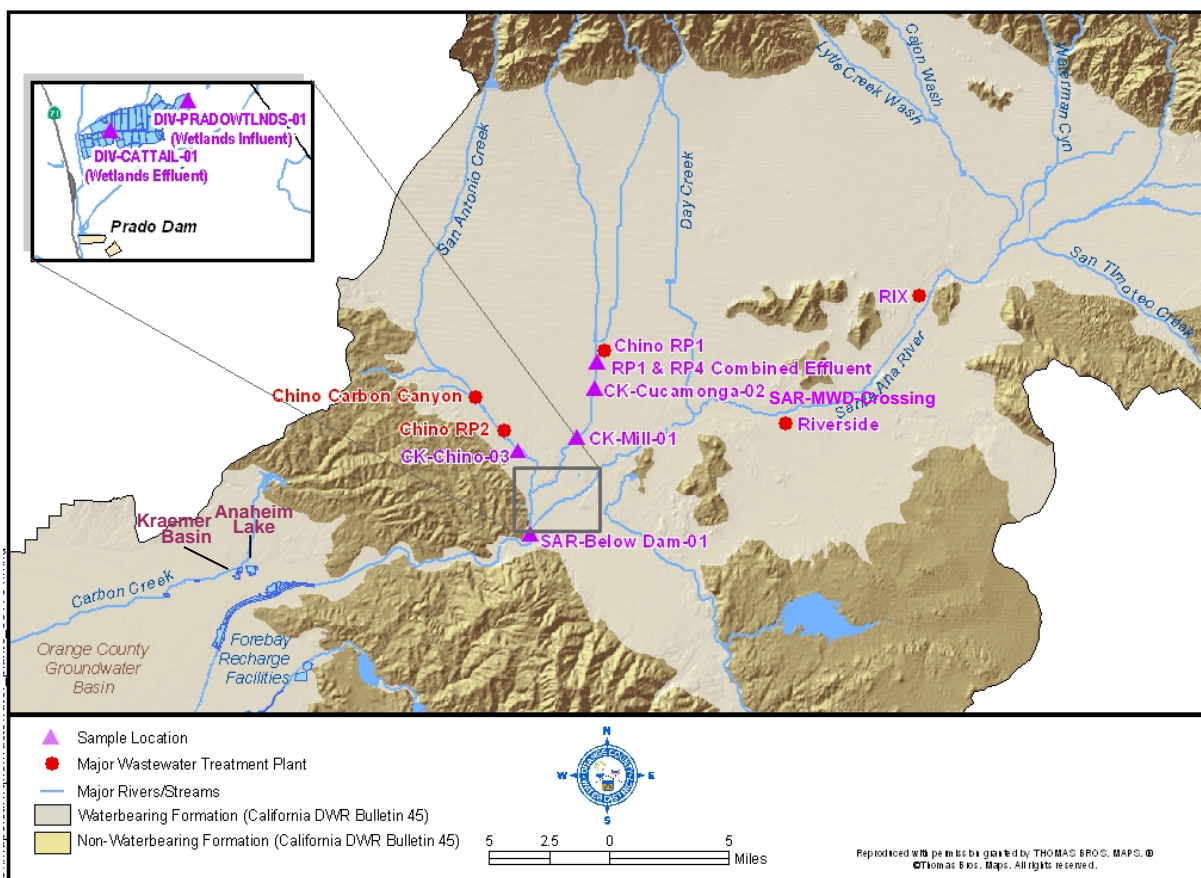


Figure 66 Map showing the major wastewater discharge locations and surface water features of the Santa Ana River system. Reprinted with permission from reference [236], figure 1. Copyright 2007, American Water Works Association

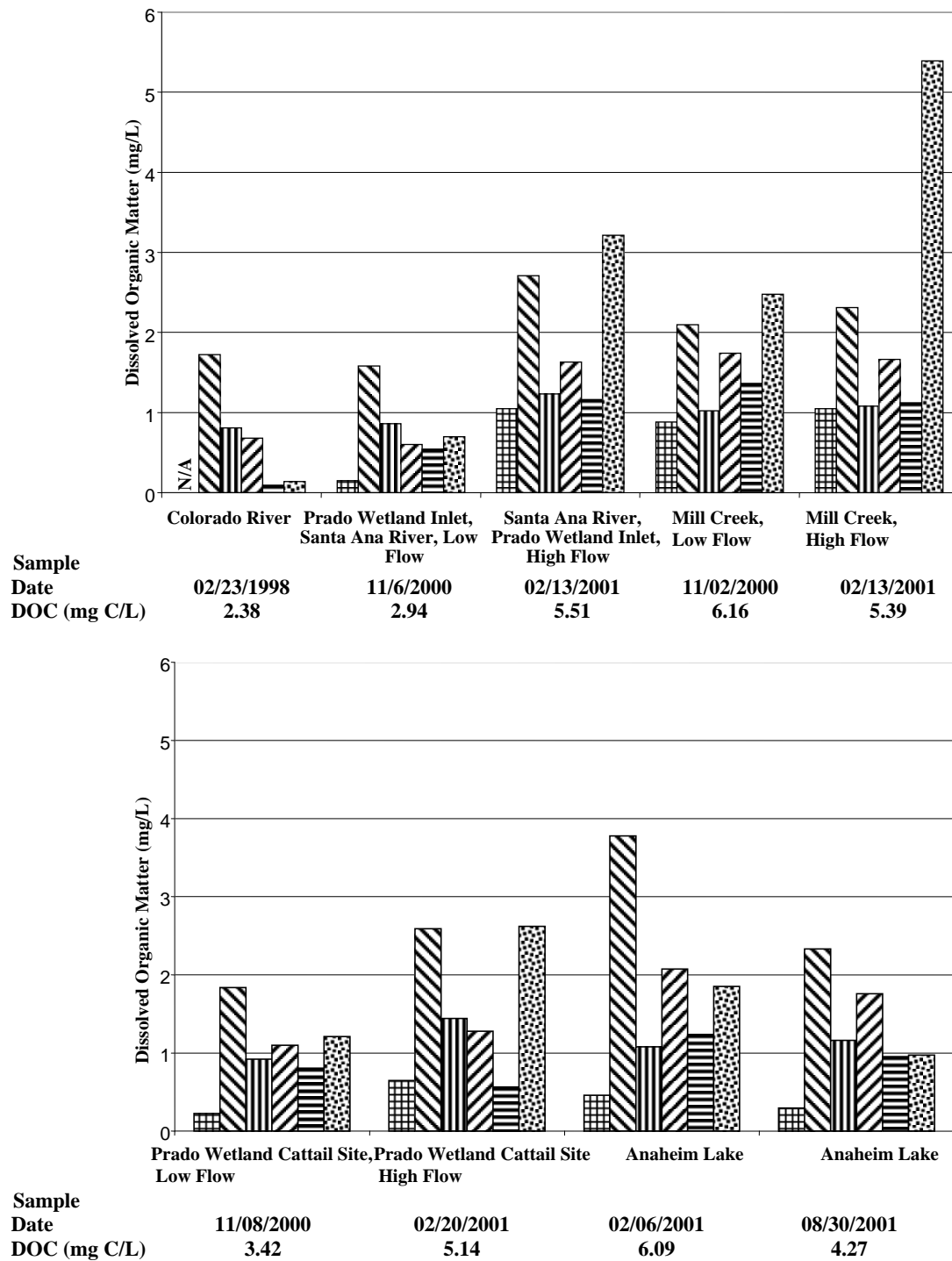


Figure 67 Bar diagrams of surface-water DOM fractionations [grid] Hydrophobic neutrals (HPO-N), [diagonal lines /] Hydrophobic acids (HPO-A), [diagonal lines \] Transphilic acids plus neutrals (TPI-A+N), [diagonal lines -] Hydrophilic acids plus neutrals (HPI-A+N), [diagonal lines =] Hydrophilic bases (HPI-B), [dots] Colloids N/A = Data not available. Reprinted with permission from reference [236], figure 9. Copyright 2007, American Water Works Association

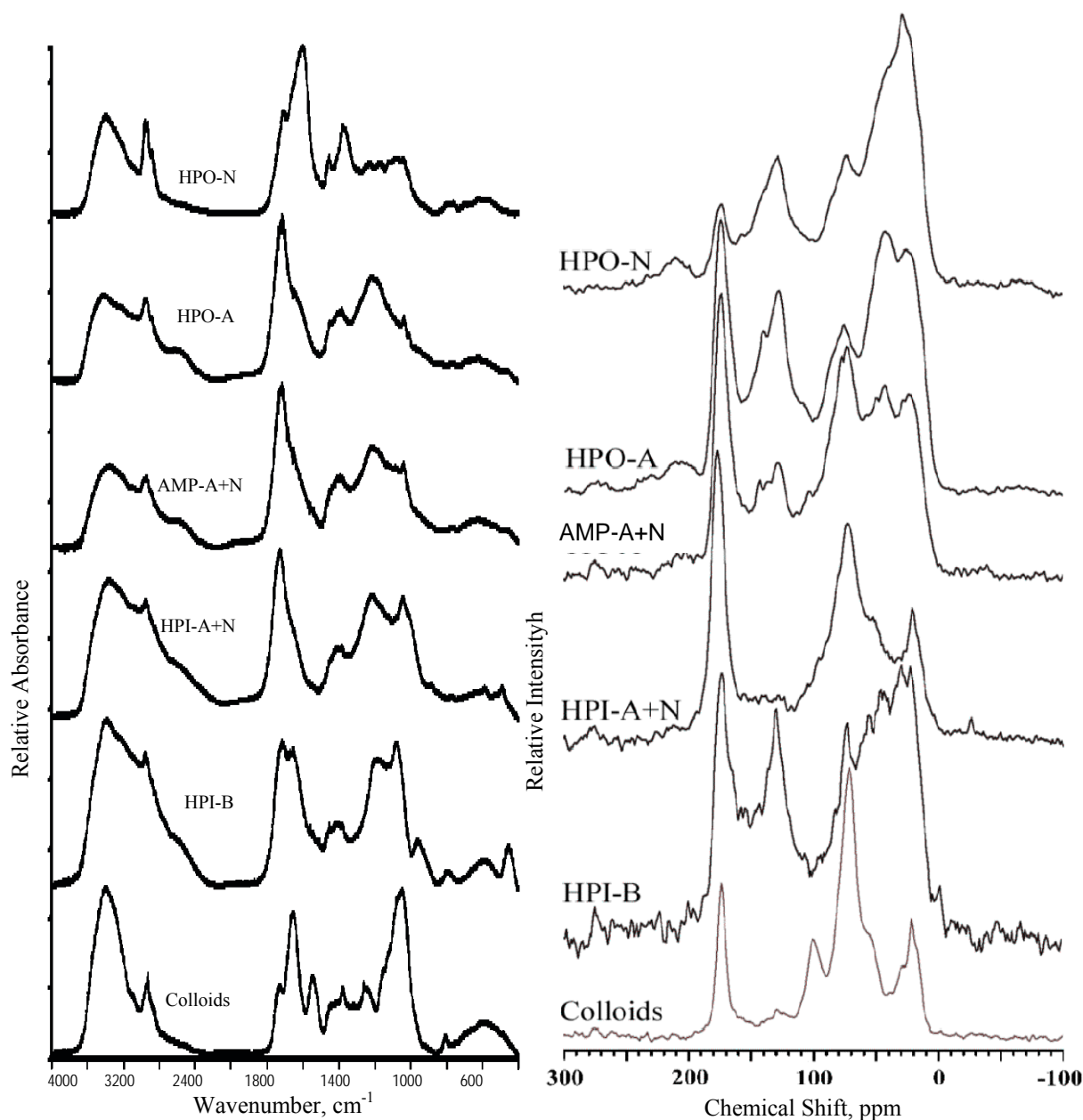


Figure 68 Infrared (on left) and ^{13}C -NMR (on right) spectra of DOM fractions from Anaheim Lake sampled August 30, 2001; DOM fractions include hydrophobic neutrals (HPO-N), hydrophobic acids (HPO-A), amphiphilic acids plus neutrals (AMP-A+N), hydrophilic acids plus neutrals (HPI-A+N), hydrophilic bases (HPI-B), and colloids. Reprinted with permission from reference [236], figure 10. Copyright 2007, American Water Works Association

The colloid fraction has distinctive IR and ^{13}C -NMR spectra indicative of N-acetyl aminosugars most likely derived from bacterial cell walls [18]. The infrared spectrum of this fraction shows secondary amide bands near 1660 and 1550 cm^{-1} , and the methyl

groups of the N-acetyl groups are shown by bands at 1380 cm^{-1} in the infrared spectrum and 20 ppm in the ^{13}C -NMR spectrum. The HPI-A+N fraction appears to contain acidic degradation products of the colloid fraction because the same amide and methyl bands

described for the colloid fraction appear in the HPI-A+N fraction, along with major bands for the carboxylic acid group (1720 cm^{-1} and 175 ppm). The composition of the HPI-B fraction is indicative of aminoacids, peptides, and degraded porphyrins, by the 1660 cm^{-1} amide peak (IR spectrum) and broad $45\text{-}60\text{ ppm}$ peak in the ^{13}C -NMR spectrum.

9.2. Attenuation of Dissolved Organic Matter during Ground Water Recharge

This study [125] focused on the attenuation of dissolved organic matter during the process of ground water recharge from the Anaheim Lake infiltration basin shown in Figure 69. The same parcel of water was sampled in the series of observation wells shown in Figure 69 during its migration in ground water during 2001. The comprehensive DOM fractionation procedure used was the same as that used for the surface water study of the Santa Ana River Basin discussed previously. The DOM fractionation patterns are shown in Figure 70.

Anaheim Lake had been drained and scraped to remove fine sediments that plugged the basin a few days before the beginning of this infiltration experiment. Monitor well DP-ALK1-15 sampled water 15 feet below the bottom of the lake, and the other observation wells sampled ground water during its migration about 0.6 miles during a 10 month period as shown in Figure 70. Almost all the colloid fraction was removed from recharge water during the first 15 feet of infiltration. This colloid removal process was not due to filtration because much larger algal cells were observed to be in suspension in ground water samples from well DP-ALK1-15 and the deeper well AMD 9/1. Therefore, colloid removal is most likely a combination of sorption and biodegradation processes. All of the DOM fractions decreased in concentration during infiltration and migration in ground water as shown in Figure 70.

Compositional changes in the hydrophobic acid fraction are shown in the CP/MAS ^{13}C -NMR spectra of Figure 71. The aromatic carbon peak in the hydrophobic acid fraction decreases during infiltration at Anaheim Lake and during ground water migration (soil/aquifer treatment).

Another compositional change is the deepening of the valley at 30 ppm and the emergence of the peak at 15 ppm in the ^{13}C -NMR spectra of Figure 71. The dipolar-dephased ^{13}C -NMR spectrum of the Well AM 44/1 sample gives a spectrum characteristic of terpenoid-derived fulvic acid shown previously in Figure 38. The spectral region near 30 ppm is mainly

methylene carbon that is becoming depleted during soil aquifer treatment. These results showing selective preservation of terpenoid-derived fulvic acids in ground water are consistent with the resistance of terpenoids to biodegradation and with the fact that they are not removed by sorption on sesquioxide coatings on minerals.

9.3. Total Organic Matter in Stormflows, Santa Ana River Basin

Assessment of total organic matter in stormflows of the Santa Ana River was the most comprehensive and complex of the NOM analyses studies presented in this account. The 2003-2004 stormflow study [74] done by the USGS in cooperation with the Orange County Water District, and its purpose was to characterize the organic substances in stormflows in greater detail than had been performed in the previous Santa Ana River Water Quality and Health study [236]. Samples from Mill Creek, from an urban drain near the Santa Ana River at the Imperial Highway site (Figure 66), and from the Santa Ana River at the Imperial Highway were collected immediately before the storm, at peak flows during the storm, and at the recessional flow after the storm (designated samples SAR-1 through SAR-4, respectively). A significant part of the mountainous portion of the Santa Ana River watershed had burned just before the beginning of the stormflow study, which added to the sediment transport and NOM complexity during the first storm. Three storms were sampled. The hydrographs, DOC concentrations, and sampling times of the Santa Ana River at the Imperial Highway are presented in Figure 72.

The hydrographs do not show especially high flows because of the storage capacity and buffering effects of the Prado Wetlands upstream from the sampling sites, as shown in Figure 66. The hydrographs of the Mill Creek and urban drain sites had much greater extremes in flow.

Data from the Santa Ana River was selected for the example of comprehensive TOM analysis because it is more representative of stormflows in streams than the Mill Creek and urban drain samples, which are more characteristic of urban runoff. Unfiltered samples (20 L) were collected, immediately chilled on ice, and shipped in coolers to the USGS National Water Quality Laboratory in Denver for TOM fractionation (Figure 21). The TOC fractionation bar charts for the Santa Ana River samples in the third storm are shown in Figure 73.

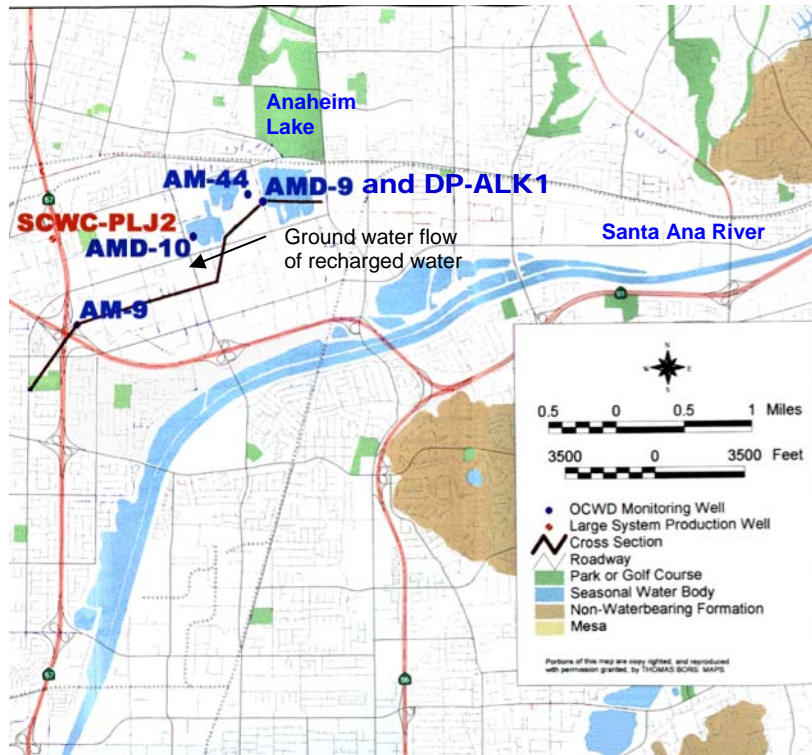


Figure 69 Map of OCWD monitoring wells sites sampled for recharge basin infiltration study [125]. Final number in well designation refers to multilevel sampler label

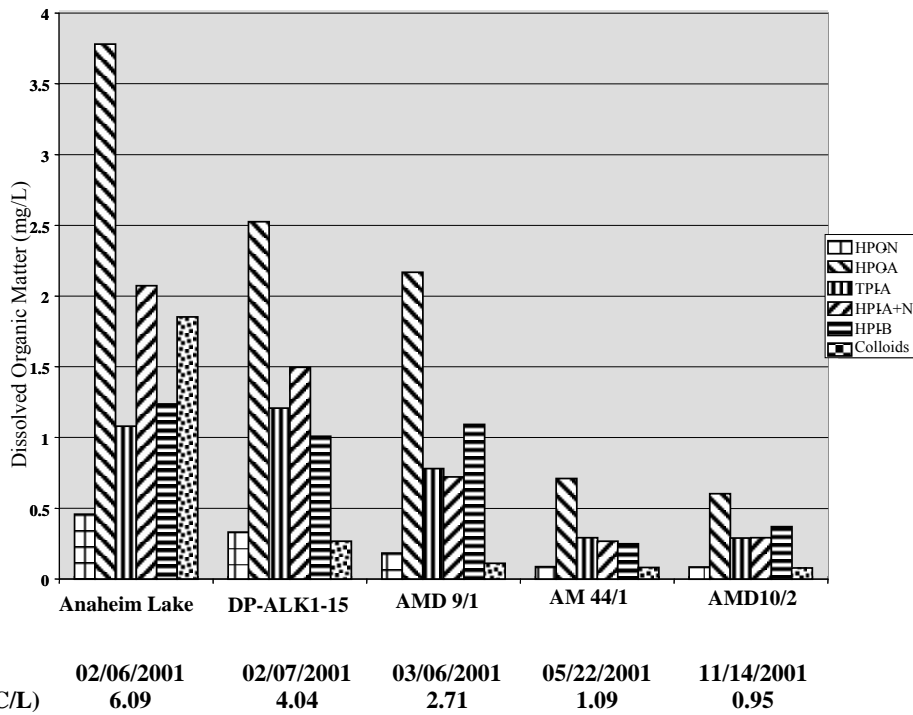


Figure 70 Bar diagrams of DOM fractionations of infiltrated Anaheim Lake water

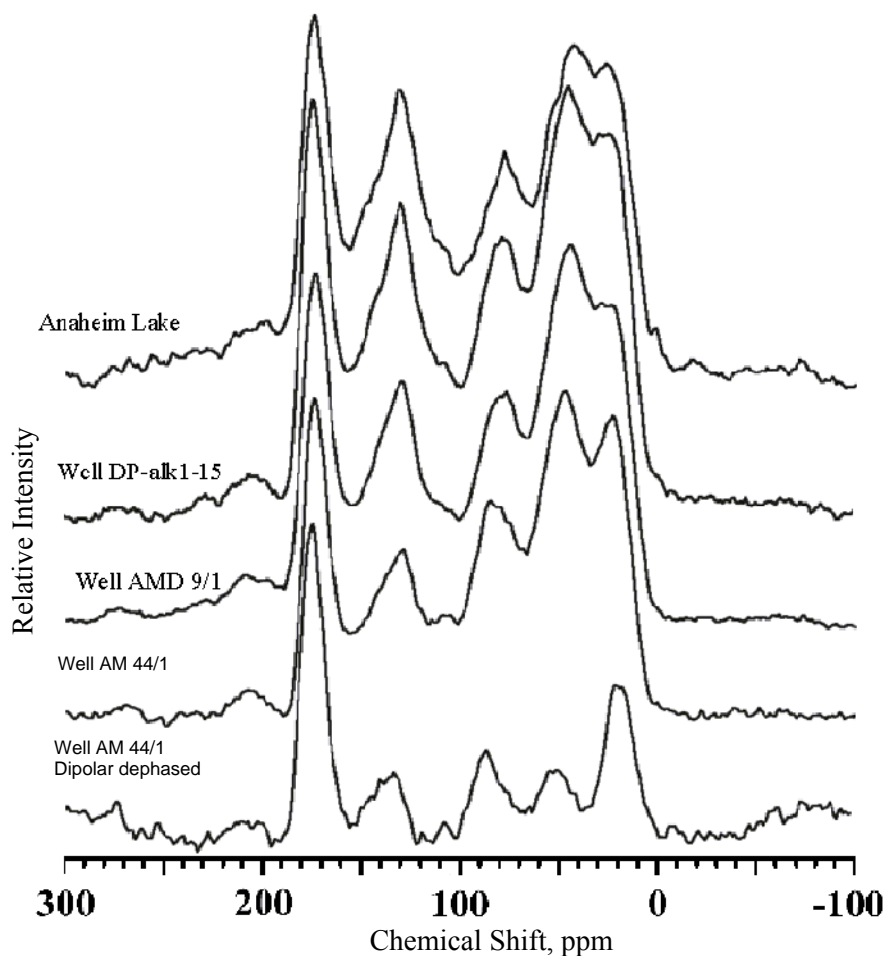


Figure 71 CP/MAS ^{13}C -NMR spectra that illustrate changes in the hydrophobic acid fraction during soil/aquifer treatment

TOC rather than TOM concentrations were plotted in Figure 73 because of some residual ash and water contents in certain fractions. The DOC fraction concentrations are relatively constant, with most of the variability in the extractable organic matter (EOM), humic acid, and humin fractions of the fine particulate portions of the suspended sediment. In the first two storms, variability in the particulate TOC fractions was much greater and its particulate concentrations in the first storm following the forest fire dwarfed the DOC-fraction concentrations (data not shown). This means that particulate concentrations in the third storm are reduced by the flushing effects of the prior two storms. The TOC concentration of the coarse particulate fraction (CPOM) is greatest in the fourth sample, whereas the TOC concentrations of the EOM, humic acid, and humin fractions are greatest in the third sample, indicating differential transport of the coarse and fine particulates.

The atomic C:N ratios of the TOC fractions are presented in Figure 74. The atomic C:N ratio of the CPOM is near 20, which is typical for vegetative litter. The C:N ratios for the humic acid, humin, colloid, TPI-A+N, and HPI-A+N fraction are near 10, which reflects a loss of nitrogen-deficient lipids and carbohydrates in the NOM degradation process. The decrease in the C:N ratio of the HPI-A+N from twelve to five with successive samples results from increasing percentages of cyanuric acid, which has a C:N ratio of 1 [75]. The larger C:N ratios of EOM, hydrophobic neutral (HPO-N), and hydrophobic acid (HPO-A) fractions reflect the nitrogen-deficient lipid precursors from which these fractions were derived. The C:N ratio pattern of the extractable organic matter reflects the presence of extractable nitrogen-rich chlorophyll in the low-flow samples 1 and 2, whereas nitrogen-deficient lipids and hydrocarbons are present in the high-flow samples 3 and 4 derived from terrestrial runoff.

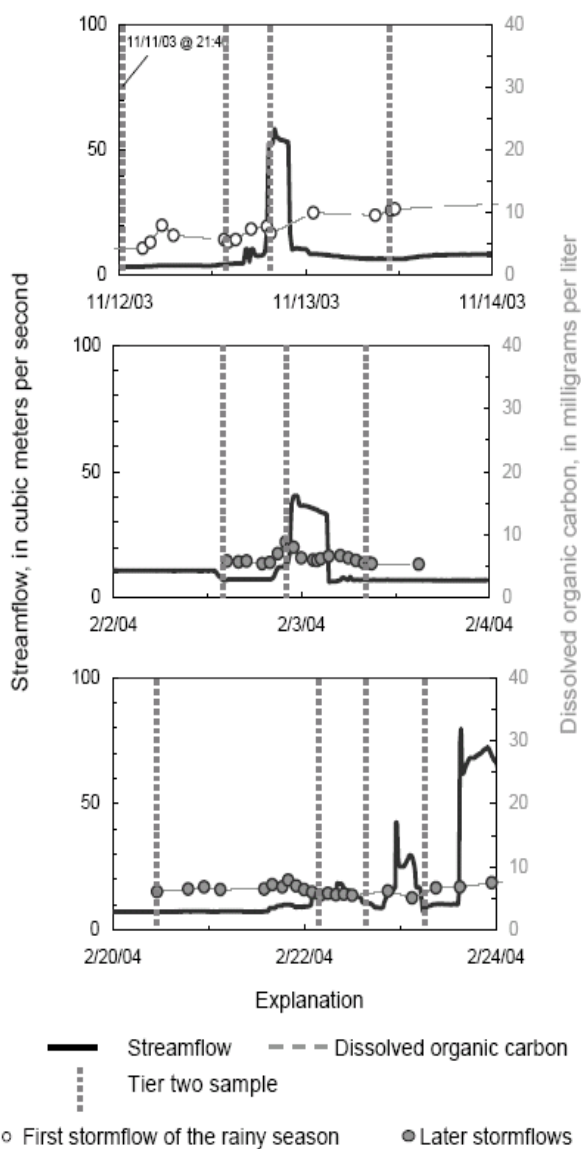


Figure 72 Streamflow and DOC concentrations from selected streamflows in the Santa Ana River at the diversion downstream from the Imperial Highway, southern California, 2003-04 rainy season

The infrared spectra of TOM fractions for the fourth sample collected from the Santa Ana River in the third storm are shown in Figure 75. Peaks indicative of carbohydrates and lipids in vegetation are readily apparent in the CPOM fraction. Lipid peaks are not observed in the EOM fraction because of contamination of this fraction by inorganic salt hydrates during the fractionation procedure. Protein amide 1 and 2 peaks are observed in the humic acid

fraction at 1640 and 1440 cm^{-1} , but they are not readily apparent in the humin fraction because of the interference of black carbon components in the humin. The colloid fraction gives the typical IR spectrum for N-acetyl aminosugars. The IR spectra of the HPO-N, HPO-A, and AMP-A+N are dominated by terpenoid-derived fulvic acids, although the amide 1 peak of proteins near 1660 cm^{-1} is observed in each fraction. The HPI-A+N fraction has sharp peaks near 3200, 1500-1400, and 500 cm^{-1} that were subsequently identified as the anthropogenic contaminant cyanuric acid [75]. The cyanuric acid discovery was first made by infrared spectrometry, demonstrating the value of comprehensive NOM analyses for the occasional discovery of non-targeted contaminants. The infrared spectrum of the base fraction indicates nitrogen-rich compounds that likely contain aminoacids, peptides, and porphyrin and nucleic acid degradation products. The specific compound-class composition of the base fraction is difficult to determine from the infrared spectrum.

The CP/MAS ^{13}C -NMR spectra of selected TOM fractions for the fourth sample taken from the Santa Ana River in the third storm are shown in Figure 76. The CPOM spectrum is dominated by carbohydrate peaks, and a moderate peak near 30 ppm indicative of straight-chain lipids is observed. Small peaks for aromatic methoxy groups, indicative of lipids, and a broad shoulder from 50-60 ppm, indicative of proteins, are also seen. The humic acid and humin fractions also have peaks indicative of carbohydrates, lipids, and proteins, and the acid/amide carbonyl peak near 175 ppm is much greater than in the spectrum of the CPOM fraction, which indicates oxidative degradation of NOM. The large symmetrical aromatic peak in the humic acid and humin fractions is an indication of black carbon derived from the recent forest fire. The sharp peak near 0 ppm in the humin fractions results from contamination by silicone grease during the fractionation procedure [75,81]. CP/MAS ^{13}C -NMR spectra were not determined for the HPO-N, HPO-A, and AMP-A+N fractions, as the IR spectra were sufficiently definitive to determine compound-class composition. The spectrum of the colloid fraction is typical of N-acetyl aminosugars. The HPI-A+N spectrum has a peak near 165 ppm that was identified as the partially enolized form of cyanuric acid (1,3,5-triazine-2,4,6-triol) [75]. The integral of this cyanuric-acid peak was used to quantify its concentration in the Santa Ana River. Lastly, low signal-to-noise of the spectrum of the base fraction illustrates the problem of small fraction size in determining CP/MAS ^{13}C -NMR spectra.

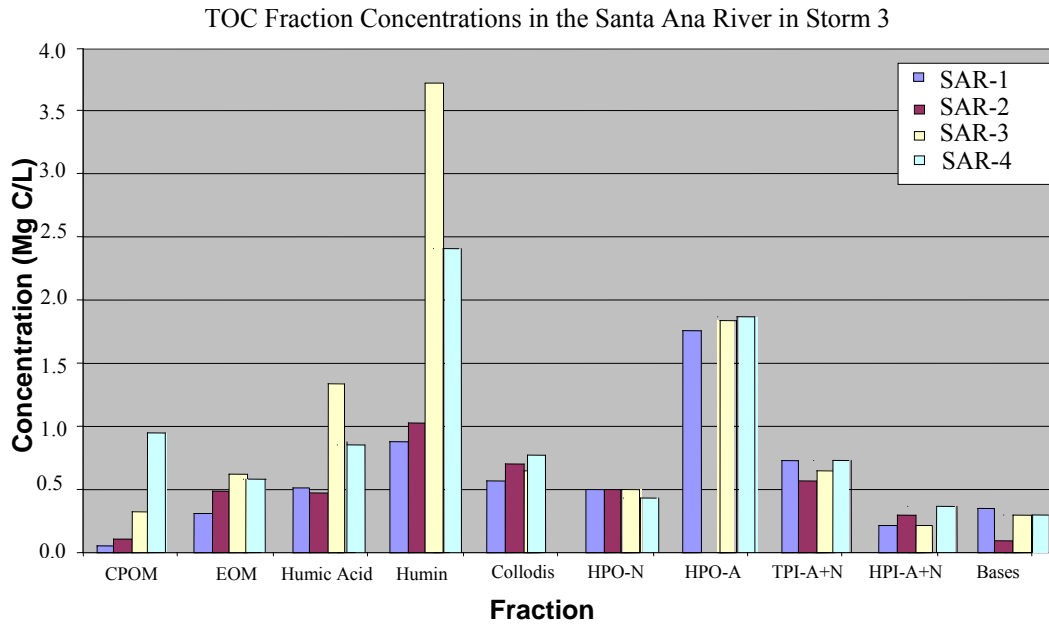


Figure 73 TOC fraction concentrations in the Santa Ana River in the third storm, 1, 2, 3, 4 = Sample number

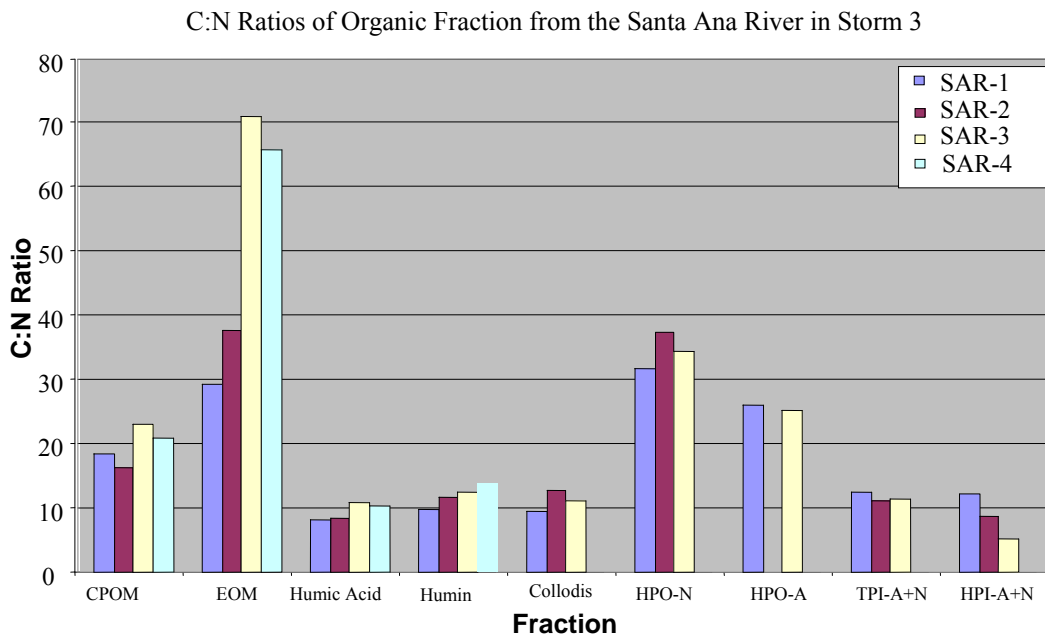


Figure 74 C:N ratios of TOM fractions from the Santa Ana River in the third storm, 1, 2, 3, 4 = Sample number

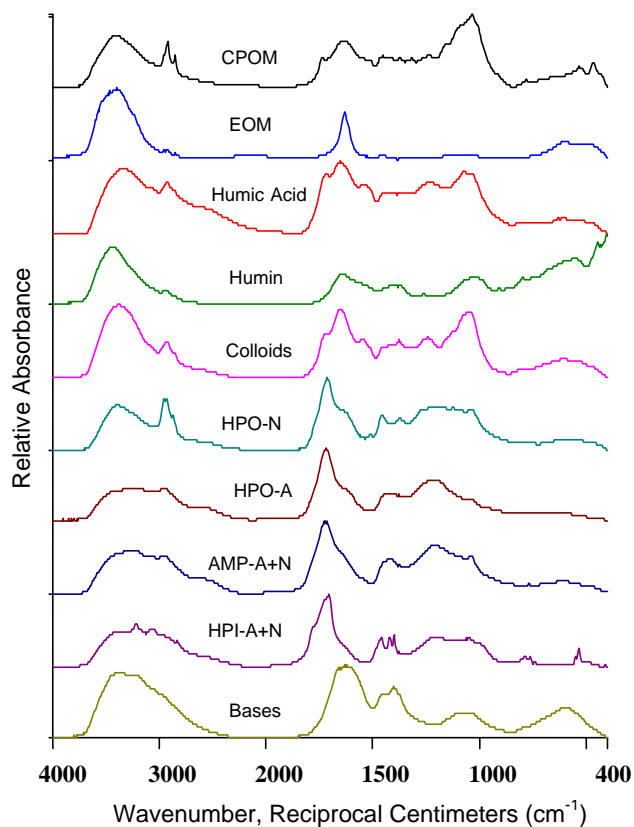


Figure 75 Infrared spectra of TOM fractions from the fourth sample collected from the Santa Ana River in the third storm

Negative ion ESI/MS spectra of the HPI-A+N fraction in samples from the Santa Ana River in the third storm are presented in Figure 77. The progressive increase of cyanuric acid with sample number is clearly shown by the increase of the m/z 128 ion relative to the NOM ions in this fraction. Cyanuric acid was independently identified by infrared (Figure 75), CP/MAS ^{13}C -NMR (Figure 76), and negative ion ESI/MS spectra (Figure 77).

This study of total organic matter in stormflows in the Santa Ana River Basin illustrates how the combination of cooperative funding effort (between the U.S. Geological Survey and the Orange County Water District), project planning, defining of objectives, strategic sampling, hydrologic measurements, TOM fractionation, and spectral analyses result in a comprehensive understanding of TOM composition and transport during baseflow and stormflow conditions. In addition, an unexpected discovery was made regarding the presence and possible origin of cyanuric acid as a degradation product of triazine

herbicides [75]. The transport characteristics and occurrence of black carbon in most TOM fractions in stormflow samples was also a significant finding.

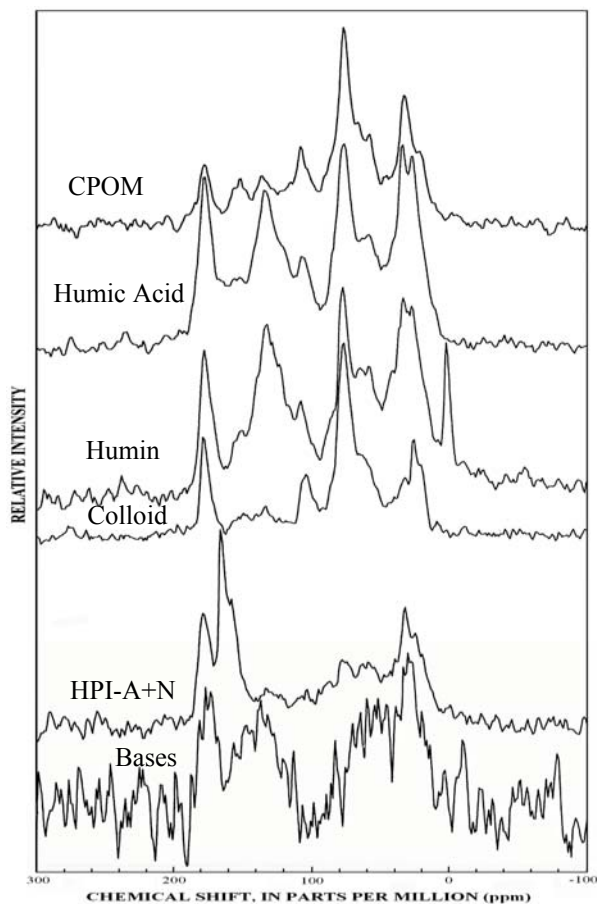


Figure 76 CP/MAS ^{13}C -NMR of selected TOM fractions from the fourth sample collected from the Santa Ana River in the third storm

9.4. Characterization of DOM in Domestic Wastewater Treatment Plant Effluents

Several studies have characterized DOM in domestic wastewater treatment plant effluents (reclaimed water) [78,125,235,237,238]. The DOM fractionation and composition of reclaimed water effluents are not substantially different with respect to major compound classes from natural lake water with DOM derived from autochthonous sources, with the exception of large percentages of surfactants and their metabolites. A number of neutral ethoxyalkylphenol surfactants (APEO's) and their carboxylated metabolites (APEC's) and anionic linear alkylsulfonates (LAS) and their carboxylated metabolites (SPC's and DATS)

were identified by GC-MS of volatile derivatives in reclaimed water infiltrated into ground water in Cape Cod, Massachusetts [237]. Sulfonated anionic surfactants and their metabolites are readily identified as a compound class by infrared spectrometry (Figure 34) and CP/MAS ^{13}C -NMR spectrometry (Figure 37).

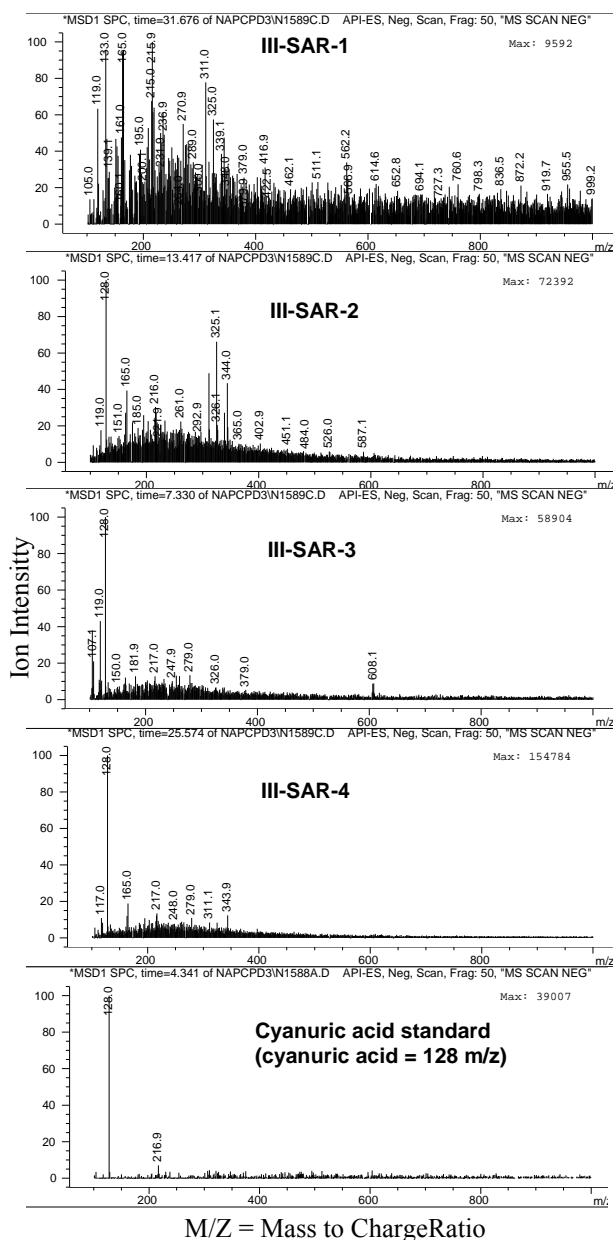


Figure 77 Electrospray/mass spectra (negative ion) of hydrophilic-acid-plus-neutral fractions from the Santa Ana River and cyanuric acid standard (SAR = Santa Ana River; I, II, III = Storm number; 1, 2, 3, 4 = sample number)

Water infiltrated into Anaheim Lake on August 30, 2001, contained 12% of the DOC as aromatic sulfonates (as measured by ^{13}C -NMR spectrometry) from anionic surfactants in reclaimed-water sources [125].

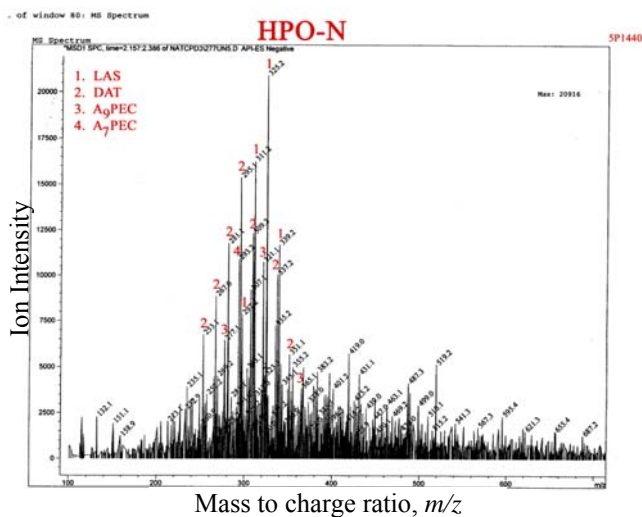


Figure 78 Negative ion ESI/MS of hydrophobic-neutral (HPO-N) fraction from Anaheim Lake showing ions assigned to linear alkyl sulfonates (LAS), dialkyltetralin sulfonates (DAT), and alkylphenol polyethylene glycol carboxylates (APEC)

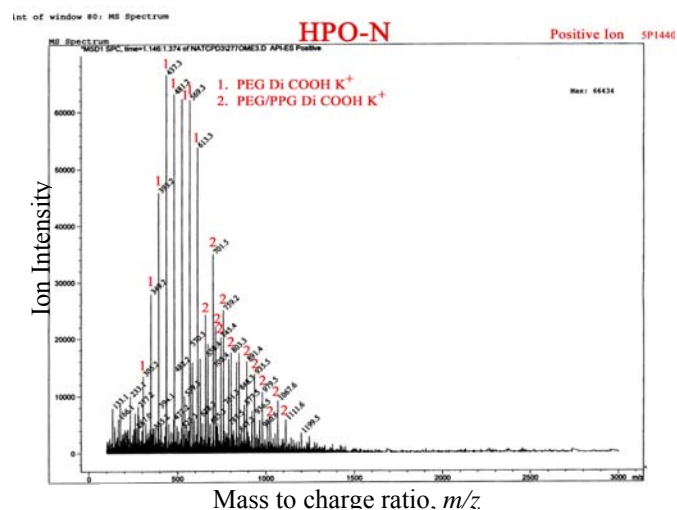


Figure 79 Positive ion ESI/MS of hydrophobic-neutral (HPO-N) fraction from Anaheim Lake showing ions assigned to potassium ion adducts with polyethylene glycol dicarboxylates (PEG Di COOH) and polyethylene glycol/polypropylene glycol copolymer dicarboxylates (PEG/PPG Di COOH)

The electrospray/MS data on the DOM fractions from the August 30 Anaheim Lake sample provide a molecular-level assay of various surfactant-degradation products compared to natural-DOM components. The names, acronyms, and structures of these surfactant degradation products are shown in Table 10. The surfactant degradation product structures presented in Table 10 were determined for the most abundant ion of each homologous series in the mass spectra of Figures 78 to 82. These identifications are tentative in that they were not confirmed with standards and additional fragmentation and chromatographic criteria; however, these structures conform to what is reported in a large body of literature on surfactant degradation products. The dicarboxylic acids could be distinguished from the monocarboxylic acid upon methylation, whereas the monocarboxylic acids shifted by 14 m/z . The hydrophobic-neutral fraction contains mainly the parent LAS and DATS surfactants; the hydrophobic acid fraction contains mainly the monocarboxylate degradation products of LAS and DATS, and the amphiphilic acid fraction contains mainly the dicarboxylate degradation products of LAS and DATS.

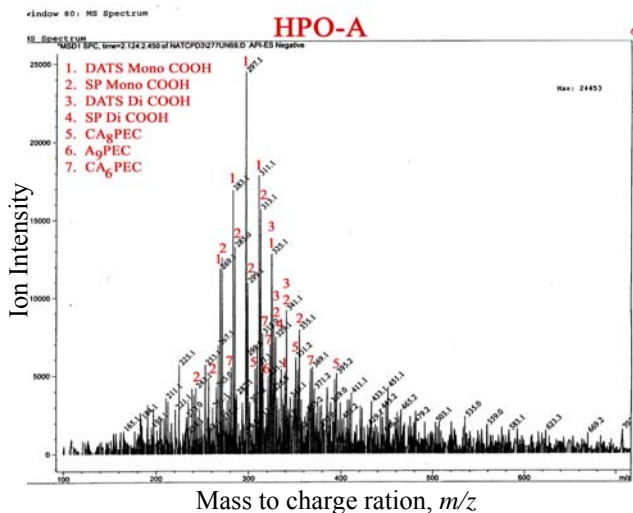


Figure 80 Negative ion ESI/MS of the hydrophobic acid fraction (HPO-A) from Anaheim Lake showing ions assigned to dialkyltetralin sulfonate monocarboxylates (DATS mono COOH), sulphophenyl monocarboxylates (SP Mono COOH), dialkyltetralin sulfonate dicarboxylates (DATS Di COOH), sulphophenyl dicarboxylates (SP Di COOH), alkylphenol polyethylene glycol carboxylates (APEC), and carboxyalkylphenol polyethylene glycol carboxylates (CAPEC)

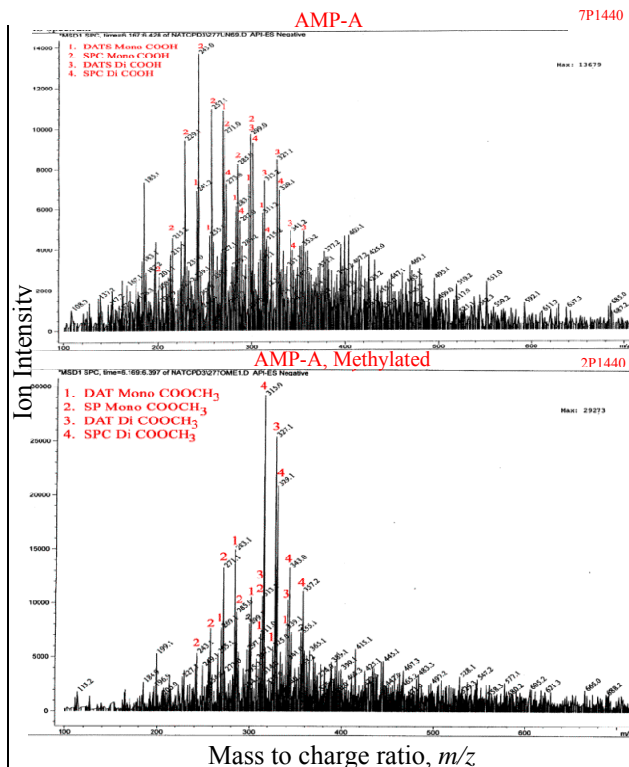
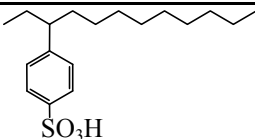
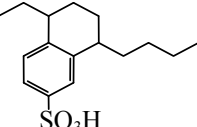
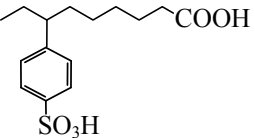
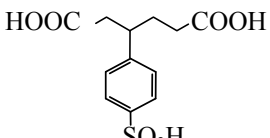
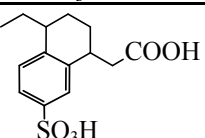
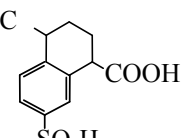
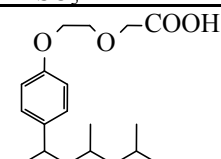
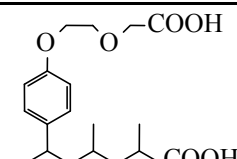
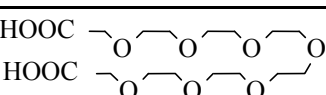
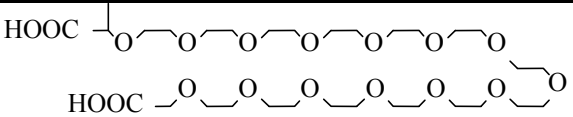


Table 10 Names, acronyms, and structures of surfactant degradation products

Chemical Name	Acronym	Structure	Molar Mass (g/mole)
Linear alkyl sulfonate	LAS		326
Dialkyltetralin sulfonate	DATS		296
Sulphophenyl monocarboxylate	SP Mono COOH		314
Sulphophenyl dicarboxylate	SP Di COOH		302
Dialkyltetralin sulfonate monocarboxylate	DATS Mono COOH		298
Dialkyltetralin sulfonate dicarboxylate	DATS Di COOH		300
Alkylphenol polyethylene glycol carboxylate	APEC		322
Carboxyalkylphenol polyethylene glycol carboxylate	CAPEC		352
Polyethylene glycol dicarboxylate	PEG Di COOH		398
Polyethylene glycol polypropylene glycol dicarboxylate	PEG/PPG Di COOH		720

The hydrophilic-acid-plus-neutral fraction contains an ion that corresponds to an aliphatic sulfonic acid degradation product that may result from opening the aromatic sulfonic acid ring. The two spectra presented in Figure 81 illustrate the ion shifts upon methylation.

The repeating series of ions for the aromatic sulfonate degradation products occurs at m/z differences of 14 (an ethylene group); by m/z differences of 44 (ethoxy group) for the PEG, APEC, and CAPEC degradation products; and by m/z differences of 58 (propoxy group) for the PEG/PPG Di-COOH degradation products. The aromatic sulfonates are derived primarily from anionic surfactants (LAS and its DATS impurities). The PEG, APEC, and CAPEC degradation products are derived from neutral surfactants. The PEG/PPG Di COOH degradation products are derived from PEG/PPG block copolymers, which are components of low-foam detergents used in dishwashers and have been found in significant concentrations in a number of surface waters, including the Mississippi River [238]. These examples of ESI/MS spectra of DOM fractions illustrate how DOM fractionation of reclaimed water effluents can be used as a preparative method for specific contaminant analyses. Surfactant molecules are especially suited for ESI/MS analyses because their surface-active properties allow them to be efficiently ionized [108].

9.5. Characterization of DOM at the Stringfellow Hazardous-Waste Disposal Site, southern California

Stringfellow, in southern California, was previously (1956-1972) a hazardous waste disposal site for disposal of liquid industrial waste from various sources including metal finishing, electroplating, and pesticide (DDT) production [240]. The site is located in Pyrite Canyon, approximately one mile north of Glen Avon in Riverside County. Ground water collected at the disposal site is highly acidic, with pH near 0; it contains very large concentrations of toxic metals and pesticide production wastes. About half of the DOC in the waste was previously determined to be *p*-chlorobenzenesulfonic acid. A USGS research project was begun to characterize the remaining DOC, to determine the DOC removed by a wastewater treatment plant specifically constructed at the site to remove hazardous wastes, and to characterize the DOC in a contaminated ground water plume that extended into Glen Avon [240].

The preparative DOM fractionation was a two-stage procedure whereby organic and inorganic solutes were fractionated into acid, base, and neutral fractions based on the procedure of Figure 17 [50]. The acid fractions desorbed from the Duolite A-7 resin were then sub-fractionated into hydrophobic, amphiphilic, and hydrophilic fractions. The amphiphilic fraction was omitted for the treatment plant influent waste sample because the high DOM concentrations exceeded the capacity of the XAD-4 column. A significant modification to the sub-fractionation procedure was that the pH of the acid fraction was adjusted to pH 0 instead of pH 2 to protonate the strongly acidic sulfonic acids so that their adsorption on XAD resins would be increased. The hydrophilic acid fraction was desalted by zeotropic distillation with acetic acid and selective precipitations described previously [18]. The major DOM constituent, *p*-chlorobenzenesulfonic acid, was extracted from the hydrophilic acid and amphiphilic acid fractions with 80% benzene/20% acetonitrile.

DOM fractionation bar diagrams of the treatment plant influent, of well OW-1 that supplies a portion of the ground water to the treatment plant effluent, and of two samples of the treatment plant effluent are shown in Figure 83. Very large DOM concentrations were observed in the amphiphilic and hydrophilic acid fractions of the treatment plant influent. Waste treatment significantly lowered all of the DOM fraction concentrations, with the amphiphilic acid, found to consist of *p*-chlorobenzenesulfonic acid [240], being the major compound that passed through the treatment plant.

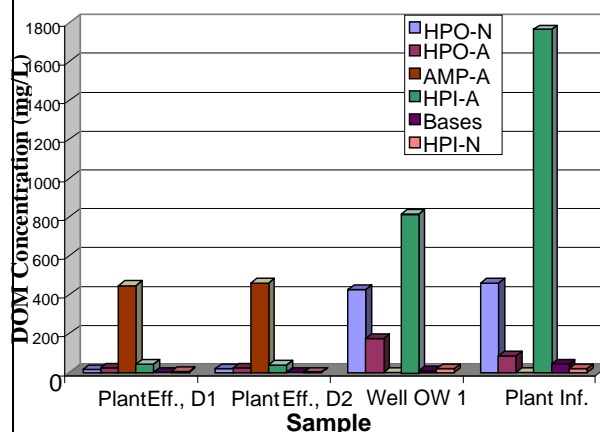


Figure 83 Bar diagram of DOM fraction concentrations for treatment plant influents (inf.) and effluents (eff.) at the Stringfellow Hazardous Waste Site, southern California

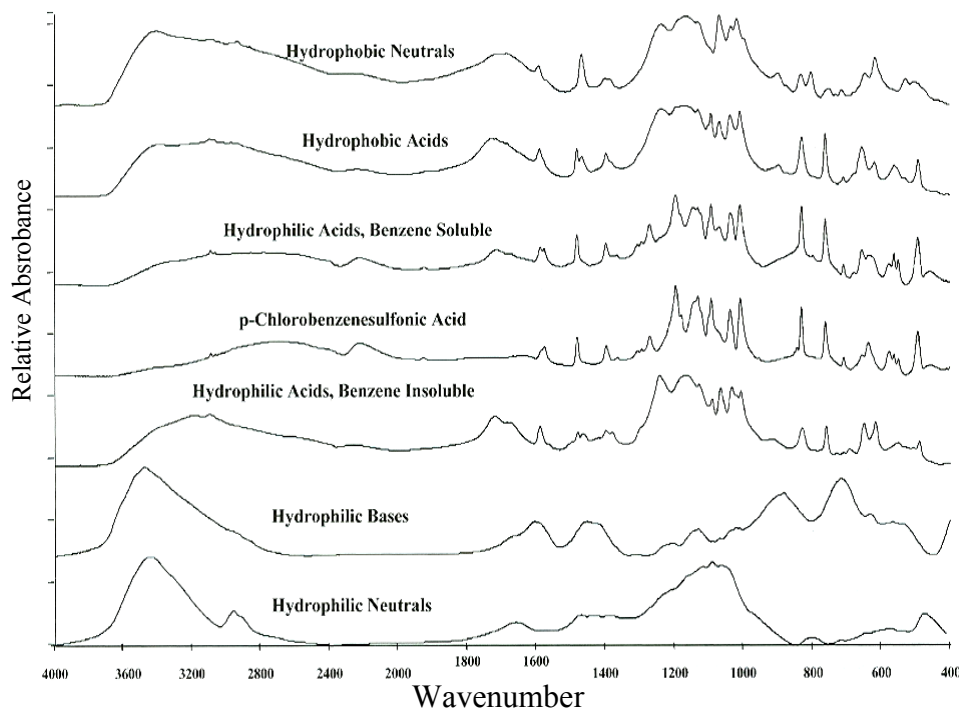


Figure 84 Infrared spectra of DOM fractions isolated from the treatment-plant influent at the Stringfellow Hazardous Waste site, southern California

Table 11 Elemental analyses of selected organic fractions in plant-influent samples (NA = not analyzed)

Fraction	% C	% H	% O	% N	% S	% Cl	% Br	% F	% P	% Ash	% Total
Hydrophobic neutral	37.79	2.59	22.30	0.10	11.46	26.11	<0.1	0.05	0.02	1.29	101.71
Hydrophobic acid	36.35	2.96	29.19	0.18	13.5	18.43	NA	NA	NA	0.98	101.59
Hydrophilic acid, benzene soluble	36.5	3.52	28.56	0.46	16.11	17.01	NA	NA	NA	0.90	108.06
Hydrophilic acid, benzene insoluble	31.36	3.51	36.30	0.94	13.78	13.21	NA	NA	NA	1.27	100.37
Hydrophilic neutral	30.53	5.72	34.56	0.99	0.30	0.60	NA	NA	NA	27.25	99.95

Infrared spectra of the various DOM fractions and sub-fractions are shown in Figure 84. The spectrum of *p*-chlorobenzenesulfonic acid standard is nearly identical to the benzene extract of the hydrophilic acid fraction. The other acid fractions have several peaks in common with the *p*-chlorobenzenesulfonic acid, indicating that this previously uncharacterized DOM belongs to the same compound class of chlorinated benzene sulfonic acids. The ¹³C-NMR spectra of these acid fractions (spectra not shown) revealed only aromatic carbons attached to sulfonic acid and chlorine substituents.

Elemental analyses of selected organic fractions found in the plant influent are presented in Table 11.

All of the acid fractions have large percentages of sulfur and chlorine, indicative of chlorinated sulfonic acid by-products of DDT pesticide synthesis wastes. The chlorine content of the fraction increases as the polarity decreases, indicating that chlorine content is partly responsible for the hydrophobic character of the fraction. The low ash contents of the acid fractions show the efficiency of the isolation procedures in removing very high concentrations of inorganic solutes.

The Stringfellow hazardous waste characterization study [240] is presented to show the applicability of the comprehensive organic analytical approach to a wastewater that contains little NOM. The organic

analytical approach was customized based upon the chemical characteristics of the waste DOM. The distinct fractionation patterns, infrared spectra, ^{13}C -NMR spectra, and elemental analyses were sufficient to identify the waste DOC as synthetic chlorinated sulfonic acids with varying degrees of substitution of aromatic rings with chlorine and sulfonic acid groups. The *p*-chlorobenzenesulfonic acid that passed through the waste treatment plant was found to disappear after infiltration in the ground water plume, but the chlorinated sulfonic acids found in the hydrophobic-neutral and hydrophobic acid fractions persisted in the ground water contaminant plume sampled in wells, with DOC concentrations as low as 2.8 mg/L.

9.6. Characterization of Organic Matter in a Swine Waste Retention Basin

The objective of this study was to determine how pharmaceuticals added to swine feed may interact with NOM in a swine waste retention basin. Organic matter in wastewater sampled from a swine waste retention basin in Iowa was fractionated into 14 fractions on the basis of size (particulate, colloid, and dissolved); volatility; polarity (hydrophobic, amphiphilic, hydrophilic); acid, base, and neutral characteristics; and precipitate or floc formation upon acidification [84]. Particulates in a whole 1 Liter sample were separated by centrifugation and were sub-fractionated into coarse, medium, and fine fractions by wet sieving. The supernatant was vacuum rotary evaporated to 100 mL, and the distillate containing volatile acids was neutralized with NaOH to pH 8 and dried to isolate volatile acids as their sodium salts. Colloids were isolated by dialysis of the non-volatile evaporated concentrate, and they were sub-fractionated by acid precipitation into precipitate colloids and soluble colloids. Non-volatile dissolved organic matter in the permeate from the dialysis procedure was fractionated by the procedure of Figure 18. A bar diagram of this TOM fractionation is presented in Figure 85.

The compound-class composition of each of these fractions was determined by infrared and ^{13}C -NMR spectral analyses. Volatile acids were the largest fraction, with acetic acid being the major component of this fraction. The second most abundant fraction was fine particulate organic matter that consisted of bacterial cells; these were sub-fractionated into extractable lipids consisting of straight-chain fatty acids, peptidoglycan components of bacterial cell

walls, and protein globulin components of cellular plasma. The large lipid content of the particulate fraction suggests that non-polar contaminants, such as certain pharmaceuticals added to swine feed, probably associate with the particulate fraction through partitioning interactions. The precipitate colloid fraction had spectra characteristic of peptidoglycans, and the soluble colloids had spectra characteristic of N-acetyl aminosugars. Cinnamic acid is a major constituent of the hydrophobic neutral fraction, and hydrocinnamic acid is the major constituent of the hydrophobic acid and base fractions. Hydrocinnamic acid, while not a base, isolated on the resin matrix of the MSC-1H cation-exchange resin in the procedure of Figure 18. The hydrophilic-acid-plus-neutral fraction consisted of N-acetyl hydroxy acids derived from degradation of N-acetyl aminosugars. The characteristics of NOM produced by anaerobic degradation are markedly different from NOM produced by aerobic degradation. The large concentrations of bacterial cell components, straight-chain lipids, acetic acid, and cinnamic and hydrocinnamic acids derived from lignin are characteristic of anaerobic degradation processes discussed previously in Reaction 4 [205,206].

9.7. Characterization of Organic Matter in Fog Water

The objective of this study was to obtain an improved understanding of organic matter composition and structure in the atmosphere. The results of this study supported by the Department of Atmospheric Science at Colorado State University are published by Herckes et al [241]. Fog and aerosol samples were collected in the winter of 2003/2004 in Fresno, California, at the experimental farm of California State University. Samples were collected during a 3-week period with a larger version of the Caltech Active Strand Cloudwater Collector. Samples were collected in a 20 L polyethylene carboy to which 48 grams of sodium hydrogen sulfate was added to lower the pH to 1.7 to suppress biological activity. A total of 4.95 L of sample was collected during this three-week period.

The sample was rotary vacuum evaporated to 100 mL. The distillate containing volatile organic acids was titrated to pH 7.5 with 0.1 M NaOH. This distillate was vacuum evaporated and freeze-dried to isolate the sodium salts of volatile organic acids. The sample concentrate was fractionated according to the procedure previously presented in Figure 18.

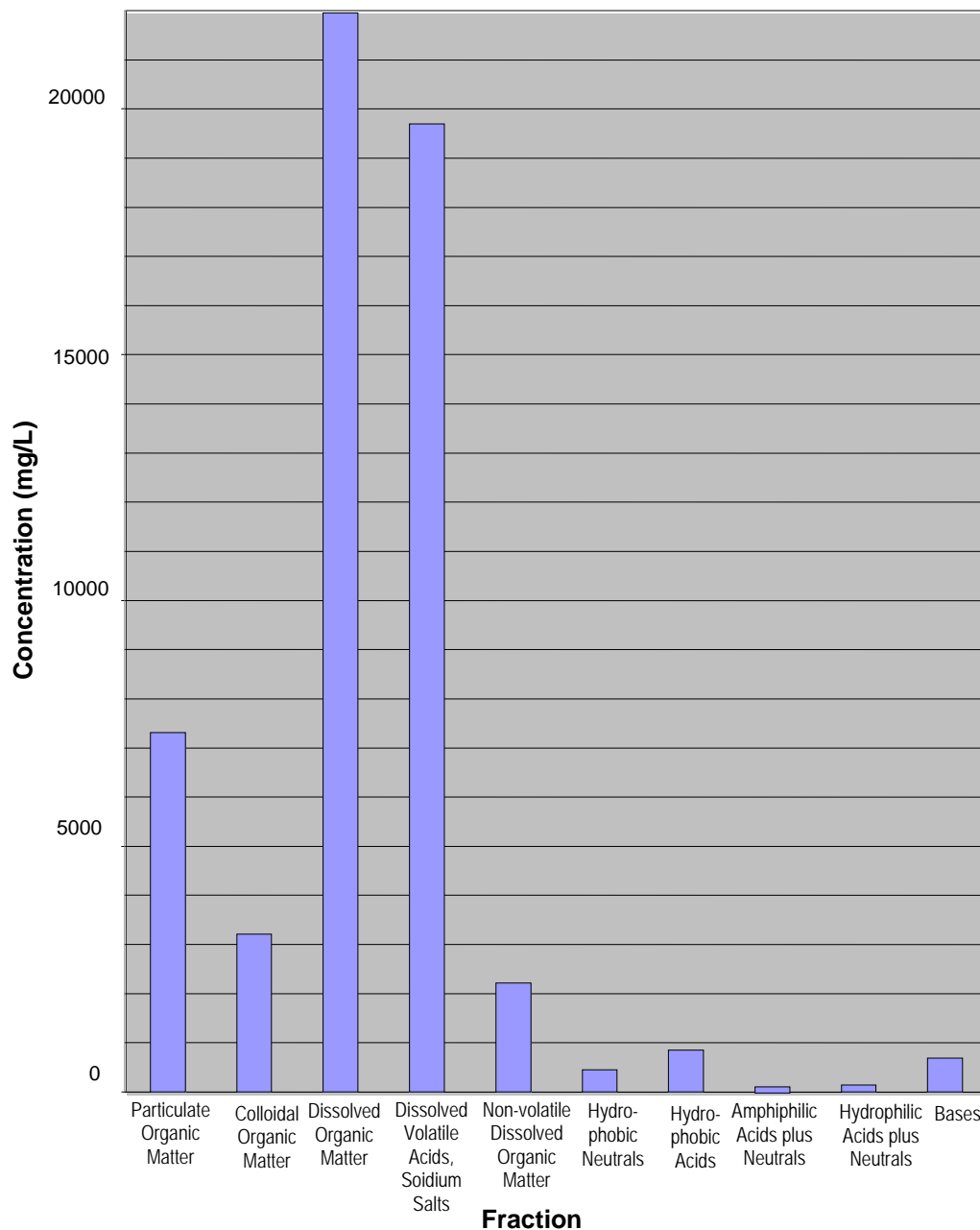


Figure 85 Bar diagram of organic matter fraction concentrations isolated from water in swine waste-retention basin, Iowa.

The amounts of organic carbon isolated in each fraction of the fog water sample are presented in Figure 86. The mass of organic carbon in the sample determined by TOC analysis was 77.9 mg/L, and a total of 62.8 mg was recovered, yielding an organic carbon recovery of 80.6%.

The compound-class compositions of the various fractions were determined from the CP/MAS ¹³C-NMR and FT-IR spectra presented in Figure 87. The major peaks in the FT-IR spectrum of the particulate fractions indicate a mixture of sodium hydrogen

sulfate and sodium sulfate that was not completely removed by dialysis. The color of the particulate fraction was black, but the ¹³C-NMR spectrum detected low aromatic carbon content. The broad bands near 1720, 1650, and 1550 cm⁻¹ in the FT-IR spectrum possibly indicate proteins and N-acetyl aminosugars, and the aliphatic hydrocarbon peak in the ¹³C-NMR spectrum indicative of straight-chain lipids is suggestive of bacterial cell components in the particulate fraction.

The volatile acid fractions have spectra in Figure 87 that show acetic acid as the major component, with lesser amounts of formic acid and a mixture of longer-chain acids such as propanoic and butyric acids. The hydrophobic-neutral fraction gave several peaks in the FT-IR spectra that are typically found in NOM samples from surface and ground water. Peaks (atypical for surface and ground water NOM) at 1630 and 1280 cm^{-1} are indicative of nitrate esters, and the broad, intense peak at 1380 cm^{-1} may indicate N-nitroso and/or C-nitroso compounds. A series of aliphatic N-nitroso compounds in this fog-water sample was independently detected by gas chromatography with nitrogen chemiluminescence detection [241]. The hydrophobic acid fraction also gave nitrate ester peaks in the FT-IR spectrum, and the ^{13}C -NMR spectrum indicated that the bulk composition of the hydrophobic acid fraction was similar to aquatic fulvic acids derived from terpenoid precursors [44]. The amphiphic-acid-plus-neutral fraction also has terpenoid characteristics along with proteinaceous DOM indicated by the amide I and II peaks at 1680 and 1540 cm^{-1} in the FT-IR spectrum. The hydrophilic-acid-plus-neutral fraction is the most abundant fraction (Figure 86), and the spectra (Figure 87) are characteristic of aliphatic hydroxyl acids. The base fraction contained only 3.5% elemental carbon, and the peaks in the FT-IR spectra result from inorganic components in this fraction. The ^{13}C -NMR spectrum of the base fraction indicates a mixture of aliphatic and aromatic amines.

The analytical challenge of the fog water study was to obtain ^{13}C -NMR spectra on small samples, as it was difficult to collect large volumes of fog water to obtain larger samples. ^{13}C -NMR spectra were obtained on samples as small as 12 mg for the hydrophobic neutral fractions, but it took several days to obtain a spectrum with a sufficiently large signal-to-noise ratio to be acceptable. However, the comprehensive analytical approach combined with the complementary information provided by FT-IR and ^{13}C -NMR spectra made it possible to achieve the project objective of an improved understanding of the composition of organic matter in the atmosphere.

9.8. Characterization of Organic Matter in Atmospheric Aerosols

The objective of this study, supported by the Department of Atmospheric Science at Colorado State University, was the same as the objective of the previous study described in this account, namely to obtain an improved understanding of organic matter

composition and structure in the atmosphere. Ambient aerosol samples were collected at five locations in the city of Fresno, California, from December 24, 2003, until January 15, 2004, during the same time period in which fog water was collected [240]. All samplers were equipped with a Tisch Series 231 2.5 micron particulate matter ($\text{PM}_{2.5}$) impactor plate, providing simultaneous coarse particle samples (on a slotted pre-filter) and $\text{PM}_{2.5}$ samples. The aerosol characterization study focused only on $\text{PM}_{2.5}$ samples collected on quartz fiber filters.

In order to provide enough particulate organic carbon for fractionation and analysis, a single composite sample was prepared by combining portions of each of the individual $\text{PM}_{2.5}$ filters. The 96 quartz fiber filter sections were divided into six 16-section portions that were inserted into six 250 mL Teflon centrifuge bottles. A solution of 200 mL of 0.01 M HCl was added to each centrifuge bottle, and the bottles were mixed by rotating on a Glas Col laboratory rotator overnight. The acid solutions were decanted and vacuum-filtered through a 47 mm, 1 μm -porosity glass-fiber filter; 200 mL of deionized water were added to each bottle, the bottles were rotated for one hour, and the water solutions were decanted, filtered, and combined with the acid solution. This water extract was vacuum-rotary evaporated to about 20 mL. The distillate containing volatile organic acids was titrated to pH 8.0 with 0.1 M NaOH. This distillate was vacuum evaporated and freeze-dried to isolate the sodium salts of volatile organic acids.

The 20 mL water extract was placed in a Spectra/Por 3 regenerated cellulose dialysis bag (29 mm diameter, 3500 Dalton pore size cutoff). It was dialyzed for 3 days against 1.1 L of deionized water. The particulate fraction in the dialysis bag was freeze-dried to give a colloid fraction free from salts. The glass-fiber filters used to filter the water extract were added to the quartz-fiber filters in the centrifuge bottles, and the filters were freeze-dried while in the centrifuge bottles. Methylene chloride (100 mL) was added to each centrifuge bottle and the sample was placed on the sample rotator overnight. The methylene chloride was vacuum-filtered through a 47 mm, 1 μm -porosity glass-fiber filter, and was vacuum-rotary evaporated to 5 mL. This 5 mL concentrate was transferred to a 5 mL previously tared glass vial and was blown down to dryness under a stream of nitrogen. This fraction is designated CH_2Cl_2 -extractable organic matter.

The quartz-fiber filters in the six centrifuge bottles and the glass-fiber filters used to filter the water and methylene chloride extracts were

transferred to six Spectra/Por 3 regenerated cellulose dialysis bags (29 mm diameter, 3500 Dalton pore size cutoff), and each bag was dialyzed against 4 L of 0.2 M HF. The HF solutions were changed daily until the filters were completely dissolved; this process took 4 days. The bags were then dialyzed against deionized water until the permeate specific conductance was less than 10 μ Siemens, and the particulate suspension inside the bags was freeze-dried to isolate the particulate organic matter fraction.

Dissolved organic matter fractionation was conducted on the dialysis permeate from the colloid-isolation step according to the procedure presented in Figure 18, except that the column size was scaled back to 20 mL and the XAD-4 column used to isolate amphiphilic DOM was omitted because of the small quantities of organic matter in the sample. The organic carbon fractionation of the aerosol sample is presented in the bar diagram of Figure 88. Each fraction was analyzed for C, H, and N, and FT-IR spectra were obtained on each fraction, but only selected major fractions were analyzed by CP/MAS 13 C-NMR spectrometry because of limitations in fraction mass as shown in Figure 88. The organic carbon recovery of the fractionation procedure was 83% based upon

summation of carbon in the isolation fractions divided by the organic carbon analyzed in the quartz-fiber filters.

The CP/MAS 13 C-NMR and FT-IR spectra of the aerosol fractions are presented in Figure 89. The particulate organic matter fraction is the largest fraction in the aerosol sample. The isolated fraction appeared black, having substantial (35.6%) aromatic (elemental) carbon (Figure 88) content based upon the 13 C-NMR spectrum (95-165 ppm) of Figure 89. The elemental carbon content determined by 13 C-NMR spectrometry is 10.2 mg, about half the content (20.1 mg) of elemental carbon directly determined on the quartz-fiber filters by the NIOSH method [242]. The infrared spectrum (Figure 89) of this fraction is free of any bands indicating inorganic substances such as the quartz-fiber filter in which the aerosols were entrained. The sharp band at 2920 cm^{-1} and the sharp peak at 30 ppm in the 13 C-NMR spectrum are indicative of methylene groups in straight-chain hydrocarbons. The band at 1700 cm^{-1} and small peak at 174 ppm indicate the presence of carboxylic acid groups. The broad band near 1620 cm^{-1} in the infrared spectrum indicates aromatic and hydrogen-bonded quinone groups.

Total Organic Carbon Fractionation of Fresno Fogwater

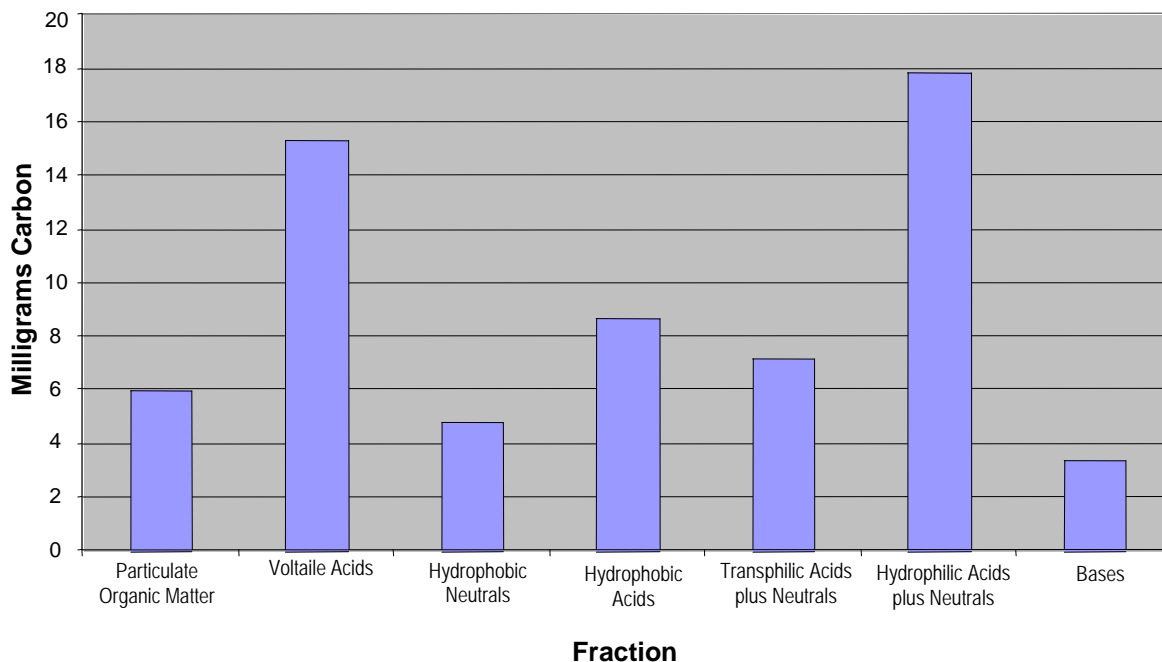


Figure 86 TOC fractionation of Fresno fog water sample. Reprinted with permission from reference [241], figure 2. Copyright 2007, American Chemical Society

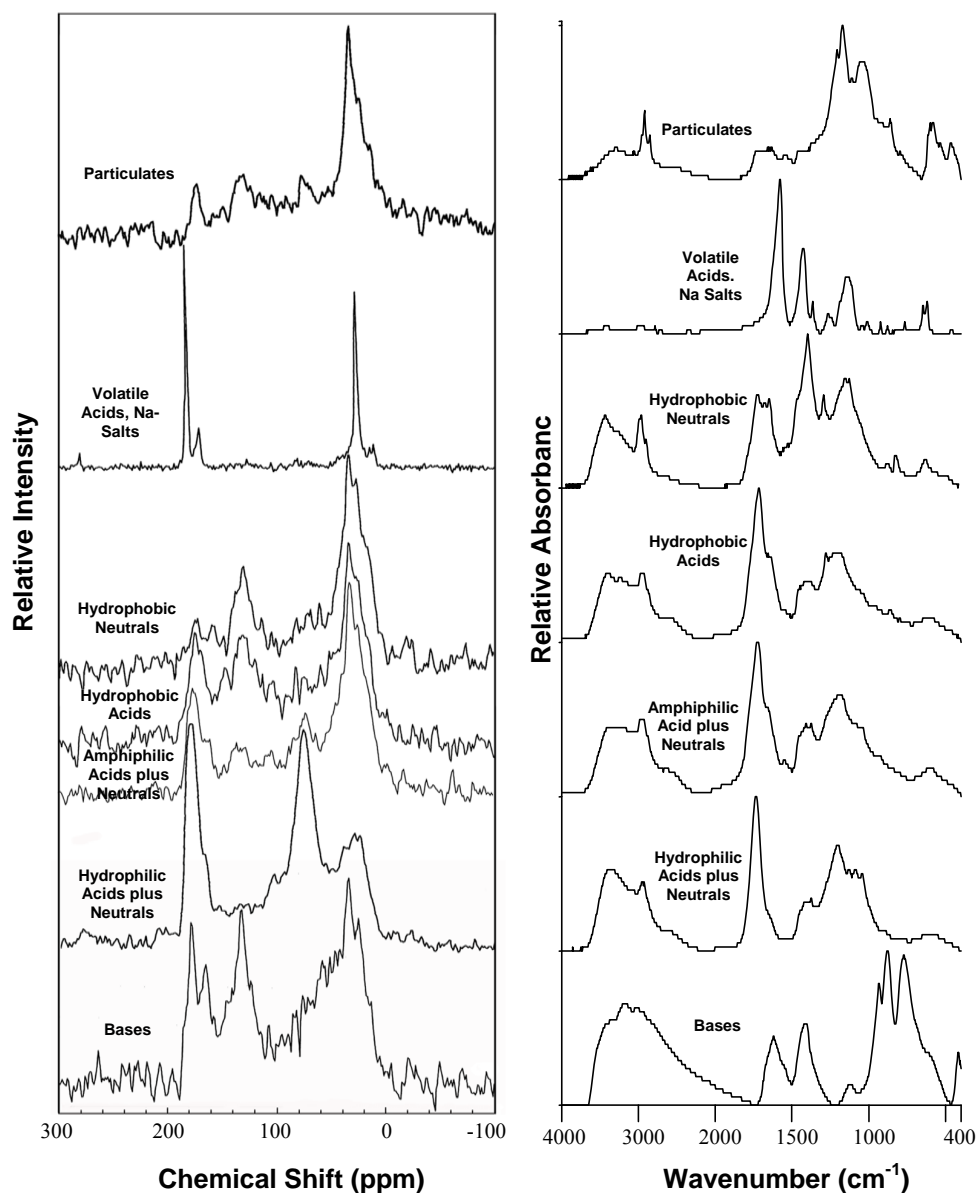


Figure 87
CP/MAS ^{13}C -NMR (left) and FT-IR (right) spectra of organic fractions isolated from Fresno fog water sample. Reprinted with permission from reference [241], figures 3 and 4. Copyright 2007, American Chemical Society

The large difference in “elemental carbon” measured by the thermo-optical method in individual filters and the aromatic (elemental) carbon content measured in the particulate organic carbon fraction is intriguing. It is unlikely that such a large difference (approximately a factor of two) can be explained by uncertainties associated with constructing the filter composite or by losses in the isolation procedure. More likely, a large fraction of what is measured as elemental carbon by the thermo-optical method is not a pure graphite (aromatic) structure but rather contains a substantial amount of other refractory organic

material. The fact that a large aliphatic component (0-55 ppm, shown in the ^{13}C -NMR spectrum of Figure 89) in the particulate organic matter fraction was not extractable with methylene chloride suggests that the aliphatic hydrocarbons are covalently bonded with the black carbon component, perhaps as the result of radical-coupling reactions. These conflicting results illustrate how an understanding of the chemical structure of soot in general and aerosol elemental carbon in particular is poor. This is not a problem unique to the aerosol science community; black carbon has also recently been found to be over-

estimated in soils and sediments because of methodological artifacts [46].

The CH_2Cl_2 -extractable organic matter fraction is the second-highest organic carbon mass fraction (see Figure 88). The extractable organic matter in the sample consisted mainly of straight-chain aliphatic hydrocarbons. These aliphatic hydrocarbons may be attached to carboxylic acid (1710 cm^{-1}), ester (1735 cm^{-1}), and aromatic (1620 cm^{-1}) structures, which contribute small peaks to the infrared spectrum of this fraction (Figure 89). Silicone bands (1260 , 1100 , 1053 and 804 cm^{-1}) are also present in the methylene chloride extract fraction as a result of contamination by silicone lubricant used on the seals in the vacuum-rotary evaporator. The silicone bands are a minor mass contaminant as the organic carbon contribution due to silicones was calculated as 3.13 mg based upon measuring the ratio of the peak intensity at 2960 cm^{-1} (methyl groups in silicones) to the peak intensity at 2920 cm^{-1} (methylene groups in sample hydrocarbons) and calculating the relative contributions of silicone versus sample components based upon absorptivity

ratios of standard compound spectra published by Pouchert [33].

The volatile acid fraction in aerosol samples constitutes a lower percentage for the mass (Figure 88) than in fog samples collected in this region (Figure 86). This is not surprising, given the high solubility of weak organic acids in the high pH (6-8) Fresno fog waters. The aerosol volatile acid fraction is also substantially different in that acetic acid (measured as acetate), which is the dominant volatile acid in the fog water samples, is a component (peak at 26 ppm in the ^{13}C -NMR spectrum), but greater amounts of longer-chain (methylene peak at 30 ppm), and branched-chain (methine peak at 38 ppm and methyl peak at 14 ppm) acids are present as well. The broad peak at 72 ppm might be indicative of volatile ether acids, and the peak at 127 ppm indicates the presence of volatile aromatic acids. The NMR peak at 171 ppm is indicative of sodium carbonate, which is also indicated by the broad band at 1440 cm^{-1} in the infrared spectrum of Figure 89. Sodium carbonate might result from drying this fraction at too high a pH value.

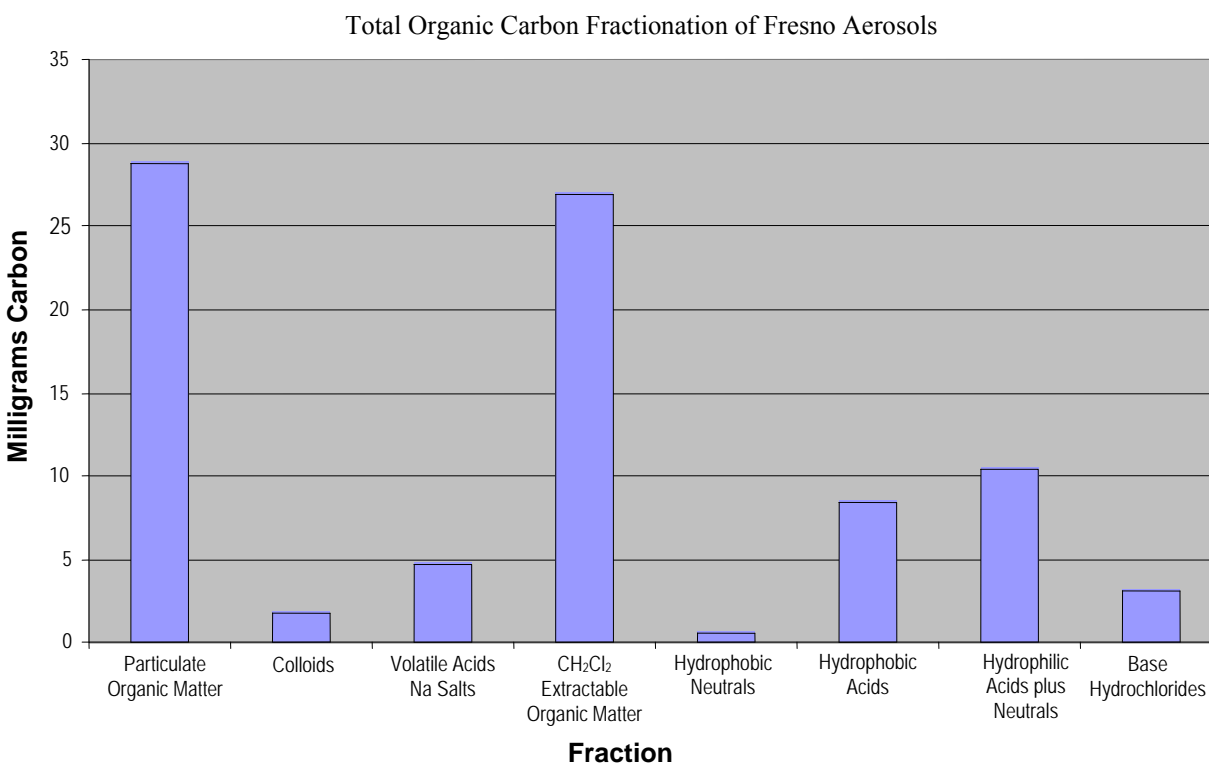


Figure 88 TOC fractionation of Fresno aerosol sample

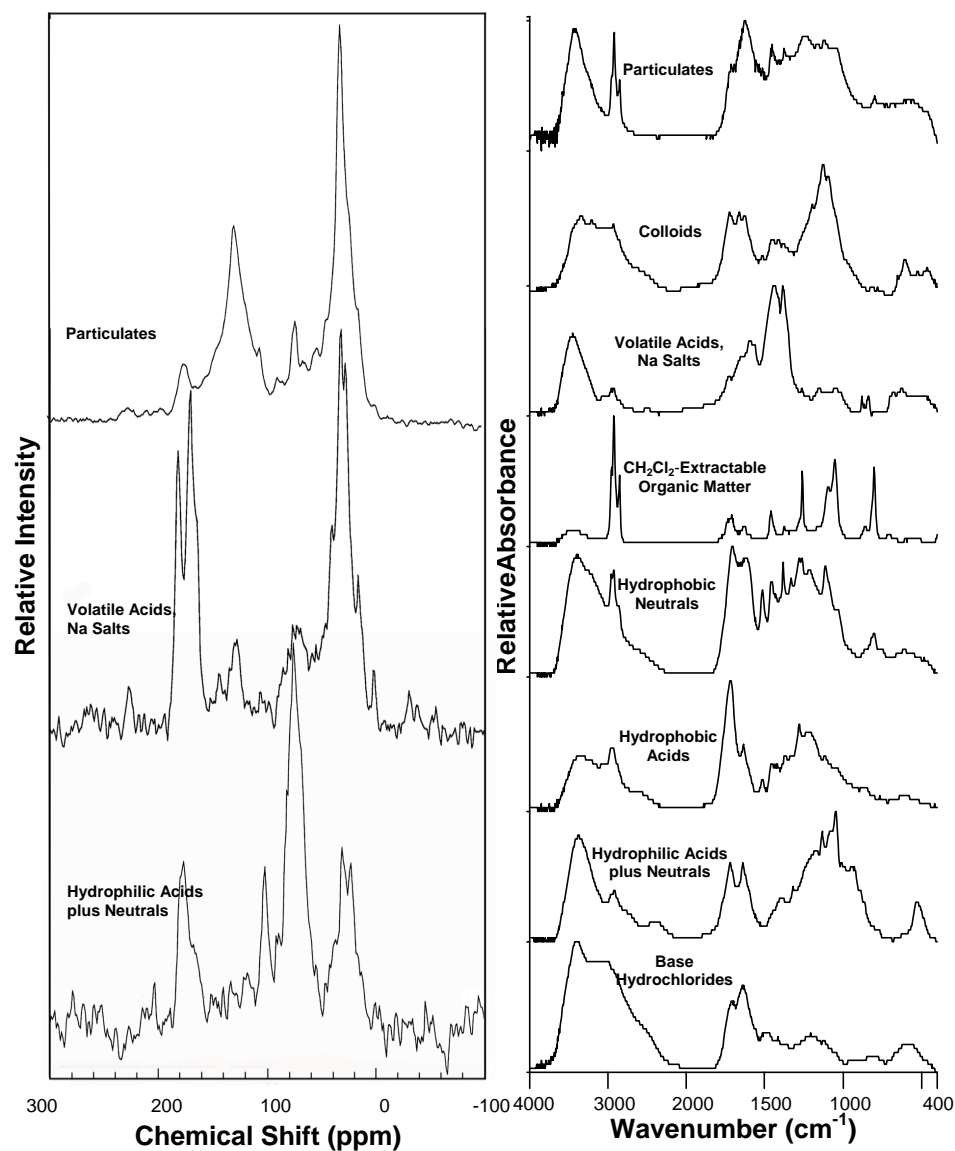


Figure 89 CP/MAS ^{13}C -NMR (left) and FT-IR (right) spectra of organic fractions isolated from Fresno aerosol sample

The mass of the colloid fraction, representing just 2% of the total recovered carbon, was sufficient only for an infrared spectrum (see Figure 88). Inorganic sulfates are indicated by bands at 1125 and 607 cm^{-1} ; silicates are indicated by bands at 1095 and 460 cm^{-1} . Organic structure bands at 1720, 1665, 1627, 1513, and 1413 cm^{-1} are suggestive of lignin structures. The hydrophobic neutral fraction contributes the smallest mass to the total organic carbon fractionation (1%), and only an infrared spectrum (Figure 89) was obtained. Organic structure bands at 1720, 1630, 1515, 1280 and 1113 cm^{-1} are again suggestive of lignin structures; the differing position of these bands relative to similar bands reported in the colloid fraction may reflect a greater degree of

oxidation and degradation of lignins in the hydrophobic neutral fraction. A small, sharp band at 1260 cm^{-1} suggests the presence of nitrate esters. Bands for nitrite esters and nitroso groups were not found in this fraction, in contrast to their presence in analysis of a Fresno composite fog water sample (Figure 87).

The hydrophobic acid fraction was isolated as a very “sticky” fraction, which precluded obtaining a ^{13}C -NMR spectrum. Sharp bands in the infrared spectrum at 1630 and 1280 cm^{-1} indicate nitrate esters. The nitrogen content of this fraction (1.95%) is consistent with the presence of nitrate esters. Bands at 1515, 1335, and 1120 cm^{-1} may indicate again degraded lignin components.

The hydrophilic-acid-plus-neutral fraction contains the majority of the water-soluble organic carbon (Figure 88). The infrared spectrum (Figure 89) has a strong C-O band at 1050 cm^{-1} and only a moderate carboxylic acid band at 1720 cm^{-1} . The ratio of these two bands indicates that neutral components rich in aliphatic alcohols are greater than carboxylic acid components. The ^{13}C -NMR spectrum (Figure 89) indicates the fraction contains carbohydrates (anomeric carbon peak at 102 ppm and alcohol peak at 72 ppm). An additional compound class in this fraction is indicated by the infrared and ^{13}C -NMR spectra showing the presence of structural methyl groups (2960 cm^{-1} band and 21 ppm peak) that are not typically found in carbohydrate structures. Methylene hydrocarbon structures are indicated by the 2920 cm^{-1} band and 30 ppm peak. No aromatic carbon structures are found in this fraction. A possible explanation for the presence of branched methyl groups in this fraction is the formation of secondary organic aerosols through photooxidation of isoprene [243]. A number of methyl branched-chain polyols are formed through this atmospheric reaction, and their structures are consistent with spectral signatures in this fraction.

The base fraction is a relatively minor component of the Fresno aerosol (4% of recovered carbon), but it is a fraction that is very rich in nitrogen, with an atomic C:N ratio of 3.5. The infrared spectrum (Figure 89) of the base hydrochlorides does not show any indication of ammonium chloride; thus, the nitrogen content of this fraction is derived from the sample and not the ammonia eluent. The broad bands at 1720 , 1600 , and 1500 cm^{-1} are typical of a mixture of amino-acids and peptide hydrochlorides [33].

Both the Fresno fog-water and aerosol studies illustrate how comprehensive NOM fractionations and characterizations developed for water and sediment samples can be adapted to atmospheric samples. The quantities of NOM isolated in each fraction were much smaller for the atmospheric samples, but the small sample requirements of FT-IR spectrometry proved to be a significant advantage over CP/MAS ^{13}C -NMR spectrometry sample requirements. Organic carbon recoveries on the atmospheric samples were comparable to organic carbon recoveries on water and sediment samples. The unique fractionations and fraction compositions of the atmospheric samples compared to water and sediment samples suggest that the results reflect NOM characteristics in differing samples and are not the results of methodological artifacts.

9.9. Characterization of NOM in Hydrophobic Soils Altered by Fire

The objective of this study was to determine the characteristics and processes by which NOM is altered by wildland fires to produce hydrophobic soils [82]. The A-horizon of burned and unburned soils developed in coniferous forests was sampled immediately after the Cerro Grande Fire near Los Alamos, New Mexico, and after the High Meadows Fire near Bailey, Colorado.

The soil samples (100 g) were sieved to < 1.0 mm, treated with 0.2 M HF to remove sesquioxide coatings, sonicated, settled, and sieved to isolate the coarse organic matter fraction as shown in Figure 21. After freeze-drying, the extractable organic matter fraction was isolated with 2:1 methylene chloride/methanol. The extracted soil was dispersed in sodium polytungstate of density 2.3 and centrifuged to separate soil organic matter from mineral matter. After washing out the sodium polytungstate by centrifugation, humic acid was extracted with 0.1 M NaOH, precipitated at pH 1, and freeze dried. The non-extractable humin was treated with 0.8 M HCl and with 1.5 M HF to destroy remaining mineral matter, and the humin was washed with water, centrifuged, and freeze-dried.

A bar diagram presenting the total organic matter fractionation of burned and unburned soil samples from the High Meadows Fire is presented in Figure 90. There were decreases in the coarse particulate organic matter and extractable organic matter fractions and increases in the humic acid and humin fractions resulting from alteration of soil organic matter by fire.

The infrared spectra of the extractable organic matter fraction in the burned and unburned soils from the High Meadows Fire are presented in Figure 91. Several peaks indicative of alkene hydrocarbons in pine resins were observed between 1000 and 600 cm^{-1} in the unburned soil, whereas these alkene peaks were absent in the burned soil. The infrared spectra of the humin fraction in the burned and unburned soils from the High Meadows Fire are presented in Figure 92. The humin fraction from the burned soil has more aliphatic hydrocarbons (peak at 2920 cm^{-1}) and aromatic ether linkages (broad peak near 1150 cm^{-1}) than are found in the unburned soil. The CP/MAS ^{13}C -NMR of these same humin fractions are presented in Figure 93. These NMR spectra show the quantitative increase in the aliphatic hydrocarbon peak near 30 ppm. These aliphatic hydrocarbons are covalently bound to the humin structure, as they were not extractable with 2:1 methylene chloride/methanol.

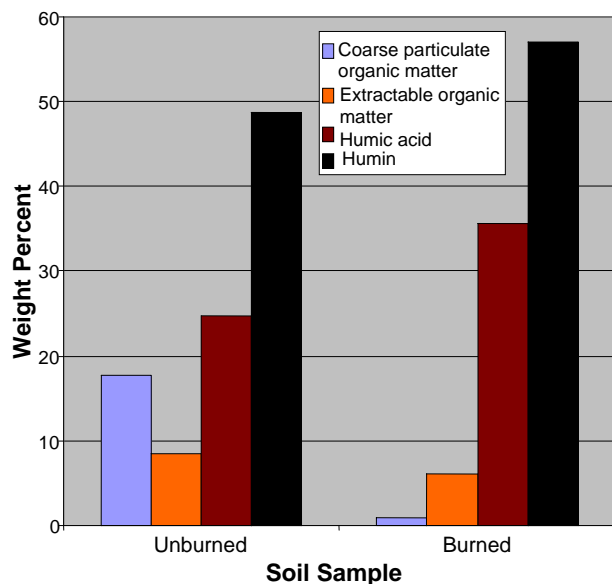


Figure 90 TOM fractionation of burned and unburned soils under lodgepole pine, High Meadows Fire

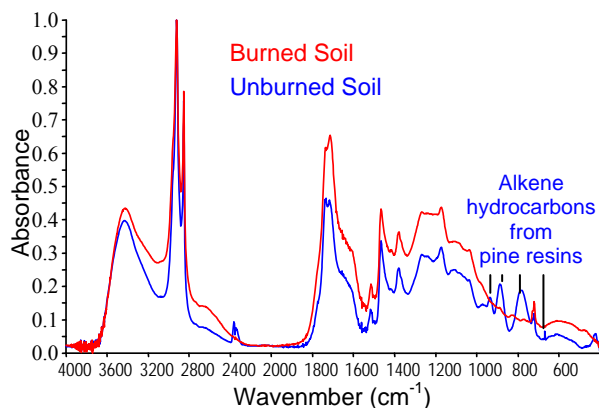


Figure 91 Infrared spectra of extractable organic matter fraction isolated from burned and unburned soils under lodgepole pine, High Meadows Fire

The NOM fractionation and spectral evidence indicates that pine-resin alkene hydrocarbons are oxidatively coupled to aromatic chars by the action of fire on NOM. This process results in an increase in the humin fractions with characteristics that lead to hydrophobic soils after a fire. Similar trends were observed with soil samples from the Cerro Grande Fire, although the changes were not as pronounced as with soil samples from the High Meadows Fire. This study illustrates how comprehensive organic analyses can be applied to soils to determine properties and processes resulting from wildland fires.

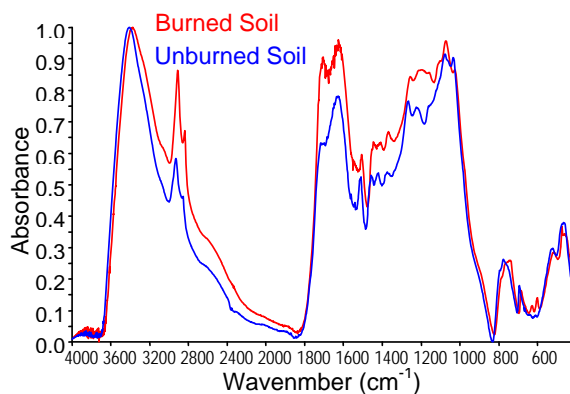


Figure 92 Infrared spectra of humin fraction isolated from burned and unburned soils under lodgepole pine, High Meadows Fire

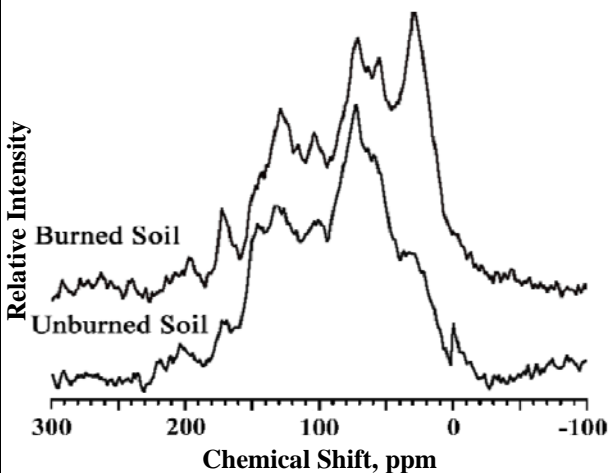


Figure 93 CP/MAS ¹³C-NMR spectra of humin fractions isolated from burned and unburned soils under lodgepole pine, High Meadows Fire

9.10. Characterization of DOM Incorporated in Calcium Carbonate Precipitated in Pyramid Lake, Nevada

The primary objective of this study [244] was to characterize the content and compound-class speciation of DOM in carbonate minerals and in lake water of Pyramid Lake, Nevada. A secondary objective was to determine the mechanisms of DOM coprecipitation with calcium carbonate. Pyramid Lake was selected for the study because of a well-documented history of carbonate mineral formation in past and present-day environments and because of past USGS research at that location [245].

Pyramid Lake has relatively fresh water (specific conductance of 7900 microSiemens). The lake surface water is super-saturated with respect to several calcium carbonate minerals (for example, calcite and aragonite), which periodically precipitate at springs and seeps located along the lake shore and occasionally as a lake-wide surface water precipitation event during summer algal blooms [246]. Calcium carbonate precipitation events associated with algal blooms are called “whittings” [246].

Carbonate rock was obtained in August, 1995, from an actively precipitating hot spring/geothermal well surrounded by loose tufa rocks. The hot spring was in the Needles area at the north end of the lake. Because of current higher lake levels than during sample collection in 1995, this site is now under water. Water samples were collected by Robert Pennington (USGS, Nevada Water Science Center) on April 6, 2006, at the marina boat dock near the Crosby Inn, Sutcliffe, Nevada.

A flow-chart for isolation and fractionation of DOM from the calcium carbonate rock sample is presented in Figure 94. The rock sample was broken up with a hammer and the fragments placed in two 4 L plastic beakers with 10% acetic acid. It took about 2 weeks for the fragments to dissolve. Acetic acid was selected to dissolve the carbonate rock because the calcium acetate reaction product has low solubility in glacial acetic acid [247] and can be removed by crystallization and filtration during zeotropic distillation of acetic acid from water. A large 2 L Buckner glass-filtration funnel with a 12 cm diameter fritted-glass filter was fitted to a 2 L glass Erlenmeyer vacuum-filtration flask, and a water aspirator was used to generate the vacuum needed to filter the large masses of calcium acetate from suspension. The calcium acetate filter cake was rinsed with glacial acetic acid until the filtrate was colorless, which indicated complete removal of DOM from the salt.

Sediments insoluble in acetic acid were removed by sieving and centrifugation. These mineral sediments were discarded because IR spectral analyses did not detect any peaks that could be ascribed to NOM. The separation of colloids from DOM was conducted against water at pH 4.9 (the pK_a of acetic acid) and against 0.01 M HCl at pH 1 because the brown color of the colloids in the dialysis bag indicated the possible presence of insoluble DOM-metal complexes that could be brought into solution at low pH. A significant amount of DOM was brought into solution at pH 1 and permeated through the dialysis membrane. Three sub-fractions of hydrophobic and amphiphilic

DOM fractions were obtained:

- 1) those that adsorbed on XAD-8 and XAD-4 resins at pH 4.9;
- 2) those that adsorbed on these resins at pH 1; and
- 3) those from the dialysis permeate at pH 1 that adsorbed on these resins.

The Pyramid Lake water sample (40.9 L) was also fractionated by a modified procedure. The major deviation from the comprehensive DOM fractionation procedure of Figure 18 is that the zeotropic distillation of acetic acid from water was conducted first to remove inorganic salts instead of after isolation of the hydrophobic and amphiphilic DOM fractions. This modification was made to make the water fractionation procedure more comparable to the rock fractionation procedure. The second modification from the DOM fractionation procedure was to fractionate hydrophobic DOM into hydrophobic-acid, -base, and -neutral fractions by the DON fractionation procedure of Figure 20. This modification was made to detect and characterize nitrogen-rich DOM fractions in lake water.

Bar diagrams presenting DOM fractionations of Pyramid Lake carbonate and water samples are presented in Figure 95. The DOM fractionation of the water sample differs from the DOM fractionation of Anaheim Lake [234], a recharge basin for the Santa Ana River in southern California subject to period algal blooms, in that the colloid and hydrophilic-acid-plus-neutral fractions in Pyramid Lake are depleted relative to the hydrophobic and amphiphilic DOM fractions in Anaheim Lake. In contrast, the DOM fractionation of the carbonate sample shows enrichment of the colloid and hydrophilic-acid-plus-neutral fractions relative to the hydrophobic and amphiphilic DOM fractions. These differing DOM fractionations of the water and carbonate rock samples suggest coprecipitation of certain components in the colloid and hydrophilic-acid-plus-neutral fractions.

The fact that the colloid fractions isolated with reasonable percentages of the DOM in both the water and rock samples was an unexpected finding of both isolation procedures. Loss of colloids was expected during the removal of salts by zeotropic distillation of water from acetic acid near the beginning of these isolation procedures. This finding about colloid recovery with these revised comprehensive DOM isolation procedures has potential application to more efficient DOM isolation procedures in saline water samples.

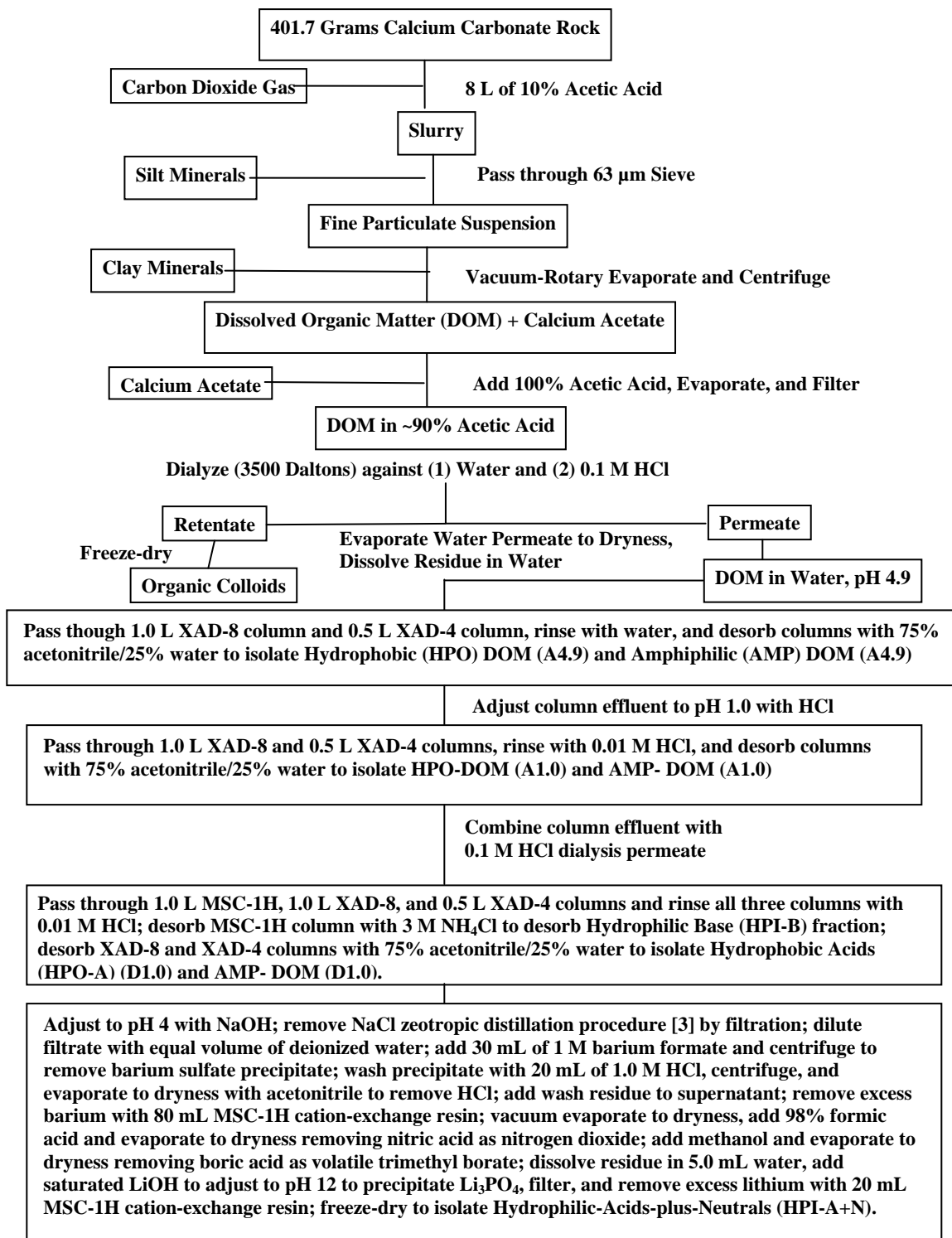


Figure 94 Flow-chart for isolation and fractionation of dissolved organic matter from calcium carbonate rock from Pyramid Lake, Nevada

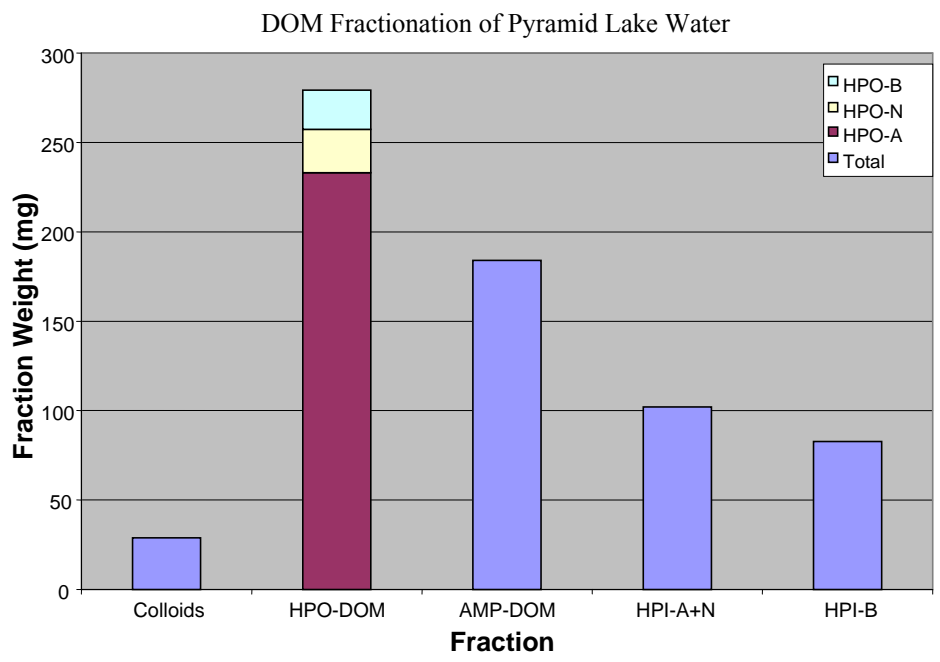
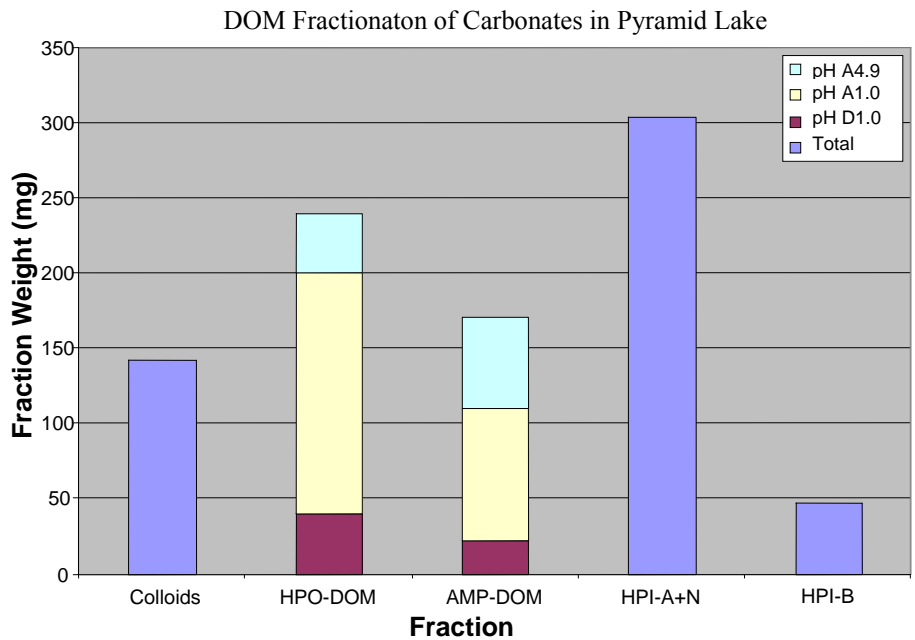


Figure 95 Bar diagrams showing DOM fractionations of Pyramid Lake carbonate and water samples. Refer to Figure 94 for pH A and D designations

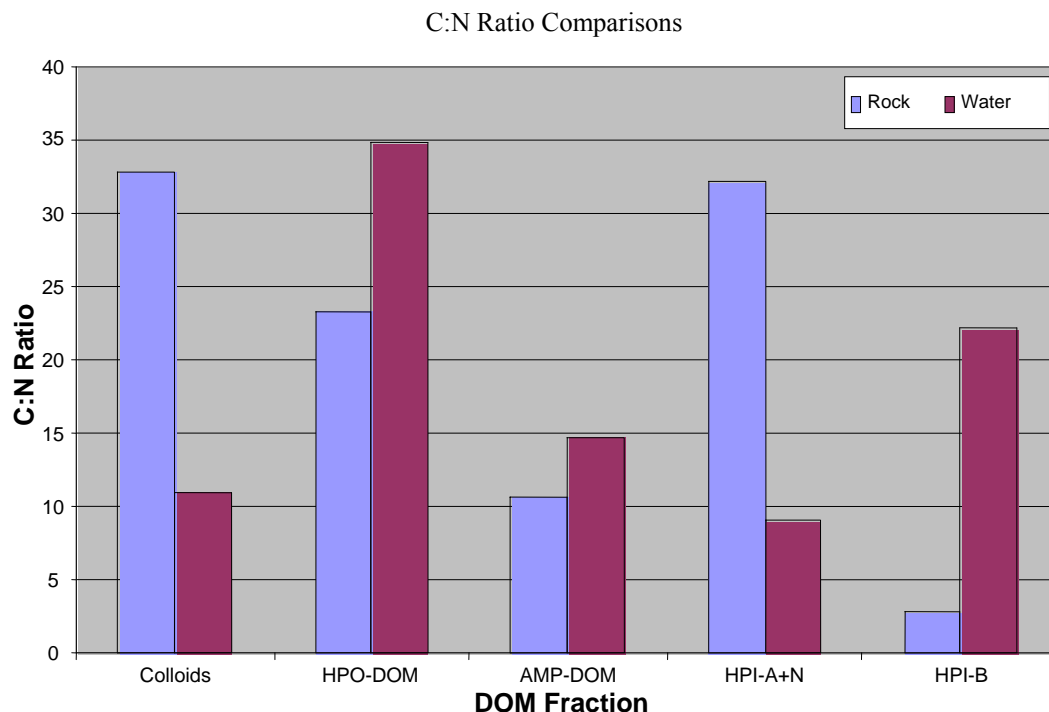


Figure 96 Bar diagrams showing atomic C:N ratios of Pyramid Lake carbonate and water samples

Atomic C:N ratios of the isolated NOM fractions from Pyramid Lake rock and water samples are presented in the bar diagrams of Figure 96. The C:N ratios of the hydrophobic and amphiphilic DOM fractions were the weight-adjusted C:N ratios of the sub-fractions presented in Figure 95. The C:N ratios of the colloid and hydrophilic-acid-plus-neutral (HPI-A+N) fractions of the rock sample are much greater than these respective fractions in the water sample, whereas the C:N ratios of the hydrophobic DOM (HPO-DOM), amphiphilic DOM (AMP-DOM), and hydrophilic base (HPI-B) fractions of the water sample are greater than these respective fractions in the rock sample. The C:N ratio data also indicates a compositional DOM fractionation resulting from coprecipitation with calcium carbonate.

The FT-IR spectra of NOM fractions isolated from the water and rock samples are presented in Figure 97. The colloid fraction from the water sample had a spectrum typical of N-acetyl aminosugars derived from bacterial cell walls, except that the carboxylic acid peak near 1720 cm^{-1} was diminished in intensity. For the colloid spectrum isolated from the rock sample, the 1720 cm^{-1} carboxylic acid peak was enhanced in intensity, and the amide 1 and 2 peaks (1660 and 1550 cm^{-1}) and the N-acetyl methyl peak at 1380 cm^{-1} were diminished in intensity relative to the carbohydrate peak near 1050 cm^{-1} . These results

indicate that acidic carbohydrates and basic aminosugar colloids are co-precipitated with calcium carbonates, and neutral N-acetyl aminosugar colloids remain in solution in lake water.

A comparison of the amide 1 and amide 2 peaks in the FT-IR spectra of selected hydrophobic DOM fractions and amphiphilic DOM (Figure 97) indicates that protein components are found almost entirely in the rock samples. A trace amount of protein was found in the infrared spectra (not shown) of the hydrophobic base and neutral fractions, but these fractions are minor constituents of hydrophobic DOM in the lake water sample (Figure 97). The hydrophobic acid and amphiphilic DOM FT-IR spectra of the lake water samples are characteristic of aquatic fulvic acids derived from terpenoids. Aquatic fulvic acids derived from tannin and lignins have a broad 1620 cm^{-1} peak caused by conjugated ketone and aromatic ring structures, and the absence of this peak in all of the DOM fractions of the water samples indicates that terrestrial DOM sources must be autochthonous.

The FT-IR spectra of the hydrophilic-acid-plus-neutral fractions of the water samples (Figure 97) appears to show hydroxycarboxylic acids similar to the rock sample, but subtle differences in the spectra coupled with major differences in the C:N ratios of this fraction indicate major compositional differences. The hydrophilic-acid-plus-neutral fraction of the rock

sample is definitely composed of hydroxycarboxylic acids, as confirmed by the large C:N ratio of 32.2, but the hydrophilic-acid-plus-neutral fraction of the water sample has a low C:N ratio of 9.1 and the IR spectrum in Figure 97 does not have nitrogenous protein and aminosugar peaks. The broad, hydrogen-bonded nitrogen N-H stretch peaks near 3100 cm^{-1} are indicated both by the intensity and position in the water sample compared to the rock sample. A possible form of nitrogen in the hydrophilic-acid-plus-neutral fraction in the water sample are lactams and cyclic imides that give carbonyl stretch peaks near 1700 cm^{-1} that are superimposed with the carboxyl stretch peaks of carboxylic acids. These lactams and cyclic imides might be derived from oxidation of pyrrole rings in porphyrin pigments in algae and/or from degradation of nucleic acids.

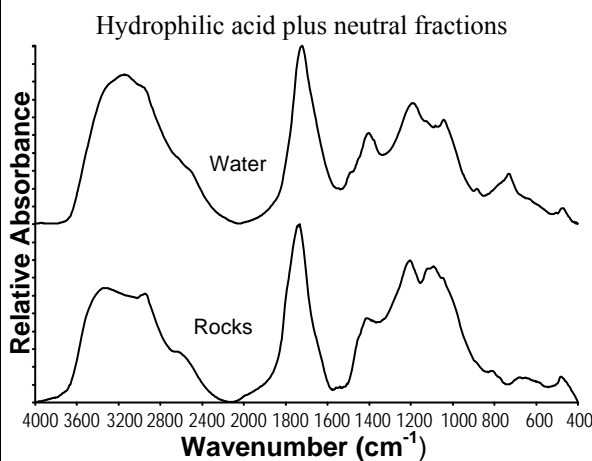
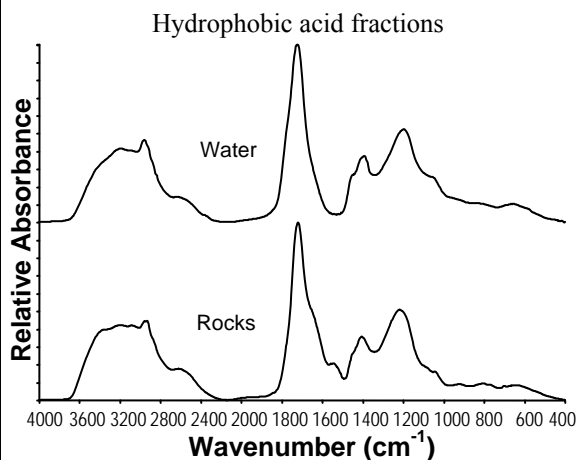
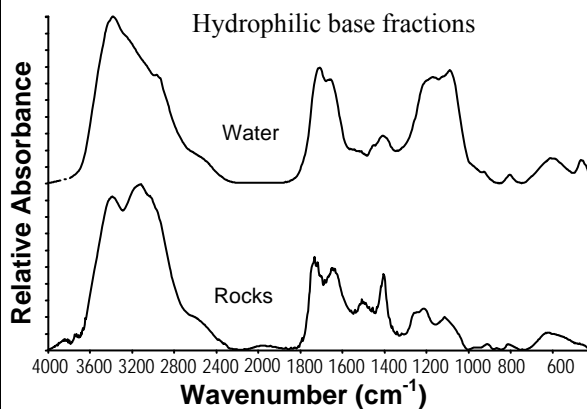
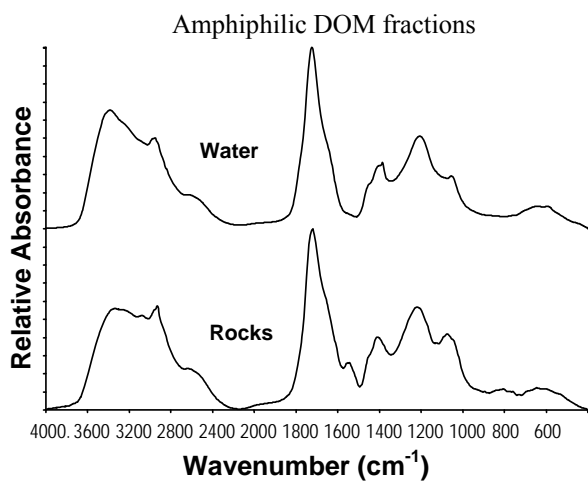
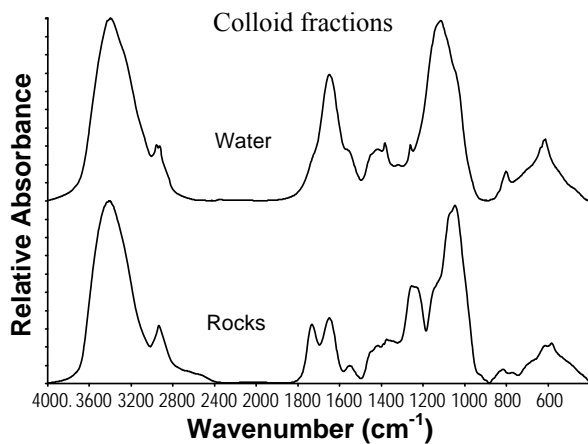


Figure 97 FT-IR spectra of NOM fractions from Pyramid Lake water and rock samples

The spectrum (Figure 97) of the hydrophilic base fraction of the water sample indicates a fraction containing proteins and carbohydrates, although the relatively large C:N ratio of 22.0 indicates a low percentage of proteins. The spectrum of the rock sample hydrophilic bases is unusual in that, while a large, broad N-H stretch peak is seen near 3100 cm^{-1} , the carbonyl stretch peaks typical of amides are not seen at their usual position near 1660 and 1550 cm^{-1} . A small peak for carboxylic acids is seen at 1630 cm^{-1} , and small peaks near 1620 and 1500 cm^{-1} may be caused by C-N stretch of protonated amino groups. The very low C:N ratio of 2.8 of the hydrophilic base fraction from the rock sample indicates the possibility of basic nucleic acids as precursors of this fraction.

Co-precipitated DOM constituted 0.23% of the calcium carbonate rock sample by weight and was enriched in polycarboxylic proteinaceous acids and hydroxyacids compared to the lake water. DOM in the lake water was composed primarily of aliphatic, alicyclic polycarboxylic acids. Precipitated DOM fractions in the rock sample were ^{14}C age-dated at 3100 to 3500 years before present [244]. The mechanism of DOM coprecipitation with calcium carbonate is believed to be formation of insoluble calcium chelate complexes with polycarboxylic proteinaceous acids and hydroxyacids that have moderately large stability constants at the alkaline pH of the lake. DOM coprecipitation results in a significant fractionation of DOM that may have practical applications to lime-softening pretreatment of drinking water to remove proteins that produce haloacetonitriles and remove hydroxy-acids that produce haloforms and haloacids upon disinfection with chlorine.

9.11. Characterization of Humic acid Sub-fractions from Lignite and Soil Samples from Greece

This humic acid sub-fractionation study was performed by Marios Drosos and Yiannis Deligiannakis of the University of Ioannina in Agrinio, Greece, in collaboration with the author at his U.S. Geological Survey laboratory. The objectives of this study were to sub-fractionate a soil and lignite humic acid to obtain compound-class structural information, and to measure proton-binding characteristics of each sub-fraction. Only the compound-class structural information is presented here.

Humic acids were extracted from the top 10 centimeters of an Alfisol forest soil and from a lignite mined in Greece with 0.5 M NaOH plus 0.1 M $\text{Na}_4\text{P}_2\text{O}_7$ using an extraction protocol recommended by the International Humic Substances Society [55].

The experimental approach of the humic acid sub-fractionation procedure was to disaggregate the humic acid by first removing metals and residual clay minerals with HCl and HF treatments; next to remove residual aluminum fluoride reaction products by dialysis against 0.1 M sodium citrate at pH 10; and lastly to dialyze against 0.1 M NaOH to completely ionize carboxyl and phenol groups to maximize charge density and disrupt hydrogen-bonded aggregates. Humic acids that permeated through the 12000 to 15000 Dalton dialysis membranes were then fractionated by a decreasing pH-gradient fractionation on XAD-8 resin as shown in Figure 98. A description of this reverse pH-gradient fractionation of humic acid is given in Section 5.

Bar diagrams of the lignite and soil humic acid fractionations are presented in Figure 99. Most of the lignite humic acid permeated the 12000 to 15000 Dalton dialysis membrane, which is consistent with its average molar mass of 3700 Daltons as measured by gel permeation chromatography. In contrast, most of the soil humic acid did not permeate the dialysis membrane, which is consistent with its average molar mass of 11800 Daltons as measured by gel-permeation chromatography.

The amount of the lignite LC2 sub-fraction exceeded the capacity of the 1 L XAD-8 column, so it was recycled after each desorption step to generate the LC21, LC 22, and LC23 sub-fractions as shown in Figure 99. A greater percentage of humic acid released with 0.1 M NaOH permeated the dialysis membrane for the soil humic acid than for the lignite humic acid. Since little lignite humic acid was obtained for fractions LN1 and LN2 as compared to LN3, and all three fractions gave essentially the same FT-IR spectra, these three fractions were combined into a composite LN fraction.

The FT-IR spectra obtained for the humic acid sub-fractionation samples are shown in Figure 100. The unfractionated humic acid samples give broad absorbance peaks with little useful compound-class structural information. Furthermore, the unfractionated humic acids contain aluminosilicates with peaks near 1050 cm^{-1} , and the broad peak extending from 600 to 400 cm^{-1} . The humic acid sub-fractions do not show the aluminosilicate peaks. In general, the soil humic acid sub-fractions have more aliphatic hydrocarbons (peak at 2920 cm^{-1}) and carbohydrates (plateau and peaks near 1050 cm^{-1}) than do the lignite humic acid; whereas the lignite humic acid sub-fractions have more conjugated ketones such as quinones (peak at 1620 cm^{-1}) than do the soil humic acid sub-fractions.

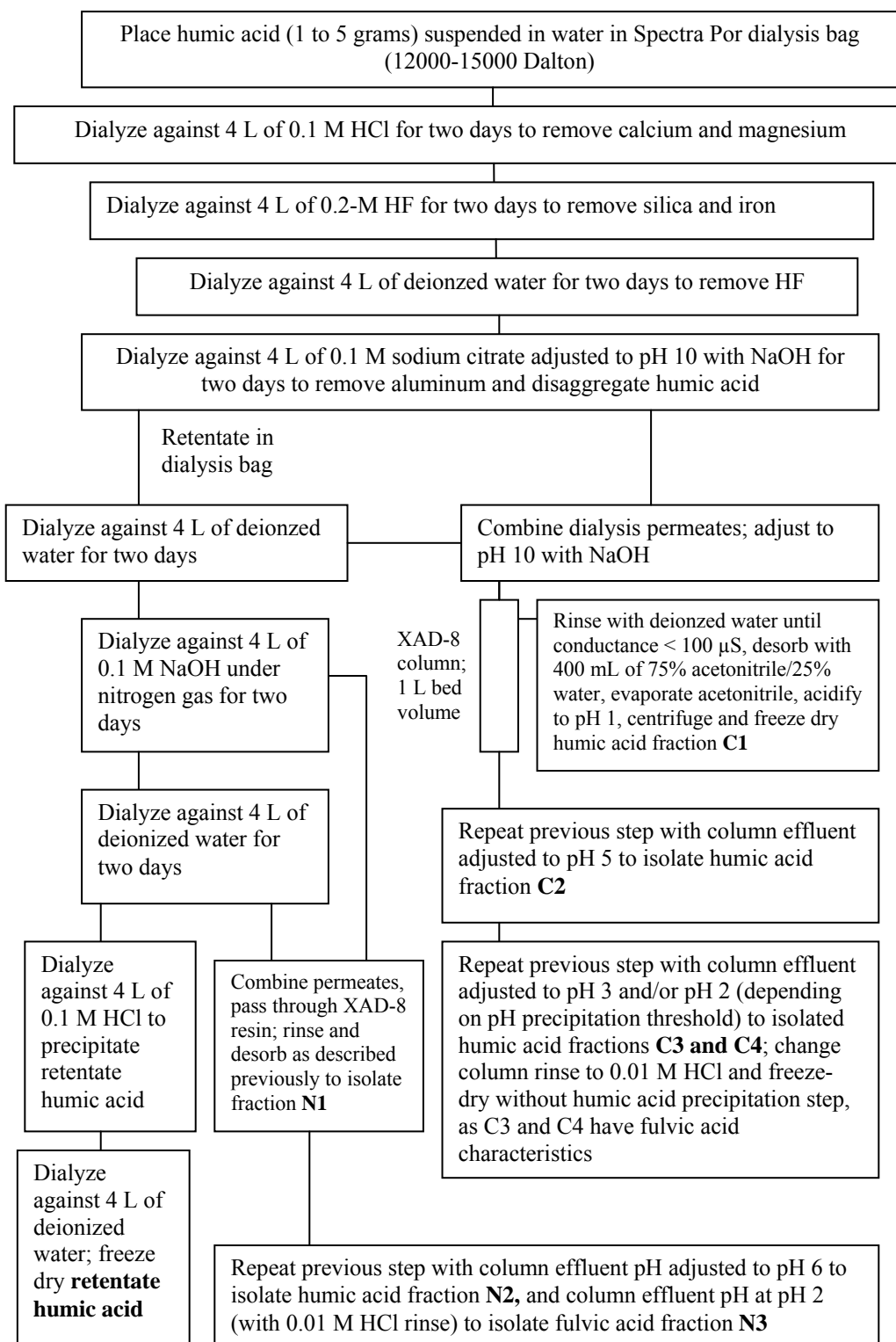


Figure 98 Humic acid sub-fractionation flow-chart

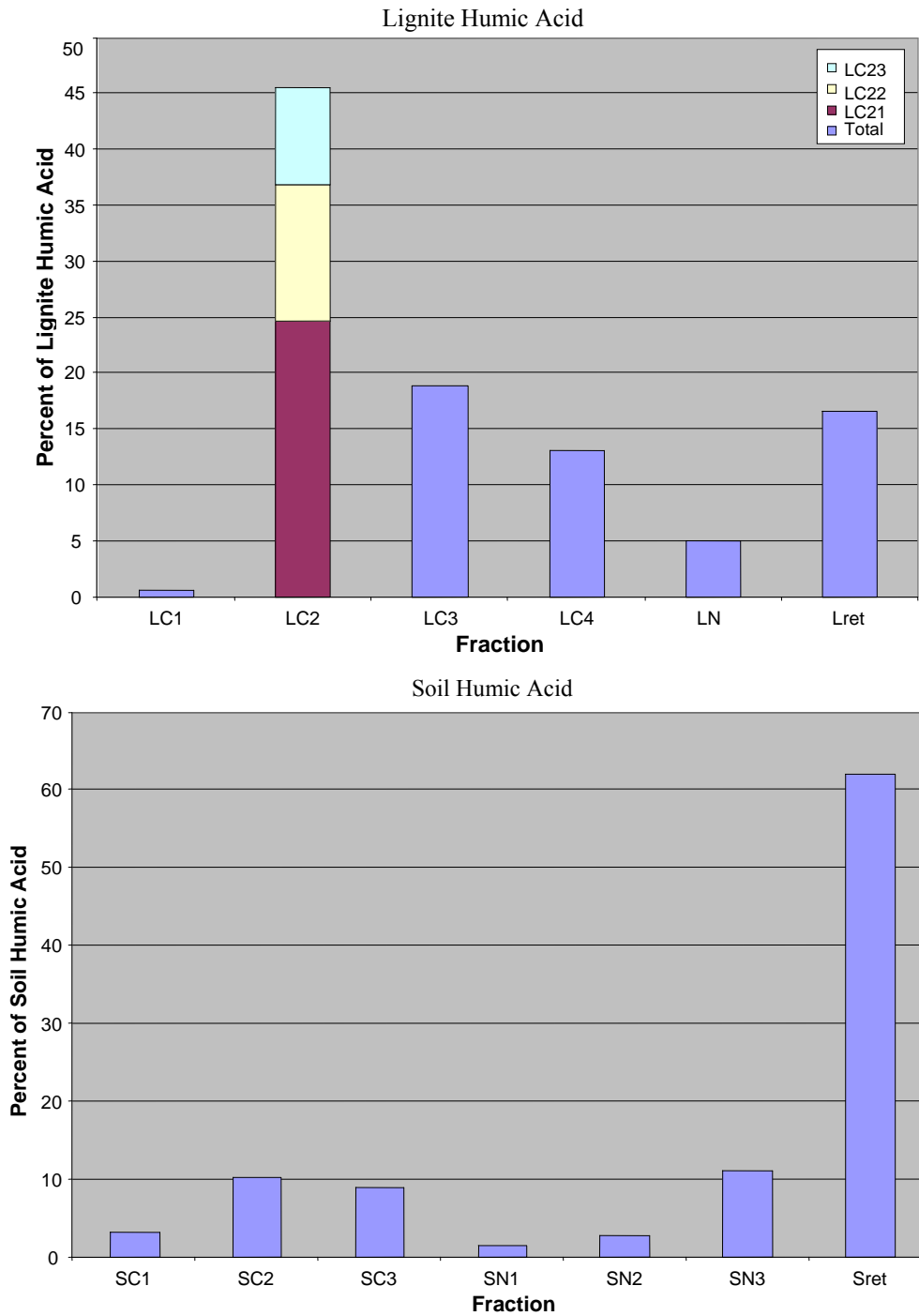


Figure 99 Bar charts of humic acid sub-fractionations; L = lignite; S = soil, C = citrate dialysis, N = sodium-hydroxide dialysis, ret = retained fraction in dialysis

The soil and lignite humic acids give significantly different fractionations (Figure 99) and FT-IR spectra (Figure 100). The Lret sub-fraction has a FT-IR spectrum that is typical for de-ashed lignite humic acid, whereas the Sret sub-fraction has a number of small sharp peaks indicating plant lignins and carbohydrates (Table 5). The LC1 sub-fraction has the lowest percentage (Figure 99) and contains the greatest aliphatic hydrocarbon content (1720 cm^{-1}) of the lignite sub-fractions. The SC1 sub-fraction is also a small fraction, and it has large aliphatic hydrocarbon content in common with the corresponding lignite sub-fraction, but it has protein (amide 1 and 2 peaks), plant lignin, and carbohydrate components.

The LC21, LC22, and LC23 fractions that constitute the majority of lignite humic acid give identical FT-IR spectra that are similar to the L_{Ret} spectra except for its lesser aliphatic hydrocarbon content. The composition of the SC2 sub-fraction is similar to the LC1 sub-fraction except for its lower aliphatic hydrocarbon content. Sub-fractions LC3, LC4, and SC3 have FT-IR spectra similar to Suwannee River fulvic acid shown in Figure 33. Soil humic acid sub-fractions SN1 and SN2 show a significant increase in aliphatic hydrocarbon composition after dialysis in 0.1 M NaOH, and specific peaks of plant lignins including the methoxy peak at 1127 cm^{-1} are an indication of lignin with little degradation. The presence of both polymethylene hydrocarbons and lignin suggests suberin [228] as the precursor compound class for sub-fractions SN1 and SN2.

The lignite LN sub-fraction differs from other lignin sub-fractions in that it has significant branched-methyl structures (peak at 2960 cm^{-1}) that are indicative of terpenoid precursors, but the conjugated ketone peak near 1620 cm^{-1} is indicative of oxidized tannins and lignins. Phloroglucinol derivatives in plants, such as humulone, incorporate terpenoid, tannin, and conjugated ketone structures into this compound class [23] that may explain the spectra of LN and also the SN3 sub-fraction that has similar FT-IR spectral characteristics.

The humic acid sub-fractionation procedure of Figure 98 that combines de-ashing (HF and citrate complexation), size fractionation (dialysis), extraction at pH 10 and pH 13, and reverse-phase chromatography on XAD-8 resin with a decreasing pH gradient provides distinct sub-fractions with unique compound-class compositions as determined by FT-IR spectrometry. The C fractions that permeate the dialysis membrane in sodium citrate at pH 10 are disaggregated by a combination of metal and mineral removal and by an increase in charge density by ionization of

carboxyl and phenol groups. The N fractions that permeate the dialysis membrane are disaggregated by a further increase in charge density by ionization of weakly acidic phenols, and possibly by hydrolysis of labile phenolic ester linkages. The humic acid retained in the dialysis membrane is probably true macromolecular material not subject to disaggregation, although additional treatments such as the urea extraction method of Hayes [85] may cause additional releases of proteinaceous humic acid sub-fractions.

10. THE PATHS TO MOLECULAR CHARACTERIZATION OF NOM

Molecular characterization of NOM has long been the ultimate objective of many analytical studies, but NOM complexity and its unique properties, especially the humic component of NOM, have frustrated molecular characterization attempts. Recent developments in analytical instrumentation have given analytical chemists unprecedented opportunities for molecular separations of extremely complex mixtures. Tandem-GC/GC separations have great potential but have not yet been applied to separations of NOM mixtures. Ultra-high-resolution ESI/FT-ICR/MS has the capability for molecular separations of NOM, but it is not yet a preparative method whereby other spectral characterizations can be performed on the ions. There are two general paths that can be followed for molecular characterization of NOM:

- 1) characterization of the phase properties of NOM whereby an understanding is obtained on how NOM molecules self-assemble in supramolecular structures; and
- 2) ultimate analyses of NOM molecular components.

10.1. Molecular Characterization of NOM Supramolecular Structures

The viewpoint of NOM as supramolecular structures is stated in the introduction of this account as “NOM as it exists in the environment should be regarded as dynamic combinatorial systems [13] and as infinitely heterogeneous with regard to the molecular composition of NOM organic phases [14].” With respect to large NOM aggregates held together by hydrophobic interactions, hydrogen bonding, and bridging by polyvalent metal cations as shown in Figures 27 and 28, the supramolecular arrangements are likely to be infinitely heterogeneous as stated by MacCarthy [14].

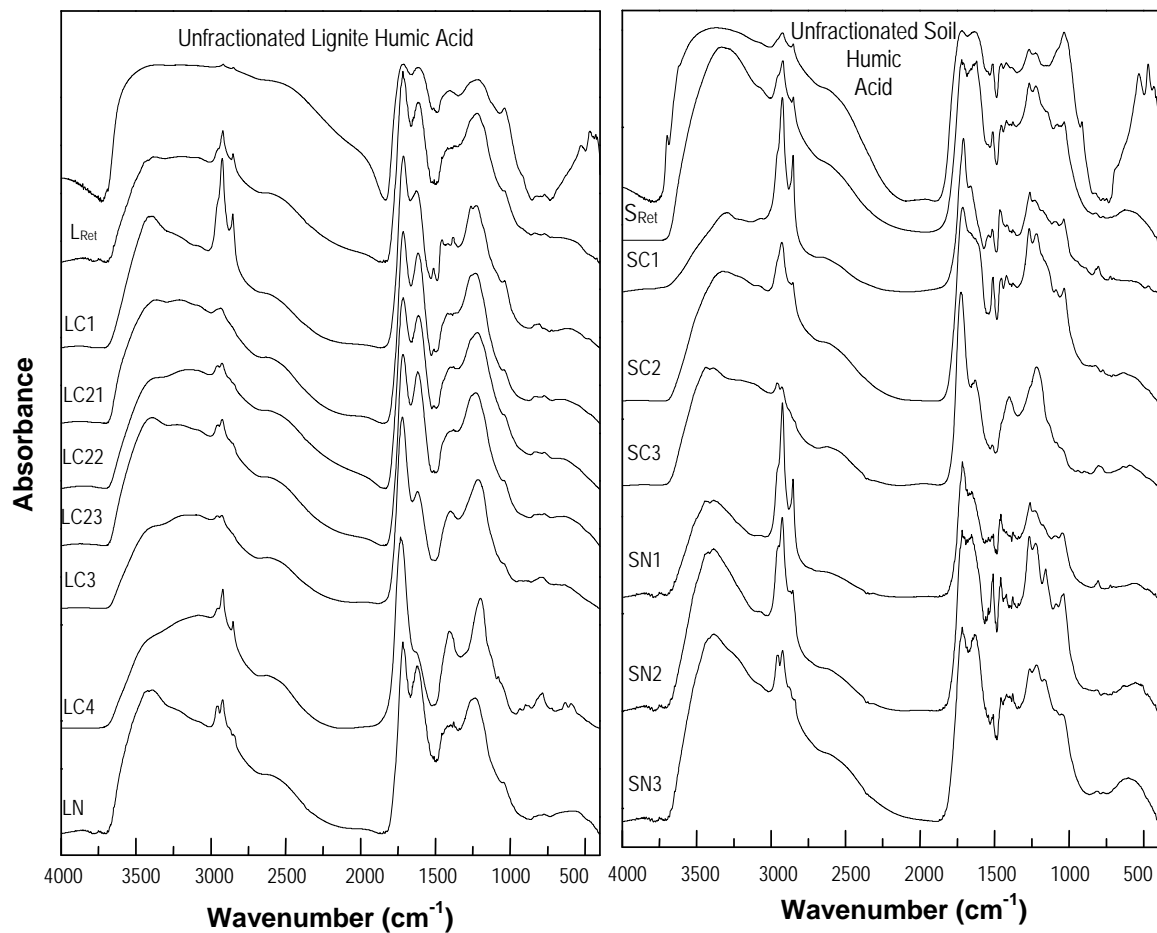
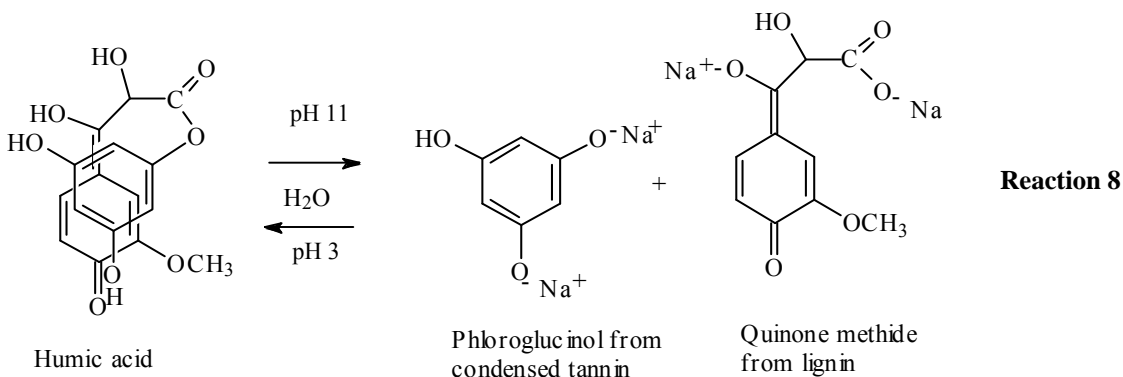


Figure 100 FT-IR spectra of lignite (on left) and soil (on right) humic acids and humic acid sub-fractions

However, smaller NOM structures such as aromatic π - π electron charge-transfer complexes as determined to be ubiquitous in humic substances by Del Vecchio and Blough [169] can be investigated at the molecular level to determine limits on molecular composition, their mechanism of formation, their

specific properties, and their derivation from precursor compound classes. A hypothetical reaction whereby a charge-transfer complex and phenolic ester of humic acid might simultaneously form or hydrolyze is presented in Reaction 8.



The covalent phenolic ester linkage was postulated to form in the humic acid charge-transfer complex based upon the finding that these complexes were intramolecular [169]. The titrimetric hysteresis curves of forward and reverse titrations (Figure 30) [115] are characteristic of phenolic esters that readily hydrolyze at pH 11 and reform as intramolecular lactones at pH 3 in water [119]. An intermolecular charge-transfer complex of humic acid would likely form phenolic esters at low pH, and especially during drying of the humic acid isolate in the acid form to become an intramolecular charge-transfer complex (shown in Reaction 8) in a manner analogous to lactone formation. Alkaline extraction of humic acid would rapidly hydrolyze this ester to the reaction products shown in Reaction 8. This labile phenolic ester linkage also might explain why some high molar mass humic components separated by gel-permeation chromatography fragment to low molar mass components when analyzed by ESI/FT/ICR/MS [106].

The quinone-methide structure in Reaction 8 is postulated to be derived from degradation of lignin. Quinones are well documented to occur in humic substances, but ortho-quinones derived from lignins are known to be unstable, degrading to substituted muconic acids as shown in Reaction 2. Para-quinones are well known to form charge-transfer complexes with phenols such as benzoquinone reacting with hydroquinone to form the quinhydrone charge-transfer complex. Para-quinone precursors of NOM are known to occur, but they are not very abundant [23]. Therefore, the quinone-methide structure of Reaction 8 was proposed to provide the correct stereochemistry for the complex, and a likely precursor source. An enolic hydroxyl group was also formed in this quinone-methide structure.

It should be possible to verify the presence of quinone methides, enol functional groups, and the formation of specific charge-transfer complexes by studies of reactions between certain model compounds shown in reaction 8. If the properties and structures of these model complexes closely approximate the molecular characteristics of humic charge-transfer complexes, a molecular level characterization of these humic complexes will be obtained that is fundamental to understanding several of the unique properties of humic substances in the environment.

10.2 Molecular Analyses of NOM

Determination of NOM components as specific molecular structures is beginning to be perceived as a tractable scientific endeavor [100]. The molar masses

of primary molecules of NOM in soil, sediment, and water are generally less than 2000 Daltons, and much of this NOM can be ionized and separated into molecules and molecular formulas that can be computed by ESI/FT/ICR/MS. The Chelsea soil humic acid has been modeled in three dimensions using quantitative experimental characterizations, computer-assisted structure elucidation, and atomistic simulations [248]. However, computer models of humic acids are limited by complex mixture characteristics, and molecular formulas that do not distinguish between isomers, and some NOM precursors such as condensed tannins and lignins that are different isomers of various hydroxyphenyl propane reactants. Therefore, additional chromatographic and spectral information is needed for molecular characterization. The following are steps needed to approach NOM molecular structures determination:

1. Select "end-member" environments for NOM characterization. These environments have well-defined autochthonous or allochthonous inputs to better define precursors, and have limited processes that degrade NOM. These environments should be selected to both bracket and constrain environmental variables for the sake of a comprehensive understanding and for reduction of complexity.
2. Develop and extend improved NOM extraction, fractionation, isolation, and purification methods. Much has already been done as illustrated by the examples in this account, but the finding that NOM molecules exist as aggregates held together by a combination of charge-transfer complexes, hydrogen bonds, metal complexes, and non-polar interactions means these interactions must be eliminated to separate the molecules. Derivatization such as acetylation or methylation is effective in disrupting hydrogen bonds, and use of reagents (hydrofluoric acid, citrate salts, ethylenediamine tetraacetic acid salts) that form stronger complexes with metals than NOM can remove complexes. The generation of homogeneous compound-class fractions should be the objective of NOM fractionation and sub-fractionation methods before ultimate molecular analyses are attempted.
3. Couple preparative-column chromatography with preparative high-performance liquid chromatography (HPLC) with a universal detector such as refractive index to generate compound-class NOM fractions. This procedure is very similar to the standard analytical approach used to separate

petroleum hydrocarbons into compound classes before chromatographic and spectrometric analyses.

4. Obtain infrared and NMR spectral analyses on compound-class fractions. Both of these spectral analyses are non-destructive and can be performed on small samples, especially with high-field NMR spectrometers. Compound-class composition can be established by these spectral analyses, especially by multidimensional NMR methods. Complementary structural group information is provided by comparing infrared and NMR spectra. Compound-class molecular models can be derived to guide subsequent mass-spectral studies.
5. Obtain both high-resolution ESI/FT/ICR/MS and ESI/multistage-tandem-MS data on the compound-class fractions. High-resolution ESI/FT/ICR/MS data give elemental composition of specific NOM molecules. Coupling reverse-phase HPLC columns with a mass spectrometer is preferred to improve molecular separations before mass spectrometry; it also gives polarity homogeneous NOM mixtures, which give more quantitative ESI/MS responses. The MS methods need to be calibrated with internal standards to better correlate ionic fragments with molecular structure and to calibrate variable response factors.
6. Derive molecular models of specific NOM molecules with known elemental composition by synthesizing independent spectral and titrimetric data from homogeneous compound-class samples. An example of this approach is provided by the model of a hydrophilic acid molecule from the deep South Atlantic Ocean DOM in Section 7.
7. Synthesize standards based upon selective postulated NOM molecules from step 5. Confirm these molecules by high-resolution chromatographic and spectral methods. This final step is likely to be expensive and may require several attempts for success; however, natural product chemists have experience in the approach outlined in this section, and they have separated and identified many complex molecules that exist in complex matrices.

This account summarizes the author's research career in developing and applying comprehensive analyses of NOM in the environment. As this final section indicates, this work is by no means complete, and there is abundant research remaining for environmental scientists to conduct on the analyses of NOM.

11. ACKNOWLEDGMENTS

This account is an outgrowth of 35 years of experience as project chief of the Comprehensive Organic Analyses of Water Project at the U.S. Geological Survey (USGS) in Denver, Colorado. Consequently, most of the experience was with water-related research that was generously supported by a number of long-term research projects in the U.S. Geological Survey. Mentoring and administrative support of this work was given by Robert C. Averett, who also edited the first publication of a comprehensive analysis, *Humic Substances in the Suwannee River, Georgia: Interactions, Properties, and Proposed Structures*. I also count Russell F. Christman of the University of North Carolina as a mentor for his lifelong interest and encouragement of my work on NOM characterizations. I regard Robert L. Wershaw as my closest colleague in the USGS who shared my interests in NOM and humic substances. Other research colleagues in the USGS (George R. Aiken, Ronald C. Antweiler, Patricia A. Brown, Larry B. Barber, Greg K. Brown, Larry G. Cox, Cary T. Chiou, Jennifer A. Field, Marvin C. Goldberg, John A. Izbicki, Ronald L. Malcolm, Diane M. McKnight, Robert H. Meade, John Moody, Ted I. Noyes, Michael M. Reddy, Terry F. Rees, Colleen E. Rostad, David W. Rutherford, Roy A. Schroeder, Harold A. Stuber, Kevin A. Thorn, and E. Mike Thurman) were important in assisting in the development and application of comprehensive analysis of NOM.

There were many NOM-characterization projects funded by governmental agencies, research foundations, water utilities, and universities that contributed to the work presented in this account. Near the beginning of this work, the U.S. Department of Energy, in a project administered by David S. Farrier of the Laramie Energy Technology Center, supported the development of the DOC fractionation procedure to characterize waters impacted by development of oil shale. In 1978, the Organization of American States supported a project administered by Ilse Walker at Instituto Nacional das Pesquisas Amazonas in Manaus, Brazil, to characterize NOM in waters and soils in the Amazon. Participation in the project *Global Carbon Transport by Major World Rivers*, funded by the United Nations Environmental Program and headed by Egon T. Degens of the University of Hamburg in Germany, gave an appreciation of the important role of NOM in the global carbon cycle. The U.S. Bureau of Reclamation provided crucial long-term support of several NOM characterization studies in wetlands used for waste-water treatment in

projects led by Eric A Styles. The American Water Works Association Research Foundation supported the development of the preparative DOM fractionation procedure in two projects involving the characterization of DOM in drinking water headed by Mark Benjamin at the University of Washington and the characterization of polar NOM in drinking-water supplies headed by Cordelia J. Hwang at the Metropolitan District of Southern California. The California Department of Toxic Substances Control, in a project led by John Hsu, supported the characterization of DOM in wastewaters and ground waters at the Stringfellow Hazardous-Waste Disposal Site. The Orange County Water District in two projects administered by Greg Woodside supported characterization of DOM in waters associated with ground water recharge, and the characterization and development of the total organic matter fractionation of stormflow waters in the Santa Ana River. The study of NOM in atmospheric aerosols and fog waters was funded by the Department of Atmospheric Sciences at Colorado State University and administered by Jeffery L. Collett. The South Atlantic deep-ocean study of DOM was funded by Alejandro Spitzzy of the University of Hamburg, Germany.

University professors who contributed to student degree programs involving NOM characterizations include Steven R. Daniel, Patrick MacCarthy, and Donald L. MacCalady at the Colorado School of Mines; Gary Amy and Harold F. Walton at the University of Colorado; Roger A. Minear at the University of Illinois; Jean-Philippe Croué at the University of Poitiers in France; Paul Westerhoff at the University of Arizona; Mark A. Nanny at the University of Oklahoma; and Yiannis Deligiannakis of the University of Ioannina in Greece. Students receiving degrees related to NOM research presented in this account include Greg K. Brown, Steve Cowling, Jennefer A. Field, Barbara S. Martin, and Colleen E. Rostad from the Colorado School of Mines; Larry B. Barber, Harold A. Stuber, Charles F. Tabor, and Jeffery H. Writer from the University of Colorado; Pierre Herckes from Colorado State University; Aaron Dotson from Arizona State University; and Marios Drosos from the University of Ioannina in Agrinio, Greece. Last, but not least, I credit my graduate professors in the Department of Agronomy at Purdue University, Paul G. Moe for my MS degree, and James L. Ahlrichs for my PhD degree, for originally stimulating my interest in NOM in soils that extended throughout my research career to comprehensive analyses of NOM in the environment.

There are many more colleagues and

collaborators too numerous to mention that I hopefully have rightfully credited in the References section of this account. However, I would like to lastly acknowledge the contributions of Stephen E. Cabaniss of the University of New Mexico who spent part of his sabbatical with my research project; Edward D. Huffman, Jr., of Huffman Laboratories in Wheat Ridge, Colorado, who continually participated in the development of the DOC fractionation procedures and applications of elemental analyses to NOM isolates; and M. Lee Davisson of the Lawrence Livermore National Laboratory who conducted and taught me the applications of carbon isotopes to NOM characterizations. I cannot emphasize enough the importance of the Humic Acid Research Group at Northeastern University in Boston under the leadership of Geoffrey Davies and Elham A. Ghabbour in organizing conferences and in originating the open-access journal *Annals of Environmental Science* in which this account is published.

Any use of trade, firm, or product name is for descriptive purposes only and does not imply endorsement by the U.S. Government.

12. REFERENCES

- [1] Shriner, RL, Fuson, RC, Curtin, DY. *The systematic identification of organic compounds*. New York: Wiley, 1964.
- [2] Wershaw, RL. Model for humus in soils and sediments. *Environ. Sci. Technol.* 1993, 27: 814-816.
- [3] Piccolo, A, Conte, P, Trivellone, E, Van Lagen, B, Buurman, P. Reduced heterogeneity of a lignite humic acid by preparative HPSEC following interaction with an organic acid. Characterization of size separates by Pyr-GC-MS and ¹H-NMR spectroscopy. *Environ. Sci. Technol.* 2002, 36: 76-84.
- [4] Black, AP, Christman, RF. Characteristics of colored surface waters, *J. Am. Wat. Works Assoc.* 1963, 55: 753-770.
- [5] Stevenson, FJ. *Humus chemistry: Genesis, Composition, Reactions*. 2nd edition. New York: Wiley, 1994.
- [6] Schnitzer, M, Khan, SU. *Soil organic matter*. New York: Elsevier, 1978.
- [7] Wrobel, K, Sadi, BBM, Wrobel, K, Castillo, JR, Caruso, JA. Effect of metal ions on the molecular weight distribution of humic substances derived from municipal compost: Ultrafiltration and SEC with spectrophotometric

- and ICP-MS detection. *Anal. Chem.* 2003, 75: 761-767.
- [8] Chauveheid, E, Denis, M. The boron-organic carbon correlation in water. *Water Research*, 2004, 38: 1663-1668.
- [9] Kinrade, SD, Del Nin, JW, Schach, AS, Sloan, TA, Wilson, KL, Knight, TG. Stable five- and six-coordinated silicate anions in aqueous solution, *Science*, 1999, 285: 1542-1545.
- [10] Leenheer, JA. Organic substance structures that facilitate contaminant transport and transformations in aquatic sediments. In: Baker, RA ed., *Organic Substances and Sediments in Water, Humics and Soils*, Chelsea, MI: Lewis Publishers, 1991: 3-22.
- [11] Simpson, AJ, Kingery, WL, Hayes, MHB, Spraul, M, Humpfer, E, Dvortsak, P, Kerssebaum, R, Godejohann, M, Hofmann, M. Molecular structures and associations of humic substances in the terrestrial environment. *Naturwissenschaften*, 2002, 89: 84-88.
- [12] Sutton, R, Sposito, G. Molecular structure in soil humic substances: The new view. *Environ. Sci. Technol.*, 2005, 39: 9009-9015.
- [13] Langford, CH, Melton, JR. When should humic substances be treated as dynamic combinatorial systems? In: Ghabbour, EA, Davies, G. eds. *Humic Substances: Molecular Details and Applications in Land and Water Conservation*. New York: Taylor and Francis, 2005: 65-78.
- [14] MacCarthy, P. The principles of humic substances: An introduction to the first principle. In: Ghabbour, EA and Davies, G, eds. *Humic Substances, Structures, Models, and Functions*. Cambridge: Royal Society of Chemistry, 2001: 19-30.
- [15] Leenheer, JA, Huffman, EWD, Jr. *Analytical method for dissolved-organic carbon fractionation*. U.S. Geol. Survey Water Resources Investigation 79-4, 1979.
- [16] Aiken, GR, McKnight, DM, Thorn, KA, Thurman, EM. Isolation of hydrophilic acids from water using macroporous resins. *Org. Geochem.* 1992, 18: 567-573.
- [17] Leenheer, JA, Croue, J-P. Characterizing aquatic dissolved organic matter. *Environ. Sci. Technol.* 2003, 37: 19A-26A.
- [18] Leenheer, JA, Croue, J-P, Benjamin, M, Korshin, GV, Hwang, CJ, Bruchet, A, Aiken, GR. Comprehensive isolation of natural organic matter for spectral characterization and reactivity testing. In: Barrett, S, Krasner, SW, Amy, GL. eds. *Natural Organic Matter and Disinfection By-Products*, American Chemical Society Symposium Series 761, Washington, DC: American Chemical Society, 2000: 68-83.
- [19] Hem, JD. *Study and interpretation of the chemical characteristics of natural water*. U.S. Geological Survey Water-Supply Paper 1473, 1970.
- [20] Stumm, W, Morgan, JJ. *Aquatic chemistry, chemical equilibria and rates in natural waters*, 3rd Edition, New York: Wiley, 1996.
- [21] Soil Conservation Service. *Soil taxonomy*. Agriculture Handbook No. 436, U.S. Department of Agriculture, 1975.
- [22] Jackson, ML. *Soil chemical analysis, advanced course*. Department of Soil Science, University of Wisconsin-Madison. 1985.
- [23] Robinson, T. *The organic constituents of higher plants*, 6th Ed., North Amherst, MA: Cordus Press, 1991.
- [24] Greenland, DJ, Hayes, MHB. *The chemistry of soil constituents*. New York: Wiley, 1978.
- [25] Thurman, EM. *Organic geochemistry of natural waters*. Dordrecht, the Netherlands: M. Nijhoff and W. Junk Publishers, 1985.
- [26] Larson, RA, Weber, EJ. *Reaction mechanisms in environmental organic chemistry*, Ann Arbor, MI: Lewis Publishers, 1994.
- [27] Gibson, DT. *Microbial degradation of organic compounds*. New York: Dekker, 1984.
- [28] Wetzel, RG. *Limnology: lake and river ecosystems*. 3rd edition. San Diego, CA: Academic Press, 2001.
- [29] Bellamy, LJ. *The infrared spectra of complex molecules, Volume 2*. London: Chapman and Hall, 1980.
- [30] Wexler, AS. Integrated intensities of absorption bands in infrared spectroscopy, *Applied Spectroscopy Reviews*, 1967, 1: 29-98.
- [31] Wilson, MA. *NMR techniques and applications in geochemistry and soil chemistry*. New York: Pergamon Press, 1987.
- [32] Nanny, MA, Minear, RA, Leenheer, JA. *Nuclear magnetic resonance in environmental chemistry*. New York: Oxford University Press, 1997.
- [33] Pouchert, CJ. *The Aldrich library of FT-IR spectra, edition 1*. Milwaukee, WI: The Aldrich Chemical Company, Inc., 1985.
- [34] Simons, WW. *The Sadtler handbook of proton NMR spectra*. Philadelphia: Sadtler Research Laboratories, Inc., PA. 1978.
- [35] Simons, WW. *The Sadtler guide to carbon-13 NMR spectra*. Philadelphia: Sadtler Research

- Laboratories, Inc., 1983.
- [36] Gould, SJ. *Planet of the bacteria: Full house*. New York: Harmony Books, 1996: 175-192.
- [37] Haslam, E. *Practical polyphenolics, from structure to molecular recognition and physiological action*. Cambridge: Cambridge University Press, 1998.
- [38] Wershaw, RL, Aiken, GR, Leenheer, JA, Tregellas, JR. Structural-group quantitation by CP/MAS ¹³C-NMR measurements of dissolved organic matter from natural surface waters, In: Ghabbour, EA, Davies, G. eds., *Humic Substances, Versatile Components of Plants, Soils, and Water*, Cambridge: Royal Society of Chemistry, 2000: 63-82.
- [39] Leenheer, JA, Brown, GK, MacCarthy, P, Cabaniss, SE. Models of metal-binding structures in fulvic acid from the Suwannee River. *Environ. Sci. Technol.* 1998, 32: 2410-2416.
- [40] Leenheer, JA, Wershaw, RL, Brown, GK, Reddy, MM. Characterization and diagenesis of strong-acid carboxyl groups in humic substances. *Applied Geochemistry*, 2003, 18: 471-482.
- [41] Ranby, B, Rabek. JF. *Photodegradation, Photooxidation and Photostabilization of Polymers*, New York: Wiley, 1975.
- [42] Harvey, GR, Boran, DA. Geochemistry of humic substances in seawater. In: Aiken, GR, McKnight, DM, Wershaw, RL, MacCarthy, P. eds. *Humic Substances in Soil, Sediment, and Water, Geochemistry, Isolation, and Characterization*. New York: Wiley, 1985: 233-248.
- [43] Trudgill, PW. Microbial degradation of the alicyclic ring: Structural relationships and metabolic pathways, In: Gibson, DT ed. *Microbial Degradation of Organic Compounds*. New York: Dekker, 1984: 131-180.
- [44] Leenheer, JA, Nanny, MA, McIntyre, C. Terpenoids as major precursors of dissolved organic matter in landfill leachates, surface water, and groundwater. *Environ. Sci. Technol.* 2003, 37: 2323-2331.
- [45] Chefetz, B, Salloum, MJ, Deshmukh, AP, Hatcher, PG. Structural components of humic acids as determined by chemical modifications and carbon-13 NMR, pyrolysis-, and thermochemolysis-gas chromatography/mass spectrometry. *Soil Sci. Soc. Amer. J.* 2002, 66: 1159-1171.
- [46] Simpson, MJ, Hatcher, PG. Overestimates of black carbon in soils and sediments. *Naturwissenschaften*, 2004, 91: 436-440.
- [47] Leenheer, JA. Chemistry of dissolved organic matter in rivers, lakes, and reservoirs, In: Baker, LA ed., *Environmental chemistry of lakes and reservoirs*, Advances in Chemistry Series 237, Washington DC: American Chemical Society, 1994: 195-222.
- [48] Aiken, GR, McKnight, DM, Harnish, RA, Wershaw, RL. Geochemistry of aquatic humic substances in the Lake Fryxell Basin, Antarctica.: *Biogeochem.*, 1996, 34: 157-188.
- [49] Meade, RH, Moody, JA, Stevens, HH, Jr., Sampling the big rivers, In: Meade, RH, ed. *Contaminants in the Mississippi River, 1987-92*. U.S. Geological Survey Circular 1133, Denver, CO. 1995: 41-51.
- [50] Leenheer, JA, Noyes, TI. *A filtration and column-adsorption system for onsite concentration and fractionation of organic substances from large volumes of water*: U.S. Geological Survey Water Supply Paper 2230, 1984.
- [51] Wershaw, RL, Leenheer, JA, Kennedy, KR. Use of ¹³C-NMR and FTIR for elucidation of degradation pathways during senescence and litter decomposition of aspen leaves, Characterization of leachate from different types of leaves. In Ghabbour, EA, Davies, G eds. *Understanding Humic Substances: Advanced Methods, Properties and Applications*: Cambridge: Royal Society of Chemistry, 1999: 19-30.
- [52] Fireman, M, Reeve, RC. Some characteristics of saline and alkali soils in Gem County, Idaho. *Soil Sci. Soc. Amer. Proc.* 1948, 13: 494-498.
- [53] Leenheer, JA. Concentration, partitioning, and isolation techniques for organic substances in water, In: Minear, R ed., *Treatise on water analysis, volume 3*. New York: Academic Press, 1984: 83-166.
- [54] Leenheer, JA. Fractionation techniques for aquatic humic substances: In: Aiken, GR, McKnight, DM, Wershaw, RL, MacCarthy, P eds. *Humic Substances in Soil, Sediment, and Water: Geochemistry, Isolation, and Characterization*, New York: Wiley, 1985: 387-408.
- [55] Hayes, MHB. Extraction of humic substances from soil, In: Aiken, GR, McKnight, DM, Wershaw, RL, MacCarthy, P eds., *Humic Substances in Soil, Sediment, and Water: Geochemistry, Isolation, and Characterization*,

- New York: Wiley, 1985: 329-362.
- [56] Wershaw, RL, Aiken, GR. Molecular size and weight measurements of humic substances, In: Aiken, GR, McKnight DM, Wershaw, RL, MacCarthy, P eds., *Humic Substances in Soil, Sediment, and Water*, Wiley, New York, 1985: 477-492.
- [57] Sirotkina, IS, Varshall, GM, Lur'e, YY, Stepanova, NP. Use of cellulose sorbents and Sephadexes in the systematic analysis of organic matter in natural water. *Zh. Anal. Khim.*, 1974, 29: 1626-1632.
- [58] Leenheer, JA, Huffman, EWD, Jr. Classification of organic solutes in water by using macroreteticular resins: *J. Res. U.S. Geological Survey*, 1976, 4: 737-751.
- [59] Christman, RF, Hruitfiord, BF. Water-quality standards for organic contaminants: Analytical limitations and possibilities. Proc. 15th Water Quality Conference, Urbana, Ill., 1973: 63-72.
- [60] Simpson, RM. *The separation of organic chemicals from water*: Philadelphia: Rohm and Hass, 1972.
- [61] Burnham, AK, Calder, GV, Fritz, JS, Junk, GA, Svec, HJ, Willis, R. Identification and estimation of neutral organic contaminants in potable water. *Anal. Chem.*, 1972, 44: 139-142.
- [62] Junk, GA, Richard, JJ, Grieser, MD, Witiak, JL, Arguello, MD, Vick, R, Svec, HJ, Fritz, JS, Calder, GV. Use of macroreticular resins in the analysis of water for trace organic contaminants, *J. Chromatography*, 1974, 99: 745-762.
- [63] Rieman, W, Walton, HF. *Ion exchange in analytical chemistry*, New York: Pergamon Press, 1970: 197-203.
- [64] Thurman, EM, Malcolm, RL, Aiken, GR. Prediction of capacity factors for aqueous organic solutes on a porous acrylic resin. *Anal. Chem.*, 1978, 50: 775-779.
- [65] Aiken, GR, Thurman, EM, Malcolm, RL, Walton, HF. Comparison of XAD macroporous resins for the concentration of fulvic acid from aqueous solution. *Anal. Chem.*, 1979, 51: 1799-1803.
- [66] Thurman, EM, Malcolm, RL. Preparative isolation of aquatic humic substances. *Environ. Sci. Technol.*, 1981, 15: 463-466.
- [67] Leenheer, JA. Comprehensive approach to preparative isolation and fractionation of dissolved organic carbon from natural waters and wastewater. *Environ. Sci. Technol.* 1981, 15: 578-587.
- [68] Leenheer, JA, Brown, PA, Stiles, EA. Isolation of nonvolatile, organic solutes from natural waters by zeotropic distillation of water from N,N-dimethylformamide. *Anal. Chem.*, 1987, 59: 1313-1319.
- [69] Aiken, GR, Leenheer, JA. Isolation and chemical characterization of dissolved and colloidal organic matter. *Chemistry and Ecology*, 1993, 8: 135-151.
- [70] Leenheer, JA, Meade, RH, Taylor, HE, Pereira, WE. Sampling, fractionation, and dewatering of suspended sediment from the Mississippi River for geochemical and trace-contaminant analysis. In: Mallard, GE, Ragone, SE eds. *U.S. Geological Survey Toxic Substances Hydrology Program—Proceedings of the Technical Meeting, Phoenix, Arizona, Sept. 26-30, 1988*, U.S. Geological Survey Water Resources Investigations Report 88-4220, 1989: 501-512.
- [71] Leenheer, JA. Fractionation, isolation, and characterization of hydrophilic constituents of dissolved organic matter in water. Proceedings of the Natural Organic Matter Workshop, Poitiers, France, 1996: 4-1 to 4-5.
- [72] AWWA Research Foundation. *Characterization of natural organic matter in drinking water*. Denver, CO: American Water Works Association Research Foundation, Report 90780, 2000.
- [73] Leenheer, JA. Fractionation and comprehensive isolation of NOM for spectral characterizations and reactivity testing. In *Polar NOM: Characterization, DBP's, Treatment*, Denver, CO: AWWA Research Foundation, Report 90877, Chapter 3, 2001: 3-1 to 3-26.
- [74] Leenheer, JA, Izbicki, JA, Aiken, GR. Characterization of organic matter in stormflow in the Santa Ana River and selected tributaries (2003-2004), Fountain Valley, CA, Organic County Water District, 2005.
- [75] Leenheer, JA, Izbicki, JA, Rostad, CE, Noyes, TI, Woodside, G. Discovery of cyanuric acid during an assessment of natural organic matter in stormflow water of the Santa Ana River, 2003-2004. U.S. Geological Survey Scientific Investigations Report 2007-5048, 2007.
- [76] Leenheer, JA, Noyes, TI, Rostad, CE, Davisson, ML. Characterization and origin of polar dissolved organic matter from the Great Salt Lake. *Biogeochem.*, 2004, 69: 125-141.
- [77] Reemtsma, T, These, A, Linscheid, M, Leenheer, JA, Spitzzy, A. Molecular and structural characterization of dissolved organic

- matter from the deep ocean by FT-ICR-MS, including hydrophilic nitrogenous organic molecules. *Environ. Sci. Technol.*, 2008, 42: 1430-1437.
- [78] Leenheer, JA, Dotson, A, Westerhoff, P. Dissolved organic nitrogen fractionation. *Ann. Environ. Sci.*, 2007, 1: 45-56.
- [79] Knicker, H, Frund, R, Ludemann, HD. Characterization of nitrogen in plant composts and native humic materials by natural abundance ¹⁵N-CPMAS and solution NMR spectra. In: Nanny, MA, Minear, RA, Leenheer, JA eds. *Nuclear Magnetic Resonance Spectroscopy in Environmental Chemistry*, New York: Oxford University Press, 1997: 272-294.
- [80] Kroeff, EP, Pietrzyk, DJ. Investigation of the retention and separation of aminoacids, peptides, and derivatives on porous copolymers by high performance liquid chromatography. *Anal. Chem.*, 1978, 50: 502-511.
- [81] Leenheer, JA. Total organic matter fractionation. Proceedings of the 13th meeting of the International Humic Substances Society, July 30-August 4, Karlsruhe, Germany, 2006: 25-28.
- [82] Leenheer, JA, Martin, DA, Rutherford, DW. Fire induced changes in soil organic matter properties that contribute to hydrophobic soils. In: Coffelt, JL, Livingston, RK eds. Second U.S. Geological Survey Wildland Fire Workshop: Oct. 31-Nov. 3, Los Alamos, New Mexico, U.S. Geological Survey Open File Report 2002-11, 2002.
- [83] Wershaw, RL, Leenheer, JA, Cox, LG. Characterization of dissolved and particulate natural organic matter (NOM) in Neversink Reservoir, New York. U.S. Geological Survey Scientific Investigations Report 2005-5108, Colorado, 2005.
- [84] Leenheer, JA, Rostad, CE. Fractionation and characterization of organic matter in wastewater from a swine waste-retention basin. U.S. Geological Survey Scientific Investigations Report 2004-5217, 2004.
- [85] Hayes, MHB. Solvent systems for the isolation of organic components from soils. *Soil Sci. Soc. Amer. J.*, 2006, 70: 986-994.
- [86] Leenheer, JA, Brown, PA, Noyes, TI. Implications of mixture characteristics on humic substance chemistry, In: Suffet, IH, MacCarthy, P eds. *Aquatic Humic Substances: Influence on Fate and Treatment of Pollutants*, Advances in Chemistry Series 219, Washington, DC: American Chemical Society, 1989: 41-54.
- [87] Leenheer, JA, Wershaw, RL, Reddy, MM. Strong-acid, carboxyl groups structures in fulvic acid from the Suwannee River, Georgia. 1. Minor structures. *Environ. Sci. Technol.*, 1995, 29: 393-398.
- [88] Leenheer, JA, Wershaw, RL, Reddy, MM. Strong-acid, carboxyl groups structures in fulvic acid from the Suwannee River, Georgia. 2. Major structures. *Environ. Sci. Technol.*, 1995, 29: 399-405.
- [89] Brown, GK, MacCarthy, P, Leenheer, JA. Simultaneous determination of Ca, Cu, Ni, Zn, and Cd binding strengths with fulvic acid fractions by Schubert's method, *Anal. Chim. Acta*, 1999, 402: 169-181.
- [90] Brown, GK, Cabaniss, SE, MacCarthy, P, Leenheer, JA. Cu(II) binding by a pH-fractionated fulvic acid, *Anal. Chim. Acta*, 1999, 402: 183-193.
- [91] Leenheer, JA, Rostad, CE. Tannins and terpenoids as major precursors of Suwannee River fulvic acid, U.S. Geological Survey Scientific Investigations Report 2004-5276, 2004.
- [92] Huffman, EWD, Jr., Stuber, HA. Analytical methodology for elemental analyses of humic substances. In: Aiken, GR, McKnight, DM, Wershaw, RL, MacCarthy, P eds. *Humic Substances in Soil, Sediment, and Water: Geochemistry, Isolation, and Characterization*, New York: Wiley, 1985: 433-455.
- [93] Reddy, MM, Leenheer, JA, Malcolm, RL. Elemental analyses and heat of combustion of fulvic acid from the Suwannee River, In: Averett, RC, Leenheer, JA, McKnight, DM, Thorn, KA eds. *Humic Substances in the Suwannee River, Georgia: Interactions, Properties, and Proposed Structures*, U.S. Geological Survey Water Supply Paper 2373, 1994: 81-88.
- [94] Perdue, EM, Richie, JD. Dissolved organic matter in fresh water, In: Holland, HD, Turekian, KK eds. *Treatise on Geochemistry, Volume 5: Surface and Ground Water, Weathering, Erosion, and Soils* (Drever, JI ed.), Chaper 11, New York: Elsevier, 2003.
- [95] Telang, SA, Pocklington, R, Naidu, AS, Romankevich, EA, Gitelson, II, Gladyshev, MI. Carbon and mineral transport in major North American, Russian Arctic, and Siberian Rivers: the St Lawrence, the Mackenzie, the Yukon, the Arctic Alaskan Rivers, the Arctic Basin Rivers

- in the Soviet Union, and the Yenisei. In: Degens, ET, Kempe, S, Richey, J eds. *Biogeochemistry of Major World Rivers*, Chapter 4, SCOPE 42, London: Wiley, 1991.
- [96] Redfield, AC. On the proportions of organic derivations in sea water and their relation to the composition of plankton. In: Daniel, RJ ed. *James Johnson Memorial Volume*. Liverpool: University Press, 1934: 177-192.
- [97] Stuer-Lauridsen, F, Pederson, F. On the influence of the polarity index of organic matter in predicting environmental sorption of chemicals. *Chemosphere*, 1997, 35: 761-773.
- [98] van Krevelen, DW. *Coal: typology- physics-chemistry constitution.*, New York: Elsevier, 1993.
- [99] Aiken, GR. The nature of nonvolatile organic acids in Antarctic Lakes, Ph.D. Dissertation, Colorado School of Mines, Golden, CO, 1991.
- [100] Leenheer, JA. Progression from model structures to molecular structures of natural organic matter components. *Ann. Environ. Sci.*, 2007, 1: 57-68.
- [101] Her, N, Amy, G, Foss, D, Cho, J. Variations in molecular weight estimation by HP-size exclusion chromatography with UVA versus online DOC detection. *Environ. Sci. Technol.*, 2002, 36: 3393-3399.
- [102] Reszat, TN, Hendry, MJ. Characterizing dissolved organic carbon using asymmetrical flow field-flow fractionation with on-line UV and DOC detection. *Anal. Chem.*, 2005, 77: 4194-4200.
- [103] Leenheer, JA, Rostad, CE, Gates, PM, Furlong, ET, Ferrer, I. Molecular resolution and fragmentation of fulvic acid by electrospray ionization/multistage tandem mass spectrometry. *Anal. Chem.*, 2001, 73: 1461-1471.
- [104] Leenheer, JA, Ferrer, I, Furlong, ET, Rostad, CE. Charge characteristics and fragmentation of polycarboxylic acids by electrospray ionization-multistage tandem mass spectrometry. In: Ferrer, I, Thurman, EM eds., *Liquid Chromatography/Mass Spectrometry, MS/MS, and Time of Flight MS, Analysis of Emerging Contaminants*, ACS Symposium Series 850, Washington, DC: American Chemical Society, 2003: 312-324.
- [105] Aiken, GR, Brown, PA, Noyes, TI, Pinckney, DJ. Molecular size and weight of fulvic and humic acids from the Suwannee River. In: Averett, RC, Leenheer, JA, McKnight, DM, Thorn, KA eds. *Humic Substances in the Suwannee River, Georgia: Interactions, Properties, and Proposed Structures*, U.S. Geological Survey Water Supply Paper 2373, 1994: 89-98.
- [106] Reemtsma, T, These, A, Springer, A, Linscheid, M. Differences in the molecular composition of fulvic acid size fractions detected by size-exclusion chromatography-online Fourier transform ion cyclotron resonance (FT-ICR) mass spectrometry. *Wat. Res.*, 2008, 42: 63-72.
- [107] Plancque, G, Amekraz, B, Moulin, V, Taulhoat, P, Moulin, C. Molecular structure of fulvic acid by electrospray with quadrupole/time-of-flight mass spectrometry, *Rapid Commun. Mass Spectrom*, 2001, 15: 827-835.
- [108] Rostad, CE, Leenheer, JA. Factors that affect the molecular weight distribution of Suwannee River fulvic acid as determined by electrospray ionization/mass spectrometry. *Anal. Chim. Acta*, 2004, 523: 269-278.
- [109] Traube, J. Über das molekularvolumen, *Berichte der Deutschen Chemischen Gesellschaft*, 1895, 28: 2722-2728.
- [110] Brown, PA, Leenheer, JA. Significance of density determinations in molecular structures comprising fulvic acid from the Suwannee River. In: Averett, RC, Leenheer, JA, McKnight, DM, Thorn, KA eds. *Humic Substances in the Suwannee River, Georgia: Interactions, Properties, and Proposed Structures*. U.S. Geological Survey Water Supply Paper 2373, 1994: 183-194.
- [111] American Society for Testing and Materials. Standard test method for density and relative density (specific gravity) of liquids by Lipkin bicapillary pycnometer, Standard D941, Philadelphia: American Society for Testing and Materials, 1955.
- [112] Averett, RC, Leenheer, JA, McKnight, DM, Thorn, KA. eds. *Humic substances in the Suwannee River, Georgia: Interactions, properties, and proposed structures*. Appendix of data on humic substances from the Suwannee River, III. Composition of humic substances isolated from the Suwannee River, A. Major constituents, 2. Organic functional groups (a) fulvic acid, U.S. Geological Survey Water-Supply Paper 2373, 1994: 218.
- [113] Perdue, EM. Acidic functional groups of humic substances. In: Aiken, GR, McKnight, DM, Wershaw, RL, MacCarthy, P eds., *Humic Substances in Soil, Sediment, and Water*, New

- York: Wiley, 1985: 493-526.
- [114] Perdue, EM, Reuter, JH, Parrish, RS. A statistical model of proton binding by humus, *Geochim. Cosmochim. Acta*, 1984, 48: 1257-1263.
- [115] Bowles, EC, Antweiler, RC, MacCarthy, P. Acid-base titration and hydrolysis of fulvic acid from the Suwannee River. In: Averett, RC, Leenheer, JA, McKnight, DM, Thorn, KA eds. *Humic Substances in the Suwannee River, Georgia: Interactions, Properties, and Proposed Structures*, U.S. Geological Survey Water Supply Paper 2373, 1994: 115-128.
- [116] Westheimer, FH, Kirkwood, JG. The electrostatic influence of substituents on the dissociation constants of organic acids. II. *J. Chem. Phys.* 1938, 6: 513-560.
- [117] Sonnenberg, LB, Johnson, JD, Christman, RF. Chemical degradation of humic substances for structural characterization, In: Suffet, IH, MacCarthy, P eds. *Aquatic Humic Substances, Influence on Fate and Treatment of Pollutants*, Advances in Chemistry Series 219, Washington DC: American Chemical Society, 1989: 3-24.
- [118] Schnitzer, M. Humic substances: Chemistry and reactions. In: Schnitzer, M, Khan, SU eds. *Soil Organic Matter*, New York: Elsevier, 1978: 1-64.
- [119] Antweiler, RC. The hydrolysis of Suwannee River fulvic acid. In: Baker, RA ed., *Organic Substances in Sediments and Water, Volume 1, Humics and Soils*. Chelsea, MI: Lewis Publishers, 1991: 163-177.
- [120] Boehm, H-P, Diehl, E, Heck, W, Sappok, R. Surface oxides of carbon. *Angewante Chemie International Edition*, 1964, 3: 669-677.
- [121] Rutherford, DW, Wershaw, RL, Reeves, JB. Development of acid functional groups and lactones during the thermal degradation of wood and wood components. U.S. Geological Survey Scientific Investigations Report 2007-5013, 2007.
- [122] Croué, J-P, Benedetti, MF, Violleau, D, Leenheer, JA. Characterization and copper binding of humic and nonhumic organic matter isolated from the South Platte River: Evidence for the presence of a nitrogeneous binding site. *Environ. Sci. Technol.*, 2003, 37: 328-336.
- [123] Leenheer, JA. Detection of unusual structures in organic matter by NMR spectrometry, Abstracts of the 2001 Annual Meeting, Soil Science Society of America, October, Charlotte, North Carolina. 2001.
- [124] Wershaw, RL, Rutherford, DW, Leenheer, JA, Kennedy, KR, Cox, LG, Koci, DR. Biogeochemical processes that produce dissolved organic matter from wheat straw. U.S. Geological Survey Water Resources Investigations Report 03-4213, 2003.
- [125] Leenheer, JA. Comprehensive characterization of dissolved and colloidal organic matter in waters associated with groundwater recharge at the Orange County Water District, Final Report to the Orange County Water District, Fountain Valley, California, 2003.
- [126] Flett, MSt.C. Intensities of some group-characteristic infra-red bands. *Spectrochimica Acta*, 1962, 18: 1537-1556.
- [127] Cabaniss, SE. Carboxylic acid content of a fulvic acid determined by potentiometry and aqueous Fourier transform infrared spectrometry, *Analytica Chim. Acta*, 1991, 255: 23-30.
- [128] Cabaniss, SE, Leenheer, JA, McVey, IF. Aqueous infrared carboxylate absorbances: aliphatic di-acids. *Spectrochimica. Acta*, 1998, 54: 449-458.
- [129] Leenheer, JA, Noyes, TI. Derivatization of humic substances for structural studies, In: Hayes, MHB, MacCarthy, P, Malcolm, RL, Swift, RS eds. *Humic Substances II. In Search of Structure*, New York: Wiley, 1989: 257-280.
- [130] Herbert, BE, Bertsch, PM. A ^{19}F and ^2H NMR spectroscopic investigation of the interaction between nonionic organic contaminants and dissolved humic material, In Nanny, MA, Minear, RA, Leenheer, JA eds. *Nuclear Magnetic Resonance in Environmental Chemistry*, New York: Oxford University Press, 1997: 73-90.
- [131] Thorn, KA, Folan, DW, MacCarthy, P. Characterization of the International Humic Substances Society reference fulvic and humic acids by solution state carbon-13 (^{13}C) and hydrogen-1 (^1H) nuclear magnetic resonance spectrometry. U.S. Geological Survey Water-Resources Investigations Report 89-4196, 1989.
- [132] Hatcher, PG, Wilson, MA. The effect of sample hydration on ^{13}C -CPMAS NMR spectra of fulvic acid. *Org. Geochem.*, 1991, 12: 293-299.
- [133] Alemany, LB, Grant, DM, Pugmire, RJ, Alger, TD, Zilm, KW. Cross polarization and magic angle spinning NMR spectra of model organic compounds. 2. Molecules of low or remote protonation, *J. Am. Chem. Soc.*, 1983, 105: 2142-2147.

- [134] Wilson, MA, Hatcher, PG. Detection of tannins in modern and fossil barks and in plant residues by high-resolution solid-state ^{13}C nuclear magnetic resonance. *Org. Geochem.*, 1988, 12: 539-546.
- [135] Preston, CM, Trofymow, JA, Sayer, BG, Niu, J. ^{13}C nuclear magnetic resonance spectroscopy with cross-polarization and magic-angle spinning investigation of the proximate-analysis fractions used to assess litter quality in decomposition studies. 1997, *Can. J. Bot.*, 75: 1601-1613.
- [136] Rutherford, DW, Wershaw, RL, Cox, LG. Changes in composition and porosity occurring during thermal degradation of wood and wood components. U.S. Geological Survey Scientific Investigations Report 2004-5292, 2004.
- [137] Novotny, EH, Hayes, MHB, deAzevedo, ER, Bonagamba. TJ. Characterization of black carbon-rich samples by ^{13}C solid state nuclear magnetic resonance. *Naturwissenschaften*, 2006, 93: 447-450.
- [138] Simpson, MJ, Hatcher, PG. Determination of black carbon in natural organic matter by chemical oxidation and solid-state ^{13}C -nuclear magnetic resonance spectroscopy. *Org. Geochem.* 2004, 35: 923-935.
- [139] Leenheer, JA, McKnight, DM, Thurman, EM, MacCarthy, P. Structural components and proposed structural models for fulvic acid from the Suwannee River. In: Averett, RC, Leenheer, JA, McKnight, DM, Thorn, KA eds. *Humic Substances in the Suwannee River, Georgia: Interactions, Properties, and Proposed Structures*, U.S. Geological Survey Water Supply Paper 2373, 1994: 195-211.
- [140] Leenheer, JA, Noyes, TI, Wershaw, RL. Acquisition and interpretation of liquid-state ^1H -NMR spectra of humic and fulvic acids. In: Nanny, MA, Minear, RA, Leenheer, JA eds. *Nuclear Magnetic Resonance in Environmental Chemistry*, New York: Oxford University Press, 1997: 295-303.
- [141] Thorn, KA. Nuclear-magnetic-resonance spectrometry investigations of fulvic humic acids from the Suwannee River. In: Averett, RC, Leenheer, JA, McKnight, DM, Thorn, KA eds. *Humic Substances in the Suwannee River, Georgia: Interactions, Properties, and Proposed Structures*, U.S. Geological Survey Water Supply Paper 2373, 1994: 141-182.
- [142] Noyes, TI, Leenheer, JA. Proton nuclear-magnetic-resonance studies of fulvic acid from the Suwannee River, In: Averett, RC, Leenheer, JA, McKnight, DM, Thorn, KA eds. *Humic Substances in the Suwannee River, Georgia: Interactions, Properties, and Proposed Structures*, U.S. Geological Survey Water Supply Paper 2373, 1994: 129-139.
- [143] Leenheer, JA, Wilson, MA, Malcolm, RL. Presence and potential significance of aromatic ketone groups in aquatic humic substances. *Org. Geochem.*, 1987: 11: 273-280.
- [144] Thorn, KA. Biogeochemistry and environmental chemistry of nitrogen (available at http://wwwbrr/cr.usgs.gov/projects/SWC_Chem_Nitrogen/), 2008.
- [145] Thorn, KA, Arterburn, JB, Mikita, MA. ^{15}N and ^{13}C NMR investigation of hydroxylamine-derivatized humic substances. *Environ. Sci. Technol.*, 1992, 26: 107-116.
- [146] Nanny, MA, Minear, RA. ^{31}P -NMR of concentrated lake water samples. In Nanny, MA, Minear, RA, Leenheer, JA eds., *Nuclear Magnetic Resonance in Environmental Chemistry*, New York: Oxford University Press, 1997: 221-246.
- [147] Condron, LM, Frossard, E, Newman, RH, Tekely, P, Morel, J-L. Use of ^{31}P NMR in the study of soils and the environment. In Nanny, MA, Minear, RA, Leenheer, JA eds. *Nuclear Magnetic Resonance in Environmental Chemistry*, New York: Oxford University Press, 1997: 247-271.
- [148] Howe, RF, Lu, X, Hook, J, Johnson, WD. Reaction of aquatic humic substances with aluminum: A ^{27}Al NMR study, *Mar. Freshwater Res.*, 1997, 48: 377-383.
- [149] Lemarchand, E, Schott, J, Gallardet, J. Boron isotopic fractionation related to boron sorption on humic acid and the structure of surface complexes formed. *Geochim Cosmochim. Acta*, 2005, 69: 3519-3533.
- [150] Hertkorn, N, Perdue, EM, Ketruprt, A. A Potentiometric and ^{113}Cd -NMR study of cadmium complexation by natural organic matter at two different magnetic field strengths. *Anal. Chem.*, 2004, 76: 6327-6341.
- [151] Xu, X, Kalinichev, AG, Kirkpatrick, RJ. ^{133}Cs and ^{35}Cl NMR spectroscopy and molecular dynamics modeling of Cs^+ and Cl^- complexation with natural organic matter. *Geochim. Cosmochim. Acta*, 2006, 70: 4319-4331.
- [152] Simpson, AJ. Multidimensional solution state NMR of humic substances: a practical guide and review. *Soil Sci.*, 2001, 166: 795-809.

- [153] Simpson, AJ, Kingery, WL, Hatcher, PG. The identification of plant derived structures in humic materials using three-dimensional NMR spectroscopy. *Environ. Sci. Technol.*, 2003, 37: 337-342.
- [154] Mao, J-D, Hundal, LS, Schmidt-Rohr, K, Thompson, ML. Nuclear magnetic resonance and diffuse-reflectance infrared Fourier transform spectroscopy of biosolids-derived biocolloidal organic matter. *Environ. Sci. Technol.*, 2003, 37: 1751-1757.
- [155] Mao, J-D, Xing, B, Schnide-Rohr, K. New structural information on a humic acid from two-dimensional ^1H - ^{13}C correlation solid-state nuclear magnetic resonance. *Environ. Sci. Technol.*, 2001, 35: 1928-1934.
- [156] Herbert, CG, Johnstone, RAW. *Mass spectrometry basics*. New York, CRC Press, 2003.
- [157] Yamashita, M, Fenn, JB. Negative ion production with the electrospray ion source. *J. Phys. Chem.*, 1984, 88: 4671-4675.
- [158] Cole, RB. ed. *Electrospray ionization mass spectrometry*, New York: Wiley, 1997.
- [159] McIntyre, C, Batts, BD, Jardine, DR. Electrospray mass spectrometry of groundwater organic acids. *J. Mass Spectrometry*, 1997, 32: 328-330.
- [160] Stenson, AC, Landing, WM, Marshall, AG, Cooper, WT. Ionization and fragmentation of humic substances in electrospray ionization Fourier transform ion cyclotron resonance mass spectrometry. *Anal. Chem.*, 2002, 74: 4397-4409.
- [161] Sleighter, RL, Hatcher, PG. The application of electrospray ionization coupled to ultrahigh resolution mass spectrometry for the molecular characterization of natural organic matter. *J. Mass Spectrom.*, 2007, 42: 559-574.
- [162] Kim, S, Kramer, RW, Hatcher, PG. Graphical method of analyses of ultrahigh-resolution broadband mass spectrometry of natural organic matter: The van Krevelin diagram. *Anal. Chem.*, 2003, 75: 5336-5344.
- [163] Korshin, GV, Li, C-W, Benjamin, MM. Monitoring the properties of natural organic matter through UV spectroscopy. Evaluation of a consistent theory, *Water Res.* 1997, 31: 1787-1795.
- [164] Traina, SJ, Novak, J, Smeck, NE. An ultraviolet method of estimating the percent aromatic carbon in humic acids. *J. Environ. Qual.*, 1990, 19: 151-153.
- [165] Chin, Y-P, Aiken, GR, O'Loughlin, E. Molecular weight, polydispersity, and spectroscopic properties of aquatic humic substances. *Environ. Sci. Technol.*, 1994, 28: 1853-1858.
- [166] Oliver, BG, Thurman, EM. Influence of aquatic humic substance properties on trihalomethane potential. In: Jolley, RL, Brungs, WA, Cotruvo, JA, Cumming, RB, Mattice, JS, Jacobs, VA eds. *Water Chlorination: Chemistry, Environmental Impact, and Health Effects*, Ann Arbor, MI: Ann Arbor Science, 1983, v. 4, pp. 235-252.
- [167] Reckhow, DA, Singer, PC, Malcolm, RL. Chlorination of humic materials: Byproduct formation and chemical interpretations. *Environ. Sci. Technol.*, 1990, 24: 1655-1664.
- [168] Hwang, CJ, Scilimenti, MJ, Krasner, SW. Disinfection by-product formation reactivities of natural organic matter fractions of a low-humic water. In: Barrett, SE, Krasner, SW, Amy, GL eds., *Natural Organic Matter and Disinfection By-Products: Characterization and Control in Drinking Water*, ACS Symposium Series 761, Wash. DC: American Chemical Society, 2000: 173-187.
- [169] Del Vecchio, R, Blough, NV. On the origin of the optical properties of humic substances. *Environ. Sci. Technol.*, 2004, 38: 3885-3891.
- [170] Chen, Y, Senesi, N, Schnitzer, M. Information provided on humic substances by E_4/E_6 ratios. *Soil Sci. Soc. Am. J.*, 1977, 41: 352-358.
- [171] Lapen, AJ, Seitz, WR. Fluorescence polarization studies of the conformation of soil fulvic acid. *Anal. Chim. Acta*, 1982, 134: 31-38.
- [172] Goldberg, MC, Weiner, ER. Fluorescence measurements of the volume, shape, and fluorophore composition of fulvic acid from the Suwannee River. In: Averett, RC, Leenheer, JA, McKnight, DM, Thorn, KA eds. *Humic Substances in the Suwannee River, Georgia: Interactions, Properties, and Proposed Structures*, U.S. Geological Survey Water Supply Paper 2373, 1994: 99-113.
- [173] Coble, PG. Characterization of marine and terrestrial DOM in seawater using excitation-emission matrix spectroscopy. *Marine Chem.*, 1996, 51: 325-346.
- [174] Cory, RM, McKnight, DM. Fluorescence spectroscopy reveals ubiquitous presence of oxidized and reduced quinones in dissolved organic matter. *Environ. Sci. Technol.* 2005, 39: 8142-8149.
- [175] Marhaba, TG, Lippincott, RL, Van, D.

- Characterizing dissolved organic matter fractions using spectral fluorescent signatures and post processing by principal component analysis. *Fresenius' J. Anal. Chem*, 2000, 366: 22-25.
- [176] McKnight, DM, Boyer, EW, Westerhoff, PK, Doran, PT, Kulbe, T, Andersen, DT. Spectrofluorometric characterization of dissolved organic matter for indication of precursor organic material and aromaticity. *Limnol. Oceanogr.*, 2001, 46: 38-48.
- [177] Izbicki, JA, Pimental, MI, Leddy, M, Bergamaschi, B. Microbial and dissolved organic carbon characterization of stormflow in the Santa Ana River at Imperial Highway, southern California, 1999-2002. U.S. Geological Survey Scientific Investigations Report 2004-5116, 2004.
- [178] Korshin, GV, Frenkel, AI, Stern, EA. EXAFS study of the inner shell structure in copper(II) complexes with humic substances. *Environ. Sci. Technol.*, 1998, 32: 2699-2705.
- [179] Koningsberger, DC, Prins, R eds. *X-ray absorption: principles, applications, techniques of EXAFS, SEXAFS, and XANES*, New York: Wiley, 1988.
- [180] Frenkel, AI, Korshin, GV, Ankudinov, AL. XANES study of Cu²⁺- binding sites in aquatic humic substances. *Environ. Sci. Technol.*, 2000, 34: 2138-2142.
- [181] Xia, K, Weesner, F, Bleam, WF, Bloom, PR, Skyllberg, UL, Helmke, PA. XANES studies of oxidation states of sulfur in aquatic and soil humic substances. *Soil Sci. Soc. Amer. J.*, 1998, 62: 1240-1246.
- [182] Skyllberg, U, Xia, K, Bloom, PR, Nater, EA, Bleam, WF. Binding of mercury(II) to reduced sulfur in soil organic matter along upland-peat soil transects. *J. Environ. Qual.*, 2000, 29: 855-865.
- [183] Christman, RF, Norwood, DL, Seo, Y, Frimmel, F. Oxidative degradation of humic substances from freshwater environments. In Hayes, MHB, MacCarthy, P, Malcolm, RL, Swift, RS eds. *Humic Substances II, In Search of Structure*, New York: Wiley, 1989: 34-67.
- [184] Griffith, SM, Schnitzer, M. Oxidative degradation of soil humic substances. In: Hayes, MHB, MacCarthy, P, Malcolm, RL, Swift, RS eds. *Humic Substances II, In Search of Structure*, New York: Wiley, 1989: 69-142.
- [185] Hayes, MHB, Swift, RS. The chemistry of soil organic colloids. In: Greenland, DJ, Hayes, MHB eds. *The Chemistry of Soil Constituents*, New York: Wiley, 1978: 179-320.
- [186] Hedges, JI, Ertel, JR. Characterization of lignin by gas capillary chromatography of cupric oxide oxidation products. *Anal. Chem.*, 1982, 54: 174-178.
- [187] Stevenson, FJ. Reductive cleavage of humic substances. In: Hayes, MHB, MacCarthy, P, Malcolm, RL, Swift, RS eds. *Humic Substances II, In Search of Structure*, New York: Wiley, 1989: 121-142.
- [188] Nimmagadda, RD, McRae, C. Characterization of the backbone structures of several fulvic acids using a novel selective chemical reduction method. *Org. Geochem.*, 2007, 38: 1061-1072.
- [189] Cheshire, MV, Cranwell, PA, Haworth, RD. Humic acid-III. *Tetrahedron*, 1968, 24: 1669-1682.
- [190] Hayes, MHB, O'Callaghan, MR. Degradations with sodium sulfide and phenol. In: Hayes, MHB, MacCarthy, P, Malcolm, RL, Swift, RS eds. *Humic Substances II, In Search of Structure*, New York: Wiley, 1989: 143-180.
- [191] Jackson, HP, Swift, RS, Posner, AM, Knox, JR. Phenolic degradation of humic acid, *Soil Sci.*, 1972, 114: 75-78.
- [192] Parsons, JW. Hydrolytic degradations of humic substances. In: Hayes, MHB, MacCarthy, P, Malcolm, RL, Swift, RS eds. *Humic Substances II, In Search of Structure*, New York: Wiley, 1989: 99-120.
- [193] Anderson, HA, Bick, W, Hepburn, A, Stewart, M. Nitrogen in humic substances. In: Hayes, MHB, MacCarthy, P, Malcolm, RL, Swift, RS eds. *Humic Substances II, In Search of Structure*, New York: Wiley, 1989: 223-253.
- [194] Martens, DA, Loeffelmann, KL. Soil aminoacid composition quantified by acid hydrolysis and anion chromatography-pulsed amperometry. *J. Agri. Food Chem.*, 2003, 51: 6521-6529.
- [195] Bracewell, JM, Haider, K, Larter, SR, Schulten, H-R. Thermal degradation relevant to structural studies of humic substances. In: Hayes, MHB, MacCarthy, P, Malcolm, RL, Swift, RS eds. *Humic Substances II, In Search of Structure*, New York: Wiley, 1989: 181-222.
- [196] Page, D. Characterization of organic matter from air, water, soils, and waste materials by analytical pyrolysis, In: Nollet, LMN ed. *Chromatographic Analysis of the Environment, Third Edition*, Chapter 8, Boca Raton, Florida: CRC Press, 2006: 287-310.
- [197] Bruchet, A, Rousseau, C, Mallevalle, J.

- Pyrolysis-GC-MS for investigating high-molecular-weight THM precursors and other refractory organics. *J. Amer. Water Works Assoc.*, 1990, 82: 66-74.
- [198] AWWA Research Foundation. *Polar NOM: Characterization, DBPs, Treatment*, Denver, CO: American Water Works Association Research Foundation, Report 90877, 2001.
- [199] Saiz-Jimenez, C. Pyrolysis/methylation of soil fulvic acids: Benzenecarboxylic acids revisited. *Environ. Sci. Technol.*, 1994, 28: 197-200.
- [200] Martin, F, del Rio, JC, González-Vila, FJ, Verdejo, T. Pyrolysis derivatization of humic substances 2. Pyrolysis of soil humic acids in the presence of tetramethylammonium hydroxide. *J. Anal. Appl. Pyrol.*, 1995, 31 75-83.
- [201] Lewan, MD. Experiments on the role of water in petroleum formation. *Geochim. Cosmochim. Acta*, 1997, 61: 3691-3723.
- [202] Greenwood, PF, Leenheer, JA, McIntyre, C, Franzmann, PD. Bacterial biomarkers thermally released from dissolved organic matter. *Org. Geochem.*, 2006, 37: 597-609.
- [203] Abbt-Braun, G, Lankes, U, Frimmel, FH., Structural characterization of aquatic humic substances – The need for a multiple method approach. *Aquat. Sci.*, 2004, 66: 151-170.
- [204] Wikipedia, Definition of consilience. <http://en.wikipedia.org/wiki/consilience>. Accessed December 4, 2008.
- [205] Crawford, RL. *Lignin biodegradation and transformation*. New York: Wiley, 1981.
- [206] Young, LY. Anaerobic degradation of aromatic compounds, In: Gibson, DT ed. *Microbial Degradation of Organic Compounds*, New York: Dekker, 1984: 487-523.
- [207] Healy, JB, Jr., Young, LY, Reinhard, M. Methanogenic decomposition of ferulic acid, a model lignin derivative. *Appl. Environ. Microbiol.*, 1980, 39: 436-444.
- [208] Harvey, GR, Boran, DA, Chesal, LA, Tokar, JM. The structure of marine fulvic and humic acid. *Mar. Chem.*, 1983, 12: 119-132.
- [209] Britton, LM. Microbial degradation of aliphatic hydrocarbons. In: Gibson, DT ed., *Microbial Degradation of Organic Compounds*, New York: Dekker, 1984: 89-129.
- [210] Leenheer, JA, Wershaw, RL. Solubility controls that determine dissolved organic matter composition of surface- and ground waters, Goldschmidt Conference Abstracts, May 2005, University of Idaho, Moscow, Idaho, 2005: A182.
- [211] Averett, RC, Leenheer, JA, McKnight, DM, Thorn, KA. eds. *Humic substances in the Suwannee River, Georgia: Interactions, properties, and proposed structures*. U.S. Geological Survey Water-Supply Paper 2373, 1994.
- [212] Windholtz, M, Budavari, S, Stroumstos, LY, Fertig, MN. *The Merck Index, Ninth Edition*, Rahway, New Jersey: Merck and Co., 1976: 9542.
- [213] Wershaw, RL, Leenheer, JA, Kennedy, KR. Use of ¹³C-NMR and FTIR for elucidation of degradation pathways during natural litter decomposition and composting, III. Characterization of leachate from different types of leaves. In: Davies, G, Ghabbour, EA eds. *Humic Substances-Structures, Properties, and Uses*, Cambridge: Royal Society of Chemistry, 1998: 47-60.
- [214] Larson, RA. *Naturally occurring antioxidants*, New York: Lewis Publishers, 1997.
- [215] Jaap, S, Damste, S, van Duin, ACT, Hollander, D, Kohnen, EL, De Leeuw, JW. Early diagenesis of bacterioplanepolyol derivatives. *Geochim. Cosmochim. Acta*, 1995, 59: 5141-5147.
- [216] Madyastha, KM, Bhattacharyya, PK, Vaidyanathan, CS. Metabolism of monoterpene alcohol, linalool, by a soil pseudomonad. *Can. J. Microbiol.*, 1977, 23: 230-239.
- [217] Kowalenko, CG. Organic nitrogen, phosphorus and sulphur in soils. In: Schnitzer, M, Khan, SU eds. *Soil Organic Matter. Developments in Soil Science 8*. Amsterdam: Elsevier, 1978: 95-136.
- [218] Kemp, ALW, Mudrochova, A. The distribution and nature of aminoacids and other nitrogen-containing compounds in Lake Ontario surface sediments. *Geochim. Cosmochim. Acta*, 1973, 37: 2191-2206.
- [219] White, A, Handler, P, Smith, EL. *Principles of biochemistry, 3rd ed.*, New York: McGraw-Hill, 1964.
- [220] Repeta, DJ, Quan, TM, Aluwihare, LI, Accardi, A. Chemical characterization of high molecular weight dissolved organic matter in fresh and marine waters. *Geochim. Cosmochim. Acta*, 2002, 66: 955-962.
- [221] Kaufman, DD. ed. *Bound and conjugated pesticide residues*, ACS Symposium Series No. 29, Washington, DC: American Chemical Society, 1976.
- [222] Baker, EW, Palmer, SE. Geochemistry of

- porphyrins, In: Dolphin, D ed. *The Porphyrins*, Vol. 1, New York: Academic Press, 1978: pp. 485-511.
- [223] Chiou, CT. *Partitioning and adsorption of organic contaminants in environmental systems*, Hoboken, New Jersey: Wiley, 2002.
- [224] Hu, W-G, Mao, J, Xing, B, Schmidt-Rohr, K. Poly(methylene) crystallites in humic substances detected by nuclear magnetic resonance. *Environ. Sci. Technol.* 2000, 34: 530-534.
- [225] Tegelaar, EW, de Leeuw, JW, Saiz-Jimenez, C. Possible origin of aliphatic moieties in humic substances. *The Science of the Total Environment*, 1989, 81/82: 1-17.
- [226] Holloway, PJ. Cutins and suberins, the polymeric plant lipids. In: Mangold, HK ed. *CRC Handbook of Chromatography, Lipids*, Vol. 1, Boca Raton, Florida: CRC Press, 1984: 321-334.
- [227] Kolattukudy, PE. Biopolyester membranes of plants: cutin and suberin. *Science*, 1980, 208: 990-999.
- [228] Tegelaar, EW, Hollman, G, Van Der Vegt, P, De Leeuw, JW, Holloway, PJ. Chemical characterization of the periderm tissue of some angiosperm species: recognition of an insoluble, non-hydrolyzable, aliphatic biomacromolecule (Suberan). *Org. Geochem.*, 1995, 23: 239-250.
- [229] Kuhlbusch, TAJ, Crutzen, PJ. Toward a global estimate of black carbon in residues of vegetation fires representing a sink of atmospheric CO₂ and a source of O₂. *Global Biogeochem. Cycles*, 1995, 9: 491-501.
- [230] Glaser, B, Haumaier, L, Guggenberger, G, Zech, W. The "Terra Preta" phenomenon: A model for sustainable agriculture in the humid tropics. *Naturwissenschaften*, 2001, 88: 37-41.
- [231] Chun, Y, Sheng, G, Chiou, CT. Evaluation of current techniques for isolation of chars as natural adsorbents. *Environ. Sci. Technol.*, 2004, 38: 4227-4232.
- [232] Schmidt, MWI, Skjemstad, JO, Czimczik, CI, Glaser, B, Prentice, KM, Gelinas, Y, Kuhlbusch, TAJ. Comparative analyses of black carbon in soils. *Global Biogeochemical Cycles*, 2001, 15: 163-167.
- [233] Kramer, RW, Kujawinski, EB, Hatcher, PG. Identification of black carbon derived structures in a volcanic soil by Fourier transform ion cyclotron resonance mass spectrometry. *Environ. Sci. Technol.*, 2004, 38: 3387-3396.
- [234] González-Vila, FJ, González, JA, Polvillo, O, Almendros, G, Knicker, H. Nature of refractory forms of organic carbon in soils affected by fires. Pyrolytic and spectroscopic approaches, In: Viegas, DX ed. *Forest Fire Research & Wildland Fire Safety*, Rotterdam, Netherlands: Millpress, 2002.
- [235] Leenheer, JA, Aiken, GR, Woodside, G, O'Connor-Patel, K. DOM in recharge waters of the Santa Ana River basin. *J. Am. Wat. Works Assoc.*, 2007, 99: 118-131.
- [236] O'Connor-Patel, K, Woodside, G. *Santa Ana water quality and health study*, Fountain Valley, CA: Orange County Water District, 2004,
- [237] Field, JA, Leenheer, JA, Thorn, KA, Barber, LB, Rostad, CE, Macalady, DL, Daniel, SR. Comprehensive approach for identifying anionic surfactant-derived chemicals in sewage effluent and ground water. *J. Cont. Hydrol.*, 1992, 9: 55-78.
- [238] Leenheer, JA, Rostad, CE, Barber, LB, Schroeder, RA, Anders, R, Davisson, ML. Nature and chlorine reactivity of organic constituents from reclaimed water in groundwater. Los Angeles County, California, *Environ. Sci. Technol.*, 2001, 35: 3869-3876.
- [239] Leenheer, JA, Wershaw, RL, Brown, PA, Noyes, TI. Detection of poly-ethylene glycol residues from nonionic surfactants in surface water by ¹H- and ¹³C-nuclear magnetic resonance spectrometry. *Environ. Sci. Technol.*, 1991, 25: 161-168.
- [240] Leenheer, JA, Hsu, J, Barber, LB. Transport and fate of organic wastes in groundwater at the Stringfellow Hazardous Waste Disposal Site. *J. Cont. Hydrol.*, 2001, 51: 163-178.
- [241] Herckes, P, Leenheer, JA, Collett, JL, Jr. Comprehensive characterization of atmospheric organic matter in Fresno, California fog water. *Environ. Sci. Technol.*, 2007, 41: 393-399.
- [242] Birch, ME, Cary, RA. Elemental carbon-based method for monitoring occupational exposures to particulate diesel exhaust. *Aerosol Sci. Technol.*, 1996, 25: 221-241.
- [243] Claeys, M, Wang, W, Ion, AC, Kourtchev, I, Gelencser, A, Maenhaut, W. Formation of secondary organic aerosols from isoprene and its gas-phase oxidation products through reaction with hydrogen peroxide. *Atmos. Env.*, 2004, 38: 4093-4098.
- [244] Leenheer, JA, Reddy, MM. Co-precipitation of dissolved organic matter by calcium carbonate in Pyramid Lake, Nevada, *Ann. Environ. Sci.*, 2008, 2: 11-25.

- [245] Reddy, MM. Carbonate precipitation in Pyramid Lake, Nevada. In Amjad, Z. *Mineral Scale Formation and Inhibition*, New York City NY, Plenum Press, 1995: 21-32.
- [246] Arp, G, Thiel, V, Reiner, A. Biofilm exopolymers control microbialite formation at thermal springs discharging into the alkaline Pyramid Lake, Nevada, USA. *U. S. Sedimentary Geology*, 1999, 126: 159-176.
- [247] Audrieth, LF, Kleinberg, J. *Non-aqueous solvents, applications as media for chemical reactions*, Chapter 8, Acetic Acid, New York: Wiley, 1953: 148-151.
- [248] 248. Diallo, MS, Simpson, A, Gassman, P, Faulon, JL, Johnson, JH, Jr., Goddard III, WA, Hatcher, PG. 3-D structural modeling of humic acids through experimental characterization, computer assisted structure elucidation and atomistic simulations. 1. Chelsea soil humic acid. *Environ. Sci. Technol.*, 2003, 37: 1783-1793.

AES8430

© Northeastern University, 2009